University of Alberta

Cambrian-Ordovician successions and detrital zircon geochronology of North Wales and Nova Scotia

by

Hayley Dawn Pothier

A thesis submitted to the Faculty of Graduate Studies and Research in partial fulfillment of the requirements for the degree of

Master of Science

Department of Earth and Atmospheric Sciences

Spring 2014
Edmonton, Alberta

ABSTRACT

The Appalachian-Caledonide Orogen resulted in the collision of Laurentia, Baltica and many peri-Gondwanan terranes, of which two share similar histories. The Harlech Dome and St. Tudwal's Peninsula, in North Wales, and the Meguma Terrane of southern Nova Scotia, in Atlantic Canada, preserve similar sedimentary successions of Cambrian age. U-Pb detrital zircon data from these regions show a West African source in the Cambrian. In the Harlech Dome this is replaced by a probable Ganderian source by the Tremadocian. Correlative rocks of the Lumsden Dam Formation of the Meguma terrane lack this Ganderian signature. This suggests North Wales was juxtaposed with the Monian Composite Terrane by this time along the Menai Strait Fault System, which has a history of sinistral strike-slip movement. This strike-slip tectonic regime could also account for the removal of the Meguma Terrane from an original position adjacent to the Harlech Dome and the basins' divergent Ordovician histories.

ACKNOWLEDGEMENTS

First and foremost I would like to gratefully acknowledge my supervisor Dr. John Waldron for offering me this great opportunity to work with him. His guidance, useful critiques, and his willingness to give his time so generously has been very much appreciated. Special thanks are given to Andy DuFrane for his advice on data reduction involved in this project. Thanks is also extended to David Schofield, Chris White, and Sandra Barr who volunteered their time to assist with field work and to Morgan Snyder and Maryam Dzulkefli for being excellent field assistants. I wish to acknowledge the help provided by Matthew Kliffer, Heather Clough and Robert Dokken with mineral separation and preparation. Assistance provided by the technicians of the University of Alberta Department of Earth and Atmospheric Sciences operating the equipment is also greatly appreciated. Funding for this research is provided by the Natural Sciences and Engineering Research Council of Canada Discovery Grants. Finally I wish to thank my family and friends for their support and encouragement throughout this work.

CONTENTS

CHAPTER 2: DETRITAL ZIRCON GEOCHRONOLOGY OF THE CAMBRIAN-ORDOVICIAN SUCCESSION OF NORTH WALES

CHAPTER 3: PROVENANCE AND DEPOSITIONAL ENVIRONMENT OF THE EARLY ORDOVICIAN CLASTIC ROCKS OF THE MEGUMA TERRANE

LIST OF FIGURES

CHAPTER 1: INTRODUCTION

1.1 INTRODUCTION

Detrital zircon geochronology is a key tool used in unraveling the complex histories of terrane interactions in ancient orogens (e.g., Dickinson 1974; Cawood et al. 2007). Identifying potential source regions for basin sediments helps to determine the basin's proximity to surrounding terranes. The timing of terrane juxtaposition can be determined by changes in the detrital zircon record through time.

The Appalachian-Caledonide Orogen involved a series of geological events that occurred from Early Ordovician to Middle Devonian time and resulting from the collision of Laurentia, Baltica, and several peri-Gondwanan terranes, including Ganderia, Avalonia, and the Meguma terrane of Nova Scotia (e.g., McKerrow et al. 2000). Several tools have been used to help provide constraints on the tectonic reconstructions of these terranes, including paleomagnetic data, faunal evidence (e.g., Thompson et al. 2010; Cocks and Torsvik 2002), and provenance studies (e.g., Barr et al. 2003; Waldron et al. 2009, 2011), but the timing of amalgamation and the paleogeographic positions of terranes involved in the orogen are still poorly constrained.

This study focuses on using detrital zircon analyses to provide insight into the history of two terranes, the Meguma terrane of Nova Scotia and the Harlech Dome succession in North Wales, for which Waldron et al. (2011) suggested a correlation. In North Wales detrital zircon samples were collected from the Arfon Basin and the northern Welsh Basin for comparison with samples collected from the adjacent Monian Composite Terrane by Collins and Buchan (2004). An additional detrital zircon sample was collected from the upper Halifax Group of the Meguma terrane for further comparison. Chapter 1 includes an introduction to the geologic setting and stratigraphy of the Meguma terrane and North Wales and outlines the analytical methods used.

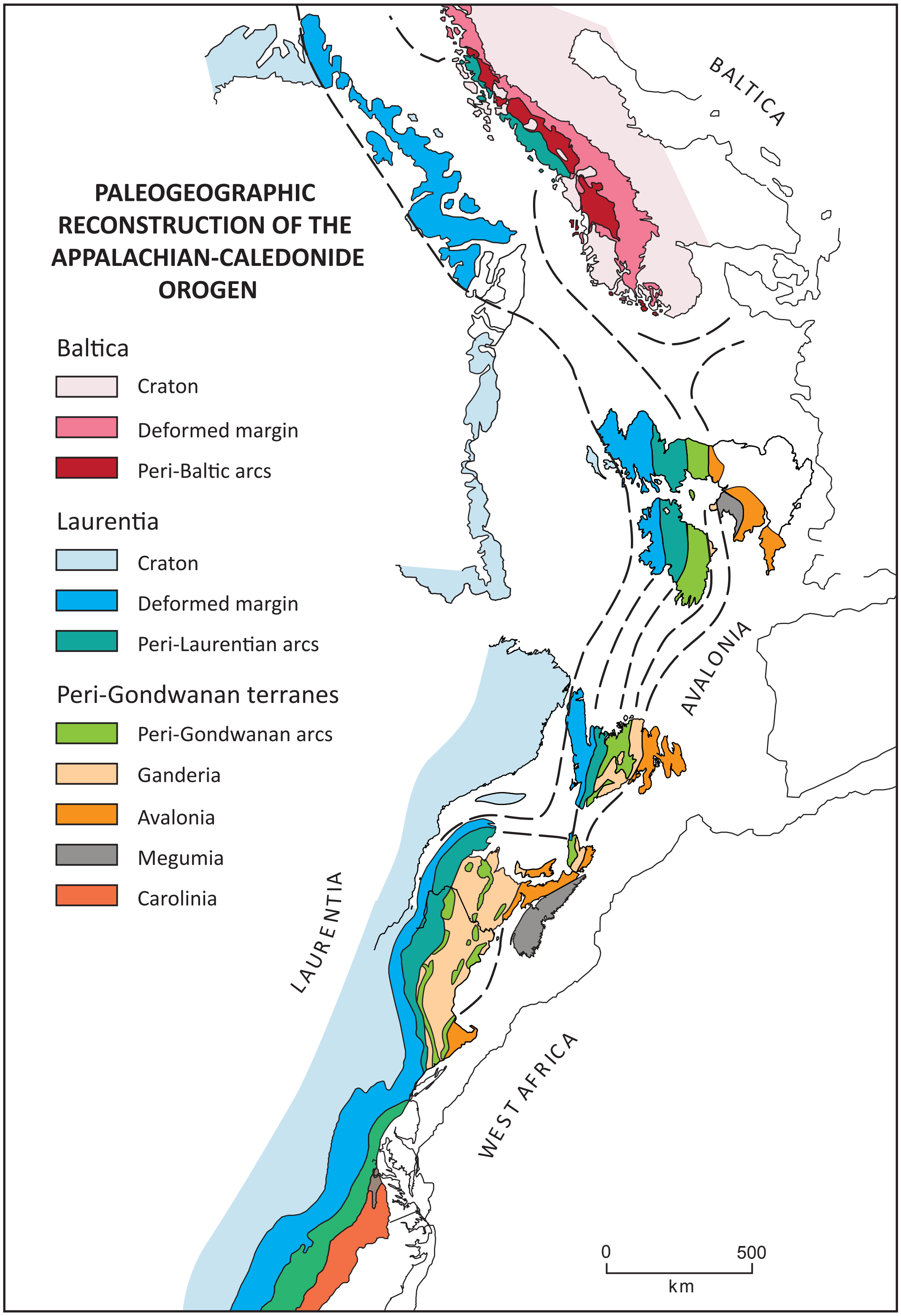

Figure 1.1: Paleocontinental reconstruction prior to the opening of the Atlantic Ocean showing the Components of the Appalachian-Caledonide orogen. Data compiled from Knott et al. (1993), van Staal et al. (1998), Barnes et al. (2007) Hibbard et al. (2007), and Waldron et al. (2011).

1.2 APPALACHIAN-CALEDONIDE OROGEN

The Appalachian-Caledonide Orogen is a Paleozoic orogen that resulted from the closure of the Iapetus Ocean and the collision of Laurentia, Baltica, and peri-Gondwanan terranes (e.g., van Staal 1998; McKerrow et al. 2000; Hibbard et al. 2007). The remnants of the orogen are found on either side of the Atlantic Ocean from the southeastern United States of America to the Caledonides of the British Isles, eastern Greenland, and Scandinavia (Fig. 1.1).

The deformed Laurentian margin forms a nearly continuous band along the entire length of the orogen (Fig. 1.1). Adjacent to the Laurentian margin are remnants of a peri-Laurentian microcontinent and peri-Laurentian arcs (Waldron and van Staal 2001; Hibbard et al. 2007). Outboard of the Laurentian realm are a series of less continuous peri-Gondwanan domains identified by Hibbard et al. (2007). In Atlantic Canada, these consist of Ganderia, West Avalonia and the Meguma terrane. Ganderia is found in New Brunswick, northern Cape Breton Island, Nova Scotia, and central Newfoundland. West Avalonia spans northern Nova Scotia and western Newfoundland. The Meguma terrane is only found in southern Nova Scotia (Fig. 1.2).

In the British Caledonides the peri-Gondwanan realm roughly corresponds to England, Wales, and the southeastern part of Ireland (Fig. 1.2). This entire region is commonly referred to as 'East' Avalonia (e.g., Brenchley et al. 2006), but it can be divided into multiple domains on multiple scales (e.g., Bluck et al. 1992). The Leinster-Lakesman terrane is the northernmost terrane included in the peri-Gondwanan realm and spans southern Ireland and northern England. The island of Anglesey in North Wales, together with the most southeastern tip of Ireland, makes up the narrow Monian-Rosslare terrane. To the south are the Welsh Basin, Midland Platform, and Anglian Basin (Fig. 1.2).

Similarities identified between peri-Gondwanan terranes on either side of the Atlantic have led to the correlation of several terranes. The Leinster-Lakesman terrane and Monian-Rosslare terrane (Fig. 1.2) have been correlated with Ganderia in Atlantic Canada (e.g., van Staal et al. 1996 and references therein, 1998) on the basis of lithological similarities. Avalonia is characterized by Precambrian arc-related volcanic suites that are overlain by a lower Paleozoic platformal sedimentary succession that contains Acado-Baltic fauna (Nance 1991;

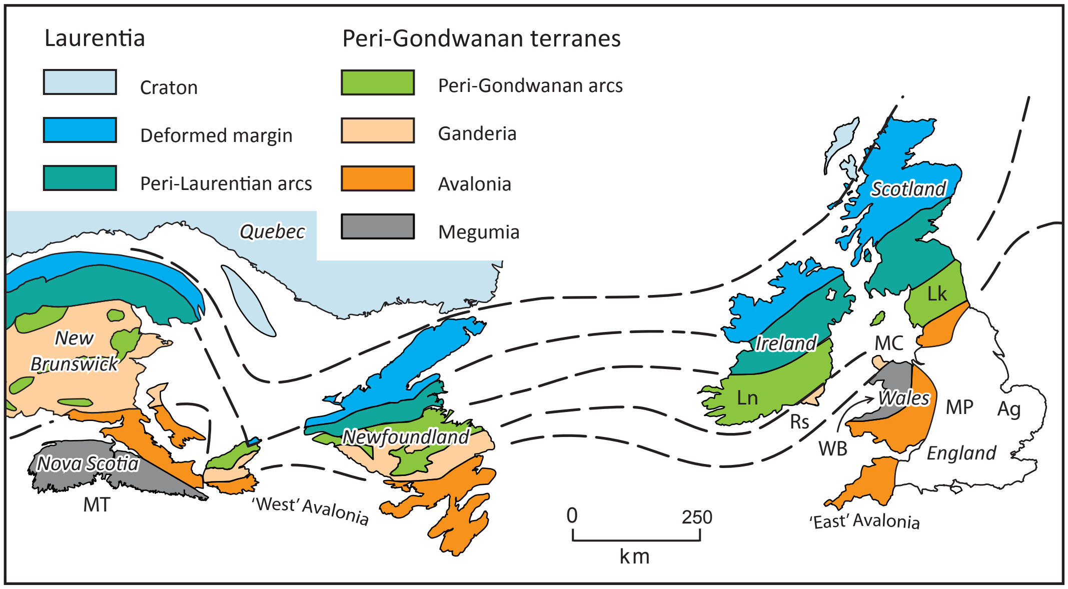

Figure 1.2: Terrane Map of the North America Appalachians and British Caledonides. Abbreviations: Ag-Anglian Basin; Lk-Lakesman Terrane; Ln-Leinster Terrane; MC-Monian Composite Terrane; MP-Midland Platform; MT-Meguma Terrane; Rs-Rosslare Terrane; WB-Welsh Basin. Data compiled from van Staal et al. (1998), Barnes et al. (2007) Hibbard et al. (2007) and Waldron et al. (2011).

Nance and Murphy 1994). 'East' and 'West' Avalonia describe correlative parts of this domain on the east and west side of the Atlantic Ocean (Fig. 1.2). Waldron et al. (2011) have recognized lithostratigraphic and provenance similarities between the early Cambrian to Tremadocian successions of the Meguma terrane and the Harlech Dome in the Welsh Basin assigning both to the domain"Megumia" (Fig. 1.2). The work done in this study is designed to test and explore the implications of that hypothesis.

The paleogeographic positions of several terranes involved in the Appalachian-Caledonide Orogen are poorly constrained, but there is a consensus (e.g., Murphy et al. 2004; Hibbard et al. 2007) that many of them – including Avalonia, Ganderia, and the Meguma terrane – originated along the Gondwanan margin. However, the relative positions of even these terranes are poorly known.

1.3 NORTH WALES

1.3.1 Geologic Setting

North Wales can be divided into three Precambrian to Tremadocian zones (Fig. 1.3), the Monian Composite Terrane, the Arfon Basin, and the Harlech Dome of the Welsh Basin, all of which contain distinct lithostratigraphic successions (Fig. 1.4).

The Monian Composite terrane (part of the Monian-Rosslare terrane) is located on the island of Anglesey and the Llŷn Peninsula (Fig. 1.3). It comprises three discrete tectonic units, each bounded by faults and shear zones (Gibbons and Horák 1990). These include the Monian Supergroup, the Coedana Complex, and the Aethwy terrane (Fig. 1.3). The first of these, the Monian Supergroup, is exposed on the northwestern part of the island and consists of an early Cambrian to Tremadocian sedimentary succession discussed in further detail in section 1.3.2. The second is the Precambrian Coedana Complex, which runs SW-NE through the centre of the island. It consists of the Coedana granite and a suite of gneisses that have been altered to hornfels in places (Gibbons 1983). The granite has been dated at 613 ± 4 Ma (Tucker and Pharaoh 1991). The third is the Aethwy terrane, preserved in a thin slice in southeast Anglesey. It consists of metabasite and metasedimentary rocks metamorphosed to blueschist facies (Gibbons 1987; Gibbons and Horák 1990). These have produced $^{40}Ar/^{39}Ar$ dates of 580-590 Ma and 550-560 Ma, which are interpreted to represent the time of respective greenschist and blueschist metamorphic events (Dallmeyer and Gibbons 1987).

The Monian Composite terrane is bounded to the southeast by the Menai Strait Fault System (Fig. 1.3). The NE-striking system contains a series of steep faults and shear zones, most significantly the Berw, Dinorwic, and Aber-Dinlle faults, that have a history of sinistral transcurrent movement (Gibbons and Horák 1990). Gibbons (1987) suggested the existence of a terrane boundary along the Menai Strait Fault System based on contrasts in basement characteristics on either side of the fault system and the presence of an early ductile shear zone.

The southwestern extension of the Menai Strait Fault System in North Wales is the Llŷn Shear Zone (Fig. 1.3). In this region, the highest unit of the Monian Supergroup is exposed to the north of the shear zone and to the south is the Sarn Igneous Complex which produced a U-Pb date of 615 ± 2 Ma (Horák et al. 1996).

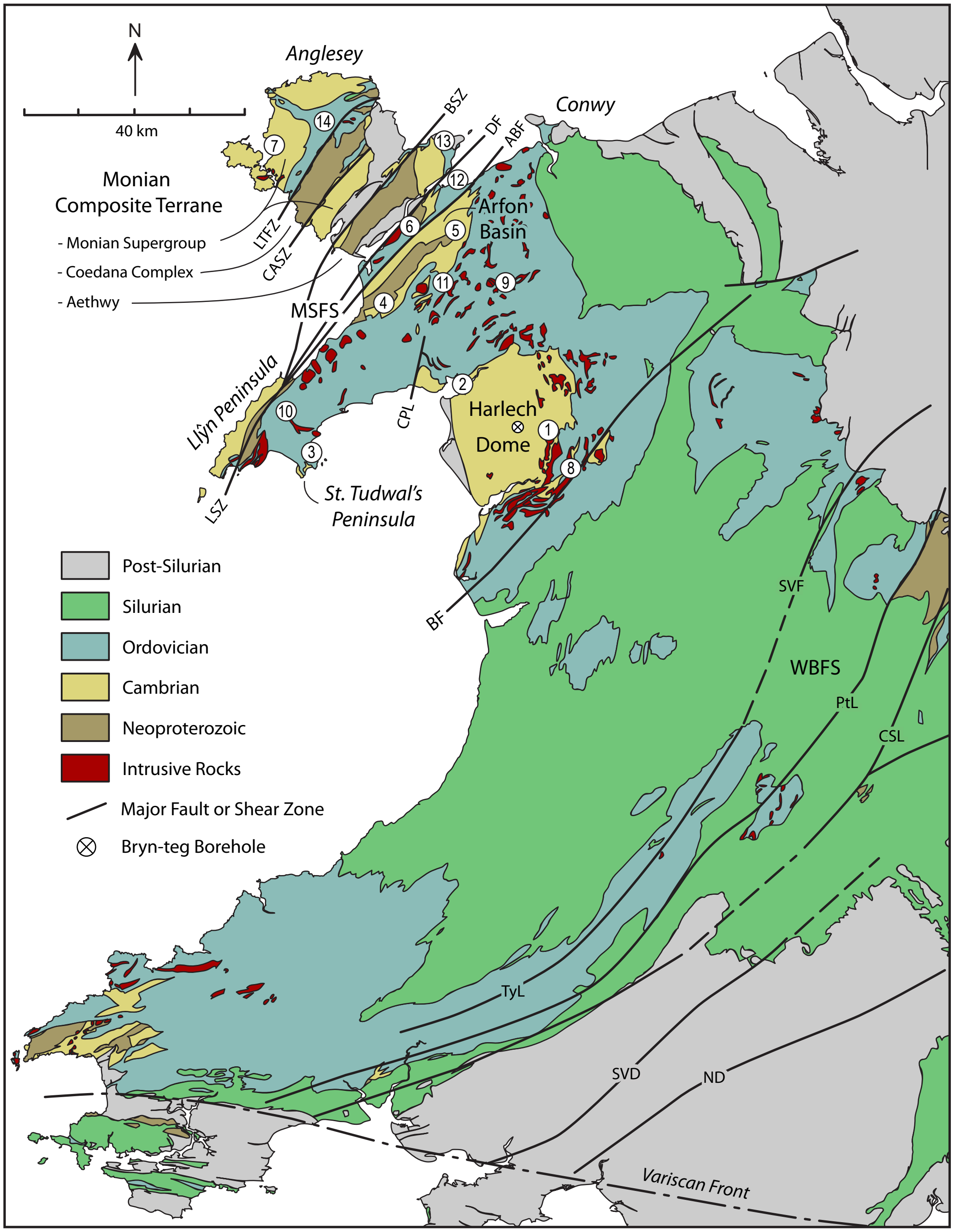

Figure 1.3: Geological map of Wales (from British Geological Survey 2007). Circled numbers indicate locations of columns shown in Fig. 1.4 and 1.5. Abbreviations: ADF-Aber-Dinlle Fault; BF-Bala Fault; BSZ-Berw Shear Zone; CASZ-Central Anglesey Shear Zone; CSL-Church-Stretton Lineament; DF-Dinowic Fault; LSZ-Llŷn Shear Zone; LTFZ-Llyn Traffwll Fault Zone; MSFS-Menai Strait Fault System; ND-Neath Disturbance; PtL-Pontesford Lineament; SVD-Swansea Valley Disturbance; SVF-Seven Valley Fault; TyL-Tywi Lineament; and WBFS-Welsh Borderland Fault System.

Preserved to the south of the Dinorwic fault and between the Monian Composite terrane and the Welsh Basin is the Precambrian to Cambrian volcano-sedimentary succession of the Arfon Basin (Fig. 1.3). The relationship of these rocks with the successions to the northwest and southeast is unknown. The faulted northwestern contact with the Monian terrane hides the nature of the relationship of the Arfon Basin with Monian rocks, and Ordovician cover conceals the southeastern boundary between it and the Cambrian deposits of the Harlech Dome in the Welsh Basin (Fig. 1.3).

The Welsh Basin contains a thick early Cambrian to early Devonian sedimentary succession of both clastic metasedimentary and volcanic rocks described in more detail in section 1.3.4. Little is known about the basin's basement as there are only small exposures of Neoproterozoic rocks around its borders (Fig. 1.3) and within the Bryn-teg borehole in the Harlech Dome region (Allen and Jackson 1978; McIlroy and Horák 2006).

1.3.2 Monian Supergroup

The Monian Supergroup (the bedded succession of Greenly 1919) consists of early Cambrian to Tremadocian mainly sedimentary rocks that have been metamorphosed to greenschist facies. Historically, these rocks were believed to be Precambrian (e.g., Greenly 1919; Shackleton 1969), but paleontological evidence indicates a Cambrian age for most of the succession (Muir et al. 1979; Brenchley et al. 2006).

The Monian Supergroup as described by Gibbons and Ball (1991) is divided into three groups. The South Stack Group, the lowest unit (Fig. 1.4), consists of massive quartzite and quartzose turbiditic greywacke with minor slate (Greenly 1919). These rocks contain post-Neoproterozoic trace fossils *Skolithos* and early Cambrian trace fossil *Trichophycus* (Muir et al. 1979). A detrital zircon sample from the Holyhead formation of the South Stack Group produced an age of 501 ± 1 Ma, which has been interpreted by Collins and Buchan (2004) to represent a maximum depositional age. The overlying New Harbour Group (Fig. 1.4) consists of pelite with subordinate serpentinite, gabbro, basalt, and chert (Gibbons 1983). The Gwna Group (Fig. 1.4) is the youngest unit in the Monian Supergroup. It has been described as a mélange that contains continental and deep-water clasts including pillow lava, chert, sandstone, limestone, and granite

(Gibbons 1987). This unit was initially interpreted to be the result of tectonic disruption by Greenly (1919) and was later described by Shackleton (1954, 1969, 1975) as a deformed olistostrome. There is little evidence to constrain the age the New Harbour and Gwna Groups; however, Floian sedimentary rocks rest unconformably over the Gwna Group providing a maximum depositional age for this unit (Greenly 1919; Bates 1968).

The Ordovician record on the Monian Composite Terrane ranges from the Dapingian to the late Sandbian (Rushton and Fortey 2000) and is not as complete as the record on mainland Wales (Fig. 1.5). Ordovician rocks appear only as outliers. They consist mainly of mudstone and there is no record of significant volcanic activity (Bates 1972). Silurian (436 Ma) rocks on the Monian Composite Terrane are only preserved in northern Anglesey (Parrish 1999). These rocks rest above Darriwillian sedimentary rocks and are overlain by mid-Llandovery graptolite-bearing slate (Greenly 1919).

1.3.3 Arfon Basin

The Arfon Basin is located to the northwest of the Welsh Basin and to the southeast of the Monian Composite terrane along the Menai Strait Fault System (Fig. 1.3). The northwestern boundary with the Monian Composite Terrane is the Dinorwic Fault (Fig. 1.3) and the nature of the southwestern contact with the Harlech Dome succession is hidden beneath Ordovician cover.

Arfon Group

At the base of the Arfon Basin is the approximately 4000 m thick Arfon Group (Fig. 1.4) (Reedman et al. 1984). The lowest unit in the Afron Group, the Padarn Tuff Formation, has been dated by Tucker and Pharaoh (1991) and Compston et al. (2002) who reported U-Pb ages of 614 ± 2 Ma and 605 ± 2 Ma respectively. It comprises welded felsic ash flow tuffs. Its base is not exposed. Enveloped within the Padarn Tuff is the Twt Hill Granite dated at 615 ± 1.3 Ma (Schofield et

Figure 1.4: (next page) Stratigraphic columns showing Cambrian units of the northern Welsh Basin, Arfon Basin, and Monian Composite Terrane. Data compiled from Pharaoh and Carney (2000), Brenchley and Rawson (2006), Rushton and Molyneux (2011). Abbreviations: ABF-Aber-Dinlle Fault; DG-Dorothea Grit; DF-Dinorwic Fault; CPL-Cwm Pennant Lineament; and WBFS-Welsh Borderland Fault System. Using time scale of Peng et al. (2012).

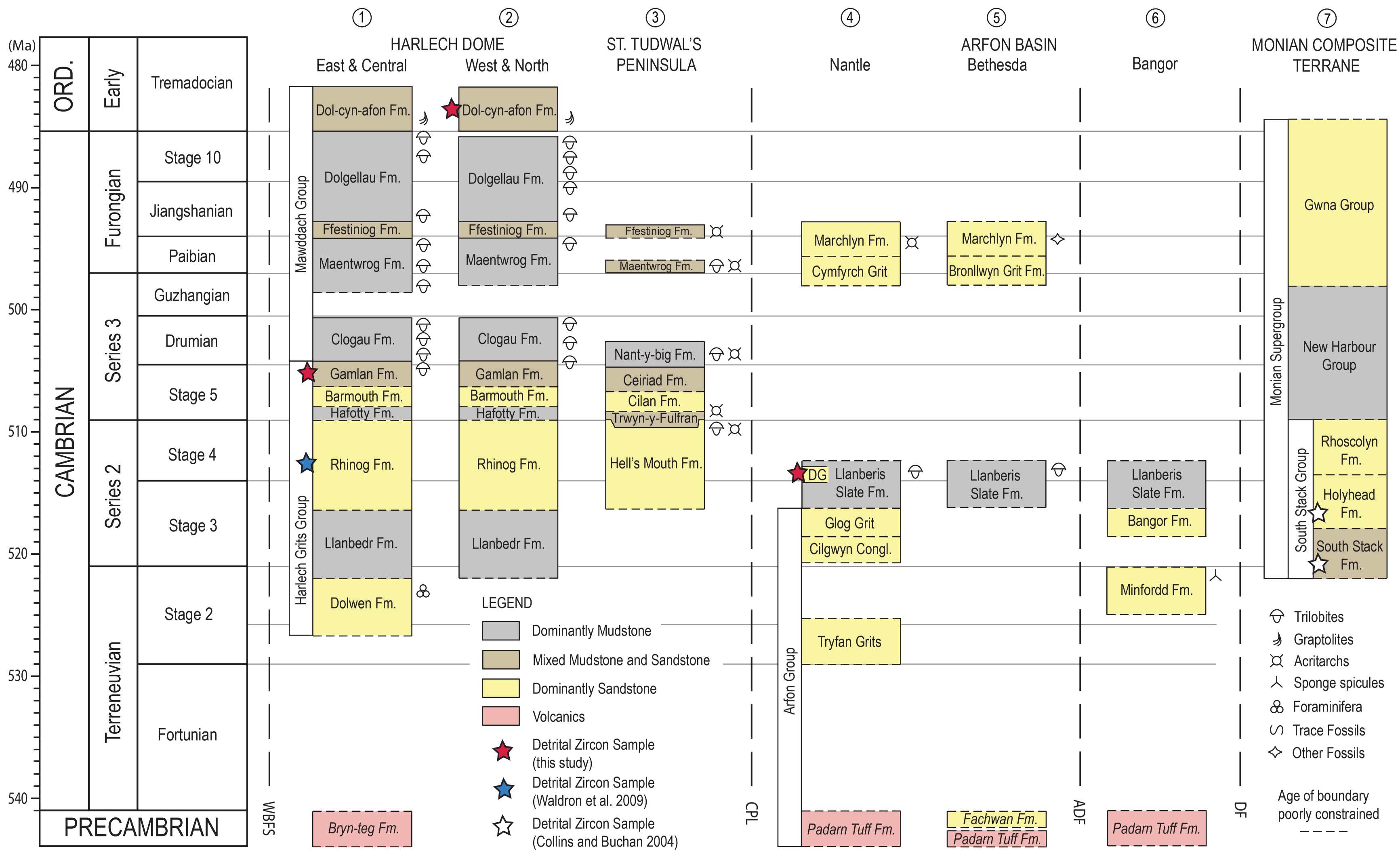

(Ma)
480
490
500
510
520
530
540
ORD.
Early
Tremadocian
CAMBRIAN
Furongian
Stage 10
Jiangshanian
Paibian
Series 3
Guzhangian
Drumian
Stage 5
Series 2
Stage 4
Stage 3
Terreneuvian
Stage 2
Fortunian
PRECAMBRIAN
WBFS
CPL
ADF
DF
① HARLECH DOME East & Central
② West & North
③ ST. TUDWAL'S PENINSULA
④ Nantle
⑤ ARFON BASIN Bethesda
⑥ Bangor
⑦ MONIAN COMPOSITE TERRANE
Mawddach Group
Harlech Grits Group
Dol-cyn-afon Fm.
Dolgellau Fm.
Ffestiniog Fm.
Maentwrog Fm.
Clogau Fm.
Gamlan Fm.
Barmouth Fm.
Hafotty Fm.
Rhinog Fm.
Llanbedr Fm.
Dolwen Fm.
Bryn-teg Fm.
Nant-y-big Fm.
Ceiriad Fm.
Cilan Fm.
Trwyn-y-Fulfran
Hell's Mouth Fm.
Marchlyn Fm.
Cymfyrch Grit
DG
Llanberis Slate Fm.
Glog Grit
Cilgwyn Congl.
Tryfan Grits
Arfon Group
Padarn Tuff Fm.
Bronllwyn Grit Fm.
Fachwen Fm.
Bangor Fm.
Minffordd Fm.
Monian Supergroup
Gwna Group
New Harbour Group
South Stack Group
Rhoscolyn Fm.
Holyhead Fm.
South Stack Fm.
LEGEND
Dominantly Mudstone
Mixed Mudstone and Sandstone
Dominantly Sandstone
Volcanics
Detrital Zircon Sample (this study)
Detrital Zircon Sample (Waldron et al. 2009)
Detrital Zircon Sample (Collins and Buchan 2004)
Trilobites
Graptolites
Acritarchs
Sponge spicules
Foraminifera
Trace Fossils
Other Fossils
Age of boundary poorly constrained

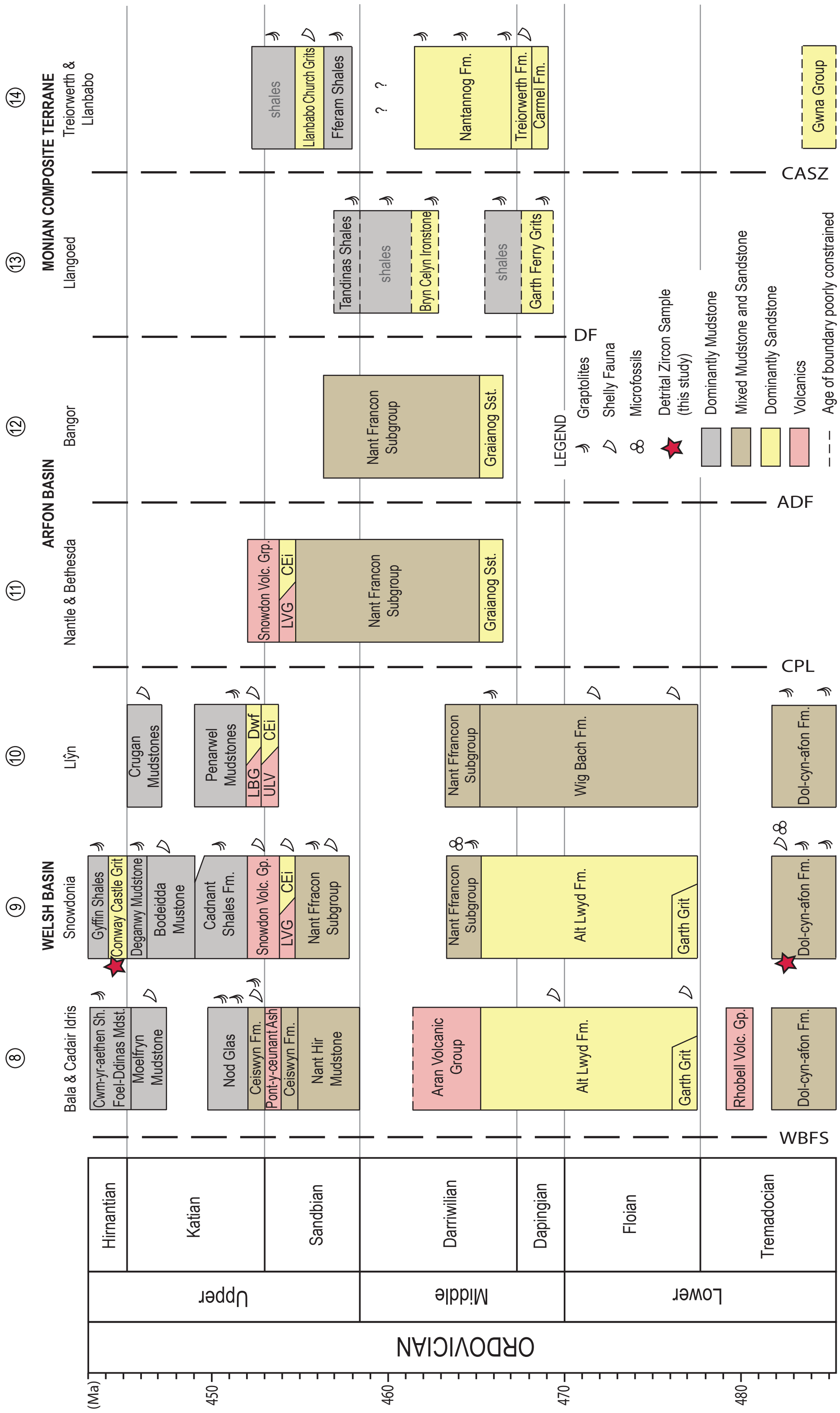
ORDOVICIAN
Upper
Middle
Lower
Hirnantian
Katian
Sandbian
Darriwilian
Dapingian
Floian
Tremadocian
(Ma)
450
460
470
480
WBFS
CPL
ADF
DF
CASZ
WELSH BASIN
ARFON BASIN
MONIAN COMPOSITE TERRANE
8
Bala & Cadair Idris
9
Snowdonia
10
Llŷn
11
Nantle & Bethesda
12
Bangor
13
Llangoed
14
Treiorwerth & Llanbabo
Cwm-yr-aethen Sh.
Foel-Ddinas Mdst.
Moelfryn Mudstone
Nod Glas
Ceiswyn Fm.
Pont-y-ceunant Ash
Ceiswyn Fm.
Nant Hir Mudstone
Aran Volcanic Group
Alt Lwyd Fm.
Garth Grit
Rhobell Volc. Gp.
Dol-cyn-afon Fm.
Gyffin Shales
Conway Castle Grit
Deganwy Mudstone
Bodeidda Mustone
Cadnant Shales Fm.
Snowdon Volc. Gp.
LVG
CEi
Nant Ffracon Subgroup
Nant Ffrancon Subgroup
Alt Lwyd Fm.
Garth Grit
Dol-cyn-afon Fm.
Crugan Mudstones
Penarwel Mudstones
LBG
ULV
Dwf
CEi
Nant Ffrancon Subgroup
Wig Bach Fm.
Dol-cyn-afon Fm.
Snowdon Volc. Grp.
LVG
CEi
Nant Francon Subgroup
Graianog Sst.
Nant Francon Subgroup
Graianog Sst.
Tandinas Shales
shales
Bryn Celyn Ironstone
shales
Garth Ferry Grits
shales
Llanbabo Church Grits
Fferam Shales
? ?
Nantannog Fm.
Treiorwerth Fm.
Carmel Fm.
Gwna Group
LEGEND
Graptolites
Shelly Fauna
Microfossils
Detrital Zircon Sample (this study)
Dominantly Mudstone
Mixed Mudstone and Sandstone
Dominantly Sandstone
Volcanics
Age of boundary poorly constrained

Figure 1.5: (previous page) Stratigraphic columns showing Ordovician units of the northern Welsh Basin, Arfon Basin, and Monian Composite Terrane. Data from Rushton and Fortey (2000). Abbreviations for stratigraphical units are from (Rushton and Howells 1999): CEi-Cwm Eigiau Formation; Dwf-Dwyfach Formation; LlV-Llewelyn Volcanic Group; LVG-Llanbedrog Volcanic Group; and the ULG-Upper Lodge Volcanic Formation. Other abbreviations include ABF-Aber-Dinlle Fault; DF-Dinorwic Fault; CASZ-Central Anglesey Shear Zone; CPL-Cwm Pennant Lineament; WBFS-Welsh Borderland Fault System. Using time scale of Cooper and Sadler (2012).

al. 2008). The Tucker and Pharaoh (1991) age is consistent with a contemporary relationship between the Padarn Tuff and the Twt Hill Granite; however, the Compston et al. (2002) age is significantly younger. The granite's relationship with the Arfon sedimentary rocks is not known.

Unconformably overlying the Padarn Tuff (Fig. 1.4) are coarse to fine clastic rocks with intercalated pyroclastic and mixed pyroclastic and clastic rocks (Reedman et al. 1984). The only age control for the upper part of the Arfon Group includes a U-Pb date of 573 ± 1 Ma from tuff near the top of the Fachwan Formation (Compston et al. 2002) and the presence of sponge spicules within the Minfford formation (Fig. 1.4), which suggest a Cambrian age (Rushton and Molyneux 2011).

Units above the Arfon Group

Overlying the Arfon Group is the Llanberis Slates Formation (Fig. 1.4). It consists of mudstone, siltstone, and turbiditic sandstone (Crimes 1970). There are several informally recognized sandstone units within the Llanberis Slates, including the Dorothea Grit from which a detrital zircon sample was analyzed for this study (see Chapter 2). The early Cambrian trilobite *Pseudotops viola* was found stratigraphically above the Dorothea Grit indicating an early Cambrian (Epoch 2) age, younger than 521 Ma in the timescale of Peng et al. (2012). Above the Llanberis Slates, are sandstone with thin pelite beds overlain by silty mudstone and laminated sandstone (Brenchley et al. 2006). The Marchlyn Formation (Fig. 1.4) has been interpreted as upper Cambrian (Furongian) based on the presence of the trace fossil *Cruziana semiplicata* (Crimes 1970).

Affinities of the Arfon Basin

The origin of Arfon Basin succession is not known and it has not been definitively linked with either the Monian Composite terrane or the Welsh Basin. Greenly

(1919, 1944, 1946) assigned several undated sedimentary and volcaniclastic rock outliers in southern Anglesey to be correlatives to the Afron Group. However, they rest unconformably upon the Penmynedd blueschists which record metamorphism at c. 550 Ma (Dallmeyer and Gibbons 1987). Given the 573 ± 1 Ma age of the Fachwen Formation, this correlation seems unlikely. Tucker and Pharaoh (1991) suggested a link between the Coedana Granite and the Padarn Tuff both of which have been dated at approximately 614 Ma. Reedman et al. (1984) suggested a link between Greenly's outliers in Anglesey to the Minfordd Formation (Fig. 1.4) based on the presence of sponge spicules implying the Arfon Group spanned both sides of the Dinorwic Fault. The Arfon Basin shares the same Ordovician sedimentary cover succession as the Harlech Dome showing that it was definitely in contact with the remainder of the Welsh Basin by Floian time.

1.3.4 Welsh Basin

The Welsh Basin preserves a thick sedimentary succession largely composed of interleaved units of mudstone and coarse clastic turbidite deposits, with volcanic intervals in the Ordovician. Woodcock (1990) divided the succession into three megasequences, the Dyfed, Gwynedd and Powys Supergroups, each separated by basin-wide unconformities.

Little is known about the nature of the Welsh Basin's basement because of limited exposure of Neoproterozoic rocks. In the Harlech Dome region, the Bryn-teg Borehole (Fig. 1.3) penetrated into the Bryn-teg Volcanic Formation, which consists mainly of andesites and tuffite (Allen and Jackson 1978). It is thought to be Neoproterozoic, but there is no direct evidence for its age except that it is overlain by early Cambrian rocks.

Dyfed Supergroup

The Dyfed Supergroup spans the early Cambrian to Tremadocian. In North Wales it is only exposed in the Harlech Dome and St. Tudwal's Peninsula regions (Fig. 1.3). It can be divided into the lower Harlech Grits Group and upper Mawddach Group (Fig. 1.4).

At the base of the Harlech Grits Group is the Dolwen Formation. It is characterized by greenish grey sandstone with interbedded pebbly sandstone and siltstone (Allan and Jackson 1985). The Dolwen Formation yielded an early Cambrian foraminiferan *Platysolenites antiquissimus* (Allen and Jackson 1978). Overlying this is the Llanbedr Formation, which consists of grey and purple siltstone and mudstone with minor interbedded fine-grained sandstone (Allen and Jackson 1985). The Llanbedr Formation is overlain by the Rhinog Formation, which is characterized by coarse-grained pebbly sandstone. This unit was sampled for detrital zircon work by Waldron et al. (2011). This is followed by the Hafotty Formation, which is predominantly grey siltstone with some interbedded sandstone and is enriched with manganese (Allen and Jackson 1985). The Barmouth Formation is similar to the Rhinog Formation and consists of coarse-grained sandstone and siltstone (Allen and Jackson 1985). The highest unit in the Harlech Grits Groups is the Gamlan Formation. It is characterized by interbedded grey and purple siltstone and mudstone and also has manganese enrichment (Allan and Jackson 1985). Mid-Cambrian (Drumian Stage) trilobites have been identified in the uppermost beds of the Gamlan Formation (Allen et al. 1981). This unit was sampled as a part of this study (Chapter 2). The Harlech Grits Group in the St. Tudwal's Peninsula region includes the Hell's Mouth, Trwyn y Fulfran, and Cilan formations (Fig. 1.4), which have broad similarities to the Rhinog, Hafotty, and Barmouth Formations of the Harlech Dome succession (Young et al. 2009).

The Clogau Formation is the lowest unit in the Mawddach Group and is characterized by black siltly mudstone (Allan et al. 1981). The unit contains Cambrian (Stage 5) trilobites *Tomagnostus fissus, Paradoxides hicksii*, and *Eodiscus punctatus* s.l. (Allen et al. 1981). The overlying Maentwrog Formation consists of grey silty mudstone with thinly interbedded coarse siltstone and fine-grained sandstone. It contains Cambrian, Paibian Stage *Olenus Zone* fauna (Allen et al. 1981). These pass up into interbedded pale grey sandstone and grey silty mudstone of the Ffestiniog Flags Formation (Allen et al. 1981). The presence of Trilobites *Homagnotus obesus* in the lowest beds, *Parabolinoides bucephalus* in the highest beds, and the Brachiopod *Lingulella davisi* (Allen et al. 1981) indicate a Cambrian, Paibian to Stage 9 age according to the timescale of Peng et al. (2012). Above the Festiniog Flags formations is the Dollegau Formation, which comprises black siltstone and mudstone and contains Cambrian Furongian fauna (Allen at el. 1981). This is supported by a volcaniclastic sandstone from this unit that has been dated at 491 ± 1 Ma (Davidek et al. 1998) and 489 ± 0.6 Ma (Landing et al. 2000). The Dol-cyn-afon Formation is the highest preserved unit

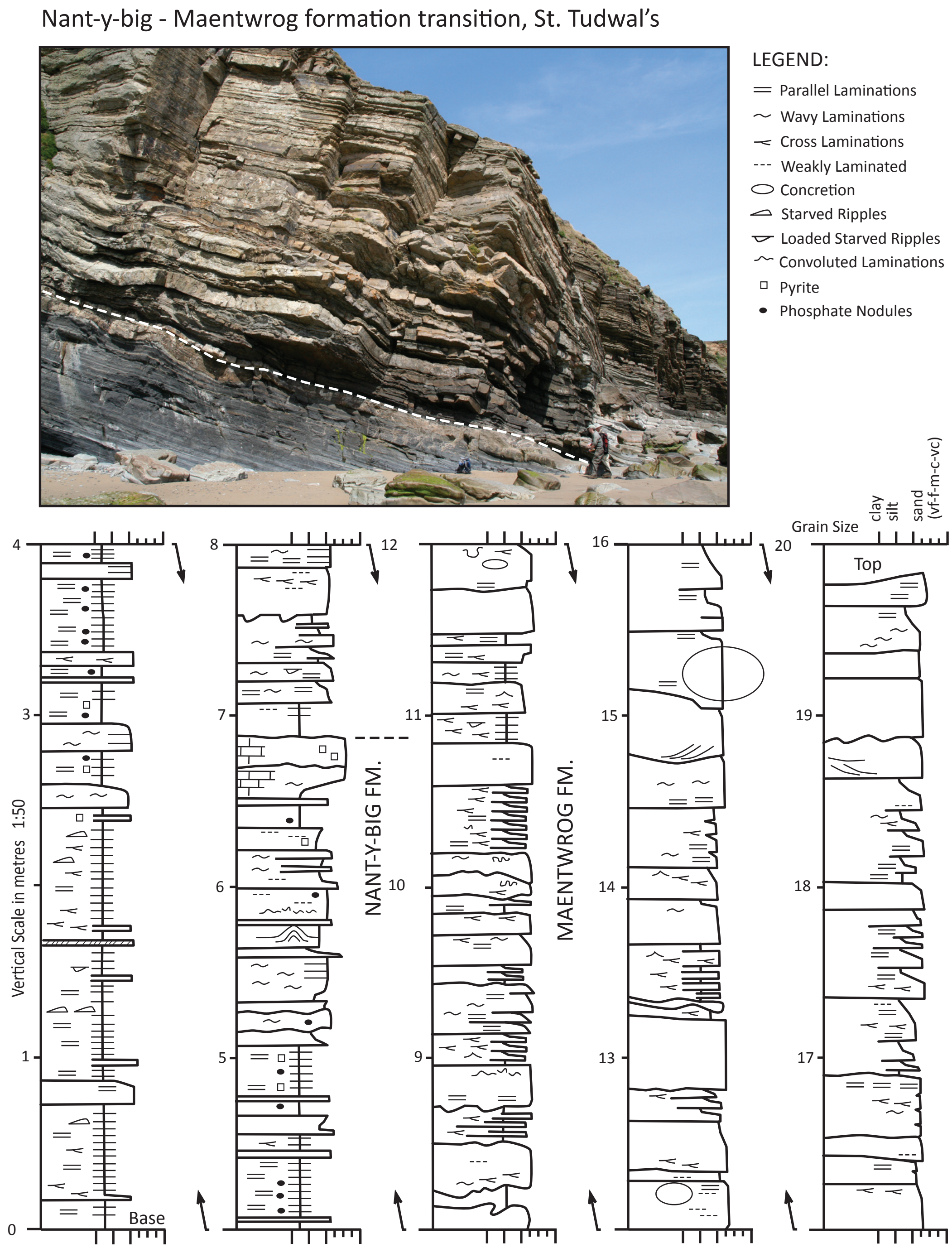

Figure 1.6: Detailed section across the middle-upper Cambrian boundary at Porth Ceriad, St. Tudwal's Peninsula in Wales. The image shows the lower dark mudstones if the Nant-y-big Formation overlain by sandstone beds of the Maentwrog Formation. The dashed line marks the boundary. The top of the Nant-y-big Formation is marked by a calcareous horizon.

in the Mawddach Group. It consists of grey siltstone and mudstone and contains the Tremadocian graptolite *Rhabdinopora flabelliformis* (Allen and Jackson 1985). This unit was sampled as a part of this study (Chapter 2).

The succession on the St. Tudwal's Peninsula records a similar Cambrian record; however it is much thinner with only ~900 m preserved (Brenchley et al. 2006) and it shows a shallowing event near the base of the Furongian marked by a disconformity (Young et al. 2002). Figure 1.6 shows the transition from dominantly laminated mudstones of the Nant-y-big Formation into the medium to thickly interbedded sandstone and mudstone of the Maentwrog Formation at St. Tudwal's Peninsula.

Gwynedd Supergroup

The overlying Gwynedd Supergroup includes the majority of the Ordovician record in North Wales (Fig. 1.5). Its base is marked by a sub-Floian unconformity where the succession was deposited over gently folded and tilted Precambrian to Tremadocian rocks. The oldest unit in the Gwynedd Supergroup is the Rhobell Volcanics Group (Fig. 1.5). It is found only to the east of the Harlech Dome. The group comprises Tremadocian basaltic lava, sandstone, conglomerate and minor sedimentary breccia (Brenchley et al. 2006). The rest of the Gwynedd Supergroup comprises mainly marine mudstone, siltstone, and sandstone interfingering with volcanic deposits that range from the Floian until the mid-Katian (Rushton and Howells 1998). The volcanics consist mainly of felsic tuffs with mixed basaltic and rhyolitic lavas and are intercalated with minor sedimentary rocks (Rushton and Howells 1998). The top of the Gwynedd Supergroup is marked by a unit of black mudstone and minor limestone (Fig. 1.5) deposited over most of the northern Welsh Basin (Rushton and Fortey 2000).

Powys Supergroup

The Powys Supergroup ranges from the late Katian to the Early Devonian. Its base is marked by a diachronous unconformity. The basal units in North Wales are characterized mainly by marine mudstone and argillaceous mudstone (Brenchley et al. 2006) that contain late Katian fauna (Brenchley and Cullen 1984). During the Hirnantian, a glacio-eustatic fall in sea-level brought coarse sediment into deep basins including the Conway Castle Grit (Rushton and Fortey 2000) sampled in this study (Chapter 2). The overlying succession is dominated by mudstones and deep-water turbidites (Cherns et al. 2006). The top of the Powys Supergroup is defined by the major unconformity attributed to the Devonian Acadian orogeny.

1.4 MEGUMA TERRANE

1.4.1 Geologic Setting

The Meguma terrane is located in southern Nova Scotia to the south of the Cobequid-Chedabucto fault zone, which separates it from the Avalon terrane to the north (Fig. 1.7). It contains the thick (~13 km) Cambrian to Early Ordovician Meguma Supergroup, and overlying Silurian to Devonian sedimentary and volcanic rocks of the Rockville Notch Group (White et al. 2012) (Fig. 1.8). The docking of the Meguma terrane to Laurentia in the Early Devonian to Early Carboniferous Neoacadian orogeny (White et al. 2007; van Staal et al. 2009) caused deformation and folded the succession into NE-SW-trending, upright, subhorizonal folds with axial planar cleavage (Reynolds and Muecke 1978; Henderson et al. 1986). Regional metamorphism ranges from greenschist facies to amphibolite facies in southwest Nova Scotia (Reynolds et al. 1981; Keppie and Muecke 1979). During the late Devonian a series of granitoids were emplaced, including the South Mountain Batholith (Clarke and Halliday 1980), which metamorphosed the metasedimentary rocks to hornblende-hornfels facies (Jamieson et al. 2012). Southwestern Nova Scotia records a second greenschist facies deformation event at c. 320 Ma (Culshaw and Reynolds 1997).

There is no exposure of basement rock anywhere in the Meguma terrane. Basement xenoliths (Eberz et al. 1991) and Meguma granitoids (Clarke et al. 1988) produced Sm/Nd ratios that indicate deeper crustal material with a younger residence age than the overlying Meguma Supergroup. U-Pb zircon and monazite dates from basement xenoliths show a population of grains between 575-630 Ma (Greenough et al. 1999) typical of Pan-African orogenic belts and Avalonia (Krogh et al. 1988; Kerr et al. 1995; O'Brien et al. 1996; Murphy et al. 1997). The upper intercept of a discordant zircon fraction is interpreted by Greenough et al. (1999) to represent a Mesoproterozoic population, which is absent in lower Meguma Supergroup sedimentary rocks (Krogh and Keppie 1990; Waldron et al. 2009). Given this, some have proposed that the Meguma Supergroup was

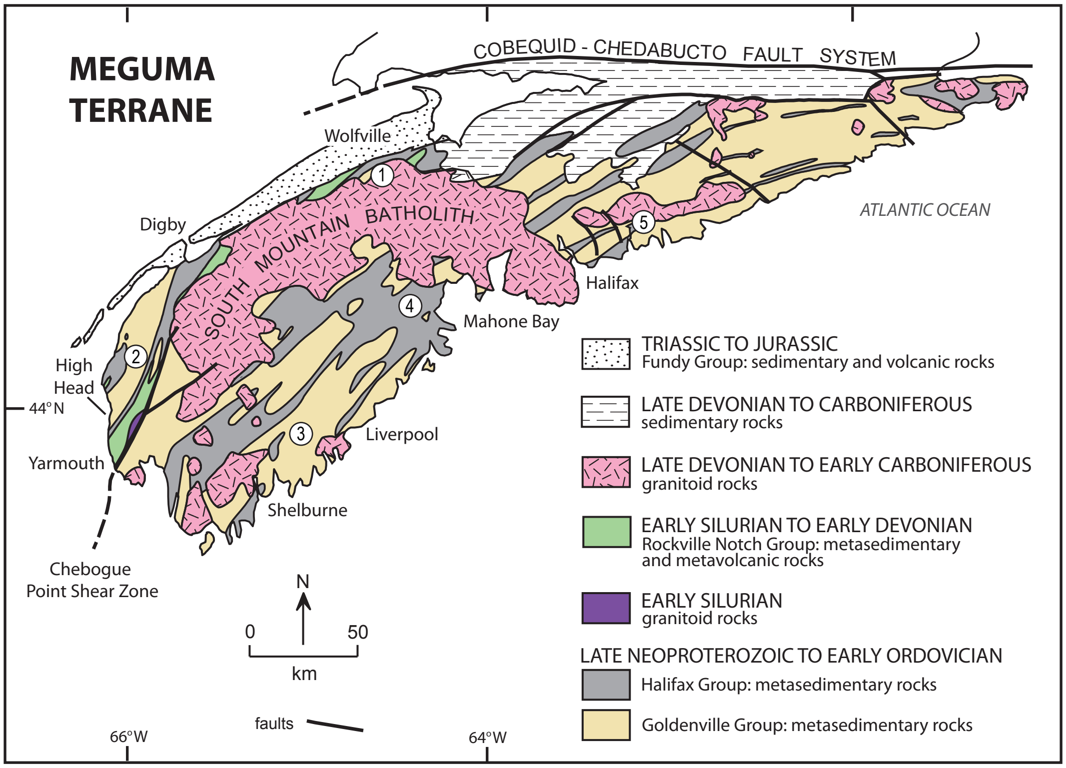

Figure 1.7: Geological map of the Meguma Terrane, Nova Scotia (after White 2010a).

deposited upon Avalonian crust and that West Avalonia and the Meguma terrane were once parts of the same microcontinent (e.g., Keppie 1997; Keppie and Krough 2000; Landing 2004; Murphy et al. 2004; Linnemann et al. 2012). Others believe that the Cobequid-Chedabucto Shear Zone (Fig. 1.7), that separates the two terranes, represents a structural contact where the Meguma terrane was thrust over crust with Avalonia characteristics (e.g., Keppie and Dallmeyer 1987; Waldron et al. 1989; Eberz et al. 1991; Clarke et al. 1997; Greenough et al. 1999).

Schenk (1983, 1997) suggested the Meguma Supergroup was deposited on a continental embankment of the passive margin of Gondwana, but preliminary whole-rock geochemistry has been interpreted to suggest deposition in an active continental margin and/or an island arc setting, not a passive margin (White et al. 2006). Waldron et al. (2009) proposed that the succession was deposited in a rift or extensional environment that subsequently became inactive. This scenario explains the upward transition from a relatively juvenile Avalonian/Pan-African source to an older more diverse source region. It also accounts for the rapid accumulation of the thick succession and the differences in the stratigraphic succession (Waldron et al. 2009). The Chebogue Point Shear Zone (CPSZ) located in southwest Nova Scotia (Fig. 1.7) strikes N-S to NE-SW (White 2010b). It cannot be traced farther east beyond its intersection with the South Mountain Batholith. The CPSZ has been described as a tectono-stratigraphic boundary, dividing the Meguma Supergroup into different, though correlative units at the formation level, to the northwest and southeast of the shear zone (White 2010b).

1.4.2 Goldenville Group

The Goldenville Group (Fig. 1.8) is the lowest unit in the Meguma Supergroup. The lower units are dominated by thick to medium-bedded metamorphosed sand-rich turbidites with local metasiltstone and slate (Harris and Schenk 1975; Waldron and Jensen 1985). The High Head member of the Church Point formation (Fig. 1.8) contains trace fossils, including *Oldhamia,* that are characteristic of the early Cambrian (Gingras et al. 2011). These are consistent with detrital zircon collected from Church Point formation (Fig. 1.8) that produced youngest ages of 544 ± 18, 537 ± 15, and 529 ± 19 Ma, providing a maximum depositional age close to the Ediacaran-Terreneuvian boundary (Waldron et al. 2009).

In southwest Nova Scotia the massive metasandstones pass up into thin to medium-bedded metasandstone and slate of the Government Point formation including the Tancook Island member (Fig. 1.8). These units are less sand-rich then the underlying New Harbor and Green Harbour formations (O'Brien 1985; Waldron 1987; Waldron 1992). The Government Point formation yielded a middle Cambrian Acado-Baltic Trilobite faunule (Pratt and Waldron 1991).

The uppermost units of the Goldenville Group (Fig. 1.8) are dominated by metasiltstone and slate, with minor fine-grained metasandstone beds (White 2010b). To the southeast of the Chebogue Point Shear Zone these units are characterized by manganese enrichment (White 2010b) and a diverse assemblage of trace fossils including locally abundant *Teichichnus.* Cambrian Series 3 to Furongian acritarchs have been identified in the Tupper Lake Brook formation (White et al. 2012). These units were formerly part of the Halifax formation (O'Brien 1986, 1988; Waldron 1992; Schenk 1995), but were later added to the Goldenville Group by White (2010b).

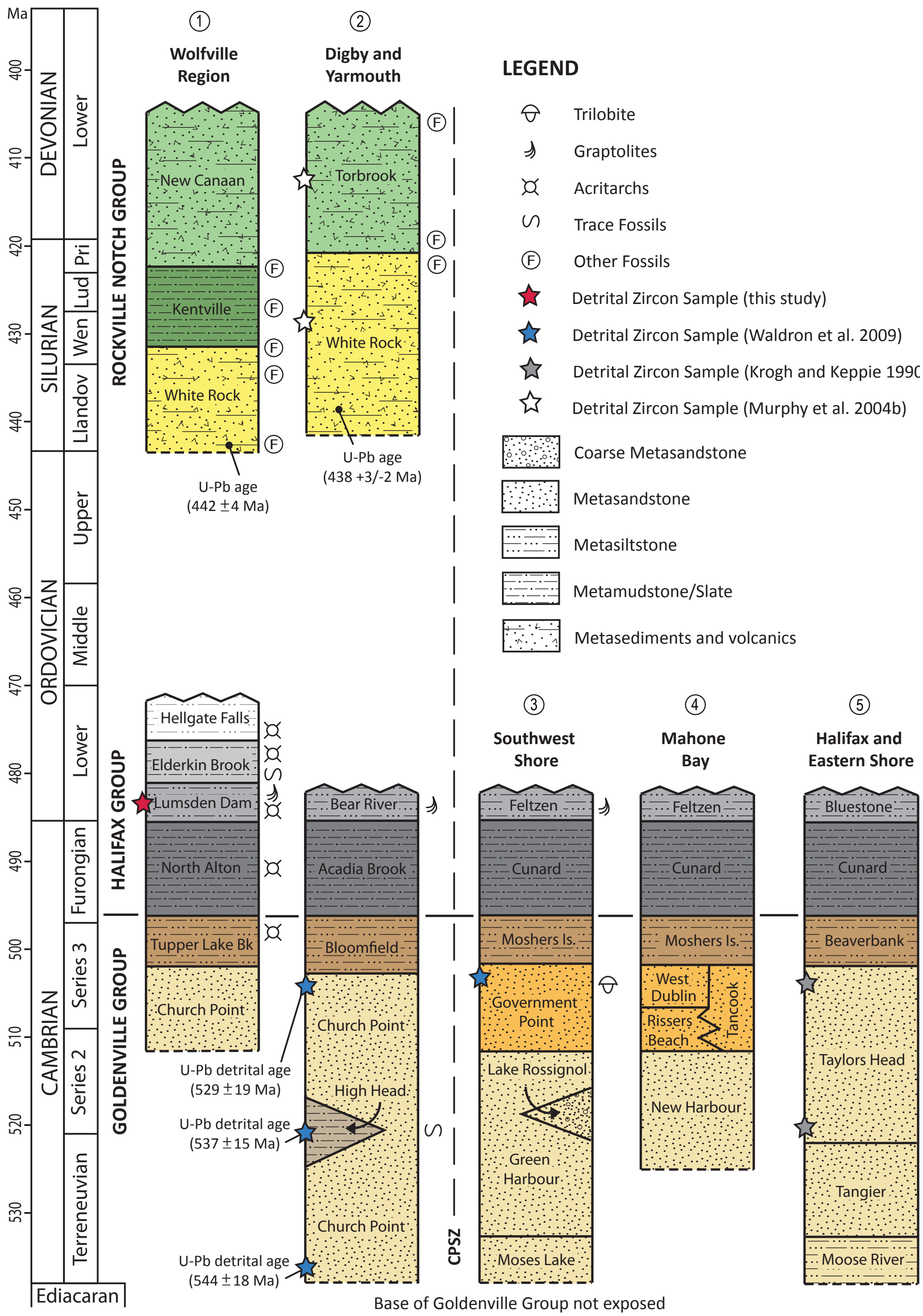

Figure 1.8: Stratigraphy of the Meguma terrane in different regions in Nova Scotia (after O'Brien 1988; Horne and Pelly 2007; White 2010b; White et al. 2012) showing the locations sampled in detrital zircon studies. Paleontological and U-Pb age data are from sources described in the text. Using time scale of Peng et al. (2012). CPSZ - Chebogue Point Shear Zone.

1.4.3 Halifax Group

The Halifax Group conformably overlies the Goldenville Group. At the base is the Cunard Formation and its lateral equivalents, Acadia Brook, and North Alton formations (Fig. 1.8). These units rest conformably over the Goldenville Group, and are characterized by organic rich black slate and siltstone, and often contain a significant amount of sulphide minerals. Acritarch assemblages found in the North Alton formation indicate a Furongian depositional age (White et al. 2012).

The overlying Lumsden Dam formation and laterally equivalent Bluestone, Bear River, and Feltzen formations (Fig. 1.8) are characterized by medium to dark grey slate interlayered with cross-laminated metasiltstone and metasandstone. The graptolite *Rhabdinopora flabelliformis* has been identified in the Lumsden Dam, Feltzen, and Bear River formations indicating a Tremadocian depositional age. Acritarch assemblages from the Lumsden Dam and Bear River formations are also consistent with an early Tremadocian age (White et al. 2012). Because this unit contains coarser-grained intervals it was chosen for sampling in this study. No detrital zircon samples have previously been analyzed within the Halifax Group.

In the Wolfville region, higher parts of the Halifax Group are persevered. The Elderkin Brook formation consists of light grey to red-brown diffusely laminated slate with minor siltstone. It locally contains abundant trace fossils (White et al. 2012). It contains a late Tremadocian acritarch assemblage. The Hellgate Falls formation is the highest unit in the Halifax Group (Fig. 1.8). It is characterized by light to dark grey slate interbedded with siltstone and sandstone. It is highly bioturbated and contains a late Tremadocian to Floian acritarch assemblage (White et al. 2012).

1.4.4 Rockville Notch Group

The Silurian to Lower Devonian Rockville Notch Group (formerly the Annapolis Supergroup of Schenk 1995) is preserved on the northwest side of the CPSZ and South Mountain Batholith (Fig. 1.7). The basal White Rock Formation rests unconformably over the Halifax Group (Fig. 1.8). This unit contains a diverse collection of rock types including metasedimentary rocks and both silicic and mafic volcanic rocks (Crosby 1951; Smitheringale 1960; Taylor 1965; MacDonald et al. 2002). Felsic tuff at and near the base of the White Rock Formation produced U-Pb ages of 442 ± 4 Ma (Keppie and Krogh 2000) and 438 ± 3 Ma (MacDonald et al. 2002) placing the base of the unit close to the Ordovician - Silurian boundary (~443 Ma). Vertebrate and crinoid remains that are limited to the Ludlow and Pridoli have been identified in the upper part of this unit in the Digby area (Bouyx et al. 1997). In the Wolfville region the White Rock Formation is overlain by interbedded slate and siltstone (Ami 1900; Smitheringale 1960; Taylor 1965) of the Kentville Formation (Fig. 1.8). This unit contains late Silurian (Ludlovian) marine fossils (Smitheringale 1960, 1973; Taylor 1965) making it equivalent to the top of the White Rock Formation to the southwest. The youngest units in the Rockville Notch Group consist of marine sedimentary and volcanic rocks (Smitheringale 1960, 1973; Taylor 1965) of the New Canaan and Torbrook Formations (Fig. 1.8). These units contain Pridoli to late Early Devonian fauna (Smitheringale 1960; Bouyx et al. 1997). Chemical analysis of the volcanic rocks in the White Rock Formation are alkalic and have been interpreted by MacDonald et al. (2002) to indicate a within-plate extensional tectonic setting.

1.4.5 Intrusive Rocks

The intrusive rocks of the Meguma terrane can be grouped into older mafic sills and younger granitoids.

In the northwestern part of the Meguma terrane two suites of sills are present (Barr et al. 1983). Type I sills are found in the Goldenville and Halifax groups. They are light grey, fine-grained and rarely exceed a thickness of 3 m (White and Barr 2004). Peperitic textures and soft-sediment deformation that have been interpreted as indicating they were emplaced penecontemporaneously with sediment deposition (Barr et al. 1983; White et al. 1999; White and Barr 2004). They have been folded with the Meguma Group rocks. These relationships, along with their absence in the overlying Rockville Notch Group, indicate emplacement between the late Neoproterozoic and Early Ordovician (White and Barr 2004). Type II sills are less abundant and occur in both the Meguma Supergroup and the overlying Rockville Notch Group. They are dark grey to black, coarse grained, and are rarely less than 5 m thick. These sills do not exhibit any structures that suggest penecontemporaneous emplacement and no folded Type II sills have been observed. However, they are deformed and cleaved and are not present in the South Mountain Batholith, suggesting that they were emplaced prior to regional deformation, constraining their age from the Early to Middle Devonian

(White and Barr 2004). Both sill types are theolitic to alkalic, the older suite being slightly more alkalic, indicating emplacement in a continental, within-plate extensional environment (Barr et al. 1983; White and Barr 2004).

Granitoid plutons intruding the Meguma Supergroup and Rockville Notch Group metasedimentary rocks are a prominent feature of the Meguma terrane and underlie approximately a third of southern Nova Scotia. Clarke et al. (1997) has identified two types of granitoids plutons that occur in the Meguma terrane. The central granitic plutons, including the South Mountain batholith, emplaced at c. 372 Ma, were likely entirely crustally derived from the underlying Meguma Supergroup rocks (Clarke et al. 1997). This complex has been interpreted to be the result of crustal thickening related to the convergence of the Meguma terrane with West Avalonia (Clarke et al. 1997). The slightly older (≥376 Ma) peripheral plutons have been interpreted by Clarke et al. (1997) to originate from the intrusion of subduction-related magmas prior to the final emplacement of the Meguma terrane.

1.4.6 Post-Devonian Stratigraphy

Unconformably overlying the Meguma terrane and Avalonia are the Late Devonian to Carboniferous succession of the Maritimes Basin consisting of non-marine clastics of the Horton Group, evaporates, carbonates, and minor clastic sedimentary rocks of the Windsor Group (Gibling et al. 2008), and non-marine fluvial deposits of the Mabou, Cumberland and Pictou groups. The mid-Triassic to Early Jurassic Fundy Group unconformably overlies the Maritimes Basin and comprises predominantly red continental clastics and tholeiitic basalt related to the opening of the Atlantic Ocean (Hubert and Mertz 1984; Withjack et al. 1995).

1.4.7 Comparison with North Wales

Similarities between the Cambrian sedimentary successions of the Meguma terrane and the North Wales succession in the Harlech Dome and St. Tudwal’s Peninsula have been recognized by Waldron et al. (2011). Both areas record thick early Cambrian continentally-derived sandstone turbidites, overlain by early to middle Cambrian alternating mud-rich and sand-rich units in which manganese is concentrated. The manganiferous interval is characterized in all regions by a diverse assemblage of trace fossils, including locally abundant *Teichichnus*. Above, the succession consists of anoxic, organic-rich turbidites, shallowing upwards into paler, early Ordovician mudstone and siltstone, which contain the graptolite *Rhabdinopora*.

In addition to the stratigraphic similarities the two basins also have a similar provenance. Detrital zircon analysis from the mid-Cambrian Rhinog Formation in the Harlech Dome (Fig. 1.4) sampled by Waldron et al. (2011) displays a similar range of ages as detrital zircon samples collected from the Goldenville group. Both basins show distributions that are dominated by early Cambrian to Late Neoproterozoic populations, a secondary 2.0 to 2.1 Ga population and a minor Archean contribution (Krogh and Keppie 1990; Waldron et al. 2009; Waldron et al. 2011).

In the Ordovician the basin histories diverge. The highest parts of the Nova Scotia succession record shallowing conditions and shelf sedimentation extending into the Early Ordovician. However, the Welsh basin successions are unconformably overlain by Tremadocian volcanics, and then by Floian sandstones and younger Ordovician volcanics.

1.5 METHODS

1.5.1 Sample Collection

Eleven samples were collected in the field as a part of this study, five of which have results reported here. Of these five, one sample was collected from the Tremadocian Lumsden Dam Formation of the Meguma terrane, and four samples were collected from North Wales that span the Cambrian (Series 3) to the latest Ordovician. Sample localities were selected based on rock type, stratigraphic position, and proximity to known fossil occurrences to help best constrain the timing of sediment deposition. Approximately 8 kg of material was collected from the coarsest part of the sampled beds.

The sample from the Lumsden Dam Formation (NB027A) was chosen for detrital zircon sampling because it would provide information for the provenance of the Halifax Group. Previous detrital zircon studies in the Meguma terrane have been on the Goldenville and Rockville Notch groups. The sample was collected roughly 20 m below the horizon bearing the graptolite *Rhabdinopora flabelliformis*.

The Dol-cyn-afon Formation (sample NA041A) in the Welsh succession is a contemporaneous unit to the Lumsden Dam Formation. It was chosen for sampling because it provided an opportunity for further comparison between the Welsh and Meguma succession. It is the youngest unit in the Mawddach Group below the sub-Floian unconformity. The sample location was chosen based on its proximity to a known fossil site of the graptolite *Rhabdinopora flabelliformis* and a volcaniclastic sandstone bed dated at 491 ± 1 Ma (Davidek et al. 1998).

The Conway Castle Grit (NA031A) was sampled to represent the latest Ordovician record. It represents one of the first coarse sediment units above a late Ordovician unconformity and although it only includes allochthonous Hirnantian fauna, the underlying Deganwy Mudstone contains late Katian fauna (Brenchley and Cullen 1984). Hirnantian graptolites in the overlying Gyffin Shales (Fig. 1.5) implying a probable Hirnantian age for the Conway Castle Grit (Rushton and Fortey 2000).

Samples from the Gamlan Formation (ML001A) and the Dorothea Grit (ML010A) were collected by Waldron and Schofield in August 2008. The mid-Cambrian Gamlan Formation was collected for further comparison between the Meguma Supergroup and the Harlech Dome succession. The Dorothea Grit sample was taken to provide insight into the origin of the Arfon Basin. Age Constraints on the Arfon Basin are poor. The sample was collected from the highest coarse-grained unit within the Llanberis slates, which is known to contain the trilobite *Pseudatops viola* near the top of the unit above the Dorothea Grit (Howell and Stubblefield 1950).

Five additional units were sampled from the Welsh Basin but were not analyzed. The Garth Grit (sample NA030A) was deposited in the Floian and lies stratigraphically between the Dol-cyn-afon Formation and the Conway Castle Grit. Samples from the Conway Castle Grit (NA031A) and Dol-cyn-afon Formation (NA041A) produced similar results. The Garth Grit lies stratigraphically between the two so it was not analyzed since it was likely to produce the same results as the overlying and underlying units. A sample from the Cwmcringly Formation (NA023A) is of similar age to the Conway Castle Grit; however, it was collected from further south in Wales and was finer-grained, so priority was given to the Conway Castle Grit, which was likely to yield more zircons. Samples from the Nant Ffrancon Subgroup (NA032A), Maentwrog Formation (NA035A) and Ffestiniog Flags Formation (NA037A) were also collected, but due to their fine-grained nature none yielded sufficient detrital zircons. One additional Meguma Supergroup sample was collected from the Cunard formation (NB011A) to use for comparison with the Maentwrog Formation in the Harlech Dome; however, since the Maentwrog Formation was not analyzed, it was no longer a priority to be completed.

1.5.2 Sample Preparation

Samples ML001A and ML010A were separated by Heather Clough and sample NB027A was separated by Hayley Pothier both at the University of Alberta. Samples NA031A and NA041A were separated at Dalhousie University by Matthew Kliffer. Both procedures involved using a rock saw to cut the sample into small pieces followed by reduction to sand-sized particles using a jaw crusher and disk mill. A Wilfley table was then used to separate dense material, and the dense fraction was then sieved to remove material greater than 210 μm. The sample was further reduced using a Frantz magnetic separator to remove magnetic material. Heavy liquids separation was then used to remove material with a density less than ~3.1 g/cm^3. The specific gravity of zircon is 4.68 (Nesse 2000). At the University of Alberta methylene iodide (3.30 - 3.33 g/cm^3) was used. At Dalhousie University sodium polytungstate (3.1 g/cm^3) and methylene iodide were used.

There are generally two protocols for the selection of zircon grains for analysis. Gehrels and Dickinson (1995) and Samson et al. (2005) use a method where grains are picked selectively to represent the greatest variety of colour and morphology in an attempt to identify as many age populations as possible. This method has an advantage in that it may pick up populations missed in random sampling (Gehrels 2000); however, it may distort the relative abundance of ages. To help eliminate the sampling bias inherited in the hand picking process, others (e.g., McLennan et al. 2001) use a protocol that involves using a random selection of grains. In this study, the zircon grains for sample ML001A (Gamlan Fm.) were picked and mounted by hand by Heather Clough. For all other samples a random sample of the separated grain fraction was used. Pyrite and other opaques minerals were removed by hand picking.

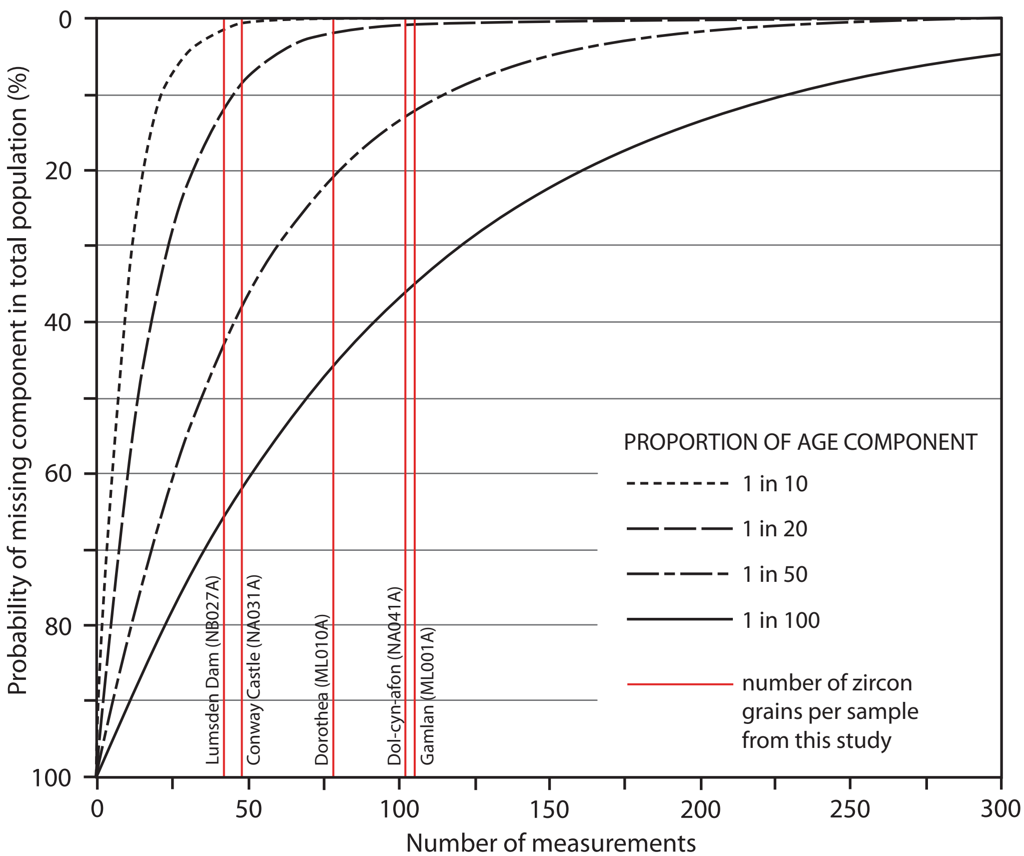

Figure 1.9: Graph illustrating the probability of missing an age component in the total population based on the number of grains analyzed (from Dodson et al. 1988; Fedo et al. 2003). The number of grains that produced concordant ages for each population sampled in this study is shown.

The grains were mounted in a synthetic resin mount. To avoid analyzing non-zircon grains that may have ended up on the mount, zirconium elemental maps of the mount surface were made using an electron microprobe or a scanning electron microscope. Electron backscatter images were aslso collected for all samples except ML001A. These images provide details of the internal structure of the zircon grains including inclusions and zoning.

1.5.3 Instrumentation and Data Acquisition

LA-MC-ICP-MS

U-Pb dating was conducted using laser ablation multi-collector inductively coupled plasma mass spectrometry (LA–MC-ICP-MS). The advantages of this method for detrital zircon studies over Thermal Ionization Mass Spectrometry

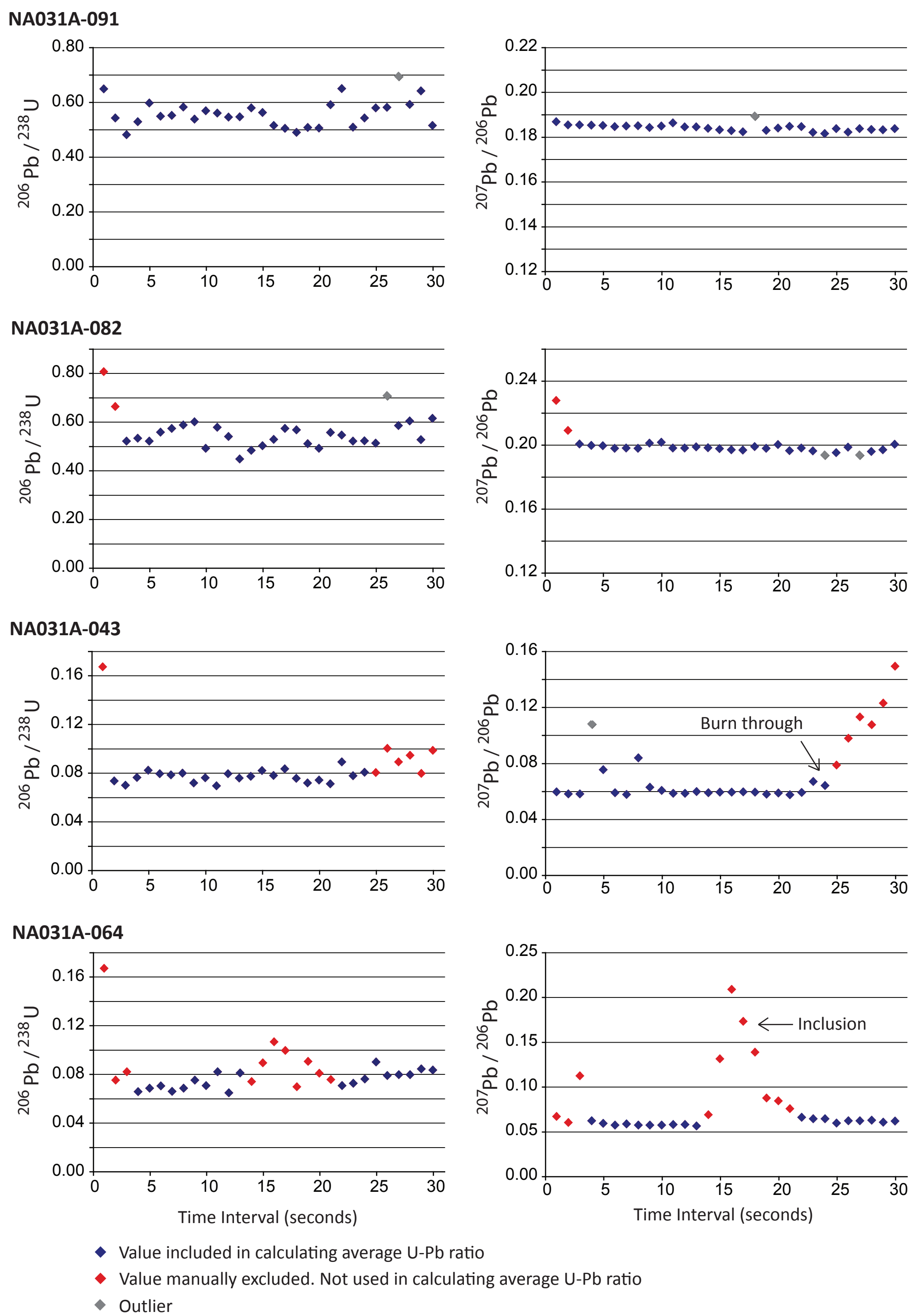

Figure 1.10: Examples of time-resolved signals from the sample NA031A Conway Castle Grit showing a) stable flat signal, b) signal with initial peak, c) signal showing entry into another zone, and d) signal showing possible inclusion.

(TIMS) and Sensitive High Resolution Mass Spectrometer (SHRIMP) are short analytical time and low cost while providing moderate spatial resolution, accuracy, and precision (Chang et al. 2006).

The instrument used in data acquisition was a Nu Plasma MC-ICP-MS (Nu Instruments, UK) coupled to a UP-213 Nd:YAG deep UV (213 nm) laser ablation system (New Wave Research, USA), at the University of Alberta, Radiogenic Isotope Facility. A beam diameter of 30 μm was used, except when the ^{206}Pb counts per second were elevated beyond the detector limit; then the beam diameter was reduced to 20 μm. Each grain was ablated for approximately 70 seconds during which 30 one-second integrations of data were collected. Two in-house standards were used. LH94-15 (1830 ± 1 Ma) is a homogeneous calc-alkaline enderbite (Ashton et al. 1999) and GJ1-32 (609 Ma) is of uncertain origin (Simonetti et al. 2008). Two analyses of LH94-15 and either one or two analyses of GJ1-32 were collected before and after runs of 10 analyses of unknowns.

It is important to obtain a high number of measurements in order to reduce the probability of missing an age component in the total population (Dodson et al. 1988). Figure 1.9 illustrates this relationship. In this study between 120 and 200 grains were analyzed for each sample.

Data Reduction

Initial data calculations were performed using a spreadsheet written by S.A. DuFrane (University of Alberta). Time-resolved signals were checked for indications of core-rim features, zoning, or inclusions. When required, a portion of the time-resolved signal was rejected in an attempt to achieve a stable flat signal (Fig. 1.10). Unusual counts at the initial part of the signal were discarded because they displayed elevated $^{206}Pb/^{238}U$ and $^{207}Pb/^{206}Pb$ and ratios likely resulting from lead contamination on the mount surface. All data are 2 standard deviation filtered.

A combination of standards LH94-15 and GJ1-32 were used for normalizing the ages of the unknown grains. Standard LH94-15 was used when the unnormalized $^{207}Pb/^{206}Pb$ ratio of the grain was greater than the average observed $^{207}Pb/^{206}Pb$ ratio of LH94-15. Standard GJ1-32 was used when the initial $^{207}Pb/^{206}Pb$ ratio of the grain was less than the average observed $^{207}Pb/^{206}Pb$ ratio of GJ1-32. Normalization was performed using a weighted combination of the two standards for grains with intermediate $^{207}Pb/^{206}Pb$ ratios. Instrument drift during the day resulted in variations in the isotopic ratios of the standards. To account for this, the standard analyses were bracketed into different groupings representing periods of consistency. These groupings of standards were then used to normalize grains analyzed within the same interval.

Common-lead correction was applied when the average ^{204}Pb counts per second for a single grain analysis counts were elevated above background levels produced by isobaric interference from mercury (^{204}Hg) present in the Argon gas supply. The two-stage evolution model of Stacey and Kramers (1975) was used in the common lead correction. This model assumes that lead originally developed from a primordial composition equal to that of the troilite lead of the Canyon Diablo meteorite where $^{238}U/^{204}Pb = 7.19$ and $^{232}Th/^{204}Pb = 32.21$ starting at 4.57 Ga. A second stage is then assumed to have started around 3.7 Ga as a result of a differentiation process that altered conditions where the new assumed values were $^{238}U/^{204}Pb = 9.74$ and $^{232}Th/^{204}Pb = 37.19$.

U-Pb dating relies on the decay of ^{235}U to ^{207}Pb, with a half-life of 703.8 Ma, and ^{238}U to ^{206}Pb, with a half-life of 4.468 Ga (Jaffey et al. 1971). The ratios of these two isotopic systems can be plotted on a concordia diagram, where concordia is a curve where $^{207}Pb/^{235}U$ and $^{206}Pb/^{238}U$ ages are equal. An age calculated from these two isotopic systems can be considered concordant if it lies on the Concordia curve within error. If it does not, then it is considered discordant.

Discordance was calculated using the formula below, which looks at the difference between the observed $^{206}Pb/^{238}U$ ratio and the expected $^{206}Pb/^{238}U$ ratio based on the $^{207}Pb/^{206}Pb$ age calculated from the observed $^{207}Pb/^{206}Pb$ ratio. Grains with a calculated discordance of greater then 10% (or less than -10%) were not included in interpretations.

$$\%\ \text{discordance} = \frac{(e^{0.000155125 \times 206Pb/207Pb\ age} - 1) - {}^{206}Pb/{}^{238}U\ \text{ratio}}{(e^{0.000155125 \times 206Pb/207Pb\ age} - 1)} \times 100$$

Due to the difference in decay rate between the different uranium isotopes, younger grains usually produce more precise $^{206}Pb/^{238}U$ ages, and older grains usually produce more precise $^{207}Pb/^{206}Pb$ ages. Given these factors, different authors have used different filters to determine which age to report. McLennan et al. (2001) and Ireland (1992) used $^{207}Pb/^{206}Pb$ ages for grains greater than 800 Ma and $^{206}Pb/^{238}U$ ages for grains less than 800 Ma (where 800 Ma is an arbitrary diving line) except when the $^{206}Pb/^{238}U$ age was younger than the age of sedimentation. Collins and Buchan (2004) used a filter where if the $^{206}Pb/^{238}U$ age was greater than 2005 Ma the $^{207}Pb/^{206}Pb$ age was used; if the $^{206}Pb/^{238}U$ age was less than 1250 Ma the $^{206}Pb/^{238}U$ was used; and if the $^{206}Pb/^{238}U$ age lies between 1250 Ma and 2005 Ma then the more precise age was used. Strachan et al. (2007) and Waldron et al. (2009, 2011) used the most precise age calculated from $^{207}Pb/^{206}Pb$ and $^{206}Pb/^{238}U$. This roughly equates to using $^{206}Pb/^{238}U$ ages for grains less than c. 1000 Ma and $^{207}Pb/^{206}Pb$ ages for grains greater than c. 1000 Ma (Strachan et al. 2007). This method was used for this study, because the majority of the data reported from other studies, that are being used for comparison, did the same.

Relative probability density plots describe the probability of any given detrital age within a sample. The area under a portion of the curve between t1 and t2 represents the probability of a zircon having an age between t1 and t2. Isoplot3 (Ludwig 2003) was used to calculate ages and to produce concordia and relative probability density plots.

1.6 PRESENTATION AND ORGANIZATION

This document has been prepared in a paper based thesis format, where chapters 2 and 3 are written as two separate papers for future journal presentation. As a result of this arrangement there will be some repetition of information across chapters.

Chapter 2 examines the results of four new detrital zircon samples collected from the North Wales succession and discusses implication of those results on the terrane interaction between East Avalonia and the Monian Composite Terrane from the mid-Cambrian to the latest Ordovician.

In Chapter 3, the Lumsden Dam Formation of the Meguma Supergroup succession is formally described and compared with the correlative Bluestone formation, also of the Meguma Supergroup. A new detrital zircon sample from the Lumsden Dam helps complete the detrital zircon record for the Meguma terrane as it is the highest sampled horizon to date within the Meguma Supergroup. The new provenance data provides further comparison with the Welsh succession for which Waldron et al. (2011) suggested a correlation.

Chapter 4 discusses the paleogeographic implications of the results and summarizes the conclusions of this study.

1.7 REFERENCES

Allen, P.M. and Jackson, A.A. 1978. Bryn-teg borehole, North Wales. Bulletin of the Geological Survey of Great Britain, 61.

Allen, P.M. and Jackson, A.A. 1985. Geology of the country around Harlech. Memoir of the British Geological Survey, Sheet 135 with part of 149. British Geological Survey, Keyworth, Nottingham.

Allen, P.M., Jackson, A.A. and Rushton, A.W.A. 1981. The Stratigraphy of the Mawddach Group in the Cambrian Succession of North Wales. Proceedings of the Yorkshire Geological Society, 43: 295–329.

Ami, A.M. 1900. Synopsis of the geology of Canada. Proceedings and Transactions of the Royal Society of Canada, New Series, 6, pp. 194–195.

Ashton, K.E., Heaman, L.M., Lewry, J.F., Hartlaub, R.P. and Shi, R. 1999. Age and origin of the Jan Lake Complex: a glimpse at the buried Archean craton of the Trans-Hudson Orogen. Canadian Journal of Earth Sciences, 36: 185–208.

Barnes, C.G., Frost, C.D., Yoshinobu, A.S., McArthur, K., Barnes, M.A., Allen, C.M., Nordgulen, Ø. and Prestvik, T. 2007. Timing of sedimentation, metamorphism, and plutonism in the Helgeland Nappe Complex, north-central Norwegian Caledonides. Geosphere, 3: 683–703.

Barr, S.M., Davis, D.W., Kamo, S. and White, C.E. 2003. Significance of U–Pb detrital zircon ages in quartzite from peri-Gondwanan terranes, New Brunswick and Nova Scotia, Canada. Precambrian Research, 126: 123–145.

Barr, S.M., Doyle, E.M. and Trapasso, L.S. 1983. Geochemistry and tectonic implications of mafic sills in Lower Paleozoic formations of southwestern Nova Scotia. Maritime Sediments and Atlantic Geology, 19: 73–87.

Bates, D.E.B. 1968. The Lower Palaeozoic Brachiopod and Trilobite Faunas of Anglesey. Bulletin of the British Museum (Natural History) Geology Series, 16, pp. 127.

Bates, D.E.B. 1972. The Stratigraphy of the Ordovician rocks of Anglesey. Geological Journal, 8: 29–58.

Bluck, B.J., Gibbons, W. and Ingham, J.K. 1992. Terranes. Geological Society, London, Memoirs, 13: 1–4.

Bouyx, E., Blaise, J., Brice, D., Degardin, J.M., Goujet, D., Gourvennec, R., Le Menn, J., Lardeux, H., Morzadec, P. and Paris, F. 1997. Biostratigraphie et paleobiogeographie du Siluro-Devonien de la zone de Meguma (Nouvelle-Écosse, Canada). Canadian Journal of Earth Sciences, 34: 1295–1309.

Brenchley, P.J. and Cullen, B. 1984. The environmental distribution of associations belonging to the Hirnantia fauna - Evidence from North Wales and Norway. *In* Aspects of the Ordovician System. *Edited by* D.L. Bruton. Palaeontological Contributions from the University of Osla, No. 295, pp. 113–125.

Brenchley, P.J. and Rawson, G. 2006. England and Wales through geologic time. *In* The Geology of England and Wales. *Edited by* P.J. Brenchley, and P.F. Rawson. Geological Society, London, pp. 1–23.

Brenchley, P.J., Rushton, A.W.A., Howells, M. and Cave, R. 2006. Cambrian and Ordovician: the early Palaeozoic tectonostratigraphic evolution of the Welsh Basin, Midland and Monian Terranes of Eastern Avalonia. *In* The Geology of England and Wales. *Edited by* P.J. Brenchley and P.F. Rawson. Geological Society, London, pp. 25–74.

British Geological Survey. 2007. Bedrock Geology UK South (South of National Grid Line 540 km N), 1:625 000 Scale, 5th edition. (Keyworth. Nottingham: British Geological Survey).

Cawood, E.A., Nemchin, A.A., Strachan, R., Prave, T. and Krabbendam, M. 2007. Sedimentary basin and detrital zircon record along East Laurentia and Baltica during assembly and breakup of Rodinia. Journal of the Geological Society, London, 164: 257–275.

Chang, Z., Vervoort, J.D., McClelland, W.C. and Knaack, C. 2006. U-Pb dating of zircon by LA-ICP-MS. Geochemistry, Geophysics, Geosystems, 7: 1–14.

Cherns, L., Cocks, L.R.M., Davies, J.R., Hillier, R.D., Waters, R.A. and Williams, M. 2006. Silurian: the influence of extensional tectonics and sea-level changes on sedimentation in the Welsh Basin and on the midland Platform. *In* The Geology of England and Wales. *Edited by* P.J. Brenchley and P.F. Rawson. Geological Society, London, pp .74–102.

Clarke, D.B. and Halliday, A.N. 1980. Strontium isotope geology of the South Mountain batholith, Nova Scotia. Geochimica et Cosmochimica Acta, 44: 1045–1058.

Clarke, D.B., Halliday, A.N. and Hamilton, P.J. 1988. Neodymium and strontium isotopic constraints on the origin of the peraluminous granitoids of the South Mountain Batholith, Nova Scotia, Canada. Chemical Geology, 73: 15–24.

Clarke, D.B., MacDonald, M.A. and Tate, M.C. 1997. Late Devonian mafic-felsic magmatism in the Meguma Zone, Nova Scotia. Geological Society of America Memoirs 191, pp. 107–127.

Cocks, L.R.M. and Torsvik, T.H. 2002. Earth geography from 500 to 400 million years ago: a faunal and palaeomagnetic review. Journal of the Geological Society, London, 159: 631–644.

Collins, A.S. and Buchan, C. 2004. Provenance and age constraints of the South Stack Group, Anglesey, UK: U–Pb SIMS detrital zircon data. Journal of the Geological Society, London, 161: 743–746.

Compston, W., Wright, A.E. and Toghill, P. 2002. Dating the Late Precambrian volcanicity of England and Wales. Journal of the Geological Society, London, 159: 323–339.

Cooper, R.A. and P.M. Sadler 2012. The Cambrian Period. *In* The Geologic Time Scale *Edited by* F.M. Gradstein, J.G. Ogg, M. Schmitz and G. Ogg. Elsevier, pp. 489-523.

Crimes, T.P. 1970. A facies analysis of the Cambrian of Wales. Palaeogeography, Palaeoclimatology, Palaeoecology, 7: 113–170.

Crosby, D.G. 1951. The Wolfville map-area, Kings and Hants counties, Nova Scotia; npub. PhD. Dissertation, Stanford University, Stanford, California.

Clushaw, N. and Reynolds, P. 1997. $^{40}Ar/^{39}Ar$ age of shear zones in the southwest Meguma Zone between Yarmouth and Meteghan, Nova Scotia. Canadian Journal of Earth Sciences, 34: 848–853.

Dallmeyer, R.D. and Gibbons, W. 1987. The age of blueschist metamorphism in Anglesey, North Wales: evidence from $^{40}Ar/^{39}Ar$ mineral dates of the Penmynydd schists. Journal of the Geological Society, London, 144: 843–850.

Davidek, K., Landing, E., Bowring, S.A., Westrop, S.R., Rushton, A.W.A., Fortey, R.A. and Adrain, A. 1998. New uppermost Cambrian U–Pb date from Avalonian Wales and the age of the Cambrian–Ordovician boundary. Geological Magazine, 135: 227–229.

Dickinson, W.R. 1974. Plate tectonics and sedimentation. *In* Tectonics and Sedimentation. *Edited by* W.R. Dickinson. Society of Economic Paleontologists and Mineralogists, Special Publications, 22: 1–27.

Dodson, M.H., Compston, W., Williams, I.S. and Wilson, J.F. 1988. A search for ancient detrital zircons in Zimbabwean sediments. Journal of the Geological Society, 145: 977–983.

Eberz, G.W., Clarke, D.B., Chatterjee, A.K. and Giles, P.S. 1991. Chemical and isotopic composition of the lower crust beneath the Meguma Lithotectonic Zone, Nova Scotia: Evidence from granulite facies xenoliths: Contributions to Mineralogy and Petrology, 109: 69–88.

Fedo, C.M., Sircombe, K.N. and Rainbird, R.H. 2003. Detrital zircon analysis of the sedimentary record. Reviews in Mineralogy and Geochemistry, 53: 277–303.

Gehrels, G.E. 2000. Introduction to detrital zircon studies of Paleozoic and Triassic strata in western Nevada and northern California. Geological Society of America Special Paper 347, pp. 1–17.

Gehrels, G.E. and Dickinson, W.R. 1995. Detrital zircon provenance of Cambrian to Triassic miogeoclinal and eugeoclinal strata in Nevada. American Journal of Science, 295:18–48.

Gibbons, W. 1983. The Monian ‘Penmynydd Zone of Metamorphism’ in Llŷn, North Wales. Geological Journal, 18: 21–41.

Gibbons, W. 1987. Menai Strait fault system: An early Caledonian terrane boundary in north Wales. Geology, 15: 744–747.

Gibbons, W. and Ball, M.J. 1991. A discussion of Monian Supergroup stratigraphy in northwest Wales. Journal of the Geological Society, London, 148: 5–8.

Gibbons, W. and Horák, J. 1990. Contrasting metamorphic terranes in northwest Wales. Geological Society, London, Special Publications, 51: 315–327.

Gibling, M.R., Culshaw, N., Rygel, M.C. and Pascucci, V. 2008. The Maritimes Basin of Atlantic Canada: Basin Creation and Destruction in the Collisional Zone of Pangea. Sedimentary Basins of the World, 5: 211–244.

Gingras, M.K., Waldron, J.W.F., White, C.E. and Barr, S.M. 2011. The evolutionary significance of a Lower Cambrian trace-fossil assemblage from the Meguma terrane, Nova Scotia. Canadian Journal of Earth Sciences, 48: 71–85.

Greenly, E. 1919. The Geology of Anglesey: Memoir of the Geological Survey of U.K. (2 vols).

Greenly, E. 1944. The Arvonian rocks of Arvon. Quarterly Journal of the Geological Society, London, 100: 269–284.

Greenly, E. 1946. The Monio-Cambrian Interval. Geological Magazine, 83: 237–240.

Greenough, J.D., Krogh, T.E., Kamo, S.L., Owen, J.V. and Ruffman, A. 1999. Precise U-Pb dating of Meguma basement xenoliths: new evidence for Avalonian underthrusting. Canadian Journal of Earth Sciences, 36: 15–22.

Harris, I.M. and Schenk P.E. 1976. The Meguma Group. Maritime Sediments, 11: 25–46.

Henderson, J.R., Wright, T.O. and Henderson, M.N. 1986. A history of cleavage and folding: An example from the Goldenville Formation, Nova Scotia. Geological Society of America Bulletin, 97: 1354–1366.

Hibbard, J.P., van Staal, C.R. and Rankin, D.W. 2007. A comparative analysis of pre-Silurian crustal building blocks of the northern and the southern Appalachian orogen. American Journal of Science, 307: 23–45.

Horák, J.M., Doig, R., Evans, J.A. and Gibbons, W. 1996. Avalonian magmatism and terrane linkage: new isotopic data from the Precambrian of North Wales. Journal of the Geological Society, London, 153: 91–99.

Horne, R. J. and Pelley, D. 2007. Geological Transect of the Meguma Terrane from Centre Musquodoboit to Tangier. *In* Mineral Resources Branch, Report of Activities 2006. Nova Scotia Department of Natural Resources, Report 2007-1, pp. 71–89.

Howell, B.F. and Stubblefield, C.J. 1950. A revision of the Fauna of the North Welsh *Conocoryphe* viola Beds implying a Lower Cambrian Age. Geological Magazine, 87: 1–16.

Hubert, J.F. and Mertz, K.A. 1984 Eolian sandstones in Upper Triassic - Lower Jurassic redbeds of the Fundy Basin, Nova Scotia. Journal of Sedimentary Petrology, 54: 798–810.

Ireland, T.R. 1992. Crustal evolution if New Zealand: evidence from age distributions of detrital zircons in Western Province paragneisses and Torlesse greywacke. Geochimica et Cosmochimica Acta, 56: 911–920.

Jackson, S.E., Pearson, N.J., Griffin, L. and Belousova, E.A. 2004. The application of laser ablation-inductively coupled plasma-mass spectrometry to in situ U-Pb zircon geochronology, 211: 47–69.

Jaffey, A.H., Flynn, K.F., Glendenin, L.E., Bentley, W.C. and Essling, A.M. 1971. Precision Measurement of Half-Lives and Specific Activities of ^{235}U and ^{238}U. Physical Review C, 4: 1889–1906.

Jamieson, R.A., Hart, G.G., Chapman, G.G. and Tobey, N.W. 2012. The contact aureole of the South Mountain Batholith in Halifax, Nova Scotia: geology, mineral assemblages, and isograds. Canadian Journal of Earth Sciences, 49: 1280–1296.

Keppie. J.D., Dostal, J., Murphy, J.B. and Cousens, B.L. 1997. Palaeozoic withinplate volcanic rocks in Nova Scotia reinterpreted: isotopic constraints on magmatic source and palaeocontinental reconstructions. Geological Magazine, 134: 425–447.

Keppie, J.D. and Dallmeyer, R.D. 1987. Dating transcurrent terrane accretion: an example from the Meguma and mAvalon Composite terranes in the Northern Appalachians. Tectonics, 6: 831–847.

Keppie, J.D. and Krogh, T.E. 2000. 440 Ma Igneous Activity in the Meguma Terrane, Nova Scotia, Canada: Part of the Appalachian overstep sequence? American Journal of Science, 300: 528–538.

Kerr, A., Jenner, G.A. and Fryer, B.J. 1995. Sm–Nd isotopic geochemistry of Precambrian to Paleozoic granitoid suites and the deep-crustal structure of the southeast margin of the Newfoundland Appalachians. Canadian Journal of Earth Sciences, 32: 224–245.

Krogh, T.E. and Keppie, J.D. 1990. Age of detrital zircon and titanite in the Meguma Group, southern Nova Scotia, Canada: Clues to the origin of the Meguma Terrane. Tectonophysics, 177: 307–323.

Krogh, T.E., Strong, D.F., O'Brien, S.J. and Papezik, V.S. 1988. Precise U–Pb zircon dates from the Avalon Terrane in Newfoundland. Canadian Journal of Earth Sciences, 25: 442–453.

Landing, E. 2004. Precambrian-Cambrian boundary interval deposition and marginal platform of the Avalon microcontinent. Journal of Geodynamics, 37: 411–435.

Landing, E., Bowring, S.A., Davidek, K.L., Rushton, A.W.A., Fortey, R.A. and Wimbledon, W.A.P. 2000. Cambrian–Ordovician boundary age and duration of the lowest Ordovician Tremadoc Series based on U–Pb zircon dates from Avalonian Wales. Geology Magazine, 137: 485–494.

Linnemann, U., Herbosch, A., Liegeois, J.P., Pin, C., Gartner, A. and Hofmann, M. 2012. The Cambrian to Devonian odyssey of the Brabant Massif within Avalonia: A review with new zircon ages, geochemistry, Sm–Nd isotopes, stratigraphy and palaeogeography. Earth-Science Reviews, 112: 126–154.

Ludwig, K.R. 2003. User's Manual for Isoplot 3.00. Berkeley Geochronology Center Special Publication, 4.

MacDonald, L.A., Barr, A.M., White, C.E. and Ketchum, W.F. 2002 Petrology, age, and tectonic setting of the White Rock Formation, Meguma terrane, Nova Scotia: evidence for Silurian continental rifting. Canadian Journal of Earth Sciences, 39: 259–277.

McIlroy, D. and Horák, J.M. 2006. Neoprterozoic: the late Precambian terranes that formed Eastern Avalonia. *In* The Geology of England and Wales. *Edited by* P.J. Brenchley, and P.F. Rawson. Geological Society, London, pp. 9–24.

McKerrow, W.S., Niocaill, C.M. and Dewey, J.F. 2000. The Caledonian Orogeny redefined. Journal of the Geological Society, London, 157: 1149–1154.

McLennan, S.M., Bock, B., Compston, W., Hemming, W.R. and McDaniel, D.K. 2001. Detrital zircon geochronology of Taconian and Acadian foreland sedimentary rocks in New England. Journal of Sedimentary Research, 71: 305–317.

Muir, M.D., Bliss, G.M., Grant, P.R. and Fisher, M.J. 1979. Palaeontological evidence for the age of some supposedly Precambrian rocks in Anglesey, North Wales. Journal of the Geological Society, London, 136: 61–64.

Murphy, J.B., Keppie, J.D., Davis, D.W. and Krogh, T.E. 1997. Regional significance of new U–Pb age data for Neoproterozoic igneous units in Avalonian rocks of northern mainland Nova Scotia, Canada. Geological Magazine, 134: 113–120.

Murphy, J.B., Pisarevsky, S.A., Nance, R.D. and Keppie, J.D. 2004. Neoproterozoic-Early Paleozoic evolution of peri-Gondwanan terranes: implications for Laurentia-Gondwana connections. International Journal of Earth Sciences, 93: 659–682.

Nance, R.D. and Murphy, J.B. 1994. Contrasting basement isotopic signatures and the palinspastic restoration of peripheral orogens: examples from the Neoproterozoic Avalonian–Cadomian belt. Geology, 22: 617–620.

Nance, R.D., Murphy, J.B., Strachan, R., D'Lemos, R.A. and Taylor, G.K. 1991. Late Proterozoic tectonostratigraphic evolution of the Avalonian and Cadomian terranes. Precambrian Geology, 53: 41–78.

Nesse, W.D. 2000. Introduction to mineralogy. New York: Oxford University Press.

O'Brien, B.H. 1985. Preliminary report on the geology of the Lahave River area, Nova Scotia. In Current research, part A. Geological Survey of Canada, Paper 85-lA, pp. 784–794.

O'Brien, B.H. 1986. Preliminary report on the Geology of the Mahone Bay area, Nova Scotia. *In* Current Research, Part A, Geological Survey of Canada, Paper 86-1A, pp. 439-444.

O'Brien, B.H. 1988. A Study of the Meguma Terrane in Lunenburg County, Nova Scotia.

Geological Survey of Canada, Open File 1823.

O'Brien, S.J., O'Brien, B.H., Dunning, G.R. and Tucker, R.D. 1996. Late Neoproterozoic Avalonian and related peri-Gondwanan rocks of the Newfoundland Appalachians. *In* Avalonian and related Peri-Gondwanan terranes of the Circum-North Atlantic. *Edited by* R.D. Nance and M.D. Thompson. Geological Society of America, Special Paper 304, pp. 9–28.

Parrish, R.R. 1999. The age of the volcanic rocks at the Parys Mountain VMS deposit, Wales. Appendix 3A. *In*, Geology and mineralization of the Parys Mountain polymetallic deposit, Wales, United Kingdom: Bangor, Wales, Anglesey Mining plc, unpublished report. *Edited by* T.J. Barrett, S.C. Tennant, and W.H. MacLean. v. 1 (text) and v. 2 (appen.).

Peng, S., Babcock, L.E. and Cooper, R.A. 2012. The Cambrian Period. *In* The Geologic Time Scale *Edited by* F.M. Gradstein, J.G. Ogg, M. Schmitz, and G. Ogg. Elsevier, pp. 437–488.

Pharaoh, T.C. and Carney, J.N. 2000. Introduction to the Precambrian rocks of England and Wales. *In* Precambrian Rocks of England and Wales. *Edited by* J.N. Carney, J.M. Horak, T.C. Pharaoh, W. Gibbons, D. Wilson, W.J. Barclay, R.E. Bevins, J.C.W. Cope and T.D. Ford,Geological Conservation Review Series, No. 20, Joint Nature Conservation Committee, Peterborough.

Pratt, B.R. and Waldron, J.W.F. 1991. A Middle Cambrian trilobite faunule from the Meguma Group of Nova Scotia. Canadian Journal of Earth Sciences, 28: 1843–1853.

Reedman, A.J., Leveridge, B.E. and Evans, R.B. 1984. The Arfon Group ('Arvonian') of North Wales. Proceedings of the Geologists' Association, 95: 313–321.

Reynolds, P.H. and Muecke, G.K. 1978. Age studies on slates: Applicability of the $^{40}Ar/^{39}Ar$ stepwise outgassing method. Earth and Planetary Science Letters, 40: 111–118.

Reynolds, P.H., Zentilli, M.I. and Muecke, G.K. 1981. K-Ar and $^{40}Ar/^{39}Ar$ geochronology of granitoid rocks from southern Nova Scotia: Its bearing on the geological evolution of the Meguma Zone of the Appalachians. Canadian Journal of Earth Sciences, 18: 386–394.

Rushton, A.W.A. and Fortey, R.A. 2000. North Wales. *In* A revised correlation of Ordovician rocks in the British Isles. *Edited by* R.A. Fortey, D.A. Harper, J.K. Ingham, A.W. Owen, M.A. Parks, A.W.A. Rushton and N.H. Woodcock. The Geological Society, Special Report 24, pp. 18–24.

Rushton, A W A. and Howells, M F. 1998. Stratigraphical framework for the Ordovician of Snowdonia and the Lleyn Peninsula. British Geological Survey Research Report, RR/99/08.

Rushton, A.W.A. and Molyneux, S.G. 2011. Welsh Basin. *In* A Revised Correlation of the Cambrian Rocks in the British Isles. *Edited by* A.W.A. Rushton, P.M. Brück, S.G. Molyneux, M. Williams and N.H. Woodcock. Geological Society, London, Special Report 25, pp. 21–27.

Samson, S., Hamilton, M., Barr, S. and White, C. 2005. U-Pb Ages From Detrital Zircon in Avalonian Sedimentary Rocks: Temporal Changes in Provenance Tied to Terrane Migration. Journal of the Geological Society, London, 162: 65–71.

Schenk, P.E. 1983. The Meguma terrane of Nova Scotia, Canada - An aid in trans-Atlantic correlation. *In* Regional trends in the geology of the Appalachian-Caledonian-Hercynian-Mauritanide orogen. *Edited by* P.E. Schenk. D. Reidel Publishing Co., pp. 121–130.

Schenk, P.E. 1995. Annapolis Belt. *In* Geology of the Appalachian-Caledonian orogen in Canada and Greenland: Geological Survey of Canada, Geology of Canada. *Edited by* H. Williams. no. 6, pp. 367–383.

Schenk, P.E. 1997. Sequence stratigraphy and provenance on Gondwana's margin: the Meguma Zone (Cambrian to Devonian) of Nova Scotia, Canada. Geological Society of America Bulletin, 109: 395–409.

Schofield, D. I., Evans, J.A., Millar, I.L., Wilby, P.R. and Aspden, J.A. 2008. New U-Pb and Rb-Sr constraints on pre-Acadian tectonism in North Wales. Journal of the Geological Society, London, 165: 892–894.

Shackleton, R.M. 1954. The structure and succession of Anglesey and the Lleyn Peninsula. Advancement of Science, London, 11: 106–108.

Shackleton, R.M. 1969. The PreCambrian of North Wales. *In* The PreCambrian and Lower Palaeozoic rocks of Wales. *Edited by* A. Wood. University of Wales Press, Cardiff, pp. 1–22.

Shackleton, R.M. 1975. Precambrian rocks of Wales. In: A correlation of the Precambrian rocks in the British Isles. Edited by A.L. Harris, R.M. Shackleton, J. Watson, C. Downie, W.B. Harland and S. Moorbath. Special Report of the Geological Society of London, 6: 76–82.

Simonetti, A., Heaman, L.M., Hartlaub, R.P., Creaser, R.A., MacHattie, T.G. and Böhm, C. 2005. U–Pb zircon dating by laser ablation-MC-ICP-MS using a new multiple ion counting Faraday collector array. Journal of Analytical Atomic Spectrometry, 20: 677–686.

Simonetti, A., Heaman, L.M. and Chacko, T. 2008. Chapter 14: Use of discrete-dynode secondary electron multipliers with faradays – A 'reduced volume' approach for in situ U-Pb dating of accessory minerals within petrographic thin section by LA-ICP-MS. *In* Mineralogical Association of Canada Short Course 40, Vancouver, pp. 241–264.

Smitheringale, W.G. 1960. Geology of the Nictaux-Torbrook map-area, Annapolis and Kings counties, Nova Scotia. Geological Survey of Canada, Paper 60-13, p. 32.

Smitheringale, W.G. 1973. Geology of parts of Digby, Bridgetown, and Gaspereau map-areas, Nova Scotia: Geological Survey of Canada Memoir 375, p. 78.

Stacey, J.S. and Kramers, J.D. 1975. Approximation of terrestrial lead isotope evolution by a two-stage model. Earth and Planetary Science Letters, 26: 207–221.

Strachan, R.A., Collins, A.S., Buchan, C., Nance, R.D., Murphy, J.B. and D'Lemos, R.S. 2007. Terrane analysis along a Neoproterozoic active margin of Gondwana: insights from U–Pb zircon geochronology. Journal of the Geological Society, London, 164: 57–60.

Taylor, F.C. 1965. Silurian stratigraphy and Ordovician-Silurian relationships in southwestern Nova Scotia. Geological Survey of Canada, Department of Mines and Technical Surveys, Paper 64-13.

Thompson, M.D., Grunow, A.M. and Ramezani. J. 2000. Cambro-Ordovician paleogeography of the Southeastern New England Avalon Zone: Implications for Gondwana breakup. Geological Society of America Bulletin, 122: 76–88.

Tucker, R.D. and Pharaoh, T.C. 1991. U–Pb zircon ages for Late Precambrian igneous rocks in southern Britain. Journal of the Geological Society, London, 148: 435–443.

van Staal, C.R., Dewey, J.F., MacNiocaill, C. and McKerrow, W.S. 1998. The Cambrian–Silurian tectonic evolution of the northern Appalachians and British Caledonides: history of a complex, west and southwest Pacific-type segment of Iapetus. *In* Lyell: the Past is the Key to the Present. *Edited by* D.J. Blundell, and A.C. Scott. Geological Society, London, Special Publications, 143: 199–242.

van Staal, C.R., Sullivan, R.W. and Whalen, J.B. 1996. Provenance of tectonic history of the Gander Zone in the Caledonian/Appalacian Orogen: Implications for the origin and assembly of Avalon. Geological Society of America, Special Paper 304, pp. 347–367.

van Staal, C.R., Whalen, J.B., Valverde-Vaquero, P., Zagorevski, A. and Rogers, N. 2009. Pre-Carboniferous, episodic accretion-related, orogenesis along the Laurentian margin of the northern Appalachians. Geological Society, London, Special Publications, 327: 271–316.

Waldron, J.W.F. 1987. Sedimentology of the Goldenville-Halifax transition in the Tancook Island area, South Shore, Nova Scotia. Geological Survey of Canada, Open File Report 1525.

Waldron, J.W.F. 1992. The Goldenville–Halifax transition, Mahone Bay, Nova Scotia: relative sea-level rise in the Meguma source terrane. Canadian Journal of Earth Sciences, 29: 1091–1105.

Waldron, J.W.F. and Jensen, L.R. 1985. Sedimentology of the Goldenville Formation, Eastern Shore, Nova Scotia. Geological Survey of Canada, Paper, 85-15.

Waldron, J.W.F., Piper, D.J.W. and Pe-Piper, G. 1989. Deformation of the Cape Chignecto Pluton, Cobequid Highlands, Nova Scotia: thrusting at the Meguma-Avalon boundary. Atlantic Geology, 25: 51–62.

Waldron, J. W. F., Schofield, D.I., White, C.E. and Barr, S.M. 2011. Cambrian successions of the Meguma Terrane, Nova Scotia, and Harlech Dome, North Wales: dispersed fragments of a peri-Gondwanan basin?. Journal of the Geological Society, 168: 83–98.

Waldron, J.W.F., White, C.E., Barr, S.M., Simonetti, A. and Heaman, L.M. 2009. Provenance of the Meguma terrane, Nova Scotia: rifted margin of early Paleozoic Gondwana. Canadian Journal of Earth Sciences, 46: 1–9.

Waldron, J.W.F. and van Staal, C.R. 2001. Taconian orogeny and the accretion of the Dashwoods block: A peri-Laurentian microcontinent in the Iapetus Ocean. Geology, 29: 811–814

White, C.E. 2010a. Pre-Carboniferous bedrock geology of the Annapolis Valley area (NTS 21A/14, 15, and 16; 21H/01 and 02), southern Nova Scotia. *In* Mineral Resources Branch, Report of Activities 2009. *Edited by* D.R. MacDonald. Nova Scotia Department of Natural Resources, Report 2010-1, pp. 137–155.

White, C.E. 2010b. Stratigraphy of the Lower Paleozoic Goldenville and Halifax groups in the western part of southern Nova Scotia. Atlantic Geology, 46: 136–154.

White, C.E. and Barr, S.M. 2004. Age and petrochemistry of mafic sills on the northwestern margin of the Meguma terrane in the Bear River–Yarmouth area of southwestern Nova Scotia. *In* Mineral Resources Branch, Report of Activities 2003. *Edited by* D.R. MacDonald. Nova Scotia Department of Natural Resources, Report 2004-1, pp. 97–117.

White, C. E., Barr, S. M., Horne, R. J. and Hamilton, M. A. 2007. The Neoacadian orogeny in the Meguma terrane, Nova Scotia, Canada. in 42nd Annual Meeting Geological Society of America, Northeastern Section, March 12-14, Abstracts with Programs, 39: 69.

White, C.E., Barr, S.M. and Toole, R.M. 2006. New insights on the origin of the Meguma Group in southwestern Nova Scotia, Canada. Nova Scotia Department of Natural Resources, Mineral Resource Branch, Open File Illustration, ME 2006-2.

White, C.E., Horne, R.J. and Hunter, J. 1999. Preliminary bedrock geology of the Digby map sheet (21A/12), southwestern Nova Scotia. Nova Scotia Department of Natural Resources, Report of Activities 1998, Report 1999-1, pp. 119–134.

White, C.E., Palacios, T., Jensen, S. and Barr, S.M. 2012. Cambrian-Ordovician acritarchs in the Meguma terrane, Nova Scotia, Canada: Resolution of early Paleozoic stratigraphy and implications for paleogeography. GSA Bulletin 124: 1773–1792.

Withjack, M.O., Olsen, P.E. and Schlische, R.W. 1995. Tectonic evolution of the Fundy rift basin, Canada: Evidence of extension and shortening during passive margin development. Tectonics, 14: 390–405.

Woodcock, N.H. 1990. Sequence stratigraphy of the Palaeozoic Welsh Basin. Journal of the Geological Society, London, 147: 537–547.

Woodcock, N. H. 2000. Introduction to the Silurian. *In* British Silurian Stratigraphy, *Edited by* D. Palmer, D.J. Siveter, P. Lane, N. Woodcock, and R. Aldridge.

Geological Conservation Review Series, No. 19, Joint Nature Conservation Committee, pp. 1–22.

Young, T.P., Gibbons, W. and McCarroll, D. 2002. Geology of the country around Pwllheli. Memoir of the British Geological Survey, Sheet 134. British Geological Survey, Keyworth, Nottingham.

Young, T., Martin, F., Dean, W.T. and Rushton, A.W.A. 2009. Cambrian stratigraphy of St. Tudwal's Peninsula, Gwynedd, northwest Wales. Geological Magazine, 131: 335–360.

CHAPTER 2: DETRITAL ZIRCON GEOCHRONOLOGY OF THE CAMBRIAN-ORDOVICIAN SUCCESSION OF NORTH WALES

A version of this chapter will be submitted for publication under the following authorship
Pothier, H., Waldron, J.W.F., Schofield, D.I. and DuFrane, S.A.

2.1 INTRODUCTION

The ages of detrital zircon grains in clastic sedimentary rocks offer important information about potential source regions for sedimentary basin fill and variations in the record over time within a particular succession may reflect changes in a basin's proximity to different source areas. In this way, detrital zircon can be used to help constrain paleogeographic positions and the timing of terrane juxtaposition.

The Caledonide-Appalachian Orogen preserves evidence of a series of geological events of Early Ordovician to Middle Devonian age that record closure of the Iapetus Ocean and the collision of Laurentia, Baltica, and peri-Gondwanan terranes (Harland and Gayer 1972; van Staal 1998; McKerrow et al. 2000; Hibbard et al. 2007). The passive margin of Laurentia, and associated peri-Laurentian terranes, span most of length of the eastern North America and part of Greenland (Fig. 1.1). Outboard of this Laurentian realm is a mosaic of terranes interpreted as a series of microcontinental blocks and arcs formed along the northern (present day coordinates) margin of Gondwana (e.g., Hibbard et al. 2007). These were classified by Hibbard et al. (2007) into several peri-Gondwanan domains including Ganderia, Avalonia, and the Meguma terrane of Nova Scotia (Fig. 1.1).

Several links have been made between peri-Gondwanan elements involved in the Caledonide Orogen in the British Isles and Appalachian Orogen of Atlantic Canada (Fig. 2.1). East and West Avalonia (Fig. 2.1) are generally characterized by lower Paleozoic platformal sedimentary successions overlying Precambrian arc-related volcanic suites (Nance 1991; Nance and Murphy 1994). The adjacent Cambrian successions of the Harlech Dome within the Welsh Basin (Fig. 2.1), previously regarded as part of Avalonia, and the Meguma terrane (Fig. 2.1)

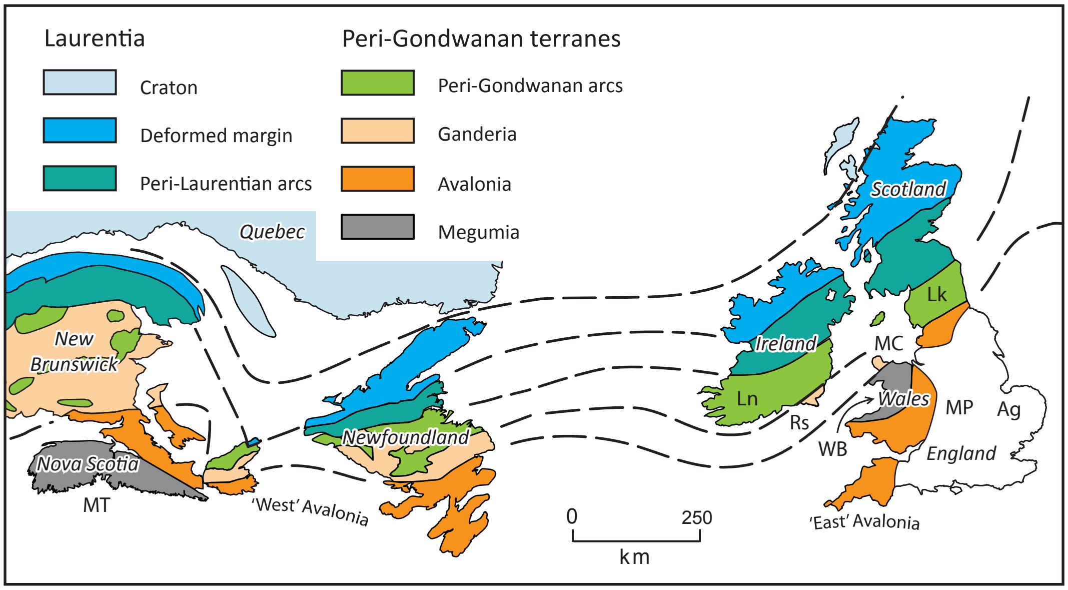

Figure 2.1: Terrane Map of the North America Appalachians and British Caledonides. Abbreviations in alphabetical order are Ag-Anglian Basin; Lk-Lakesman Terrane; Ln-Leinster Terrane; MC-Monian Composite Terrane; MP-Midland Platform; MT-Meguma Terrane; Rs-Rosslare Terrane; WB-Welsh Basin. Data compiled from van Staal et al. (1998), Barnes et al. (2007) Hibbard et al. (2007) and Waldron et al. (2011).

of Nova Scotia have been linked by Waldron et al. (2011) in a new domain, Megumia. The Monian Composite terrane and the Leinster-Lakesman terrane (Fig. 2.1) have been correlated with the Ganderia domain of Newfoundland and New Brunswick (e.g., van Staal et al. 1996 and references therein, 1998).

In discussing terrane interactions it is important to use a consistent timescale. Where possible, we use the timescales of Gradstein et al. (2012) throughout this paper. It should be noted that this includes a four-fold division of the Cambrian as documented by Peng et al. (2012). We informally use 'lower Cambrian' to include Series 1 (Terreneuvian) and 2 (unnamed); 'middle Cambrian' to include Series 3 (unnamed); and 'upper Cambrian' to include Series 4 (Furongian).

The purpose of this paper is to investigate terrane interactions by examining the detrital zircon record from four sandstone units sampled in North Wales spanning the interval from the early Cambrian to the latest Ordovician in order (1) to constrain the timing of the juxtaposition of the Welsh Basin with the Monian Composite terrane along the Menai Strait Fault System; (2) to provide new insight into the origin of the Arfon Basin, which lies along the fault system; and (3) to determine whether North Wales came into contact with Laurentia during this time interval. We build on the results of Waldron et al. (2009, 2011) who suggested a link between the early Cambrian to Tremadocian successions of the Harlech Dome in North Wales and the Meguma terrane where both were derived from sources in Gondwana. We conclude that North Wales was juxtaposed with the Monian Composite terrane by the Tremadocian, and that Laurentian detritus is not recorded in the latest Ordovician sediments, indicating that the Iapetus Ocean remained open at least until the Silurian. The Cambrian detrital zircon record from the Arfon Basin does not show definite links to either the Monian Composite terrane or the Welsh Basin and Midland Platform, and may indicate that the basin is a transported slice caught up in the fault system.

2.2 REGIONAL GEOLOGIC SETTING

Precambrian to Ordovician sedimentary basins of Wales display contrasting histories across major NE-striking fault systems. Most notable are the Welsh Borderland Fault System and the Menai Strait Fault System (Fig. 2.2). The Welsh Borderland Fault System separates the lower Paleozoic Welsh Basin from the Midland Platform to the east, and includes the long-lived Pontesford and Tywi lineaments and the Church Stretton Fault Zone (Woodcock and Gibbons 1988) (Fig. 2.2). The Menai Strait Fault System separates the Welsh Basin to the southeast from the Monian Composite terrane on Anglesey and the Llŷn Peninsula (Gibbons 1987). The system contains a series of steep NE-striking faults and shear zones, most significantly the Berw, Dinorwic and Aber-Dinlle faults (Fig. 2.2). Gibbons (1987) suggested the existence of a terrane boundary along the Menai Strait Fault System based on contrasts in basement characteristics on either side of the fault system and the presence of a ductile shear zone that was active from at least the early Cambrian to the late Carboniferous (Gibbons 1987). Between the Monian Composite Terrane and the Welsh Basin, along the Menai Straight Fault System, is the Arfon Basin. It contains a distinct Neoproterozoic to Cambrian succession that has not been definitively linked to either the Harlech Dome to the south nor to the Monian succession of Anglesey to the north (Rushton and Molyneux 2011).

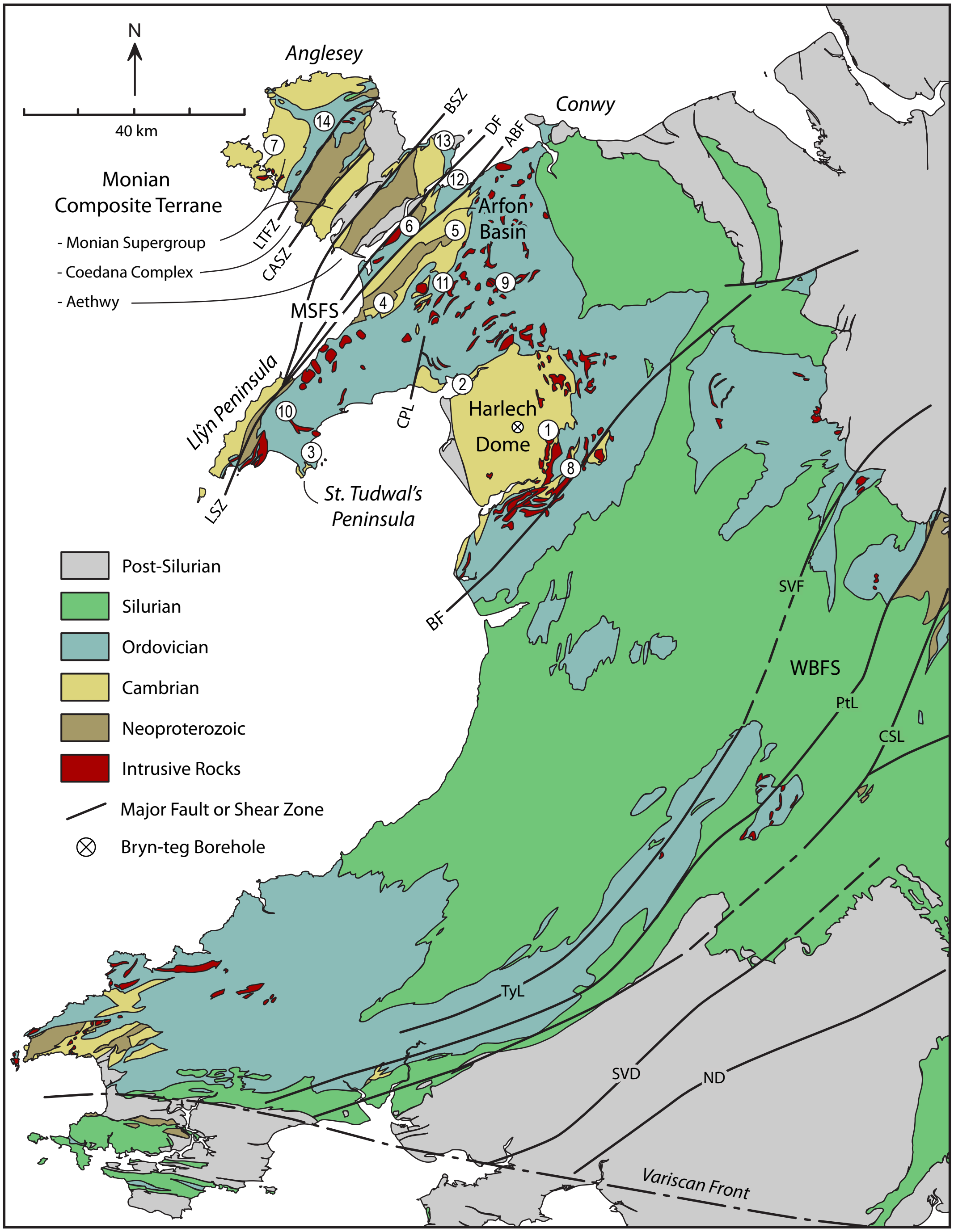

Figure 2.2: Geological map of Wales (from British Geological Survey 2007). Abbreviations in alphabetical order: ADF-Aber-Dinlle Fault; BF-Bala Fault; BSZ-Berw Shear Zone; CSL-Church-Stretton Lineament; DF-Dinowic Fault; LSZ-Llŷn Shear Zone; MSFS-Menai Strait Fault System; PtL-Pontesford Lineament; SVD-Swansea Valley Dist.; SVF-Seven Valley Fault; TL-Tywi Lineament; and WBFS-Welsh Borderland Fault System. Numbers refer to stratigraphic columns shown in Fig. 2.3 and 2.5.

2.2.1 Welsh Basin

The sedimentary fill of the Welsh Basin ranges from the early Cambrian to Early Devonian and has been divided into three megasequences, each separated by basin-wide unconformities (Woodcock 1990). The Dyfed Supergroup, the lowest of the three, spans the early Cambrian to the Tremadocian and is widely exposed in the Harlech Dome in North Wales. Its base is interpreted as an unconformity with underlying Precambrian basement (Allen and Jackson 1978) and its top is marked by a sub-Floian unconformity (sub-Arenig unconformity of older time scales), which spans both the Welsh Basin and the Monian terrane in Anglesey (Ruston and Fortey 2000).

The Dyfed Supergroup succession in the Harlech Dome (Fig. 2.3) rests upon interbedded sedimentary and volcaniclastic rocks, tuffs, and lavas of the Neo-proterozoic Bryn-teg Volcanic Formation known only from the Bryn-teg borehole (Fig. 2.4) (Allan and Jackson 1978). Above this, the Cambrian Harlech Grits Group is characterized by course-grained psammite with interbedded metasiltstone (Allen and Jackson 1985). Waldron et al. (2011) noted similarities between the Harlech Dome succession and Meguma Supergroup of Nova Scotia. The Rhinog Formation (Fig. 2.3), of the Harlech Grits Group, was sampled for detrital zircon as a part of this comparison. The upper part of the Harlech Grits Group contains mudstone, siltstone and sandstone with manganese-rich horizons in the Hafotty and Gamlan formations (Allen and Jackson 1985) (Fig. 2.3). We report new detrital zircon results from the Gamlan Formation. The overlying Mawddach Group (Drumian to Tremadocian) consists of interbedded silty mudstone and fine to coarse sandstone (Allen and Jackson 1985). We sampled the highest unit in the group, the Dol-cyn-afon Formation (Fig. 2.3). The Mawddach Group is unconformably overlain by the Tremadocian Rhobell Volcanic Group (Allen and Jackson 1985), which contains basaltic lava, sandstone, conglomerate and minor sedimentary breccia (Brenchley et al. 2006). A K-Ar age of 475 ± 12 Ma from an amphibole separate has been interpreted by Beckinsale and Rundle (1980) to represent the minimum extrusion age for the Rhobell Volcanic Group. This succession is interpreted as subduction-related (Kokelaar et al. 1984, 1988).

The overlying Ordovician succession (Fig. 2.5), assigned to the Gwynedd Supergroup of Woodcock (1990), consists mainly of marine mudstone, siltstone

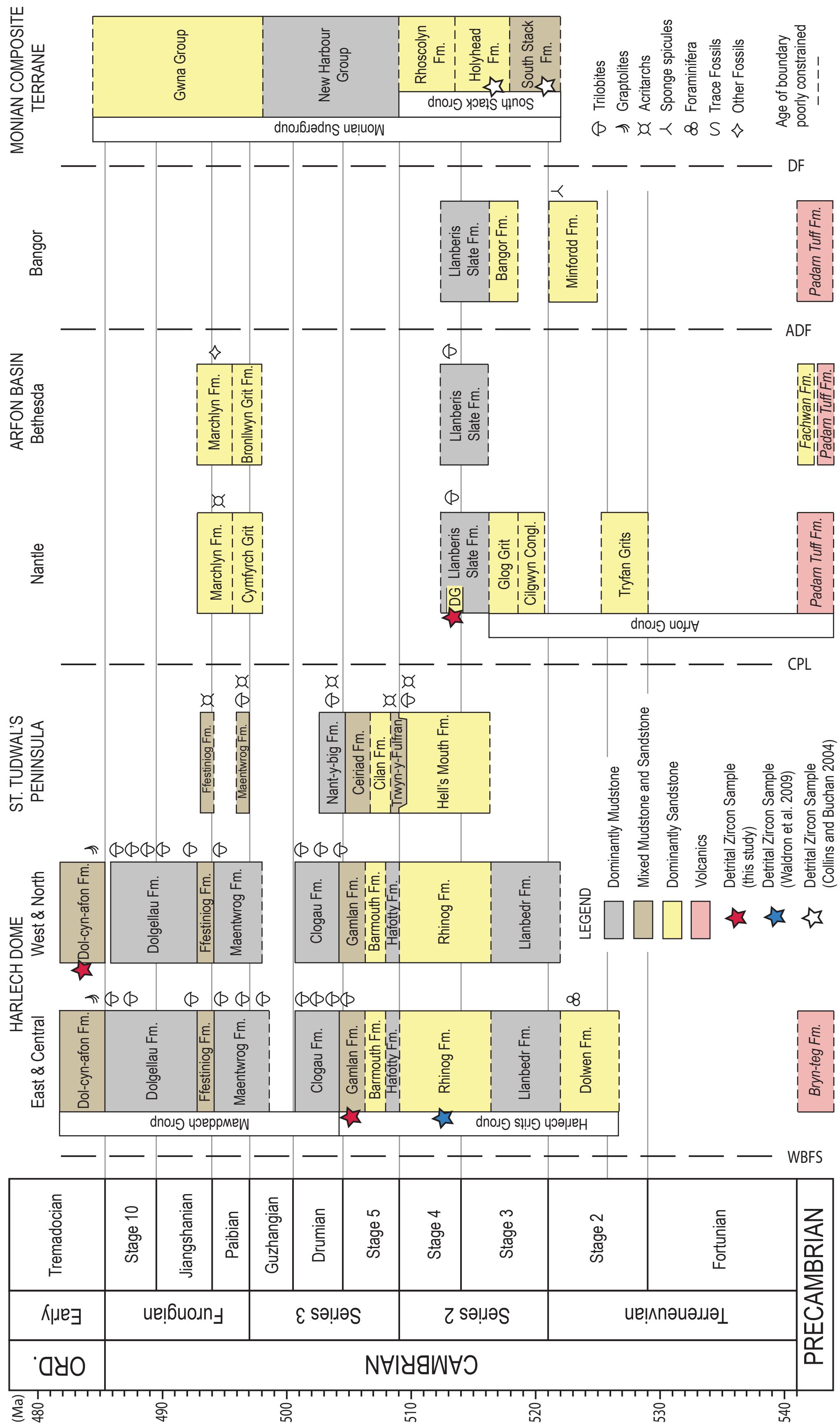

(Ma)
480
490
500
510
520
530
540
ORD.
CAMBRIAN
PRECAMBRIAN
Early
Furongian
Series 3
Series 2
Terreneuvian
Tremadocian
Stage 10
Jiangshanian
Paibian
Guzhangian
Drumian
Stage 5
Stage 4
Stage 3
Stage 2
Fortunian
WBFS
CPL
ADF
DF
① HARLECH DOME East & Central
② West & North
③ ST. TUDWAL'S PENINSULA
④ Nantle
⑤ ARFON BASIN Bethesda
⑥ Bangor
⑦ MONIAN COMPOSITE TERRANE
Dol-cyn-afon Fm.
Dolgellau Fm.
Ffestiniog Fm.
Maentwrog Fm.
Clogau Fm.
Gamlan Fm.
Barmouth Fm.
Hafotty Fm.
Rhinog Fm.
Llanbedr Fm.
Dolwen Fm.
Bryn-teg Fm.
Mawddach Group
Harlech Grits Group
Nant-y-big Fm.
Ceiriad Fm.
Cilan Fm.
Trwyn-y-Fulfran
Hell's Mouth Fm.
Marchlyn Fm.
Cymffyrch Grit
DG
Llanberis Slate Fm.
Glog Grit
Cilgwyn Congl.
Tryfan Grits
Padarn Tuff Fm.
Arfon Group
Bronllwyn Grit Fm.
Fachwen Fm.
Bangor Fm.
Minffordd Fm.
Gwna Group
New Harbour Group
Rhoscolyn Fm.
Holyhead Fm.
South Stack Fm.
South Stack Group
Monian Supergroup
LEGEND
Dominantly Mudstone
Mixed Mudstone and Sandstone
Dominantly Sandstone
Volcanics
Detrital Zircon Sample (this study)
Detrital Zircon Sample (Waldron et al. 2009)
Detrital Zircon Sample (Collins and Buchan 2004)
Trilobites
Graptolites
Acritarchs
Sponge spicules
Foraminifera
Trace Fossils
Other Fossils
Age of boundary poorly constrained

Figure 2.3: (previous page) Stratigraphic columns showing Cambrian units of the northern Welsh Basin, Arfon Basin, and Monian Composite Terrane. Data compiled from Pharaoh and Carney 2000; Brenchley and Rawson 2006; Rushton and Molyneux 2011. Abbreviations: ABF-Aber-Dinlle Fault; DF-Dinorwic Fault; CPL-Cwm Pennant Lineament; and WBFS-Welsh Borderland Fault System. Using time scale of Peng et al. (2012).

and sandstone, interfingering with volcanic deposits, that range from the Floian to mid-Katian (Rushton and Howells 1998). The Aran, Llewelyn, Llanbedrog, and Snowdon volcanic groups (Fig. 2.5) represent the main volcanic centres and span the earliest Darriwillian to the early Katian (Allen and Jackson 1985; Rushton and Howells 1998; Rushton and Fortey 2000). Katian black mudstone, above the volcanics, is overlain unconformably by mudstone, siltstone and sandstone, including the Conway Castle Grit sampled in this study, assigned to the basal

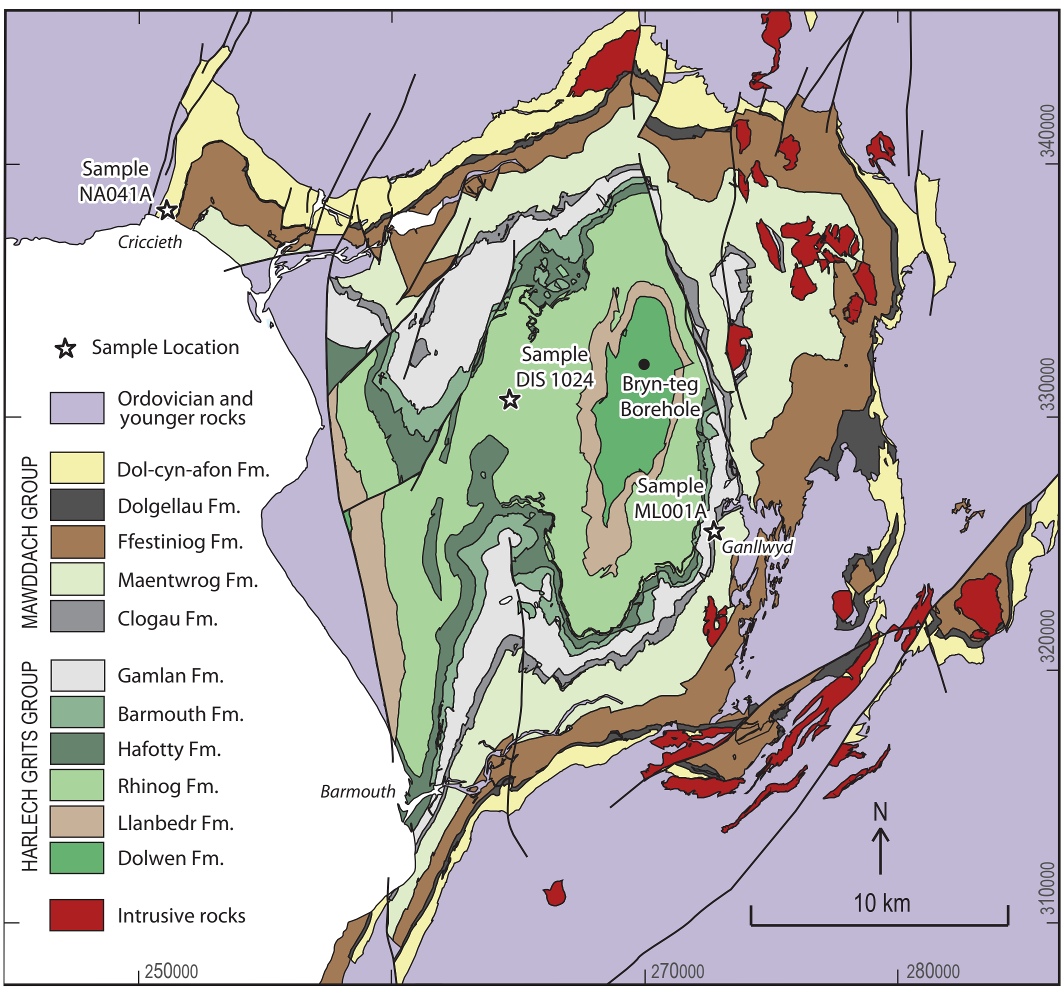

Figure 2.4: Geological map of the Harlech Dome (from British Geological Survey 1982; British Geological Survey 2013). Ordnance Survey National Grid reference system.

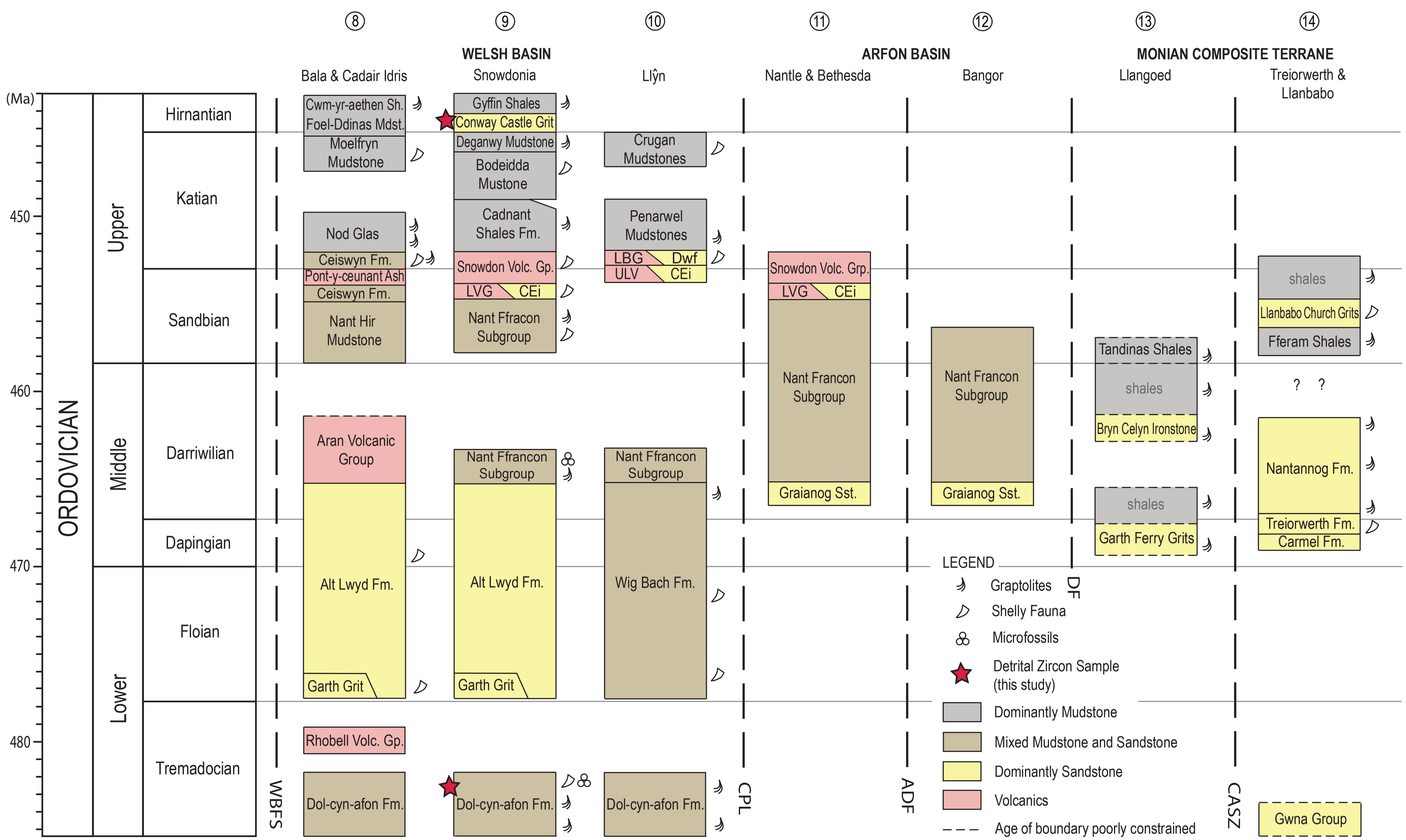

(Ma)
450
460
470
480
ORDOVICIAN
Upper
Middle
Lower
Hirnantian
Katian
Sandbian
Darriwilian
Dapingian
Floian
Tremadocian
WELSH BASIN
ARFON BASIN
MONIAN COMPOSITE TERRANE
8
9
10
11
12
13
14
Bala & Cadair Idris
Snowdonia
Llŷn
Nantle & Bethesda
Bangor
Llangoed
Treiorwerth & Llanbabo
Cwm-yr-aethen Sh.
Foel-Ddinas Mdst.
Moelfryn Mudstone
Nod Glas
Ceiswyn Fm.
Pont-y-ceunant Ash
Ceiswyn Fm.
Nant Hir Mudstone
Aran Volcanic Group
Alt Lwyd Fm.
Garth Grit
Rhobell Volc. Gp.
Dol-cyn-afon Fm.
Gyffin Shales
Conway Castle Grit
Deganwy Mudstone
Bodeidda Mustone
Cadnant Shales Fm.
Snowdon Volc. Gp.
LVG
CEi
Nant Ffracon Subgroup
Nant Ffrancon Subgroup
Alt Lwyd Fm.
Garth Grit
Dol-cyn-afon Fm.
Crugan Mudstones
Penarwel Mudstones
LBG
Dwf
ULV
CEi
Nant Ffrancon Subgroup
Wig Bach Fm.
Dol-cyn-afon Fm.
Snowdon Volc. Grp.
LVG
CEi
Nant Francon Subgroup
Graianog Sst.
Nant Francon Subgroup
Graianog Sst.
Tandinas Shales
shales
Bryn Celyn Ironstone
shales
Garth Ferry Grits
shales
Llanbabo Church Grits
Fferam Shales
? ?
Nantannog Fm.
Treiorwerth Fm.
Carmel Fm.
Gwna Group
WBFS
CPL
ADF
DF
CASZ
LEGEND
Graptolites
Shelly Fauna
Microfossils
Detrital Zircon Sample (this study)
Dominantly Mudstone
Mixed Mudstone and Sandstone
Dominantly Sandstone
Volcanics
Age of boundary poorly constrained

Figure 2.5: (previous page) Stratigraphic columns showing Ordovician units of the Northern Welsh Basin, Arfon Basin, and Monian Composite Terrane. Data from Rushton and Fortey (2000). Abbreviations for stratigraphical units are from (Rushton and Howells 1999): CEi-Cwm Eigiau Formation; Dwf-Dwyfach Formation; LlV-Llewelyn Volcanic Group; LVG-Llanbedrog Volcanic Group; and the ULG-Upper Lodge Volcanic Formation. Other abbreviations include ABF-Aber-Dinlle Fault; DF-Dinorwic Fault; CASZ-Central Anglesey Shear Zone; CPL-Cwm Pennant Lineament; WBFS-Welsh Borderland Fault System. Using time scale of Cooper and Sadler (2012).

units of the Powys Supergroup by Woodcock (1990). Ruston and Fortey (2000) interpreted this Hirnantian influx of coarser sediment into deeper part of the Welsh Basin as a result of a glacio-eustatic fall in sea-level. The overlying Silurian record in central Wales consists of thick alternating oxic and anoxic mudstones and deep-water turbidite sandstones that were deposited in sedimentary basins bounded by active extensional faults (Cherns et al. 2006).

2.2.2 Arfon Basin

The Arfon Basin is located along the Menai Strait Fault System to the northwest of the Harlech Dome (Fig. 2.2). The succession rests with an unconformity or a paraconformity upon the Precambrian felsic ash flow tuffs of the Pardarn Tuff Formation (Reedman et al. 1984) that has yielded U-Pb zircon ages of 604.7 ± 1.6 Ma (Compston et al. 2002) and 614 ± 2 Ma (Tucker and Pharaoh 1991). To the northwest, between the Aber-Dinlle and Dinorwic faults, the Arfon Group comprises tuffite, sandstone and conglomerate of the Minfordd and Bangor formations (Reedman et al. 1984) (Fig. 2.3). Sponge spicules present in the Minfordd Formation suggest they are of Cambrian rather than Precambrian age (Rushton and Molyneux 2011). Southeast of the Aber-Dinlle Fault the Arfon Group consist of the Fachwen Formation and its lateral equivalents, the Tryfan Grits, Cilgwyn Conglomerate, and Glog Grits (Rushton and Molyneux 2011). A welded ash-flow tuff within the Fachwen Formation produced an age of 572.5 ± 1.2 Ma (Compston et al. 2002). The Twt Hill Granite dated at 615 ± 1.3 Ma (Schofield et al. 2008) is enveloped within the Padarn Tuff, but its relationship with the Arfon Group sedimentary rocks is not preserved.

Above the Arfon Group, the Llanberis Slates Formation (Fig. 2.3) is characterized by silty mudstone with abundant turbiditic sandstone. The undated Dorothea Grit lower in the succession sampled in this study is one of the formally recognized sandstone units (Morris and Fearnsides 1926). Above the Dorothea Grit, early Cambrian (Series 2, from stage 3 to 4) trilobites are recorded (Howell and Stubblefield 1950; Ruston and Molyneux 2011). The Llanberis Slates Formation is overlain by the laterally equivalent sandstone-rich Bronllwyd Grit, Cymffyrch Grit formations and the Marchllyn Formation. The nature of the contact of these units with one another and the underlying Llanberis Slates is disputed (Brenchley and Rawson 2006). This whole succession is overstepped by Floian sedimentary rocks and shares the same overlying Ordovician succession as to the Harlech Dome region (Fig. 2.5).

2.2.3 Monian Composite Terrane

The Cambrian record on Anglesey is exposed in the northern part of the island (Fig. 2.2). The bedded succession was first described by Greenly (1919) and later termed the Monian Supergroup by Shackleton (1975). It comprises predominantly metasedimentary rocks that have been metamorphosed to low greenschist facies. These rocks have historically been considered Precambrian (e.g., Greenly 1919; Shackleton 1969); however, paleontological evidence (Muir et al. 1979) supports a Cambrian age for the majority of the succession. The lowest unit, the South Stack Group (Fig. 2.3), is characterized by massive quartzite and quartzose turbiditic greywacke with subordinate slate (Greenly 1919). Detrital zircons from this unit included a 522 ± 6 Ma grain (late Terreneuvian in the timescale of Peng et al. 2012) interpreted by Collins and Buchan (2004) as the maximum depositional age. This is supported by the Phanerozoic trace fossil *Skolithos* sp. and early Cambrian trace fossil *Trichophycus* found in the South Stack Group (Muir et al. 1979). The overlying New Harbour Group is characterized by pelite with subordinate serpentinite, gabbro, basalt, and chert (Gibbons 1983). The youngest unit in the Monian Supergroup is the Gwna Group, also exposed on the Llŷn Peninsula, a mélange that contains both deep-water and continental clasts including pillow lava, chert, sandstone, limestone, and granite (Gibbons 1987). Greenly (1919) interpreted the unit to be the result of tectonic disruption, but it was later described as a deformed olistostrome by Shackleton (1954, 1969, 1975). The age of these two upper units is poorly constrained; however, Floian sedimentary rocks unconformably overlie the Gwna Group, indicating these rocks are no younger than Tremadocian (Greenly 1919; Bates 1968). A number of sedimentary rock outliers were identified by Greenly (1919) in southern Anglesey. Their ages are unknown; however, the Careg Onen Beds contain sponge spicules

(Greenly 1946) and have been correlated with the Minfordd Formation of the Arfon Basin (Reedman et al.1984).

The Ordovician record in Anglesey (Fig. 2.5) appears as a series of outliers and is less complete than in mainland Wales, ranging from the Dapingian to the late Sandbian (Ruston and Fortey 2000). The facies differ from rocks of similar age in the Welsh Basin (Neuman and Bates 1978) as they are mainly mudstone and there is no evidence of significant volcanic activity (Bates 1972). Silurian rocks in Anglesey only appear in the core of the Parys Mountain syncline within the Carmel Head Thrust System in North Anglesey. The Parys Volcanic Group rests above Darriwillian sediments, and rhyolites within this unit have been dated as mid-Llandovery (Parrish 1999). Overlying these is mid-Llandovery graptolite-bearing slate (Greenly 1919).

2.3 SAMPLE DESCRIPTIONS

Four samples were collected from sandstone horizons in North Wales that span the Cambrian (Drumian Stage) to the latest Ordovician (Hirnantian), stratigraphically above the previously sampled Rhinog Formation (Waldron et al. 2011) (Fig. 2.3). Sample localities were selected based on rock type, stratigraphic position, and proximity to known fossil occurrences to help best constrain the depositional age. Petrographic images of the samples are found in Appendix A.

The Gamlan Formation is the highest unit of the Harlech Grits Group and is between 230 and 360 m thick (Fig. 2.3). It is characterized by grey, green, and purple interbedded siltstone and mudstone with thick beds of coarse-grained sandstone. The upper half of the formation is manganiferous (Allen and Jackson 1985). *Paradoxides hickii* and *Eodiscus puntatus* s.l. have been identified in the uppermost beds of the Gamlan Formation, placing the highest sediments in the *Tomagnostus fissus* zone of the Cambrian Drumian Stage (Allen et al. 1981; Allen and Jackson 1985). Typical Gamlan Formation occurs in the Barmouth area and the best exposures are on the coastal section [SH 61826 15534]. It consists of grey to greenish grey interbedded fine sandstone, siltstone, and mudstone. The beds are medium to very thinly bedded and show graded bedding and parallel laminations. Trace fossils are abundant, especially burrows. The unit is enriched in manganese, particularly in sandy layers, and manganese carbonate concretions are abundant. Sample ML001 was collected from the top of the Gamlan

Formation near Ganllwyd along the Gamlan River [SH 72601 24306] where the relationship with the overlying Clogau Formation is better exposed (Fig. 2.4). Bedding at this location dips 51° to the east. The outcrop shows an upward transition from mainly slate with very thin graded sandstone beds into medium to very thickly bedded wacke with interbedded silty slate. These are overlain by rust-weathered cleaved mudstone of the Clogau Formation. Sample ML001 is a moderately sorted, subrounded, muddy sandstone. Based on a visual estimate it contains 43% quartz, 10% polycrystalline quartz, 15% potassium feldspar, 5% chert, 3% plagioclase, 1% plutonic fragments, 1% chlorite and trace amounts of mica, zircon, and opaque minerals. The matrix comprises 22% of the rock and consists of chlorite, quartz, and white mica.

The Dol-cyn-afon Formation is the uppermost unit of the Mawddach Group (Fig. 2.3) and is 490 to 900 m thick (Allen and Jackson 1985; Howells and Smith 1997). It is characterized by grey mudstone and siltstone with minor sandstone (Rushton and Howells 1998). A crystal-rich volcaniclastic sandstone bed in the underlying Dolgellau Formation has been dated at 491 ± 1 Ma (Davidek et al. 1998), interpreted as the depositional age. The unit contains the graptolite *Rhabdinopora flabelliformis* placing it in the earliest Ordovician (Tremadocian). Sample NA041 was from the upper sandstone member of the Dol-cyn-afon Formation. It was collected from roadside outcrop east of Criccieth [SH 51060 38361] where beds dip 73° to the northwest (Fig. 2.4). The sample was taken from the base of a bed 36 cm thick from an interval of medium to thickly bedded fine sandstone that contains minor mudclasts, enveloped within well-cleaved finely laminated mudstone. It is a light grey, subrounded, moderately sorted, muddy sandstone. It is grain supported and has a weak tectonic foliation defined by the alignment of mica in the matrix. It contains 39% quartz, 13% polycrystalline quartz, 7% chert, 7% potassium feldspar, 1% plagioclase, 1% sedimentary rock fragments, 1% plutonic rock fragments and trace amounts of rounded metamorphic rock fragments, chlorite, and opaque minerals. The matrix makes up 29% of the rock and consists of chlorite, quartz and white mica.

The Conway Castle Grit is 50 m thick and occurs near the base of the Powys Supergroup (Fortey et al. 2000). It lies unconformably above the Deganwy Mudstones and is overlain by the Gyffin Shales (Fig. 2.5). The Conway Castle Grit contains only allochthonous Hirnantian fauna (Brenchley and Newall 1980);

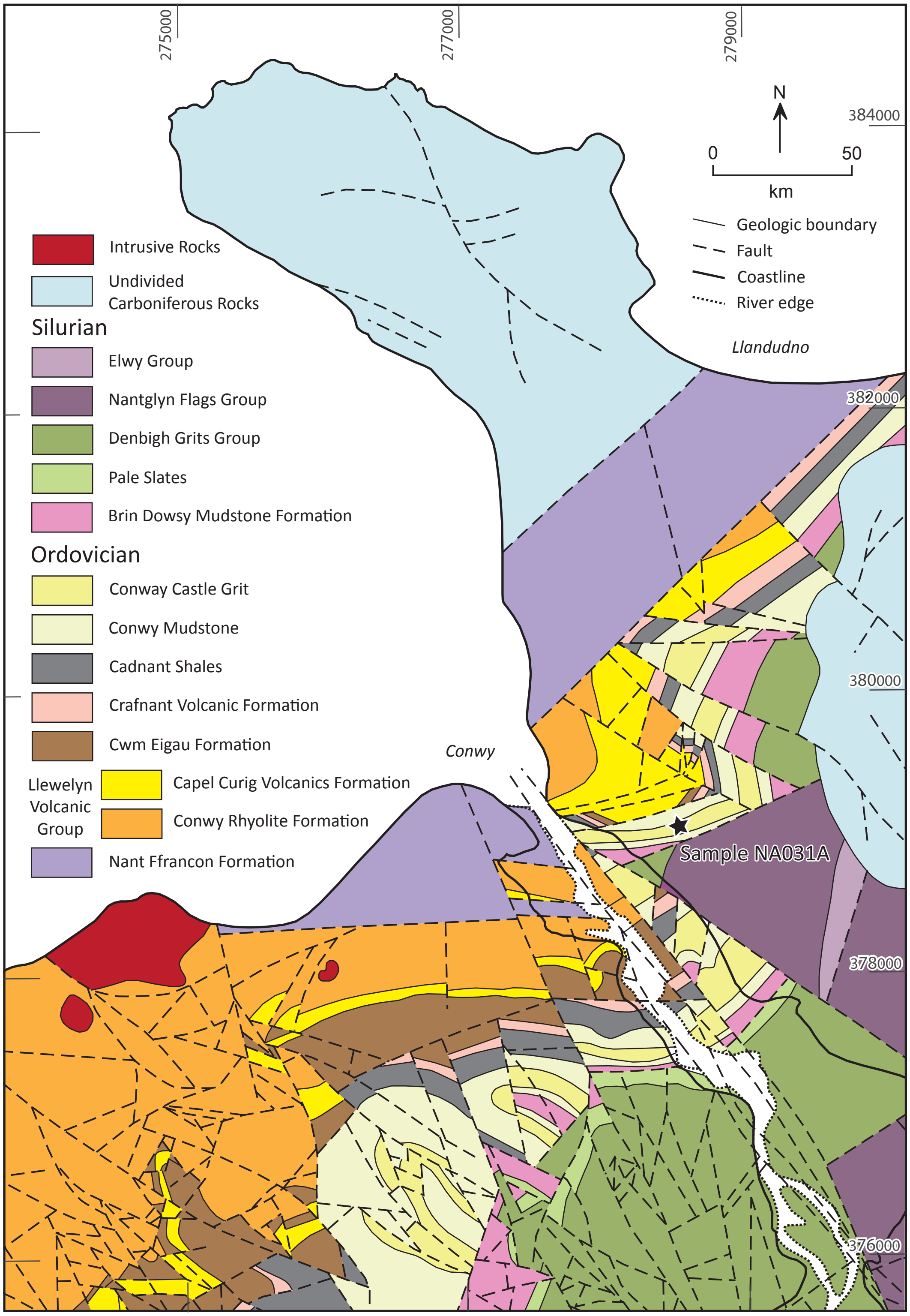

Figure 2.6: Geological map of Conwy (from British Geological Survey 1989). Ordnance Survey National Grid reference system.

however, it has been correlated with units elsewhere of Hirnantian age. The Deganwy Formation below contains late Katian fauna (Elles 1909; Brenchley and Cullen 1984) and the Gyffin Shales above contain Hirnantian graptolites (*Monograptus gregarius* zone of Elles 1909) (Rushton and Fortey 2000) implying a probable Hirnantian age. Sample NA031 was collected from the Deganwy Quarries in Deganwy [SH 78565 79060] (Fig. 2.6). The exposure contains 38 m of section with dip around 65° to the south (Rushton et al. 2000). It consists of thin to thickly bedded calcareous sandstone with minor siltstone and mudstone interbeds. Graded bedding and mud clasts (up to 15 cm) are common. The sample was collected from the base of a bed 23 cm thick, rich in carbonate material. Clasts are well sorted and rounded and comprise 26% mudstone rock fragments, 23% fossil fragments, 10% limeclasts, 4% peloids, 3% quartz, 3% opaque minerals, 1% potasium feldspar, 1% volcanic rock fragments, and trace amounts of metamorphic rock fragments, polycrystalline quartz, and chert. The matrix comprises 17% of the rock. Both carbonate and quartz cements are present and make up 8% of the rock.

The Llanberis Slates Formation (Fig. 2.3) is a succession of dominantly fine-grained sediments with minor units of graded sandstone beds (including the sampled unit, the Dorothea Grit) (Crimes 1970) within the Arfon Basin. The trace fossil *Teichichnus* has been found within the Llanberis Slates Formation (McIlroy 1998), which also contains the trilobite *Pseudatops viola* in the highest levels of the unit above the Dorothea Grits (Howell and Stubblefield 1950). These early Cambrian trilobites are assigned to the *Strenuella sabulosa* zone by Fletcher (2006) approximately equivalent to the Australian *Pararaia bunyerooensis* zone (Cambrian Series 2, Stage 3), between ~515 and 516 Ma in the Peng et al. (2012) timescale. The Llanberis Slate Formation is also stratigraphically higher than the Minffordd Formation which is believed to be Cambrian rather than Precambrian because it contains sponge spicules (Rushton and Molyneux 2011), constraining the age of the sampled horizon between 541 Ma and 515 Ma.

ML010 was collected from the green, coarse-grained sandstone of the Dorothea Grit in the Alexandra Quarry [SH 51834 56078] (Fig. 2.7). The sandstone horizon is thin to very think bedded and is enveloped with red slate. The sample is poorly sorted, subrounded, muddy sandstone. It contains approximately 49% quartz, 10% polycrystalline quartz, 9% K-feldspar, 4% volcanic rock fragments, 3% plagioclase, 3% chert, 2% sedimentary rock fragments, 2% plutonic rock

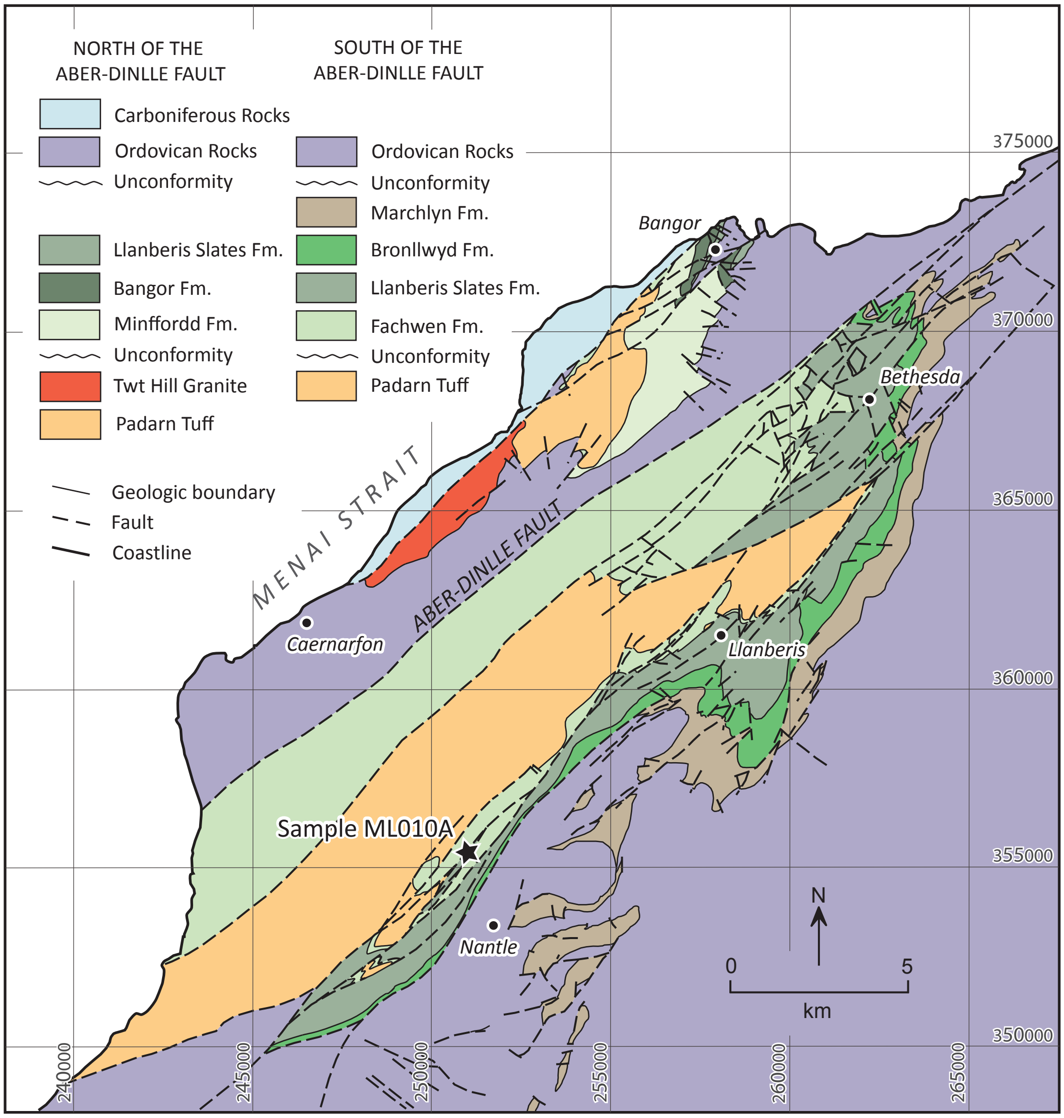

Figure 2.7: Geological map of the Arfon Basin (from British Geological Survey 1985, 1997, 2013). Ordnance Survey National Grid reference system.

fragments, and trace amounts of mica, chlorite, and opaque minerals. The matrix comprises 12% of the rock and carbonate cement makes up 6%.

2.4 ANALYTICAL TECHNIQUES

Detrital zircons from the four sandstone samples were extracted, mounted, imaged by electron backscatter, and dated using U-Pb laser ablation multicollector inductively coupled plasma mass spectrometry (LA-MC-ICP-MS). Procedures are modified from Simonetti et al. (2005). Between 120 and 200 grains were analyzed from each sample using a nominal beam diameter of 30 μm except when count rates exceeded the capacity of the ion counters in which case the spot size was reduced to a 20 μm nominal beam diameter. A fraction of grains from each sample was rejected when discordance values were elevated (>10%) or when the ^{206}Pb counts were below 10,000 cps. ^{204}Hg present in the argon gas supply produced elevated ^{204}Pb counts ranging roughly between zero and 200 cps. Only in cases where ^{204}Pb counts were elevated above background levels was the common-lead correction was applied using the two-stage evolution model of Stacey and Kramers (1975). In those cases the ^{204}Pb counts inevitably included an unpredictable background component; in most cases grains with elevated ^{204}Pb gave discordant results even after common lead correction.

A combination of $^{207}Pb/^{206}Pb$ or $^{206}Pb/^{238}U$ ages are reported depending on which result produced the lowest analytical error. The grains have been normalized using a combination of in-house standards LH94-15 (1.83 Ga, Ashton et al. 1999) and GJ1-32 (609 Ma, Simonetti et al. 2008). LH94-15 was used grains when the $^{207}Pb/^{206}Pb$ ratio of the unknown was greater than average $^{207}Pb/^{206}Pb$ ratio of the standard LH94-15. GJ1-32 was used for grains when the $^{207}Pb/^{206}Pb$ ratio of the unknown was less than the average $^{207}Pb/^{206}U$ ratio of the standard GJ1-32. For grains with intermediate $^{207}Pb/^{206}Pb$ ratios, normalization was carried out using a weighted combination of the two standards and their proportional errors, dependent on the $^{207}Pb/^{206}Pb$ ratio of the grain. Unless stated otherwise, all errors are reported using 2σ.

2.5 DETRITAL ZIRCON ANALYSIS RESULTS

The results from the detrital zircon analyses are plotted in Figures 2.8 and 2.9. The probability density plots (Fig. 2.9) describe the relative probability density of the occurrence of any given detrital age. The Cambrian (Drumian Stage) Gamlan Formation sample (ML001) shows a prominent early Cambrian cluster at c. 536 Ma and only a minor contribution of grains prior to the late Neoproterozoic. The youngest cluster of grains contains a spread of ages from 462 ± 60 to 718 ± 34 Ma with the most prominent cluster at c. 536 Ma and a second smaller peak at c. 700 Ma. In addition, there are two Mesoproterozoic grains (1238 ± 12 and 1353 ± 23 Ma), two Paleoproterozoic grains (1982 ± 8 and 1985 ± 10 Ma) and one Neoarchean grain (2657 ± 17 Ma). The early Cambrian to late Neoproterozoic peak is typical of peri-Gondwanan basins, including the Meguma

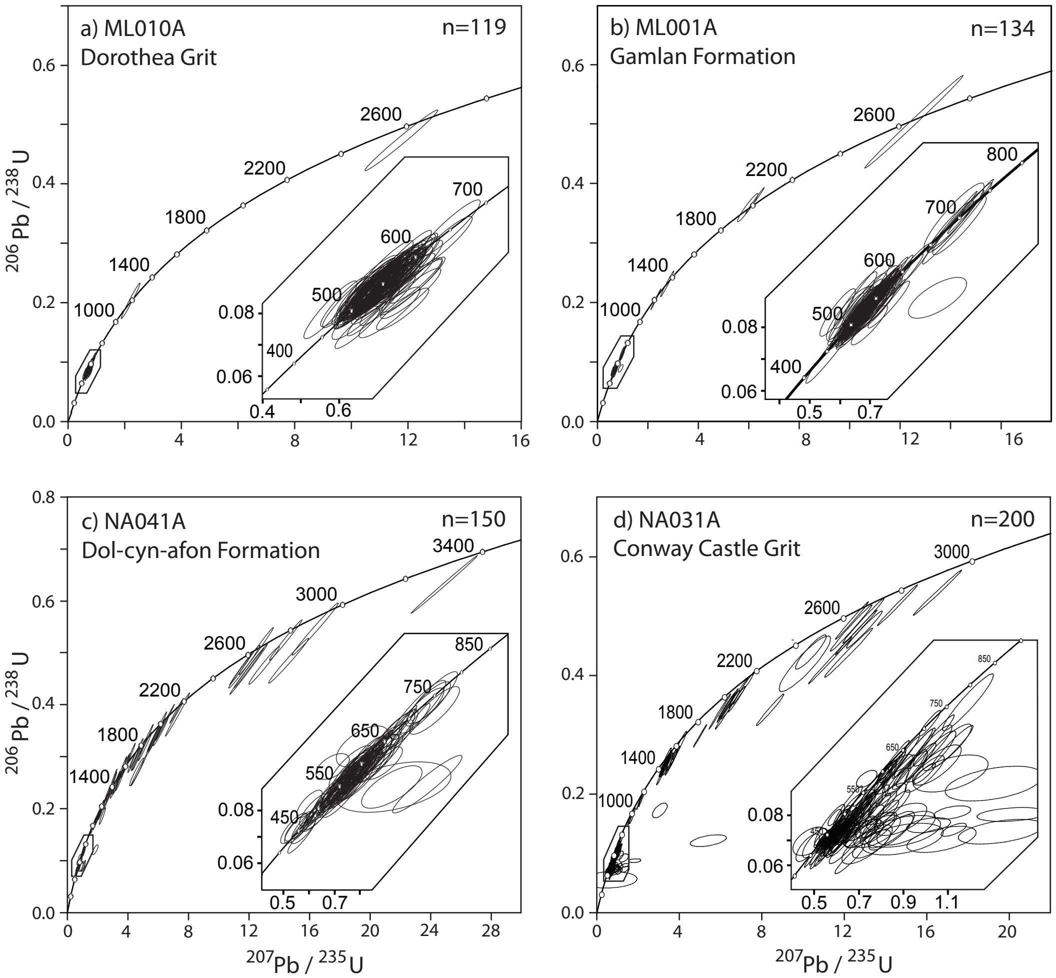

Figure 2.8: U-Pb concordia plot of all of the detrital zircon data from the a) Dorothea Grit, b) Gamlan Formation, c) Dol-cyn-afon Formation, and d) Conway Castle Grit. Ellipses represent 2-sigma uncertainties.

terrane of Nova Scotia (Krogh and Keppie 1990; Waldron et al. 2009) and eastern Avalonia (Murphy et al. 2004; Waldron et al. 2011), and reflects sources derived from within the Avalonian Panafrican orogens (Murphy et al. 2004). Northwest Africa is characterized by a lack of 1.0 to 1.7 Ga sources, so the Mesoproterozoic grains may have been derived from a source in eastern Avalonia. Similar ages are found within the early Cambrian Wrekin Quartzite (c. 535 Ma) (Murphy et al. 2004) and the Malvern Complex paragneiss (Strachan et al. 2007). However, grains of this age could have also been sourced from Amazonia (Litherland et al. 1985; Rowley and Pindell 1989). The West African (Eburnean) or Amazonian cratons are the likely source of the c. 2.0 Ga and Archean populations (Rocci et al. 1991; Lerouge et al. 2006; Waldron et al. 2009, 2011).

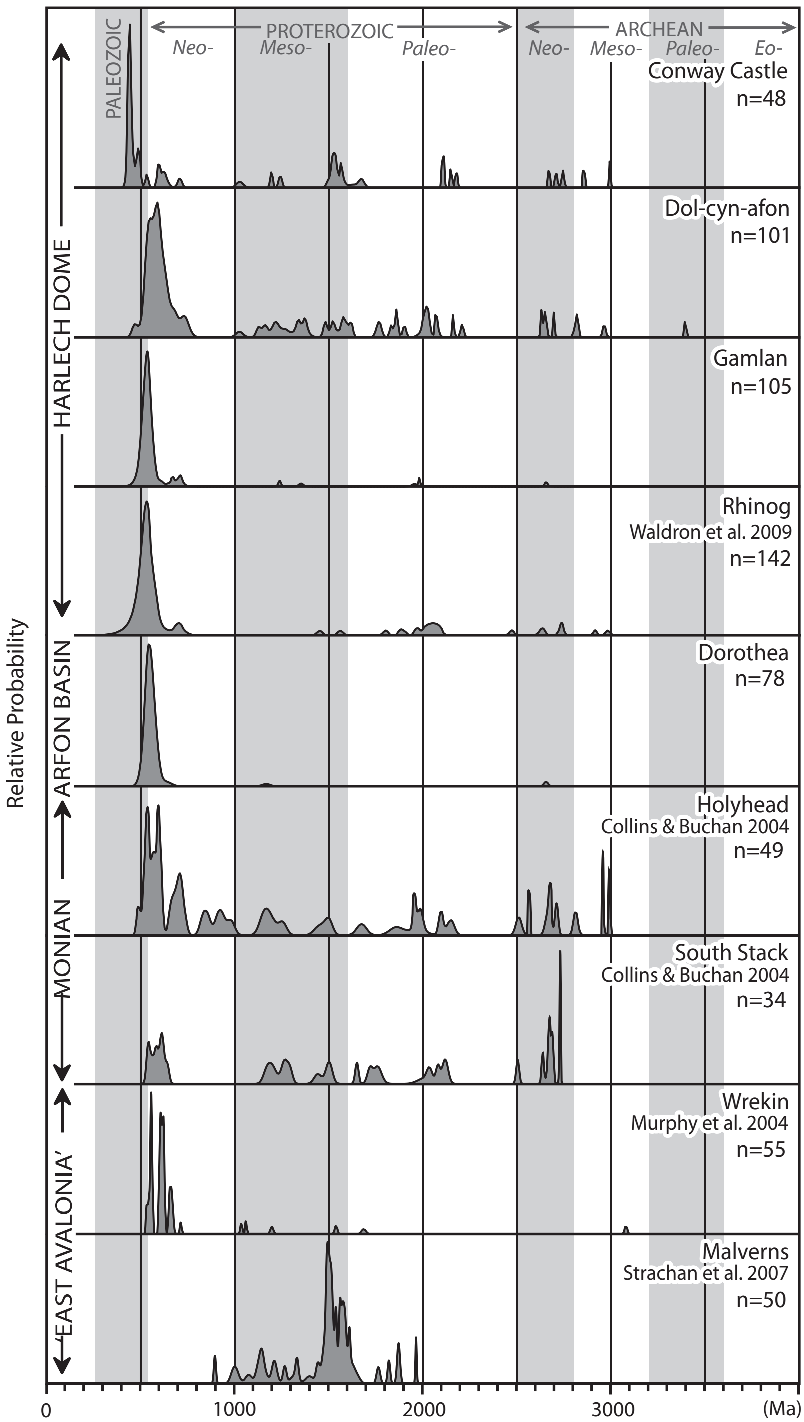

Figure 2.9: Probability density plots of detrital zircon data from North Wales compared with published results from Collins and Buchan (2004), Murphy et al. (2004), Strachan (2007) and Waldron et al. (2011). Calculations and plotting carried out with Isoplot 3.0 (Ludwig 2003).

There is a wide distribution of detrital zircon ages within the Tremadocian Dolcyn-afon sample (NA041). The most prominent peak is centered at c. 580 Ma and contains a spread of ages from 453 ± 25 to 741 ± 48 Ma (Fig. 2.9). There is a significant Mesoproterozoic and Paleoproterozoic grain population with a single grain at 967 ± 56 Ma and clusters at c. 1125 – 1380 Ma, c. 1480 – 1620 Ma, c.1760 – 1900 Ma and c. 2000 – 2200 Ma. The sample also contains seven Archean grains with ages between 2631 ± 8 to 3397 ± 7 Ma.

The Hirnantian Conway Castle Grit (sample NA031) yielded a pronounced Ordovician peak at 447 Ma and minor peak at 491 Ma. It also contains a population of late Neoproterozoic to early Paleozoic grains between 537 ± 16 and 712 ± 24 Ma. There is a significant Mesoproterozoic and Paleoproterozoic grain population with one grain at 1019 ± 31 Ma and clusters at c. 1040 – 1250, c. 1500 – 1680 Ma, and c. 2100 – 2200 Ma. The sample also contains five Archean grains between 2675 ± 9 and 2997 ± 8 Ma. This sample also recorded a number of discordant grains, most of which produced young Neoproterozoic to early Paleozoic $^{206}Pb/^{238}U$ ages.

Potential sources for the Mesoproterozoic ages in the Ordovician samples include Mesoproterozoic crust along the margin of Amazonia (Litherland et al. 1985; Rowley and Pindell 1989), recycled material from the Malverns Complex paragneiss in the Welsh Borderlands or the Coedana Complex paragneiss on Anglesey (Fig. 2.9) (Strachan et al. 2007), or from sources within the Monian Composite terrane or Leinster-Lakesman terrane (Collins and Buchan 2004; Waldron et al. *in preparation*).

The results from the Cambrian Dorothea Grits sample (ML010) show a limited source (Fig. 2.9). The largest population lies between 515 ± 38 and 653 ± 43 Ma with the most prominent peak at c. 550 Ma. A single Mesoproterozoic grain (1166 ± 42 Ma) and one Neoarchean grain at (2654 ± 23 Ma) were also present.

2.6 TECTONIC SIGNIFICANCE

2.6.1 Closure of the Iapetus Ocean

The closure of the Iapetus Ocean and the convergence of the Laurentian margin and the peri-Gondwanan terranes would likely be recorded by an influx of sediment from the newly adjacent source region. Laurentian detritus is characterized by abundant 0.95 to 1.3 Ga ages reflecting derivation from the Grenville orogen (e.g., Cawood et al. 2007; Waldron et al. 2008) and a significant increase of detritus of this age has been interpreted to record the convergence of Laurentia with other peri-Gondwanan terranes (Waldron et al. 2011; Waldron et al. *in preparation*). Although there is a small cluster between 1.0 and 1.3 Ga in the Ordovician samples, it is not the dominant age population as seen in other units derived from Laurentian sources. This indicates that the Welsh Basin was not in close proximity to Laurentia in the latest Ordovician, which is in agreement with Soper and Woodcock (1990) and Cocks and Torsvik (2002) who suggest the closure of the Iapetus Ocean occurred in the late Llandovery to Wenlock Epoch.

2.6.2 Arfon Basin

The Arfon Basin has a distinct Cambrian stratigraphy and has yet to be definitively linked to either the Harlech Dome succession or the Monian Supergroup. Brenchley et al. (2006) suggested that the basin developed along the SE margin of the Irish Sea platform in response to strike-slip movement along the Menai Strait Fault System. Reedman et al. (1984) proposed a connection between the Minffordd Formation and the outliers of the Careg Onen Beds in southern Anglesey, but only on the basis of lithology and the presence on sponge spicules (Fig. 2.3). Shackleton (1975) suggested that the basaltic material present in the Minffordd Formation was derived from Gwna Group lavas; however, it is now known that the Gwna Group is likely of the same age or younger than the Minffordd Formation and therefore not a likely source. Tucker and Pharaoh (1991) suggested a link between the Coedana Granite and the Padarn Tuff both of which have been dated at approximately 614 Ma.

The similarities between the Harlech Dome and the Arfon Basin successions are distant and few. Both Cambrian successions rest upon volcanic rocks. However the Bryn-teg Volcanics Formation consists of andesite and dacite while the

Arfon Group volcanic rocks are predominantly rhyolite and ash-flow tuff (Allan and Jackson 1978). Despite their compositional differences, Allan and Jackson (1978) proposed that a correlation may still exist based on the presence of rhyolite pebbles in the base of the Dolwen Formation, which may have been derived from a lateral equivalent, such as the Arfon Group, that was not preserved in the location of the Bryn-teg borehole.

The detrital zircon age distribution of the Dorothea Grit does not reflect any intrabasinal sources (Twt Hill Granite or Padarn Tuff) and it is different from samples from both the Harlech Dome and the Monian Composite terrane. The Dorothea Grit sample shows the same Neoproterozoic peak (c. 530 Ma) displayed in the Gamlan and Rhinog formations; however, it is lacking the c. 2.0 Ga West African population characteristic of the Harlech Dome and the Meguma terrane (Waldron et al. 2009, 2011). A detrital zircon sample collected from the Wrekin quartzite (c. 535 Ma) from the English Midlands in Shropshire (Murphy et al. 2004) shows some similarities to the Dorothea Grit. The Wrekin quartzite contains a more diverse grain population, but it does share the Neoproterozoic grain population, contains one Mesoproterozoic grain (1198 Ma) and contains no c. 2.0 Ga zircons.

If the Arfon Basin was in close proximity to the Monian Composite Terrane during the early Cambrian it is likely that the age distribution would reflect sources found there. However, the limited age distribution found in the sample suggests otherwise. The sample does not reflect any ages from the Coedana granite (613 ± 4 Ma) (Tucker and Pharaoh, 1991) or the Coedana Complex paragneiss, which contain a range of detrital zircon ages from 852 ± 27 to 2742 ± 18 Ma (Strachan et al. 2007). It also lacks the significant Meso- and Paleoproterozoic grain population found in the Holyhead and South Stack formations in Anglesey (Collins and Buchan 2004) (Fig. 2.9).

A peak c. 550 Ma in the detrital zircon record is common in parts of Ganderia and also within the east Avalonia; however, there are no known igneous bodies *in situ* of this age in east Avalonia (Murphy et al. 2004). This suggests detritus from an unseen body may have inundated the basins. West Avalonia is generally characterized by a prominent c. 620 Ma peak, but 560 – 550 Ma rocks are present (Barr et al. 2012).

The stratigraphic and provenance differences between the Arfon Basin sediments and the adjacent Monian Supergroup and Harlech Dome successions suggests that this fault-bounded basin originated elsewhere in the peri-Gondwanan realm and was emplaced into its current position during the amalgamation of the Welsh Basin with the Monian Composite Terrane.

2.6.3 Cambrian – Ordovician tectonic events in the Welsh Basin

Harlech Dome: Cambrian

The age distribution of detrital zircon grains in the Gamlan Formation sample exhibits a very similar distribution to that found in the underlying lower Cambrian Rhinog Formation (Waldron et al. 2011) (Fig. 2.9). They both display a prominent early Cambrian to late Neoproterozoic peak, minor peaks at c. 650 Ma and c. 2.0 Ga, and both contain c. 2.6 Ga grains. These similarities suggest that the source region for the Welsh Basin during the Cambrian Series 2 Drumian remained nearly unchanged since the deposition of the Rhinog Formation in the lower Cambrian. Waldron et al. (2009, 2011) suggested that the lower Harlech Dome succession was deposited in a deep-sea rift basin between the Gondwanan margin, near the West African craton, and Eastern Avalonia.

Tremadocian Events

In the Monian Composite Terrane major deformation and metamorphism to greenschist facies is recorded by fabrics and folds trending roughly NE to SW (Treagus et al. 2003; Treagus et al. 2013). The timing of this deformation is constrained between the deposition of the Gwna Group, which is no older than late Terreneuvian, and the Floian overstep sedimentary rocks.

During this general interval, in the Harlech dome, the Dol-cyn-afon Formation records shallowing and an influx of diverse zircon suggesting a source similar to Monian Composite Terrane. The region was tilted after the deposition of the Dol-cyn-afon Formation but prior to eruption of the Rhobell Volcanics in the late Tremadocian. The metamorphic grade and intensity of deformation is much lower than the Monian Composite Terrane (Allen and Jackson 1985). Pre-Floian sedimentary rocks in the Harlech Dome region are folded into NNE- to north trending folds. A second episode of deformation occurred after the extrusion of the Rhobell Volcanics Group, resulting in a second unconformity below the Floian cover. This deformation was accompanied by fracture reactivation and uplift (Kokelaar 1988), which progressively diminishes to the southeast (Shackleton 1954).

Deformation of the Arfon succession is poorly known but occurred at low metamorphic grade similar to the Harlech dome. Schofield et al (2008) suggested a Rb-Sr isochron age of 491 ± 12 Ma from the Twt Hill Granite was a deformation age, which would be consistent with 'Monian' deformation in both the adjoining terranes.

Another short-lived compressional event is recorded in the Northern Appalachian in Atlantic Canada between 486 Ma and 479 Ma (van Staal et al. 1998). This event resulted in the obduction of the Penobscot backarc basin ophiolites onto Ganderia (Colman-Sadd et al. 1992; Zagorevski et al. 2010). Although the nature of the deformation varies, the kinematic differences could be explained by an overall sinistral transpressional setting and curvature in the plate boundary.

2.6.4 Late Ordovician History

The Hirnantian Conway Castle sample yielded similar results to the Tremadocian Dol-cyn-afon sample (Fig. 2.9). They both have a prominent late Neoproterozoic to early Cambrian zircon population, and clusters between c. 1000 – 1250 Ma, c. 1500 – 1800 Ma and c. 2000 – 2200 Ma, as well as a spread of Archean grains. This indicates that the source region for North Wales was the same throughout the Ordovician.

2.6.5 Tectonic Model

During the Cambrian Period the detrital zircon record in the Harlech Dome suggests it was deposited between Avalonia and the Gondwanan margin, likely close to the West African craton. Waldron et al. (2011) proposed that it could have been positioned in a rift system between East and West Avalonia. The Cambrian detrital zircon record in the Arfon Basin suggests a slightly different source region than the sedimentary rocks of the Harlech Dome and the Monian Supergroup of the Monian Composite terrane. Movement along the Menai Strait Fault System may have resulted in the formation of several small basins. The Arfon Basin was likely one such basin, and was caught up in the fault system and emplaced between the Monian Composite terrane and the Welsh Basin. The shared post-

Tremadocian sedimentary succession across all three regions indicates that they remained in generally the same configuration after this time and that they moved as a coherent unit towards Laurentia.

Figures 2.10 and 2.11 illustrate possible terrane configurations based on these assumptions, and are also consistent with the differences in lithostratigraphy and provenance, and a sinistral strike-slip tectonic setting.

Figure 2.10a shows a paleocontinental reconstruction that places Avalonia and Ganderia in their traditional (e.g., van Staal 2010) orientations relative to the Gondwanan margin. Here the diverging Ordovician histories of the Meguma terrane and the Welsh Basin are explained by sinistral movement along a secondary fault cutting through Megumia that disconnects the basins. To accommodate sinistral movement along the Menai Strait Fault System and bring the Monian Composite terrane together with the Welsh Basin (Fig. 2.10b), Ganderia must be positioned closer to West Africa; however this contradicts the interpretation of many (e.g., van Staal et al. 2012; Pollock et al. 2009) who would place Ganderia next to Amazonia and Avalonia closer to West Africa.

Figure 2.11a shows an alternative paleocontinental reconstruction that maintains an Amazonian provenance for Ganderia and places Avalonia closer to West Africa. To maintain sinistral movement along the Menai Strait Fault System their orientations relative to the Gondwanan margin have been rotated roughly 180º. The separation of the Meguma terrane from the Welsh basin in this scenario is also explained by sinistral movement along a fault that divides Megumia. This brings the Welsh Basin and East Avalonia in contact with Ganderia. This is followed by activation of a new fault, which juxtaposed both East and West Avalonia with Ganderia.

The tectonic model illustrated in Figure 2.11 is the preferred scenario; however, it requires significant clockwise rotation of the peri-Gondwanan terranes prior to their accretion to the Laurentian margin. Waldron et al. (2011) proposed one possible East Avalonia orientation that was rotated roughly 180º from its more generally accepted orientation. There is some paleomagnetic evidence from Britain that points to a clockwise rotation up to 85º (Torsvik 1993) interpreted to have occurred during the late Carboniferous Variscan deformation, but possibly reflecting an earlier rotation trend.

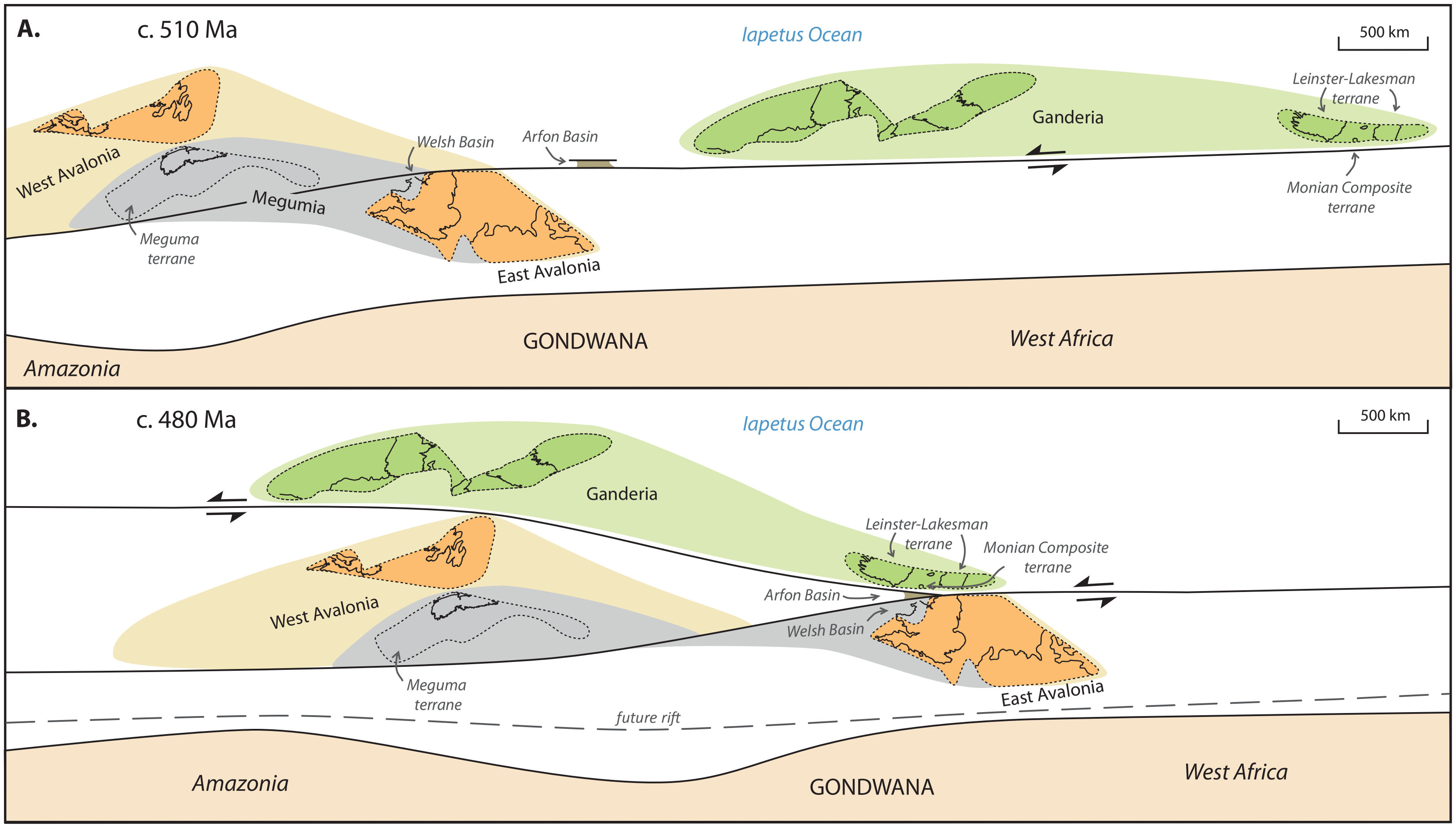

Figure 2.10: Paleogeographic reconstruction illustrating possible positions of tectonic elements along the Gondwanan margin in the Cambrian and Early Ordovician.

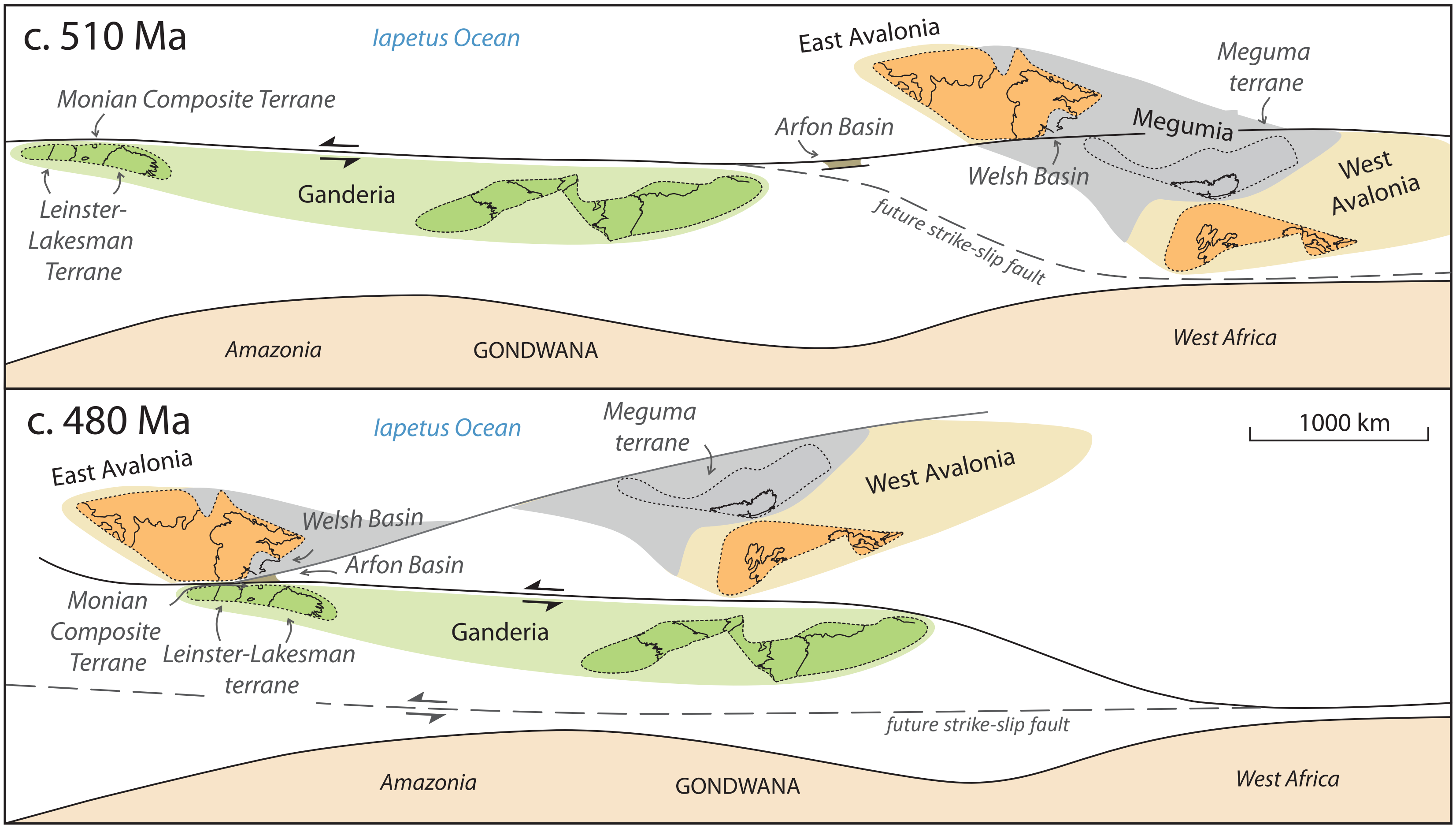

Figure 2.11: Paleogeographic reconstruction illustrating possible positions of tectonic elements along the Gondwanan margin in the Cambrian and Early Ordovician in which the domains in Fig. 2.10 have been rotated 180º.

2.7 CONCLUSIONS

The Cambrian successions of the Harlech Dome, Arfon Basin and Monian Supergroup show contrasting detrital zircon distributions in addition to distinct lithostratigraphic successions, suggesting that they were dispersed tectonic fragments receiving sediment from different source regions along the Gondwanan margin. Deformation in the Monian Composite Terrane suggests an overall environment of sinistral transpression, which brought it together with the terranes that now lie to the South. By the Tremadocian, the Welsh Basin began to see an influx of 'Monian' detritus indicating that North Wales was juxtaposed with the Monian composite terrane along the Menai Strait Fault System by this time. The same overall sinistral movement could account for the removal of the Meguma Terrane from an original position adjacent to the Harlech Dome. The shared post-Floian cover between the Harlech Dome and Arfon basins indicates these two regions were also located next to one another at this time. Derivation of sediment from the Monian composite terrane into the Welsh Basin continued at least until the Hirnantian, but the absence of Laurentian detritus indicates that collision with Laurentia was Silurian or later.

2.8 REFERENCES

Allen, P.M., Jackson, A.A. and Rushton, A.W.A. 1981. The Stratigraphy of the Mawddach Group in the Cambrian Succession of North Wales. Proceedings of the Yorkshire Geological Society, 43: 295–329.

Allen, P.M. and Jackson, A.A. 1978. Bryn-teg borehole, North Wales. Bulletin of the Geological Survey of Great Britain, 61.

Allen, P.M. and Jackson, A.A. 1985. Geology of the country around Harlech. Memoir of the British Geological Survey, Sheet 135 with part of 149. British Geological Survey, Keyworth, Nottingham.

Ashton, K.E., Heaman, L.M., Lewry, J.F., Hartlaub, R.P. and Shi, R. 1999. Age and origin of the Jan Lake Complex: a glimpse at the buried Archean craton of the Trans-Hudson Orogen. Canadian Journal of Earth Sciences, 36: 185–208.

Barnes, C.G., Frost, C.D., Yoshinobu, A.S., McArthur, K. Barnes, M.A., Allen, C.M., Nordgulen, Ø. and Prestvik, T. 2007. Timing of sedimentation, metamorphism, and plutonism in the Helgeland Nappe Complex, north-central Norwegian Caledonides. Geosphere, 3: 683–703.

Barr, S.M., Hamilton, M.A., Samson, S.D., Satkoski, A.M., White, C.E. and Murphy, J.B. 2012. Provenance variations in northern Appalachian Avalonia based on detrital zircon age patterns in Ediacaran and Cambrian sedimentary rocks, New Brunswick and Nova Scotia, Canada. Canadian Journal of Earth Sciences, 49: 533–546.

Bates, D.E.B. 1968. The Lower Palaeozoic Brachiopod and Trilobite Faunas of Anglesey. Bulletin of the British Museum (Natural History) Geology Series, 16, pp. 127.

Bates, D.E.B. 1972. The Stratigraphy of the Ordovician rocks of Anglesey. Geological Journal, 8: 29–58.

Beckinsale, R.D. and Rundle, C.C. 1980. K-Ar ages for amphibole separates from the Rhobell Volcanic Group (upper Tremadocian), Harlech Dome, North Wales. Institute of Geological Sciences, Issue 80/1, pp. 9–11.

Brenchley, P.J. and Cullen, B. 1984. The environmental distribution of associations belonging to the Hirnantia fauna - Evidence from North Wales and Norway. *In* Aspects of the Ordovician System. *Edited by* D.L. Bruton. Palaeontological Contributions from the University of Oslo, No. 295, pp. 113–125.

Brenchley P.J. and Newall, G. 1980. A Facies Analysis of Upper Ordovician Regressive Sequences in the Oslo Region, Norway - a Record of Glacio-Eustatic Changes. Palaeogeography, Palaeoclimatology, Palaeoecology, 31: 1–38.

Brenchley, P.J. and Rawson, G. 2006. England and Wales through geologic time. *In* The Geology of England and Wales. *Edited by* P.J. Brenchley and P.F. Rawson. Geological Society, London, pp. 1–23.

Brenchley, P.J., Rushton, A.W.A., Howells, M. and Cave, R. 2006. Cambrian and Ordovician: the early Palaeozoic tectonostratigraphic evolution of the Welsh Basin, Midland and Monian Terranes of Eastern Avalonia. *In* The Geology of England and Wales. *Edited by* P.J. Brenchley and P.F. Rawson. Geological Society, London, pp. 25–74.

British Geological Survey 1982. Harlech. England and Wales Sheet 135 and part of sheet 149. Solid and Drift Geology 1:50 000 (Keyworth. Nottingham: British Geological Survey).

British Geological Survey 1985. Bangor. England and Wales Sheet 106. Solid Geology 1:50 000 (Keyworth. Nottingham: British Geological Survey).

British Geological Survey 1989. Llandudno. England and Wales Sheet 94. Solid and Drift Geology 1:50 000 (Keyworth. Nottingham: British Geological Survey).

British Geological Survey 1997 Snowdon, England and Wales Sheet 119. Solid Geology 1:50 000 (Keyworth. Nottingham: British Geological Survey).

British Geological Survey 2013. Nefyn and part of Caernarfon. England and Wales Sheets 118 and part of Sheet 105. Bedrock and Superficial Deposits. 1:50 000 (Keyworth. Nottingham: British Geological Survey).

British Geological Survey 2007. Bedrock Geology UK South (South of National Grid Line 540 km N), 1:625 000, 5th edition. (Keyworth. Nottingham: British Geological Survey).

Cawood, E.A., Nemchin, A.A., Strachan, R., Prave, T. and Krabbendam, M. 2007. Sedimentary basin and detrital zircon record along East Laurentia and Baltica during assembly and breakup of Rodinia. Journal of the Geological Society, London, 164: 257–275.

Cherns, L., Cocks, L.R.M., Davies, J.R., Hillier, R.D., Waters, R.A. and Williams, M. 2006. Silurian: the influence of extensional tectonics and sea-level changes on sedimentation in the Welsh Basin and on the midland Platform. *In* The Geology of England and Wales. *Edited by* P.J. Brenchley, and P.F. Rawson. Geological Society, London, pp .74–102.

Cocks, L.R.M. and Torsvik, T.H. 2002. Earth geography from 500 to 400 million years ago: a faunal and palaeomagnetic review. Journal of the Geological Society, London, 159: 31–644.

Collins, A.S. and Buchan, C. 2004. Provenance and age constraints of the South Stack Group, Anglesey, UK: U–Pb SIMS detrital zircon data. Journal of the Geological Society, London, 161: 743–746.

Colman-Sadd, S.P., Dunning, G.R. and Dec, T. 1992. Orogeny in central Newfoundland: a sediment provenance and U/Pb age study. American Journal of Science, 292: 317–355.

Compston, W., Wright, A.E. and Toghill, P. 2002. Dating the Late Precambrian volcanicity of England and Wales. Journal of the Geological Society, London, 159: 323–339.

Cooper, R.A. and Sadler, P.M. 2012 The Cambrian Period. *In* The Geologic Time Scale *Edited by* F.M. Gradstein, J.G. Ogg, M. Schmitz, and G. Ogg. Elsevier, pp. 489–523.

Crimes, T.P. 1970. A facies analysis of the Cambrian of Wales. Palaeogeography, Palaeoclimatology, Palaeoecology, 7: 113–170.

Davidek, K., Landing, E., Bowring, S.A., Westrop, S.R., Rushton, A.W.A., Fortey, R.A. and Adrain, A. 1998. New uppermost Cambrian U–Pb date from Avalonian Wales and the age of the Cambrian–Ordovician boundary. Geological Magazine, 135, 227–229.

Elles, G.L. 1909. The relation of the Ordovician and Silurian rocks of Conway (North Wales). Quarterly Journal of the Geological Society, London, 65: 169–194.

Fletcher, T.P. 2006. Bedrock geology of the Cape St. Mary's Peninsula, southwest Avalon Peninsula, Newfoundland (incudes parts of NTS map sheets 1M/1, 1N/4, 1L/16 and 1K/13), Newfoundland. Government of Newfoundland and Labrador, Geological Survey, Department of Natural Resources, St. John's, Report 06-02.

Gibbons, W. 1987. Menai Strait fault system: An early Caledonian terrane boundary in north Wales. Geology, 15: 744–747.

Gibbons, W. 1983. The Monian 'Penmynydd Zone of Metamorphism' in Llŷn, North Wales. Geological Journal, 18: 21–41.

Greenly, E. 1919. The geology of Anglesey. United Kingdom Geological Survey Memoir (2 vols.), London.

Greenly, E. 1946. The Monio-Cambrian Interval. Geological Magazine, 83: 237–240.

Harland, W.B. and Gayer, R.A. 1972. The Arctic Caledonides and earlier Oceans. Geological Magazine, 109: 289–314.

Hibbard, J.P., van Staal, C.R. and Rankin, D.W. 2007. A comparative analysis of pre-Silurian crustal building blocks of the northern and the southern Appalachian orogen. American Journal of Science, 307: 23–45.

Howells, M.F. and Smith, M. 1997. The Geology of the country around Snowdon. Memoir of the British Geological Survey, Sheet 119 (England and Wales), London.

Howell, B.F. and Stubblefield, C.J. 1950. A Revision of the Fauna of the North Welsh Conocoryphe viola Beds implying a Lower Cambrian Age. Geological Magazine, 87: 1–16.

Kokelaar, B.P. 1988. Tectonic controls of Ordovician arc and marginal basin volcanism in Wales. Journal of the Geological Society, London, 145: 759–775.

Kokelaar, B.P., Howells, M.F., Bevins, R.E., Roach, R.A. and Dunkley, P.N. 1984. The Ordovician marginal basin of Wales. Geological Society, London, Special Publications 16: 245–269

Krogh, T.E. and Keppie, J.D. 1990. Age of detrital zircon and titanite in the Meguma

Group, southern Nova Scotia, Canada: Clues to the origin of the Meguma Terrane. Tectonophysics, 177: 307–323.

Lerouge, C., Cocherie, A., Toteu. S.F., Penaye, J., Milési, J.P., Tchameni, R. Nsifa, E.N., Fanning, C.M. and Deloule, E. 2006. Shrimp U–Pb zircon age evidence for Paleoproterozoic sedimentation and 2.05Ga syntectonic plutonism in the Nyong Group, South-Western Cameroon: consequences for the Eburnean–Transamazonian belt of NE Brazil and Central Africa. Journal of African Earth Sciences, 44: 413–427.

Litherland, M., Klinck, B.A., O'Connor, E.A. and Pitfield, P.E.J. 1985. Andean-trending mobile belts in the Brazilian Shield. Nature, 314: 345–348.

Ludwig, K.R. 2003. User's Manual for Isoplot 3.00. Berkeley Geochronology Center Special Publication, 4.

McIlroy, D., Brasier, M.D. and Moseley, J.B. 1998. The Proterozoic–Cambrian transition within the 'Charnian Supergroup' of central England and the antiquity of the Ediacara fauna. Journal of the Geological Society, London, 155: 401–411.

McKerrow, W.S., Niocaill, C.M. and Dewey, J.F. 2000. The Caledonian Orogeny redefined. Journal of the Geological Society, London, 157: 1149–1154.

Morris, T.O. and Fearnsides, W.G. 1926. The Sratigraphy and Structure of the Cambrian Slate-Belt of Nantlle, (Carnarvonshire). Quarterly Journal of the Geological Society, London, 82: 250–303.

Muir, M.D., Bliss, G.M., Grant, P.R. and Fisher, M.J. 1979. Palaeontological evidence for the age of some supposedly Precambrian rocks in Anglesey, North Wales. Journal of the Geological Society, London, 136: 61–64.

Murphy, J.B., Fernandez-Suarez, J., Jeffries, T.E. and Strachan, R.A. 2004. U–Pb (LA–ICP-MS) dating of detrital zircons from Cambrian clastic rocks in Avalonia: erosion of a Neoproterozoic arc along the northern Gondwanan margin. Journal of the Geological Society, London, 161: 243–254.

Nance, R.D. and Murphy, J.B. 1994. Contrasting basement isotopic signatures and the palinspastic restoration of peripheral orogens: examples from the Neoproterozoic Avalonian–Cadomian belt. Geology, 22: 617–620.

Nance, R.D., Murphy, J.B., Strachan, R., D'Lemos, R. A. and Taylor, G.K. 1991. Late Proterozoic tectonostratigraphic evolution of the Avalonian and Cadomian terranes. Precambrian Geology, 53: 41–78.

Neuman, R.B. and Bates, D.E.B. 1978. Reassessment of Arenig and Llanvirn age (Early Ordovician) brachiopods from Anglesey, north-west Wales. Palaeontology, 21: 571–613.

Parrish, R.R. 1999. The age of the volcanic rocks at the Parys Mountain VMS deposit, Wales. Appendix 3A. *In* Geology and mineralization of the Parys Mountain polymetallic deposit, Wales, United Kingdom: Bangor, Wales, Anglesey Mining plc, unpublished report. *Edited by* T.J. Barrett, S.C. Tennant, and W.H. MacLean.

v. 1 (text) and v. 2 (appen.).

Peng, S., Babcock, L.E. and Cooper, R.A. 2012. The Cambrian Period. *In* The Geologic Time Scale *Edited by* F.M. Gradstein, J.G. Ogg, M. Schmitz, and G. Ogg. Elsevier, pp. 437–488.

Pharaoh, T.C. and Carney, J.N. 2000. Introduction to the Precambrian rocks of England and Wales. *In* Precambrian Rocks of England and Wales. *Edited by* J.N. Carney, J.M. Horak, T.C. Pharaoh, W. Gibbons, D. Wilson, W.J. Barclay, R.E. Bevins, J.C.W. Cope and T.D. Ford, Geological Conservation Review Series, No. 20, Joint Nature Conservation Committee, Peterborough, pp. 1–17.

Pollock, J.C. Hibbard, J.P. and Sylvester, P.J. 2009. Early Ordovician rifting of Avalonia and birth of the Rheic Ocean: U−Pb detrital zircon constraints from Newfoundland. Journal of the Geological Society, London, 166: 501–515.

Reedman, A.J., Leveridge, B.E. and Evans, R.B. 1984. The Arfon Group ('Aronian') of North Wales. Proceedings of the Geologist' Association. 95: 313–321.

Rocci, G., Bronner, G. and Deschamps, M. 1991, Crystalline basement of the West African Craton. *In* The West African orogens and circum-Atlantic correlatives:. Edited by R.D. Dallmeyer and J.P. Lécorché. Springer-Verlag, Berlin, Germany, pp. 31–61.

Rowley, D.B. and Pindell. J.L. 1989. End Paleozoic-Early Mesozoic western Pangean reconstruction and its implications for the distribution of Precambrian and Paleozoic rocks around Meso-America. Precambrian Research, 42:3 411–444.

Rushton, A.W.A. and Fortey. R.A. 2000. North Wales. *In* A revised correlation of Ordovician rocks in the British Isles. *Edited by* R.A. Fortey, D.A. Harper, J.K. Ingham, A.W. Owen, M.A. Parks, A.W.A. Rushton and N.H. Woodcock. The Geological Society, Special Report 24, pp. 18–24.

Rushton, A.W.A. and Howells, M.F. 1998. Stratigraphical framework for the Ordovician of Snowdonia and the Lleyn Peninsula: a discussion of the Tremadoc to Caradoc rocks lying between the Menai Straits and the Llanderfel Syncline, and including an appendix on Cambrian rocks. Version 2. British Geological Survey Research Report RR/99/08.

Rushton, A.W.A. and Molyneux, S.G. 2011. Welsh Basin. *In* A Revised Correlation of the Cambrian Rocks in the British Isles. *Edited by* A.W.A. Rushton, P.M. Brück, S.G. Molyneux, M. Williams and N.H. Woodcock. Geological Society, London, Special Report 25, pp. 21–27.

Rushton, A.W.A., Owen, A.W., Owens, R.M. and Prigmore, J.K. 2000. British Cambrian to Ordovician Stratigraphy. Geological Conservation Review Series, No. 18, Joint Nature Conservation Committee, Peterborough.

Schofield, D.I., Evans, J.A., Millar, I.L., Wilby, P.R. and Aspden, J.A. 2008. New U-Pb and Rb-Sr constraints on pre-Acadian tectonism in North Wales. Journal of the Geological Society, London, 165: 892–894.

Shackleton, R.M. 1954. The structure and succession of Anglesey and the Lleyn Peninsula. Advancement of Science, London, 11: 106–108.

Shackleton, R.M. 1969. The PreCambrian of North Wales. *In* The PreCambrian and Lower Palaeozoic rocks of Wales. *Edited by* A. Wood. University of Wales Press, Cardiff, pp. 1–22.

Shackleton, R.M. 1975. Precambrian rocks of Wales. *In* A correlation of the Precambrian rocks in the British Isles. *Edited by* A.L. Harris, R.M. Shackleton, J. Watson, C. Downie, W.B. Harland and S. Moorbath. Special Report of the Geological Society of London, 6: 76–82.

Simonetti, A., Heaman, L.M., Hartlaub, R.P., Creaser, R.A., MacHattie, T.G. and Böhm, C. 2005. U–Pb zircon dating by laser ablation-MC-ICP-MS using a new multiple ion counting Faraday collector array. Journal of Analytical Atomic Spectrometry, 20: 677–686.

Simonetti, A., Heaman, L.M. and Chacko, T. 2008. Chapter 14: Use of discrete-dynode secondary electron multipliers with faradays – A 'reduced volume' approach for in situ U-Pb dating of accessory minerals within petrographic thin section by LA-ICP-MS. *In* Mineralogical Association of Canada Short Course 40, Vancouver, pp. 241–264.

Soper, N.J. and Woodcock, N.H. 1990. Silurian collision and sediment dispersal patterns in southern Britain. Geology Magazine, 127: 527–542.

Stacey, J.S. and Kramers, J.D. 1975. Approximation of terrestrial lead isotope evolution by a two-stage model. Earth and Planetary Science Letters, 26: 207–221.

Strachan, R.A., Collins, A.S., Buchan, C., Nance, R.D., Murphy, J.B. and D'Lemos, R.S. 2007. Terrane analysis along a Neoproterozoic active margin of Gondwana: insights from U–Pb zircon geochronology. Journal of the Geological Society, London, 164: 57–60.

Torsvik, T.H., Trench, A. Svensson, I. and Walderhaug, H.J. 1993. Palaeogeographic significance of mid-Silurian palaeomagnetic results from southern Britain—major revision of the apparent polar wander path for eastern Avalonia. Geophysical Journal International, 113: 651–661.

Treagus, S.H., Treagus, J.E. and Droop, G.T.R. 2003. Superposed deformations and their hybrid effects: the Rhoscolyn Anticline unraveled. Journal of the Geological Society, London, 160: 117–136.

Treagus, J.E., Treagus, S.H. and Woodcock, N.H. 2013. The significance of the boundary between the Rhoscolyn and New Harbour formations on Holy Island, North Wales, to the deformation history of Anglesey. Geological Magazine, 150: 519–535.

Tucker, R.D. and Pharaoh, T.C. 1991. U–Pb zircon ages for Late Precambrian igneous rocks in southern Britain. Journal of the Geological Society, London, 148: 435–443.

van Staal, C.R., Sullivan, R.W., Whalen, J.B. 1996. Provenance of tectonic history of the

Gander Zone in the Caledonian/Appalacian Orogen: Implications for the origin and assembly of Avalon. Geological Society of America Special Papers, 304: 347–367.

van Staal, C.R., Dewey, J.F., MacNiocaill, C. and McKerrow, W.S. 1998. The Cambrian–Silurian tectonic evolution of the northern Appalachians and British Caledonides: history of a complex, west and southwest Pacific-type segment of Iapetus. *In* Lyell; the Past is the Key to the Present. *Edited by* D.J. Blundell and A.C. Scott. Geological Society, London, Special Publications, 143: 199–242.

van Staal, C.R., Barr, S.B. and Murphy, J.B. 2012. Provenance and Tectonic Evolution of Ganderia: Constraints on the Evolution of the Iapetus and Rheic Oceans. Geology, 40: 987–990.

Waldron, J.W.F., White, C.E., Barr, S.M., Simonetti, A. and Heaman, L.M. 2009. Provenance of the Meguma terrane, Nova Scotia: rifted margin of early Paleozoic Gondwana. Canadian Journal of Earth Sciences, 46: 1–9.

Waldron, J. W. F., Schofield, D.I., White, C.E. and Barr, S.M. 2011. Cambrian successions of the Meguma Terrane, Nova Scotia, and Harlech Dome, North Wales: dispersed fragments of a peri-Gondwanan basin?. Journal of the Geological Society, London, 168: 83–98.

Waldron, J.W.F., Schofield, D.I., DuFrane, S.A., Floyd, J., Crowley, Q.G., Simonetti, T., Dokken, R. and Pothier, H. *in preparation*. Ganderia-Laurentia collision in the Caledonides of Great Britain and Ireland.

Waldron, J.W.F., Floyd, J.D., Simonetti, A. and Heaman, L.M. 2008. Ancient Laurentian detrital zircon in the closing Iapetus Ocean, Southern Uplands terrane, Scotland. Geology, 8: 527–530.

Woodcock, N.H. 1990. Sequence stratigraphy of the Palaeozoic Welsh Basin. Journal of the Geological Society, London, 147: 537–547.

Woodcock, N.H. and Gibbons, W. 1988. Is the Welsh Borderland fault system a terrane boundary?. Journal of the Geological Society, London, 145: 915–923.

Zagorevski, A., van Staal, C.R., Rogers, N., McNicoll, V.J. and Pollock, J. 2010. Middle Cambrian to Ordovician arc-backarc development on the leading edge of Ganderia, Newfoundland Appalachians. Geological Society of America Memoirs, 206: 367–396.

CHAPTER 3: PROVENANCE AND DEPOSITIONAL ENVIRONMENT OF THE EARLY ORDOVICIAN CLASTIC ROCKS OF THE MEGUMA TERRANE

A version of this chapter will be submitted for publication under the following authorship
Pothier, H., Waldron, J.W.F., White, C.E., and DuFrane, S.A.

3.1 INTRODUCTION

Clastic sedimentary rocks of the Meguma Terrane, the most outboard terrane of the Canadian Appalachians, have no correlatives elsewhere in Atlantic Canada, and their source has been the subject of disagreement. The terrane resided along the northern margin of Gondwana during the Cambrian; however its exact position along the margin relative to the West Africa and Amazonia, and to other peri-Gondwanan terranes, remains uncertain (e.g., Schenk 1997; Waldron 2009).

The Meguma terrane takes its name from distinctive stratigraphic unit, named the Meguma Series by Woodman (1902) and subsequently termed the Meguma Group (Stevenson 1959) or Supergroup (Schenk 1995a, 1997). It comprises the Cambrian to Early Ordovician Goldenville and Halifax Groups (Schenk 1995a; White 2010b), which are overlain by the Silurian to Devonian Rockville Notch Group, all of which are intruded by Devonian plutons (Clarke and Halliday 1980). Recent mapping of the Meguma terrane in Nova Scotia has led to the identification and division of several mappable units within the Halifax and Goldenville groups. In this paper we formally define the Lumsden Dam and Bluestone formations of the upper Halifax Group in the Wolfvillle and Halifax regions. Both units record similar sedimentological features, and the presence of a mass transport deposit in the Bluestone Formation suggests they were deposited in a slope environment.

Here we present the first detrital zircon data from the Halifax Group, which add to previous provenance studies conducted in the Goldenville and Rockville Notch groups (Krogh and Keppie 1990; Murphy et al. 2004b; Waldron et al. 2009). The data show similar distributions to underlying units, and are consistent with a primary West African source region with a minor input of Amazonian detritus.

3.2 GEOLOGIC SETTING

The Meguma terrane is exposed south of the Cobequid-Chedabucto Shear Zone in Nova Scotia (Fig. 3.1). It includes a thick (>13 km) Cambrian-Ordovician sandstone-shale succession of the Meguma Supergroup and Silurian-Devonian volcanic-sedimentary rocks of the Rockville Notch Group (White et al. 2012). The units have been deformed into SW-NE trending folds formed during the Middle Devonian Neoacadian orogeny (van Staal 2007; White et al. 2007), and have been intruded by the South Mountain Batholith and other plutons during the late Devonian (Clarke and Halliday 1980). Regional metamorphism is greenschist facies with amphibolite facies in southwest and far east of Nova Scotia (Keppie and Muecke 1979). Hornblende-hornfels facies contact metamorphism is present around the South Mountain Batholith (Jamieson et al. 2012). Unconformably overlying the Meguma terrane and adjacent Avalonia terrane are the Late Devonian to Carboniferous successions of the Maritimes Basin and the Mid-Triassic to Early Jurassic Fundy Group (Klein, 1962; Martel et al. 1993).

The Chebogue Point Shear Zone (CPSZ) is located in southwest Nova Scotia in the Yarmouth region (Fig. 3.1). It strikes N-S to NE-SW (White 2010b) and has not been traced east of its intersection with the South Mountain Batholith. White (2010b) has described the CPSZ as a tectono-stratigraphic boundary, dividing the Meguma Supergroup into the different, though correlative units at the formation level, lying to the northwest and southeast of the shear zone and South Mountain Batholith.

Basement characteristics such as age, deformation and composition normally provide critical information about a terrane's origin; however, there is no exposure of Meguma terrane basement rocks anywhere in Nova Scotia. Sm/Nd studies on Meguma granitoids (Clarke et al. 1988) and basement xenoliths (Eberz et al. 1991) indicate that deeper crustal material has a younger residence age than the overlying Meguma Supergroup. Greenough et al. (1999) dated zircons and monazites from basement xenoliths, which showed a Pan-African – Avalonian population (575-630 Ma), with a possible Mesoproterozoic grain population defined by the upper intercepts of a discordant zircon fraction known to be lacking in lower Meguma Supergroup sediments (Krogh and Keppie 1990; Waldron et al. 2009). These data are interpreted by Greenough et al. (1999) as suggesting that the Meguma succession rests upon a basement with similarities to adjacent

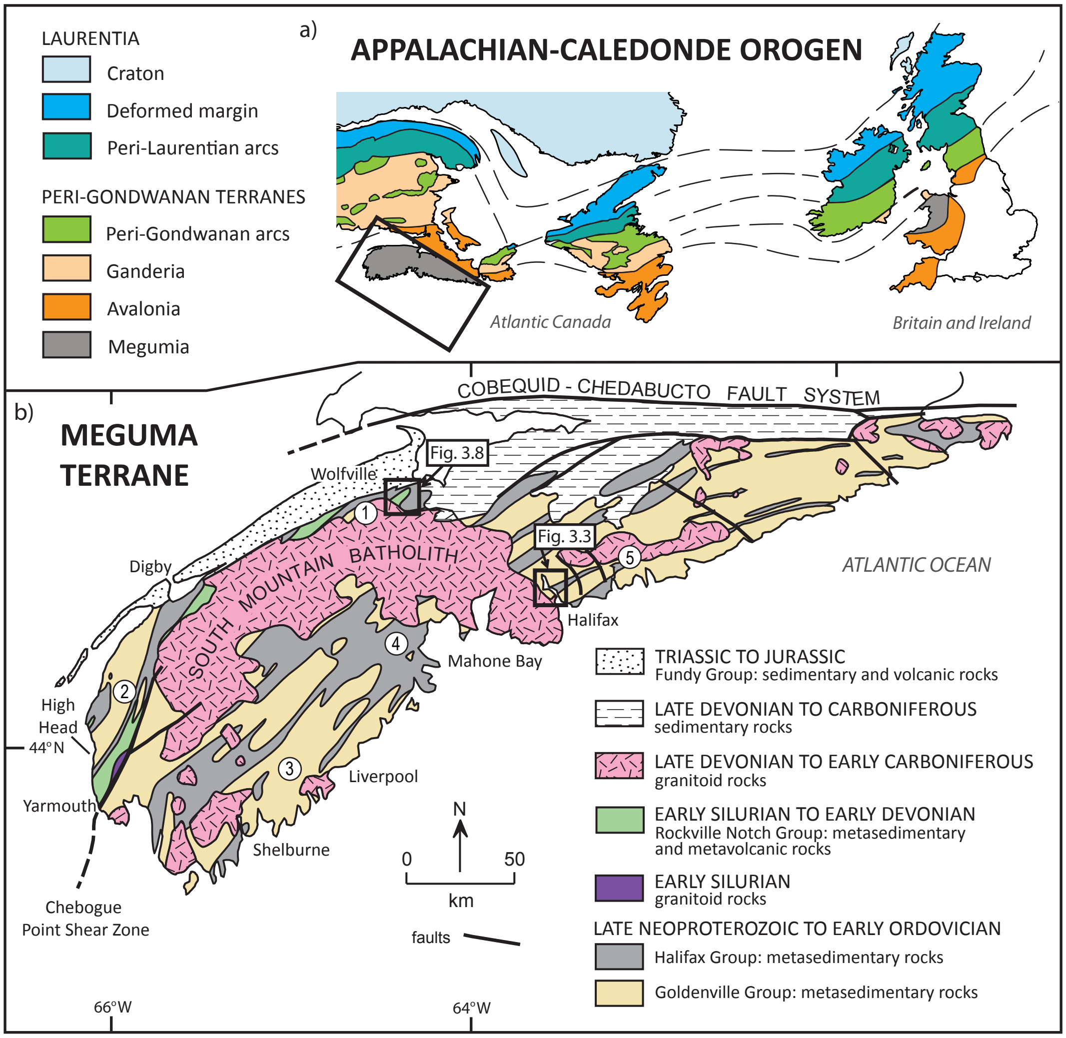

Figure 3.1: Meguma terrane (after White 2010b) with inset map showing its location in the northern Appalachian-Caledonide orogeny (after Hibbard et al. 2006). Boxes show location of maps shown in Fig. 3.3 and 3.8. Numbers refer to stratigraphic columns shown in Fig. 3.2.

Avalonia. It has been proposed that West Avalonia and the Meguma terrane once formed a part of the same microcontinent and that the Meguma succession was deposited on Avalonian crust (e.g., Keppie 1997; Landing 2004; Murphy et al. 2004a; Linnemann et al. 2012). Others believe the contact to be a structural thrust fault contact (e.g., Eberz et al. 1991; Keppie and Dallmeyer 1987; Waldron et al. 1989; Greenough et al. 1999) at which the Meguma terrane was thrust over crust with Avalonian characteristics.

3.2.1 Goldenville Group

The Goldenville Group (Fig. 3.2) is the oldest unit in the Meguma terrane and spans the early Cambrian (Terreneuvian) to the early Furongian (White et al. 2012). It is primarily composed of thick-bedded metamorphosed sand-rich turbidites with local interbedded siltstone and slate (Harris and Schenk 1975; Waldron and Jensen 1985). The highest part of the Goldenville Group is characterized by manganese-rich slate and siltstone (Waldron 1992). The Goldenville Group is estimated to have a thickness upwards of c. 8300 m (White et al. 2012). The High Head member (Fig. 3.2) contains trace fossils, including *Oldhamia*, that are characteristic of the early Cambrian (Gingras et al. 2011). These are consistent with detrital zircon collected from Church Point formation (Fig. 3.2) that produced youngest ages of 544 ± 18, 537 ± 15 and 529 ± 19 Ma, providing a maximum depositional age close to the Ediacaran-Terreneuvian boundary (Waldron et al. 2009). The Government Point formation (Fig. 3.2) yielded a middle Cambrian Acado-Baltic Trilobite faunule (Pratt and Waldron 1991).

3.2.2 Halifax Group

The Halifax Group spans the Furongian to Lower Ordovician (Fig. 3.2) and is generally much more fine grained than the underlying Goldenville Group (White et al. 2012). The lowest unit in the Halifax Group as defined by White (2010a) is the Cunard formation and its correlatives the Acadia Brook and North Alton formations in the Bear River and Wolfville regions (Fig. 3.2). Strongly cleaved, dark grey to black slates with thin metasiltstone and fine to medium-grained metasandstone lenses and beds characterize this unit. It also contains abundant sulfide minerals and weathers to a rusty-brown colour. An acritarch assemblage sampled from the North Alton formation indicates a Furongian age (Jiangshanian) (White et al. 2012). Above this are the correlative Lumsden Dam, Bluestone, Feltzen and Bear River formations (Fig. 3.2). These units, which are the focus of the remainder of the paper, are light-grey to dark-grey in colour and comprise slate interlayered with cross-laminated metasiltstone and fine-grained metasandstone. These units contain noticeably less pyrite and arsenopyrite than the underlying formation. Tremadocian graptolite fossils have been preserved in the Bear River, Feltzen and Lumsden Dam formations (White 2010a). The highest units of the Halifax Group are preserved in the Wolfville region. The

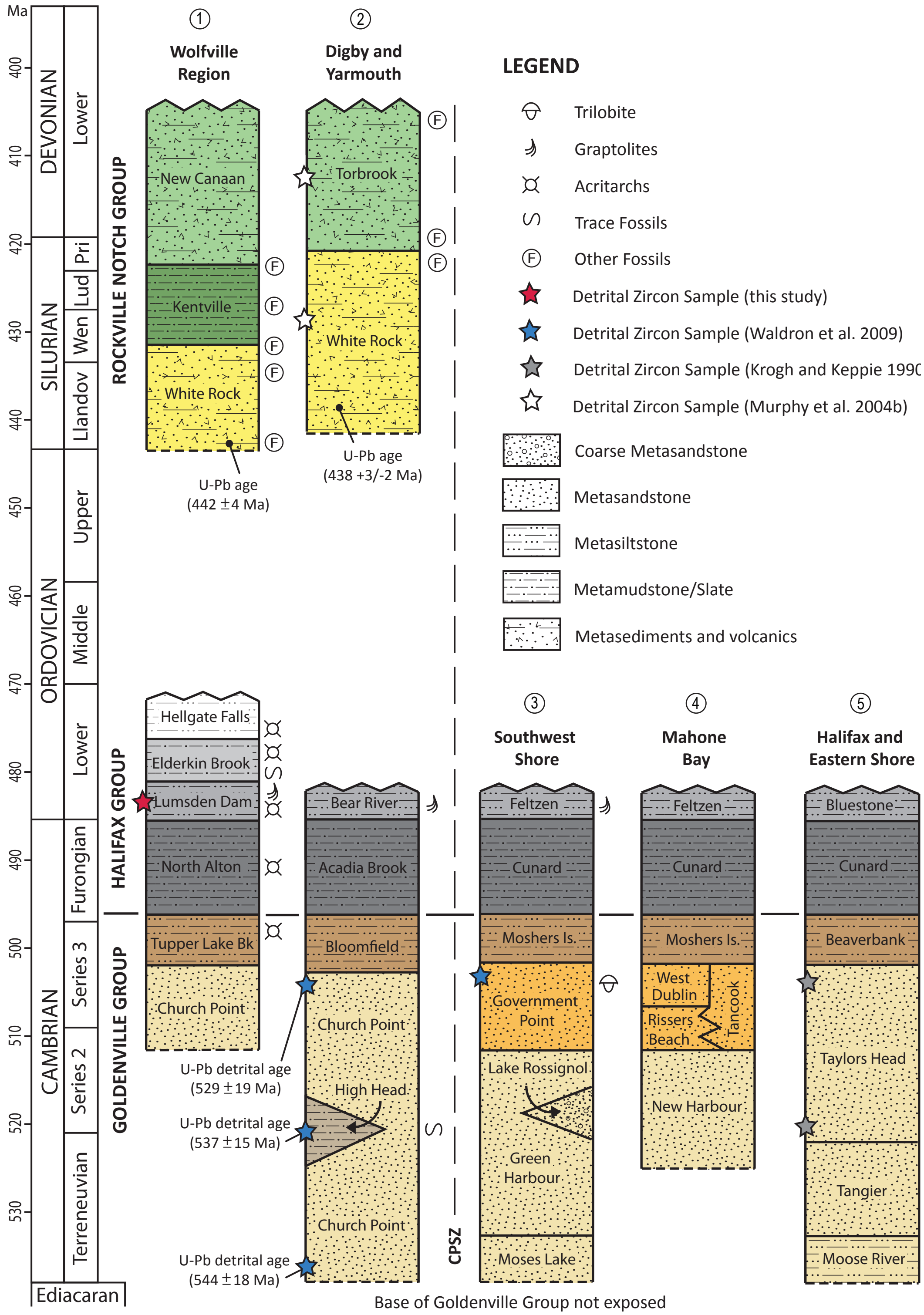

Figure 3.2: Generalized stratigraphy of the Meguma terrane in different regions in Nova Scotia (after O'Brien 1988; Horne and Pelly 2007; White 2010b; White et al. 2012) showing the locations sampled in detrital zircon studies. Paleontological and U-Pb age data are from sources described in the text. Using time scale of Peng et al. (2012).

Elderkin Brook formation (Fig. 3.2) lies above the Lumsden Dam formation. It consists of light grey to red-brown laminated slate and metamudstone and is highly bioturbated. The uppermost unit, the Hellgate Falls formation (Fig. 3.2) is light to dark grey slate interbedded with thick-bedded metasiltstone and metasandstone. Acritarch assemblages in the Elderkin Brook and Hellgate Falls formations indicate they were deposited in the late Tremadocian to Floian (White et al. 2012).

3.2.3 Rockville Notch Group

The Silurian to Lower Devonian Rockville Notch Group (formally the Annapolis Supergroup of Schenk 1995b) is preserved on the northwest side of the CPSZ and South Mountain Batholith (Fig. 3.2). The basal White Rock Formation rests unconformably over the Halifax Group (White 2010a). This unit comprises shallow marine sedimentary rocks (Lane 1975, 1981; Bouyx et al. 1997) and rift-related volcanic rocks (Schenk 1997; Keppie and Krogh 1999; MacDonald et al. 2002). A rhyolite dated near its base produced a U-Pb age of 442 ± 4 Ma (Keppie and Krogh 2000) and a felsic tuff in the Yarmouth area produced a similar age of 438 ± 3 Ma (MacDonald et al. 2002). These are overlain by metasiltstone and slate of the Kentville Formation (Smitheringale 1960; Taylor 1965). Graptolites and microfossils reported in the unit (Smitheringale 1973; Bouyx et al. 1997) identify it as upper Wenlock to lower Pridoli (Silurian). These are overlain by Pridoli to late Lower Devonian (Smitheringale 1973; Bouyx et al. 1997) marine sedimentary and volcanic rocks of the New Canaan and Torbrook formations (Smitheringale 1960; Taylor 1965).

3.3 FORMAL DESCRIPTIONS

All subdivisions of the Halifax Group have hithero been informal. We here formally define two of these units, the Bluestone and Lumsden Dam formations. All coordinates based on Universal Transverse Mercator (UTM) projection, using North American Datum 1983.

3.3.1 Bluestone Formation

The Bluestone Formation was first named by White et al. (2008) after the Bluestone member of Jamieson et al. (2005). It is mappable in the Halifax region and is exposed in the core of a SW plunging syncline adjacent to Point Pleasant Park and on the south side of the Northwest Arm (Fig. 3.3). The rocks of the Bluestone formation are interbedded light grey to beige metasandstone and metasiltstone with medium to dark grey slate and hornfels. The unit overlies darker, more pyrite-rich slate of the Cunard Formation. Bedding is continuous at the outcrop scale (several metres). Beds are graded and have sharp, flat bases, with scour structures in places. Sandstone commonly appears massive to parallel or cross-laminated; siltstone is most often cross-laminated, and slate exhibits weak parallel to wavy laminae. The cross-laminae show unidirectional current flow typically with a northward component and the ripples have sinuous crest morphologies. Trough cross-laminations and climbing-ripple cross-laminations are common (Fig. 3.4).

The Bluestone Formation lacks the abundant sulphide minerals present within the underlying Cunard formation. It contains carbonate concretions that have locally been metamorphosed to calc-silicates (Jamieson et al. 2005, 2012). The concretions are usually associated with siltstone and sandstone horizons, which also help to distinguish it from the underlying Cunard Formation. Much of the Bluestone Formation lies within the contact aureole of the South Mountain Batholith (Halifax Pluton), which has overprinted the regional greenschist facies metamorphism with hornfels facies and annealed the slaty cleavage (Jamieson et al. 2012).

The formation is here divided into four members: the Point Pleasant member, the Black Rock Beach member, the Chain Rock member, and the Quarry Pond member (following Jamieson and Waldron 2011) (Fig. 3.3).

The lowest, Point Pleasant member (approximately 295 m thick) is well exposed inland and along the shoreline in the south end of Point Pleasant Park (Fig. 3.3). It comprises thin to thickly bedded high-energy turbidite deposits and is the most sand-rich member (Fig. 3.4ab, 3.5). Bouma divisions A though to E are common, but partial Bouma sequences are also present, where the basal divisions are missing or just divisions A and E are preserved.

The Black Rock Beach member is 68 m thick and is best exposed at Black Rock Beach in the park (Fig. 3.3). The unit contains very thin to medium bedded low energy turbidite deposits (Fig. 3.4c, 3.6). Bouma divisions C-E and D-E are common.

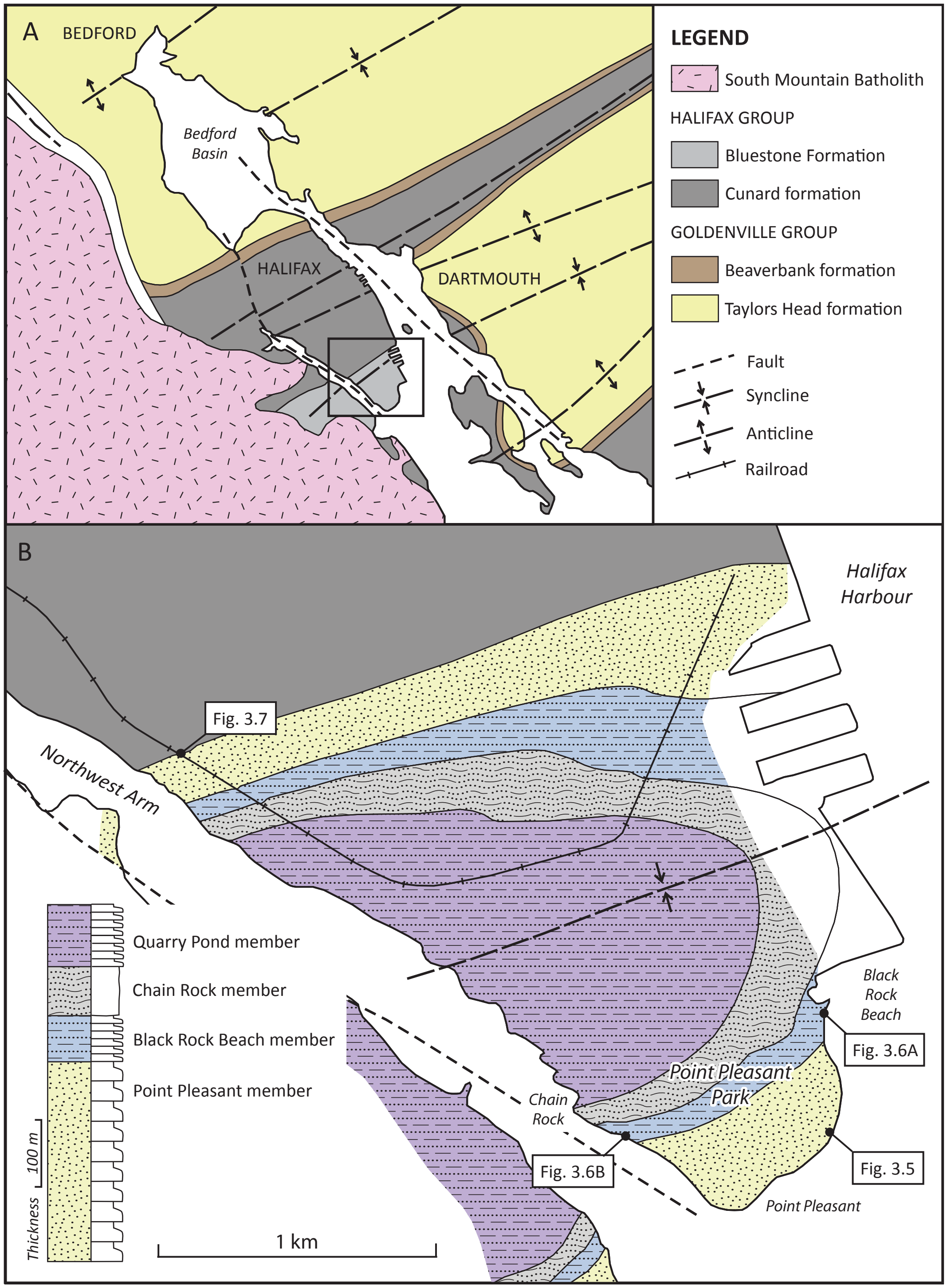

Figure 3.3: Geological map of a) the Halifax area after White et al. (2008) and b) the Bluestone Formation (after Jamieson et al. 2011).

The Chain Rock member is 75 m thick and is more resistant to erosion than the other members, forming the high ridge within the park (Fig. 3.3). It is characterized by bedding that is variably folded, discontinuous, or completely disordered, where isolated blocks of siltstone and sandstone are found within a featureless matrix (Fig. 3.4de). The deformation in this unit pre-dates the development of the regional slaty cleavage, but post-dates the formation of the carbonate concretions (Jamieson et al. 2011). On the coast of the Northwest Arm, the contact with the underlying Black Rock Beach member is visible [20T 445499E 4940918N]. A sharp contact that appears to be an erosional surface where the Chain Rock member incises into the underlying unit up to 70 cm. Due to the stratiform geometry and chaotic deformational style of the Chain Rock member it can be interpreted as a downslope mass-transport deposit (Jamieson et al. 2011).

The Quarry Pond member has a minimum thickness of 93 m. It is best exposed in the railway cutting (Fig. 3.3) and also occurs as scattered outcrops within Point Pleasant Park. This unit is very similar to the Black Rock Beach member as it also consists of very thin to medium bedded low energy turbidite deposits where Bouma divisions C-E and D-E are common (Fig. 3.4f). The Quarry Pond member is the highest unit in the Formation, exposed in the core of the Point Pleasant syncline; its top is not exposed.

The type-section for the Formation is located along the railway cutting shown in Figure 3.3 and in adjacent Point Pleasant Park, where the Bluestone Formation outcrops almost in entirety. The basal contact is exposed in the railroad cut [20T 453021E 4942263N]. It is conformable and is defined at the lowest appearance of fine-grained metasandstone beds (Point Pleasant Park member) with carbonate concretions (Fig. 3.7). The highest part of the unit in the type area occurs in the core of the Point Pleasant syncline. No overlying strata other than Quaternary deposits are observed in the Halifax region where the Bluestone Formation is the youngest exposed stratified unit; thus an upper stratigraphic contact cannot be defined. The minimum thickness of the Bluestone formation is estimated to be 531 m.

The age of the Bluestone Formation is not well constrained as no fossils have been found in this area (White et al. 2008). However, based on its stratigraphic position above the Cunard Formation, the Bluestone Formation has been

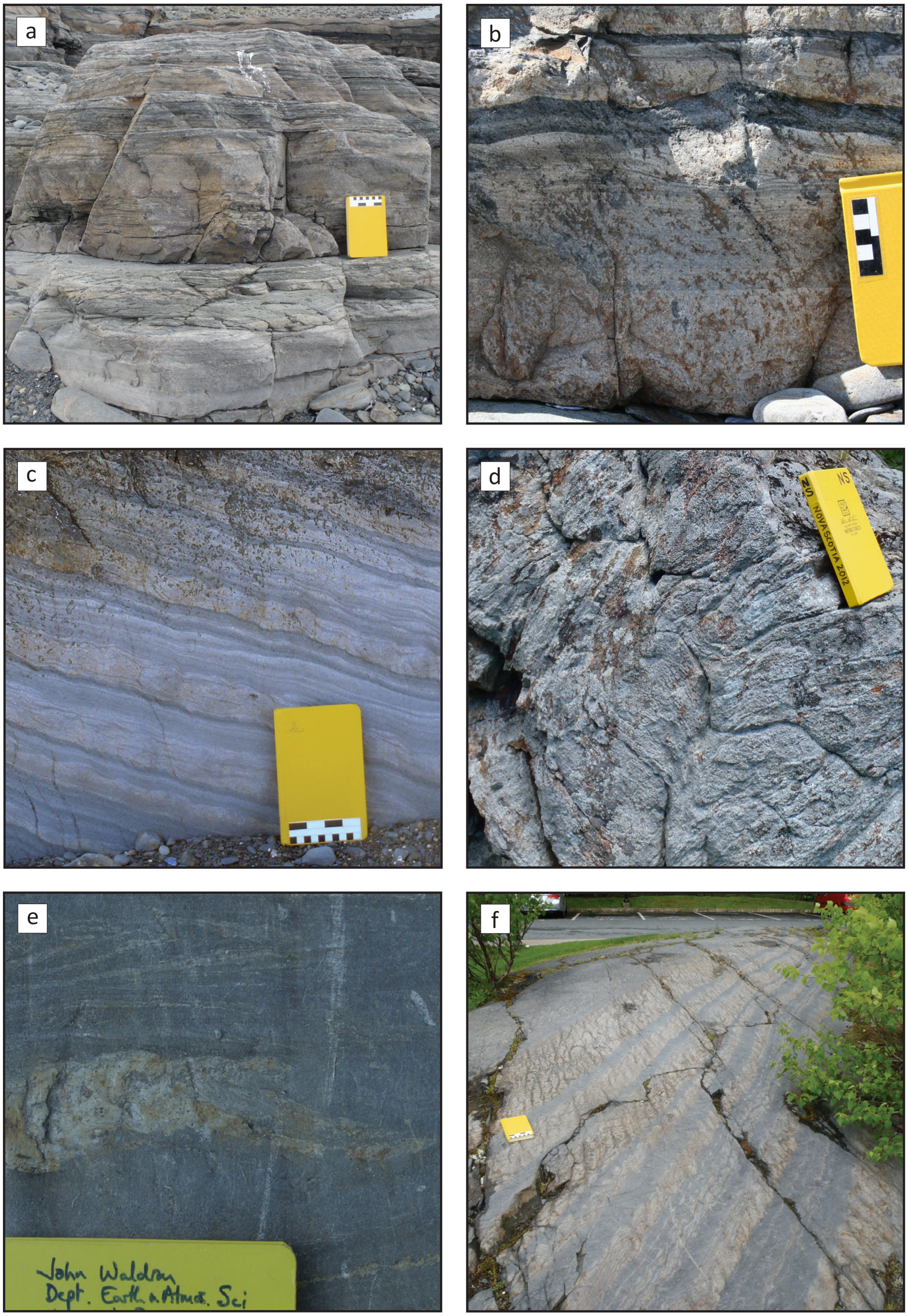

Figure 3.4: Typical field appearances of the Bluestone formation a-b) Point Pleasant member, c) Black Rock Beach member, d-e) Chain Rock member and f) Quarry Pond member.

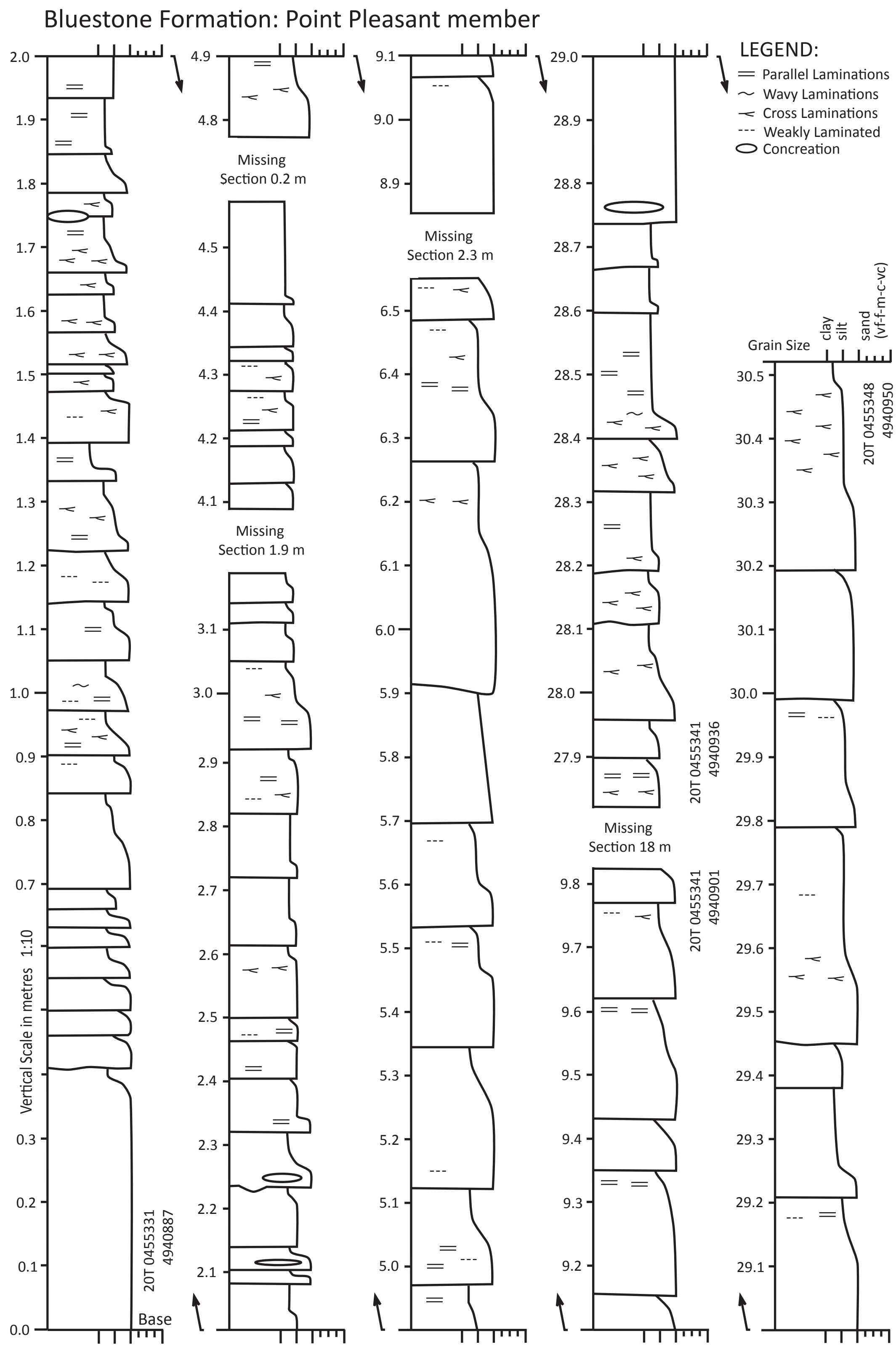

Figure 3.5: Detailed section of the Bluestone Formation Point Pleasant member.

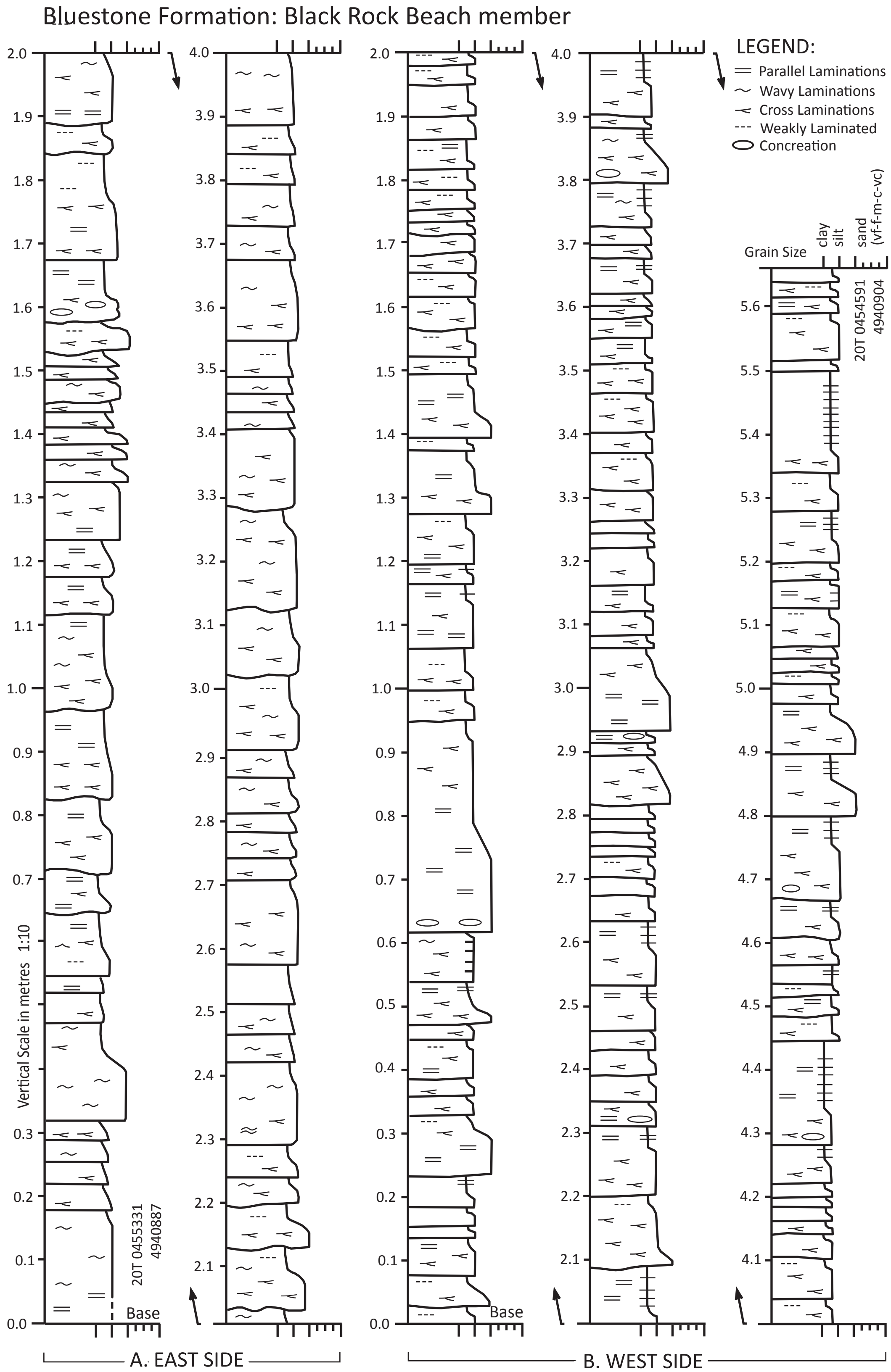

Figure 3.6: Detailed section of the Bluestone Formation Black Rock Beach member.

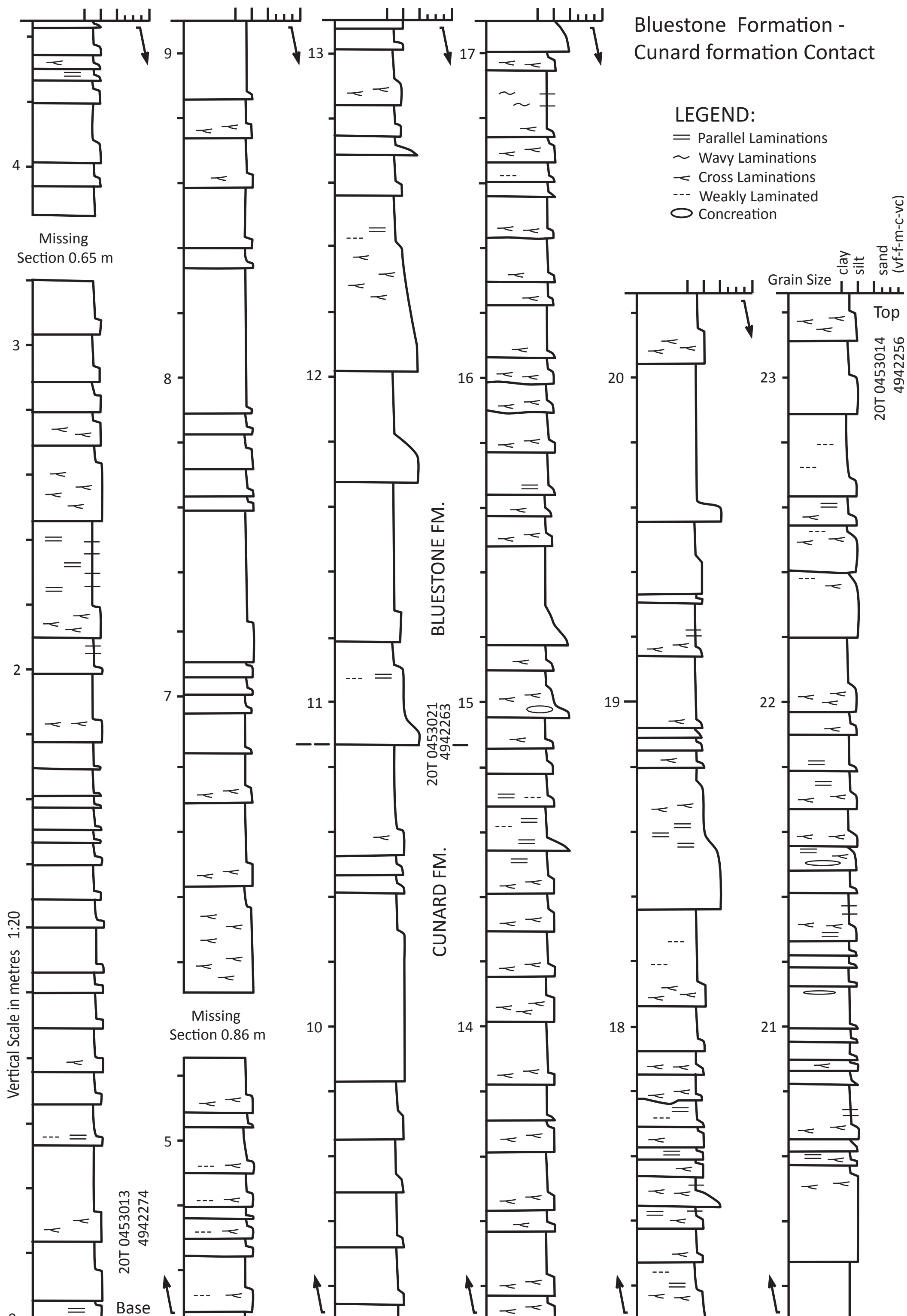

Figure 3.7: Detailed section of the contact between the Cunard and Bluestone formations.

correlated with the Lumsden Dam, Bear River and Feltzen formations, which contain graptolite and acritarch fossils of Tremadocian age (White et al. 2012). This provides the best estimate for the age of the Bluestone Formation; however, this assumes the contact is not diachronous.

3.3.2 Lumsden Dam Formation

The divisions of the Halifax Group in the Wolfville region including the Lumsden Dam Formation, were first informally named by White (2010a). In the Wolfville region, the Lumsden Dam Formation is exposed on the northwest limb of an anticline (Fig. 3.8). Excellent exposure of the unit can be seen in the Black River area, the best exposures being in an overflow channel located to the northwest of the Lumsden Dam. This type section has roughly 200 m of continuous outcrop (Fig. 3.9). The continuous outcrop terminates southward at the south end of the channel cut [20T 389943E 986789N] and to the north it disappears under vegetative cover [20T 389878E 4986982N]. Sedimentary structures were difficult to decipher along the cliff edge of the channel, but were easily seen on adjacent flat exposure. The remainder of the type section is defined in intermittent exposure to the north and south of this well exposed section.

The Lumsden Dam Formation consists mainly of light-grey siltstone and dark-grey mudstone with minor very fine-grained sandstone (Fig. 3.10). Graded beds are prevalent throughout the section and are very thin (1-3 cm) to medium (10-30 cm) bedded. Siltstone and sandstone beds are parallel laminated to cross-laminated, while most mudstone layers contain thin parallel laminations of silt. Thicker siltstone and sandstone beds are laterally continuous at the outcrop scale (several metres), but thin (less than 2 cm) cross-laminated beds commonly appear as lenses or semi-continuous and lenticular. Bed bases are sharp and flat with some scouring.

The unit contains minor sulfide minerals (less than the North Alton Fm. below) and it weathers to a rusty-brown. Rare, small (1-3 cm) carbonate concretions are also found within the siltstone and sandstone beds. The section contains four mafic sills that are parallel to bedding, which range from 90 to 120 cm thick. They can be easily confused with thick sandstone beds, as they are fine-gained and a medium grey colour (Fig. 3.11).

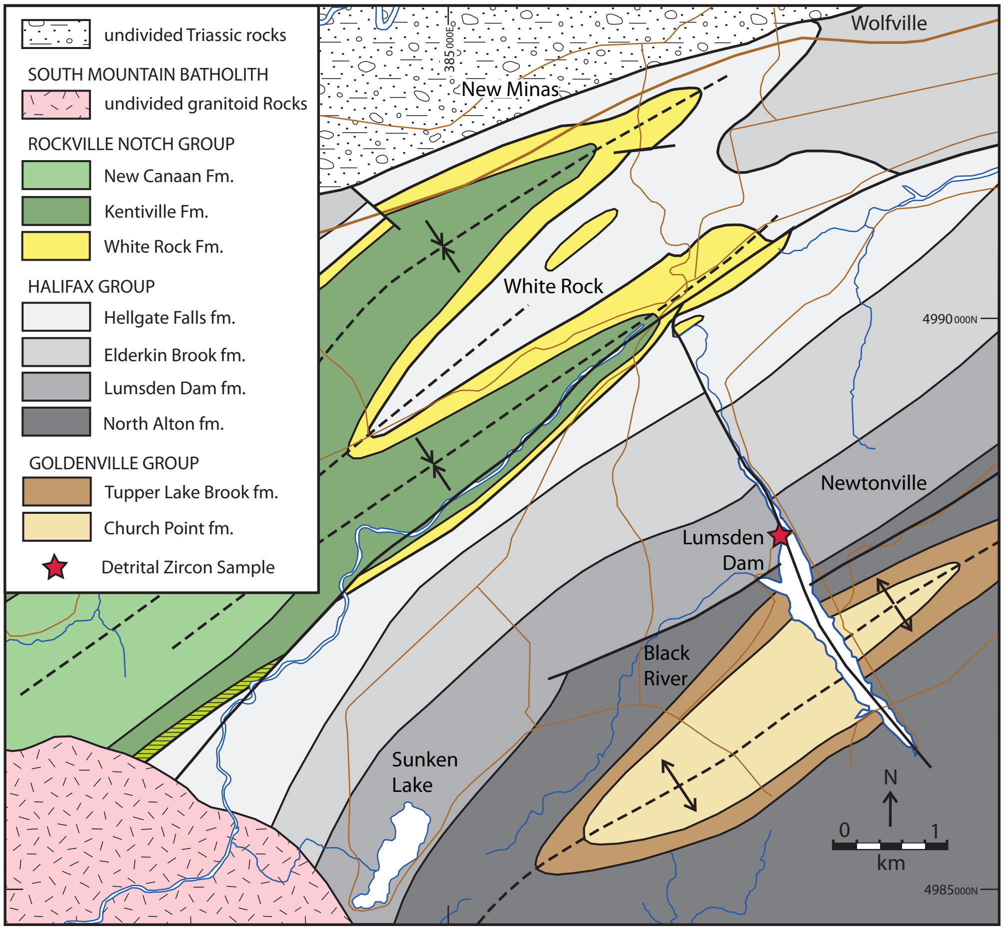

Figure 3.8: Geological map of the Wolfville area (after White 2010a).

The boundary between the Lumsden Dam Formation and the underlying North Alton formation is located along Jehill Davidson Road in Newtonville (Fig. 3.8). Intermittent exposure along the roadbed shows a change up section from dominantly medium grey to black mudstone with locally abundant sulphides and siltstone beds less than 10 cm thick, up to dominantly medium grey to greenish-grey mudstone with siltstone and sandstone beds that reach thicknesses greater than 10 cm. The boundary is placed at the lowest occurrence of a siltstone bed thickness greater than 10 cm [20T 391089E 4986980N]. White et al. (2012) have described the contact as gradational over an interval of 5 m in other parts of the region.

The boundary between the Lumsden Dam formation and the overlying Elderkin Brook formation is not visible along the east side of Black River Road, but can be constrained within 62 m between UTM coordinates 20T 389838E 4987401N

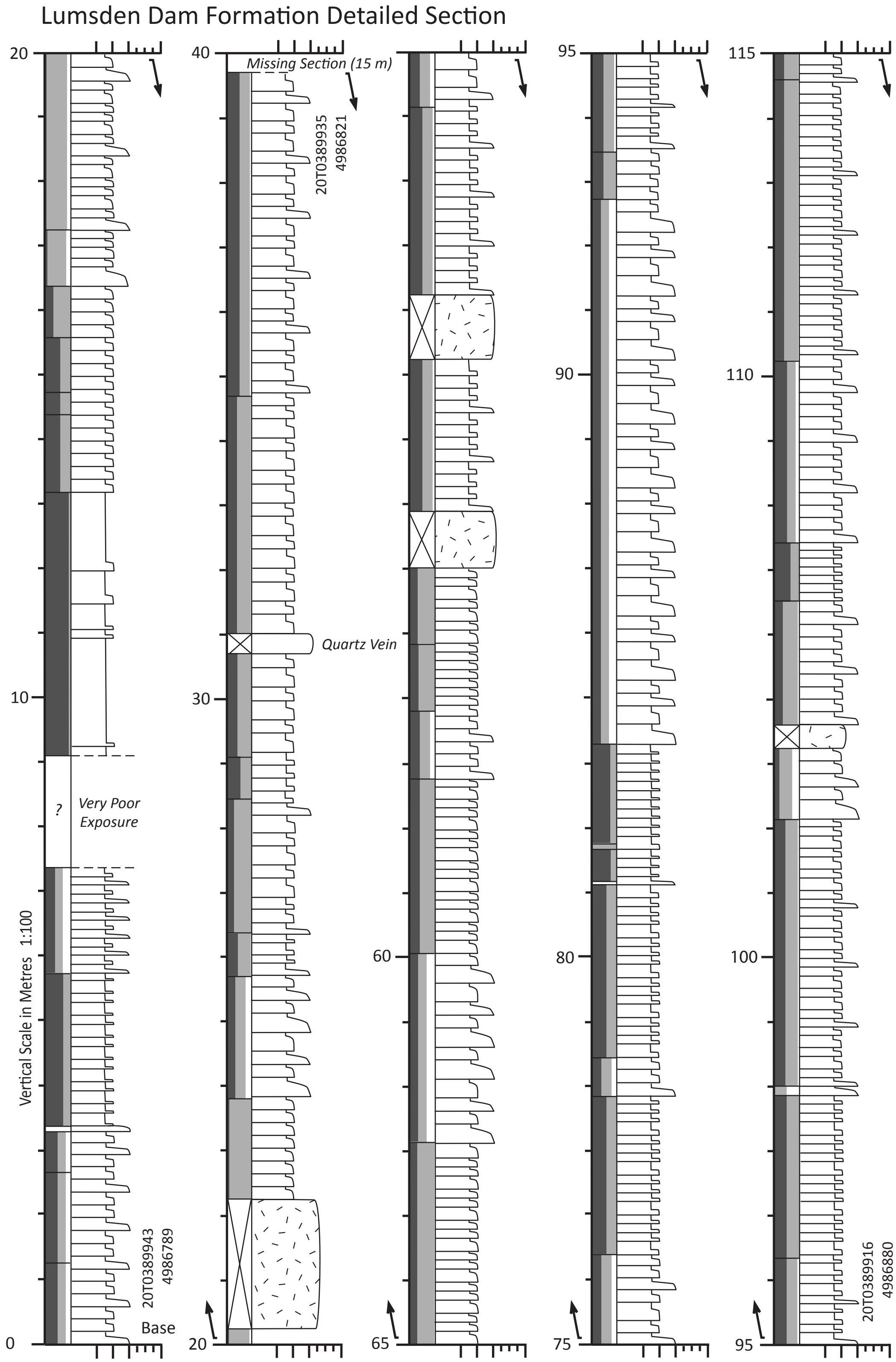

Figure 3.9: Generalized section of the Lumsden Dam Formation type area.

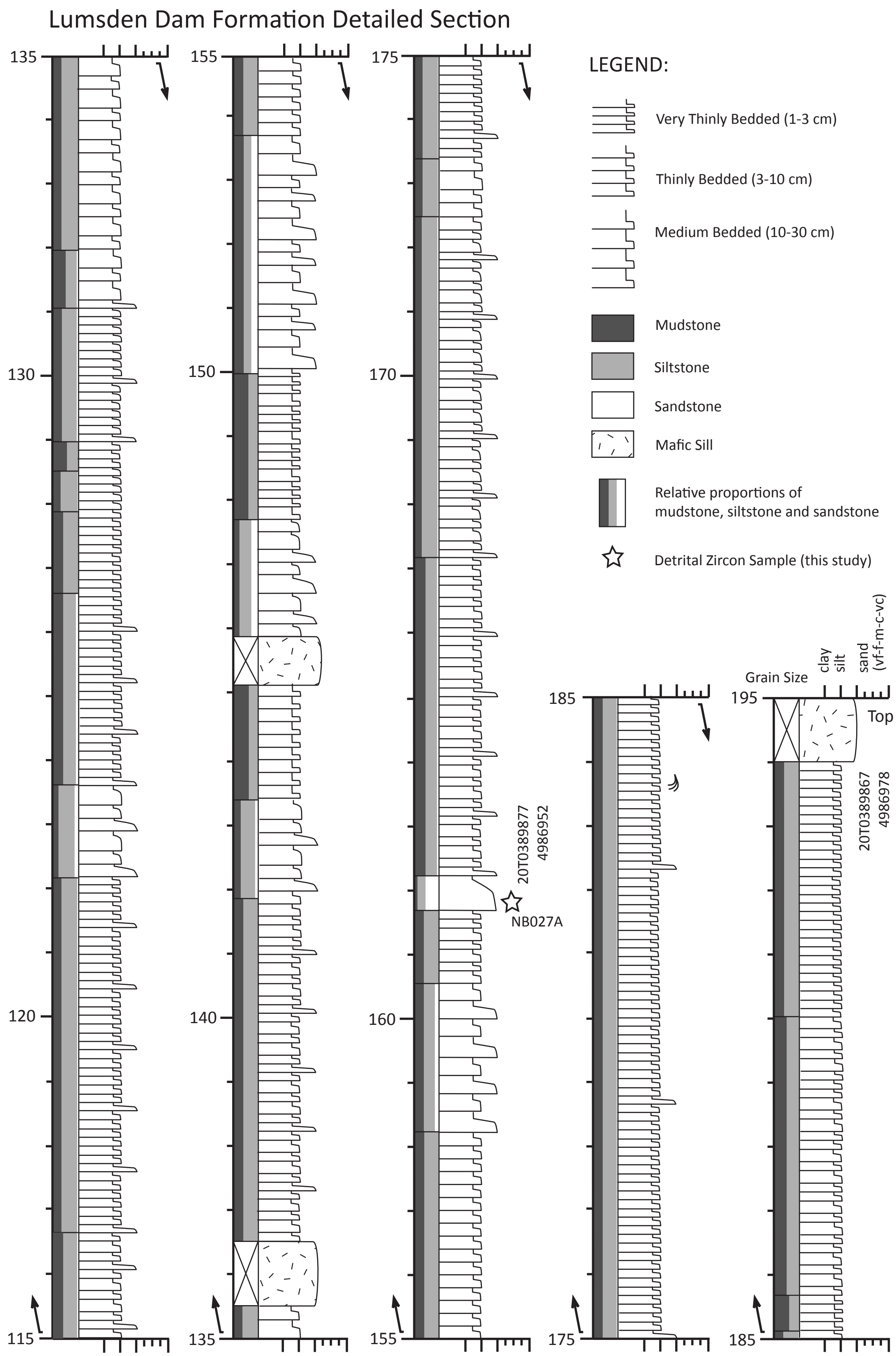
Lumsden Dam Formation Detailed Section
135
130
120
115
155
150
140
135
175
170
160
155
185
175
195
185
LEGEND:
Very Thinly Bedded (1-3 cm)
Thinly Bedded (3-10 cm)
Medium Bedded (10-30 cm)
Mudstone
Siltstone
Sandstone
Mafic Sill
Relative proportions of mudstone, siltstone and sandstone
Detrital Zircon Sample (this study)
20T0389877
4986952
NB027A
Grain Size
clay
silt
sand (vf-f-m-c-vc)
Top
20T0389867
4986978

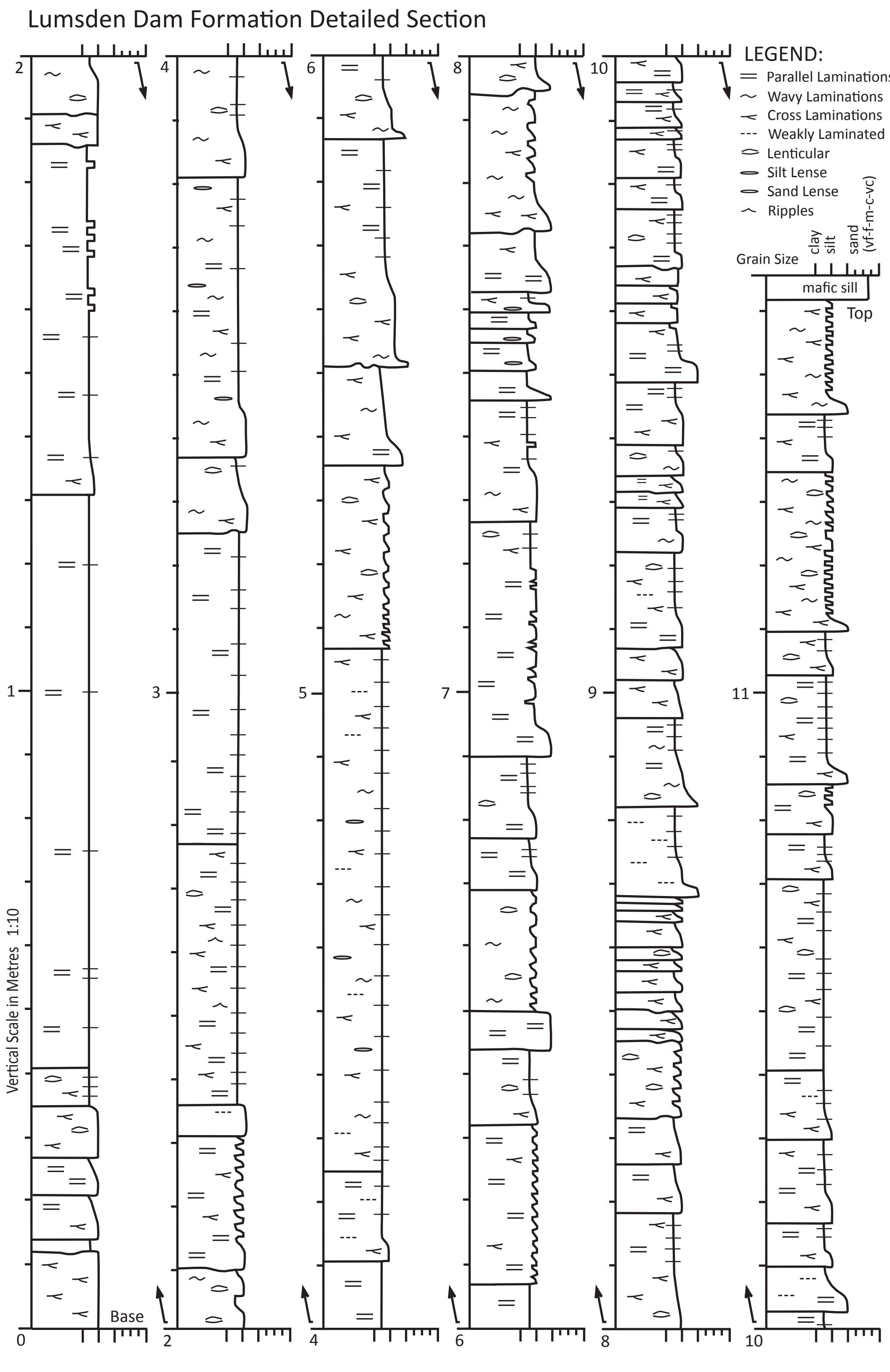

Figure 3.10: Detailed section of the Lumsden Dam Formation.

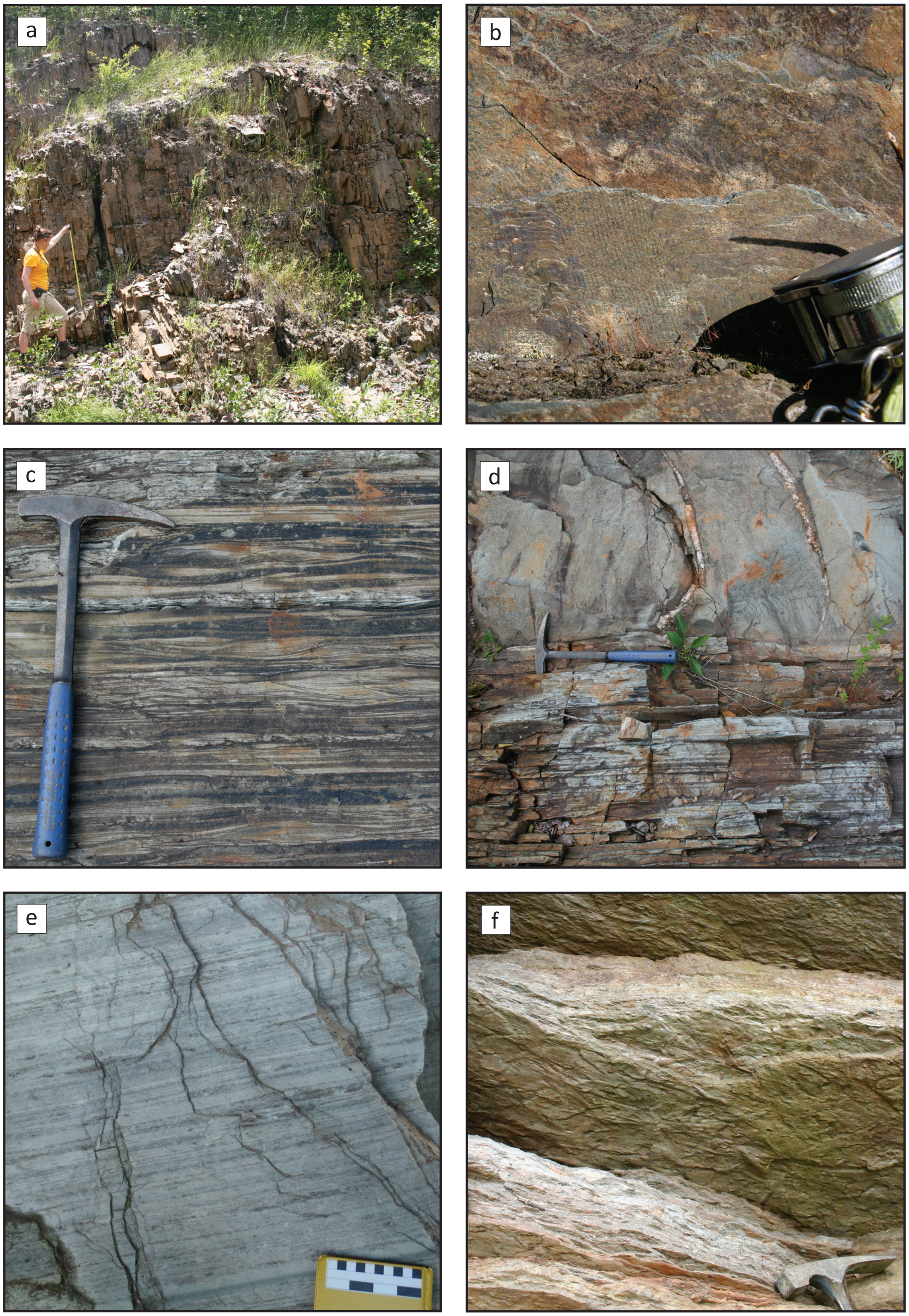

Figure 3.11: Typical field appearances of: a) Lumsden Dam Formation general view; b) graptolite fossil in Lumsden Dam Formation; c) thinly interbedded siltstone and mudstone of the Lumsden Dam Formation; d) Lumsden Dam Formation in contact with a Type I mafic sill; e) finely laminated mudstone of the Elderkin Brook formation; and f) interbedded siltstone and mudstone of the Hellgate Falls formation showing bioturbation structures.

and 20T 389815E 4987459N. Here there is a transition from the Lumsden Dam Formation, which contains siltstone and thick cross-laminated sandstone, into thick laminated mudstone with only minor siltstone. The boundary is placed at the highest occurrence of a siltstone bed thicker than 2 cm. In the studied area the Lumsden Dam Formation is estimated to be 550 m thick, although White (2010a) suggested it could reach up to 1500 m thick in some areas.

The graptolite *Rhabdinopora flabelliformis flabelliformis* (Eichwald 1840) has been identified (White et al. 2012) in beds near the middle of the Lumsden Dam Formation (Fig. 3.11) and an acritarch assemblage from lower in the Formation restricts the age of the Lumsden Dam formation to the mid-early Tremadocian (White et al. 2012).

3.3.3 Elderkin Brook Formation

The Elderkin Brook formation conformably overlies the Lumsden Dam Formation. It consists of diffusely to finely laminated, slightly disturbed, cleaved mudstone (Fig. 3.11). Unlike the Lumsden Dam Formation this unit lacks cross-laminated siltstone and sandstone beds. Its colour ranges from pale greenish grey to medium grey, and it weathers to a purple-red colour in places. The unit is mildly bioturbated and contains the trace fossils *Phycodes* sp. and large horizontal looping forms (White et al. 2012). Acritarch and trace fossils within this unit indicate a late Tremadocian age (White et al. 2012). The boundary between the Elderkin Brook and Hellgate Falls formations can be seen just north of the north end of the Lumsden Dam canal [20T 388972 4988539]. The boundary is placed at the first appearance of light coloured sandstone lenses defining bedding. The thickness is estimated to be 860 m in the studied area.

3.3.4 Hellgate Falls Formation

The Hellgate Falls formation is the highest unit in the Halifax Group and has an estimated thickness of at least 1100 m (White 2010a). It consists of light to dark grey laminated mudstone interbedded with light grey thin siltstone and sandstone beds. Lenses of cross-laminated sandstone are common. Abundant bioturbation textures and traces fossils also characterize this unit (Fig. 3.11). Locally, black slate is found at the very top of the formation (White 2010a) and is disconformably overlain by the Silurian White Rock Formation (White 2010a).

The age of the Hellgate Falls formation in constrained by acritarch fossils, whose ages range from the latest Tremadocian to Floian (White et al. 2012).

3.4 U-PB DETRITAL ZIRCON DATING

A sample for detrital zircon analysis was collected from the Lumsden Dam Formation in the overflow channel of the small Lumsden Dam [20T 0389877 4986952] approximately 20 m down-section from the *Rhabdinoporas flabelliformus* graptolite locality (Fig. 3.9). The sample was collected from a medium grey siltstone bed 8 cm thick. The grains are subrounded and well sorted. The rock has a primary fabric defined by the alignment of detrital mica grains and minor cleavage development is detectable. Based on a visual estimate it contains 50% quartz, 12% potassium feldspar, 5% detrital white mica, 3% polycrystalline quartz, 2% opaque minerals, and trace amounts of plagioclase and zircon. The matrix makes up 19% of the rock and consists of chlorite, white mica and biotite. 9% of the rock consists of calcite cement. See Appendix A for thin section images.

The sample was crushed using a jaw crusher and disk mill, then passed over a Wilfley table to isolate the heavy grain fraction. Franz and heavy liquid separation were used to isolate the zircons. A random selection of zircons was mounted and imaged by electron backscatter using a scanning electron microscope. They were dated using U-Pb laser ablation multicollector inductively coupled plasma mass spectrometry (LA-MC-ICP-MS) with a NuPlasma instrument and UP213 laser ablation system from New Wave Research™. Analytical protocol and data reduction were a modification of the procedure outlined in Simonetti et al. (2005). A 30 μm spot size was used except when elevated ^{206}Pb cps “tripped” the ion counter. When this occurred, if possible the grains were reanalyzed with a 20 μm spot size.

Two standards were used to normalize the grain ages. Standard LH94-15 with a U-Pb age of 1830 ± 1Ma is a homogeneous calc-alkaline enderbite (Ashton et al. 1999). Standard GJ1-32 with a U-Pb age of 609 Ma has an unknown source (Simonetti et al. 2008). LH94-15 was used for all grains with un-normalized ^{207}Pb/^{206}Pb ratios greater than the average observed ^{207}Pb/^{206}Pb value of LH94-15. GJ1-32 was used for all grains with un-normalized ^{207}Pb/^{206}Pb ratios less than the average observed ^{207}Pb/^{206}Pb ratio of GJ1-32. When the un-normalized ^{207}Pb/^{206}Pb ratios fell between the average observed $^{207}Pb/^{206}Pb$ ratios of the two standards, normalization was carried out using a weighted combination of the two standards and their proportional errors, dependent on the $^{207}Pb/^{206}Pb$ ratio of the grain.

Minor amounts of ^{204}Hg present in the argon gas supply led to slightly elevated background counts at atomic mass 204 and therefore would have yielded invalid ages if treated as common lead. Ages were not common-lead corrected unless levels of ^{204}Pb were higher than background levels (when counts per second of mass 204 were greater than 400). On peak zeros were collected before each set up 30 unknowns.

148 grains were analyzed from the sample; however, many analyses were discarded due to low ^{206}Pb cps (less than 10,000). 37 grains recorded ages that were between 90 and 110% concordant. The results are shown in Fig. 3.12. Either the $^{207}Pb/^{206}Pb$ or the $^{206}Pb/^{238}U$ age is reported depending on which result produced the lowest analytical error. See Appendix B for analytical results.

The detrital zircon results for the Lumsden Dam formation show a prominent Neoproterozoic peak centered at 633 Ma, defined by a cluster of ages (18 analyses) ranging from 560 to 728 Ma (Fig. 3.13). This cluster is separated by a c. 150 Ma gap from an older Neoproterozoic grain group (3 analyses) and an

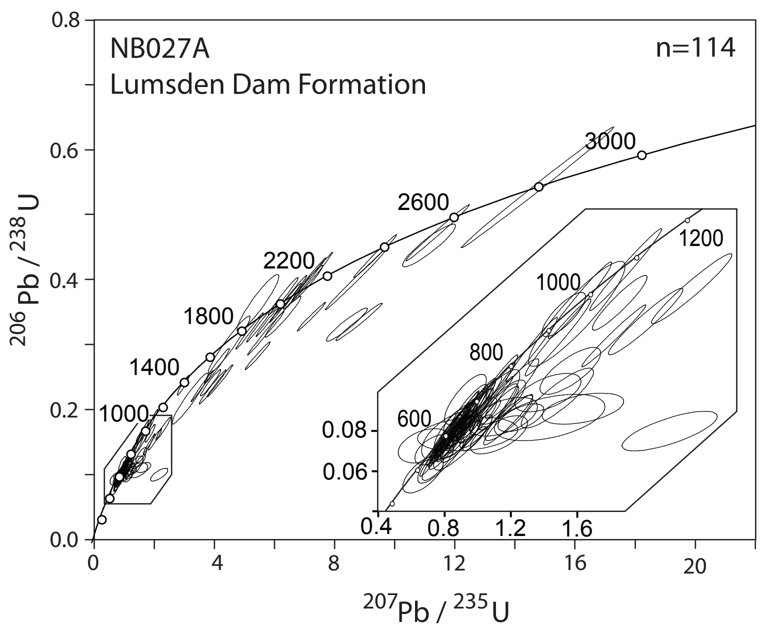

Figure 3.12: U/Pb concordia plot of detrital zircon data from the Lumsden Dam Formation sample, with 2-sigma error ellipses.

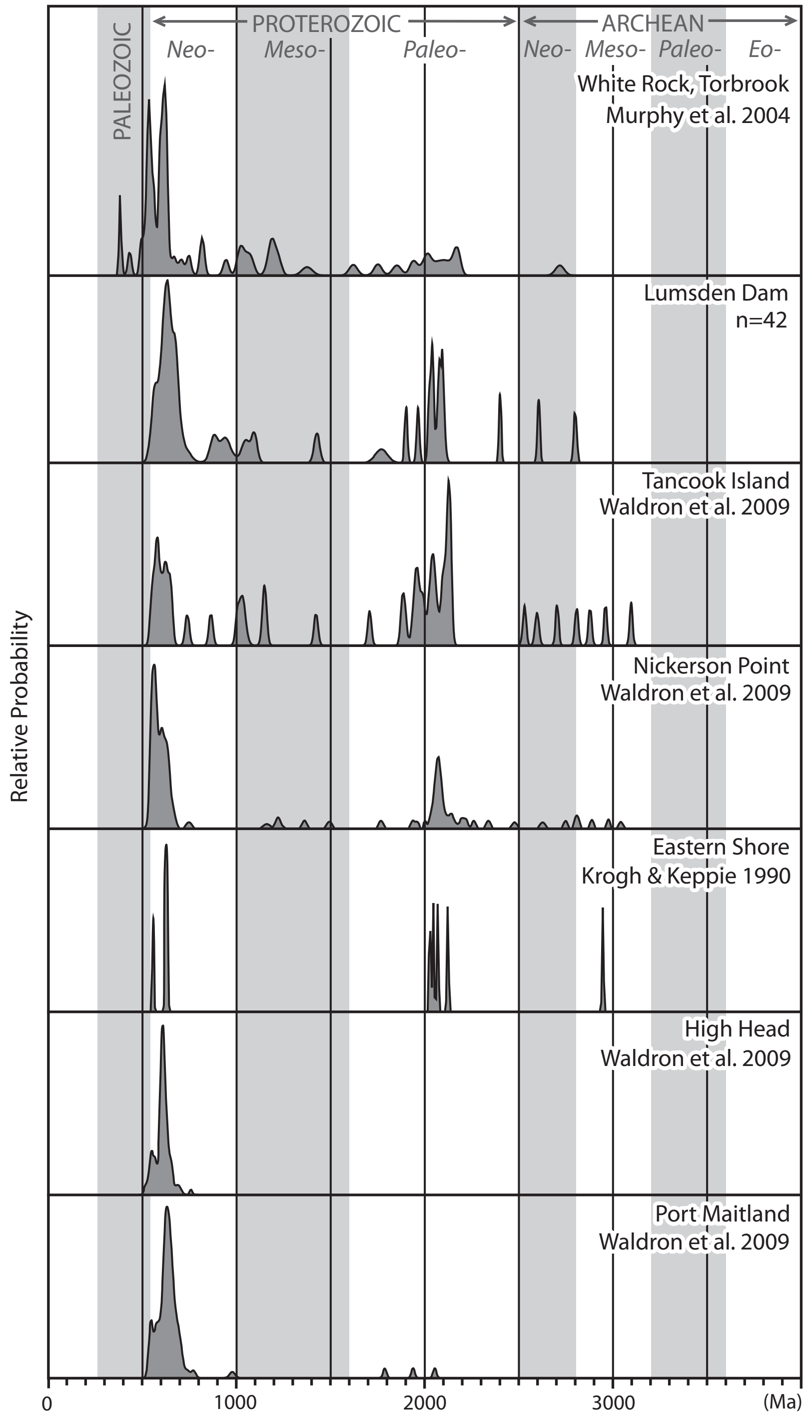

Figure 3.13: Probability density plot of detrital zircon data from the Lumsden Dam Formation, compared with results from Meguma Terrane after Krogh and Keppie (1990), Murphy et al. (2004a), Waldron et al. (2009), and Waldron et al. (2011). Calculations and plotting carried out with Isoplot 3.0 (Ludwig 2003).

early Mesoproterozoic grain group (2 analyses) with peaks at c. 930 Ma and c. 1080 Ma respectively. There were two of Mesoproterozoic age (1431 ± 30 and 1774 ± 64 Ma) and a significant Paleoproterozoic grain population with a cluster (9 analyses) ranging in age from c. 1900 to 2100 Ma. The sample also contains three Paleoproterozoic to Archean grains with ages 2405 ± 12, 2610 ± 14 and 2801 ± 16 Ma.

The average zircon grain size was approximately 50 μm. Young grains were generally euhedral to subherdral, and many exhibited oscillatory zoning. Old grains were generally sub-rounded to rounded and showed more homogeneous internal compositions with only weak zoning features (Fig. 3.14). Other features present in the grain population included core-rim structures, inclusions and fractures. These features typically were correlated with discordant ages.

3.5 DISCUSSION

3.5.1 Correlation

The Bluestone and Lumsden Dam formations have been correlated based on their lithological similarities and their stratigraphic position above the Cunard Formation and its lateral equivalent, the North Alton Formation (White 2010a). The two units comprise interbedded sandstone and siltstone with medium to dark grey mudstone and slate. The majority of beds exhibit vertical sequences of sedimentary structures described in the Bouma sequence (Bouma 1962), typical of turbidites. They are both dominantly low-energy turbidites that record Bouma divisions Tb-Te and Tc-Te and contain high-energy turbidites that record Bouma divisions Ta-e and Ta,e. Given these similarities there are also important differences. The Bluestone Formation contains a higher proportion of high-energy turbidites (Point Pleasant Park member) than the Lumsden Dam Formation and the mass transport deposits in the Bluestone Formation (Chain Rock member) are not present in the Lumsden Dam Formation. This difference can be attributed to slightly different positions relative to the basin margin, either laterally, or basinward. The slightly coarser Bluestone Formation may have been more proximal than the Lumsden Dam formation. This agrees with paleocurrent data that suggests a northwestward (present-day coordinates) flow direction, with the source region to the SE and basin to the NW (Schenk 1970).

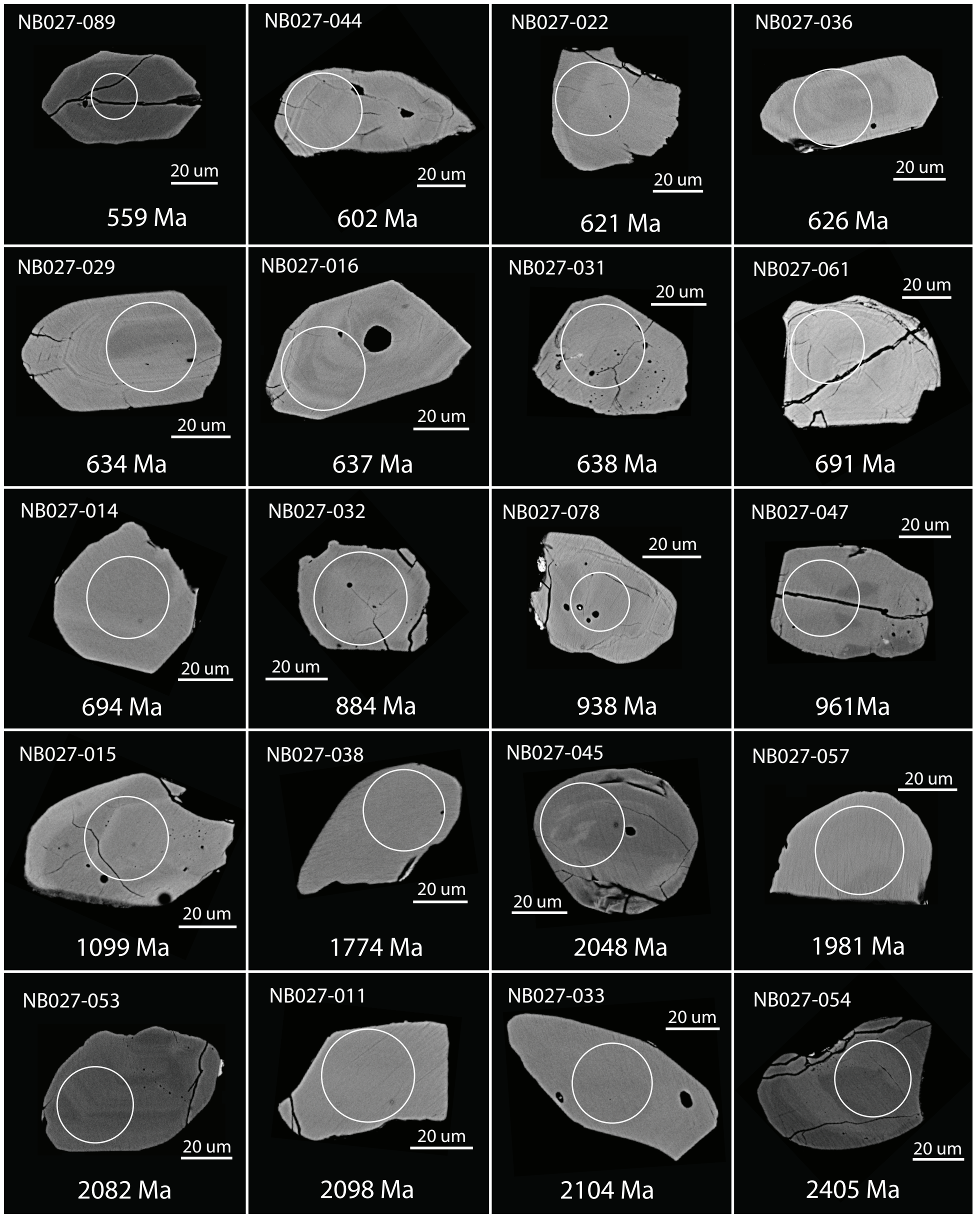

Figure 3.14: Electron backscatter images of selected zircon grains from the Lumsden Dam Formation. Ages are given in Ma. Circles represent the location of the grain sampled.

The Meguma Supergroup has been correlated with Cambrian to Tremadocian succession in the Harlech Dome of North Wales (Waldron et al. 2011). Both regions record thick early Cambrian continentally-derived sandstone turbidites, overlain by early to middle Cambrian alternating mud-rich and sand-rich units that are enriched in manganese. The manganiferous interval is characterized in all regions by numerous trace fossils, including locally abundant *Teichichnus*. Above, the succession consists of anoxic, organic-rich turbidites, shallowing upwards into paler, Tremadocian mudstone and siltstone of the Dol-cyn-afon Formation. This unit has been correlated with the Bluestone and Lumsden Dam formation of the Meguma terrane (Waldron et al. 2012; White et al. 2012) based on its age and stratigraphic position.

3.5.2 Age

The Lumsden Dam Formation contains the graptolite *Rhabdinopora flabelliformis flabelliformis* and an acritarch assemblage of Tremadocian age (White et al. 2012). No fossils have been discovered in the Bluestone Formation and attempts to extract detrital zircons were unsuccessful; hence there is still no direct evidence for the unit's age. Its stratigraphic position above the Cunard formation and the lithological similarities between it and the Lumsden Dam Formation suggests the Bluestone Formation was also deposited during the Tremadocian. However, it is possible that the top of the Cunard formation (and laterally equivalent units) represents a diachronous surface.

3.5.3 Depositional Environment

Schenk (1983) suggested the Meguma succession was deposited along the continental embankment of a passive margin; however, the bulk-rock lithochemistry has been interpreted by White et al. (2006) to suggest deposition in an active continental margin and/or an island arc setting, not a passive margin. Waldron et al. (2009) proposed a rift or extensional environment that subsequently became inactive. The latter explains the upward transition from a relatively juvenile Avalonian and Pan-African source to an older more diverse source region. It also explains the rapid accumulation of the ~13 km thick succession in ≤60 million years and the differences in the stratigraphic succession on either side of the CPSZ (Waldron et al. 2009).

The Goldenville Group is interpreted to represent a submarine, deep-sea fan deposit related to turbidity currents and other types of sediment gravity flow (e.g., Schenk 1971; Harris and Schenk 1976). The depositional environment for the shaly Cunard Formation of the lower Halifax Group has generally been interpreted as a mid- or upper-fan of a muddy deep-marine fan that prograded over the Goldenville Group (Stow et al. 1984; Schenk 1971). Waldron (1987, 1992) attributed the abundance of graphite and sulfide minerals in the Cunard Formation to anaerobic conditions on the seafloor. The Lumsden Dam and

Bluestone formations record a succession of low to high-energy turbidite deposits. The presence of a mass transport deposit in the Halifax area indicates that this unit was likely deposited in a slope environment. The Elderkin Brook and Hellgate Falls formations show a progression into a highly a bioturbated facies with abundant trace fossils that lacks turbidictic structures. This suggests a transition from a slope into an outer shelf environment by the late Tremadocian. These observations agree with Schenk (1997) who interpreted the upper formations of the Halifax Group to represent shoaling succession deposited between the upper slope of a prodelta and a muddy outer shelf.

3.5.4 Provenance

The ages of detrital zircon grains in clastic sedimentary rocks offer important information about potential source regions for sedimentary basin fill. This method has been an essential tool in determining the paleogeographic positions of many peri-Gondwanan terranes. Several detrital zircon studies (e.g., Waldron et al. 2009; Barr et al. 2012) within the Meguma terrane and West Avalonia have focused on distinguishing West African craton from Amazonian craton sources. The West African craton is characterized by Paleoproterozoic rocks (2.0 to 2.2 Ga) related to the Eburnean and Birimian orogens, and Archean rocks (Rocci et al. 1991; Lerouge et al. 2006). The Amazonian craton has Paleoproterozoic and Archean sources, as well but also has extensive Mesoproterozoioc crust including the Rio Negro belt (1.6 to 1.8 Ga) and the Rondonia-Sunsas belts (1.3 to 1.0 Ga) (Litherland et al. 1985; Rowley and Pindell 1989). The lack of a Mesoproterozoic grain population (c. 800 to 1700 Ma) has been considered an indicator of West African rather than Amazonian provenance (e.g., Nance and Murphy 1996; Linnemann et al. 2004).

Several detrital zircon samples have been analyzed from the Goldenville and Rockville Notch groups (Krogh and Keppie 1990; Murphy et al. 2004b; Waldron et al. 2009) (Fig. 3.13). Units sampled low in the Goldenville Group show a restricted distribution with prominent late Neoproterozoic grain populations. A Neoproterozoic to early Cambrian peak is common to many peri-Gondwanan terranes including Avalonia (Barr et al. 2012) and Ganderia (Fyffe et al. 2009), (Murphy et al. 2004b; Waldron et al. 2011) and reflects orogenic events that occurred between c. 540 and 700 Ma along the Gondwanan margin (Nance et al. 1991).

Later Goldenville Group samples contain a few Mesoproterozoic grains, a significant population of grains between 2.0 and 2.2 Ga and a range of Archean grains. These were interpreted by Krogh and Keppie (1990) and Waldron et al. (2009) to indicate sources in West Africa. The detrital zircon sample collected from the Lumsden Dam Formation shows a very similar distribution to the sample from the Government Point formation in the upper Goldenville Group (Fig. 3.13). In addition to the late Neoproterozoic peak it also contain a small late Mesoproterozoic peak, 1.4 Ga and 1.75 Ga grains, a significant population between 1.9 and 2.1 Ga, as well as 2.6 and 2.8 Ga Archean grains. The West African craton is believed to be the main source region for the Goldenville Group (e.g., Waldron et al. 2009; Krogh and Keppie 1990). The West African source interpreted for the Goldenville Group appears to have continued to supply detritus to the Meguma Terrane into the Ordovician.

3.5.5 Paleogeography

The Meguma terrane resided along the northern margin of Gondwana during the Cambrian (e.g., Cocks and Torsvik 2002; Landing 2005); however, its exact position, and whether it formed its own discrete terrane or was a part of West Avalonia, are still subjects of controversy. Schenk (1970, 1981, 1997) and Robinson et al. (1998) have suggested the sequence represents a continental prism that formed off northwestern African margin, while others (e.g., Landing 2004; Murphy et al. 2004a) believed it formed on the margin of West Avalonia. Some would place the Meguma terrane adjacent to the Amazonian craton (e.g., Keppie 1977; Linnemann 2012), and others closer to the West African craton (e.g., Schenk 1997; Waldron et al. 2009). Waldron et al. (2009) suggested that the succession was deposited in a rift system between East and West Avalonia and the Gondwana margin. In the early stages of basin development the uplifted flanks would supply the only source of sediment and later thermal subsidence permitted for a more extensive source region including a minor influx from Mesoproterozoic crust of Amazonia. This trend is reflected in εNd values that show a change from a restricted juvenile source to a more diverse and isotopically evolved sources (Waldron et al. 2009).

The Meguma Supergroup has been correlated with the Harlech Dome succession in North Wales (Waldron et al. 2011). Both preserve similar sedimentary successions of Cambrian age, displaying thick early Cambrian continentally-

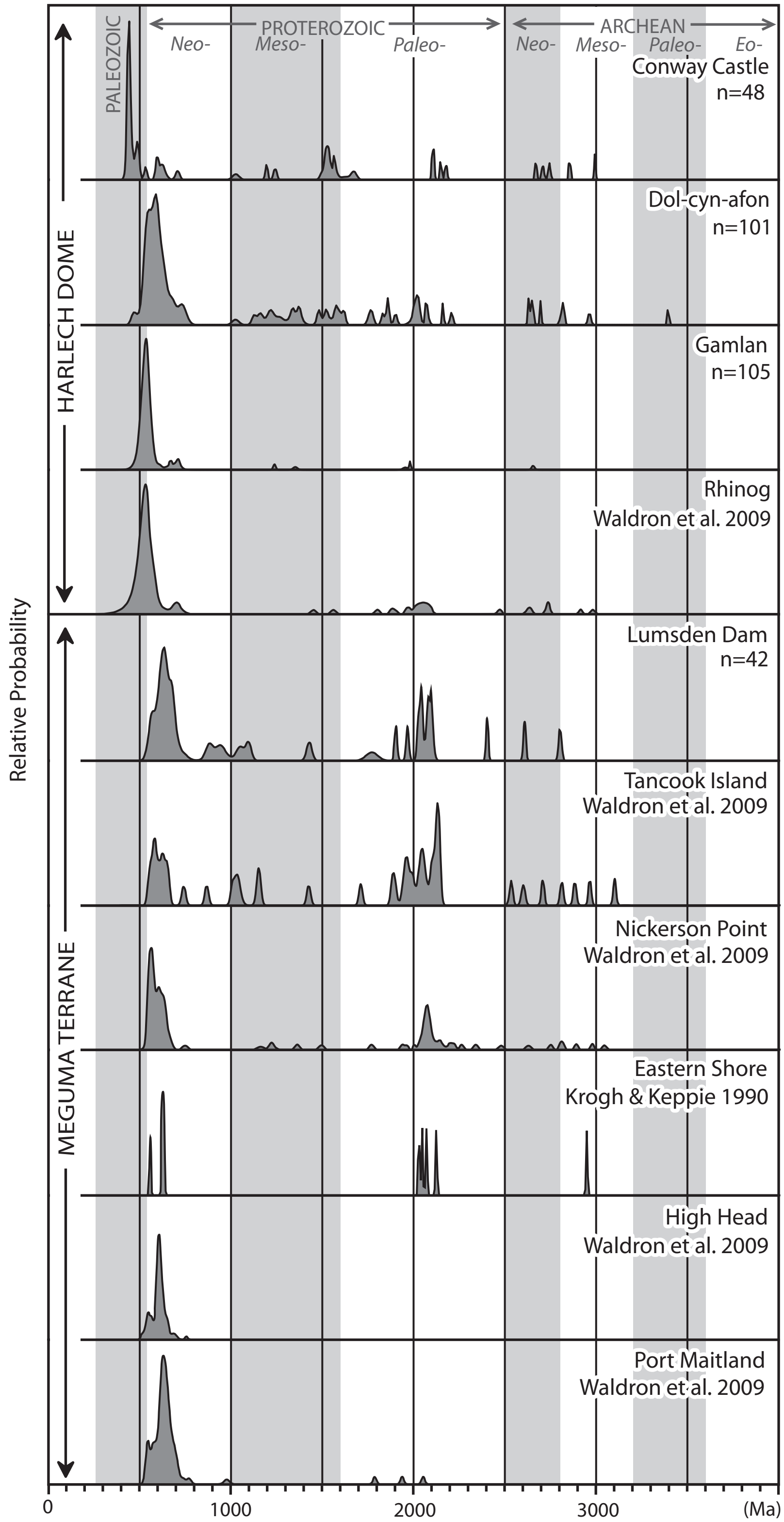

Figure 3.15: Probability density plot of detrital zircon data from the Meguma terrane compared with results from the Harlech Dome region in North Wales (Waldron et al. 2011).

derived sandstone turbidites, overlain by early to middle Cambrian alternating mud-rich and sand-rich units in which manganese is concentrated. Above, the successions comprise anoxic, organic-rich turbidites, shallowing upward into paler, Early Ordovician mudstone and siltstone that contain the graptolite *Rhabdinopora*. In the Harlech Dome region, the Tremadocian is represented by the mudstone-rich Dol-cyn-afon Formation and has previously been compared to the Lumsden Dam Formation base on its age and fossil assemblage (Waldron et al. 2011; White et al. 2012).

By the late Tremadocian the stratigraphic similarities between the Welsh Basin and the Meguma terrane end and their histories diverge. The Lumsden Dam Formation records slope conditions that transition into shelf sedimentation recorded in the Elderkin Brook and Hellgate Falls formations. This is followed by a period of non-deposition and/or erosion and is then overlain the Silurian volcano-sedimentary succession of the Rockville Notch Group. In North Wales, the Dol-cyn-afon Formation is unconformably overlain by late Tremadocian volcanics followed by Floian sandstones and back-arc volcanic rocks through to the late Ordovician.

Detrital zircon samples collected from Cambrian rocks (Rhinog and Gamlan formations) in the Harlech Dome exhibit similar distribution (Fig. 3.15) to the Cambrian Goldenville Group rocks indicating they too were likely sourced from the Pan-African – Avalonian orogen and the West African craton (Waldron et al. 2011; Chapter 2). Three possible Cambrian scenarios have been suggested by Waldron et al. (2011) to explain the similarities between the Harlech Dome and the Meguma Supergroup, one of which suggested they were positioned in a rift basin that formed between East and West Avalonia along the Gondwana margin near the West African craton in the recently identified domain Megumia (Waldron et al. 2011).

A new detrital zircon sample from the Dol-cyn-afon Formation (Chapter 2) exhibits a prominent Neoproterozoic to Cambrian grain population with a peak at c. 580 Ma; it contains a Mesoproterozoic and early Paleoproterzoic grain population that is more abundant than in the Lumsden Dam sample, and a 1.9 to 2.1 Ga population is less prominent (Fig. 3.15). While the Lumsden Dam Formation detrital zircon distribution confirms a consistent source region for the Meguma Supergroup between the Cambrian, Series 3 to Tremadocian, the

Dol-cyn-afon Formation detrital zircon distribution is more representative of the Monian Composite terrane in North Wales (Fig. 2.9), which has been correlated with Ganderia of Atlantic Canada (Collins and Buchan 2004).

The Monian Composite Terrane is separated from the Welsh basin along the NE-SW striking Menai Strait Fault System, which represents a terrane boundary in North Wales. The similarities between the Dol-cyn-afon Formation and Monian detrital zircon distributions indicate the juxtaposition of the Monian Composite Terrane with North Wales by the Tremadocian (Chapter 2). Consequently, if the Welsh basin and the Meguma basin were in in close proximity in the Tremadocian, the Lumsden Dam Formation should reflect the same Monian source as the Dol-cyn-afon Formation, which it does not. These new observations support the diverging Ordovician histories recorded for the two basins and suggests that, if the two basins were contiguous in the Cambrian period, they had parted by the Tremadocian.

Waldron et al. (2011) proposed two paleogeographic reconstructions that would allow the Meguma terrane and the Welsh Basin to be adjacent during the Cambrian. One suggests Megumia originated in a rift system located between East and West Avalonia. The other suggests that the basin was located between Avalonia and Gondwana, where East Avalonia was rotated roughly 180º from its traditionally accepted orientation.

In these scenarios, a mechanism to accommodate the diverging histories of once proximal basins would be strike-slip faulting. Late Precambrian subduction and arc activity along the Gondwanan margin transitioned into a more stable environment by the early Paleozoic, where sinistral transcurrent motion is thought to have been prevalent (Nance et al. 1991). The Menai Strait Fault System between the Monian Composite Terrane and Welsh basin was active between the early Cambrian and late Carboniferous and is thought to have a major component of sinistral strike-slip movement (Gibbons 1987; Gibbons and Horák 1990). If a continuation of this fault system were to pass through Megumia, the left-lateral migration and juxtaposition of the Monian Composite terrane with the Welsh Basin could have displaced the Meguma terrane laterally along the Gondwana margin.

Figure 3.16 shows one possible terrane configuration based on the assumption that Megumia was located within a rift system between the East and West Avalonia.

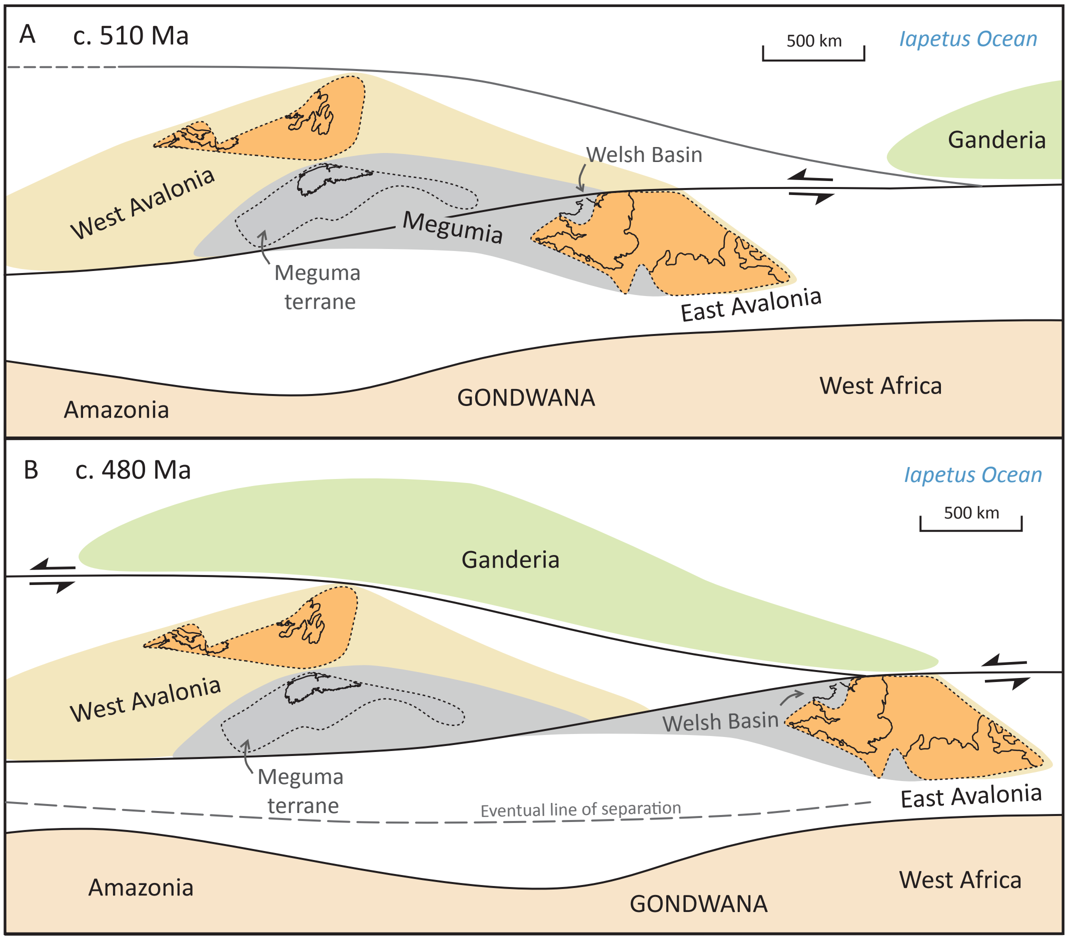

Figure 3.16: Possible paleogeographic reconstruction of the tectonic elements of the Gondwanan margin in the Cambrian and Early Ordovician.

This model is consistent with a sinistral strike-slip tectonic setting, known for the Menai Strait Fault System, and the traditional orientation of Avalonia relative to the Gondwanan margin (e.g., Nance et al. 2008). However, this configuration would require the Monian Composite Terrane, a probable piece of Ganderia, originated closer to the West African craton, when most (e.g., Pollock et al. 2009; van Staal et al. 2012) would position it along the Amazonian margin. Figure 3.17 shows an alternate configuration, which keeps Ganderia adjacent to Amazonia. It is still consistent with a sinistral strike-slip tectonic setting; however, this configuration requires that Avalonia, Ganderia, and the Meguma terrane be rotated roughly 180º from their orientations in Figure 3.16a.

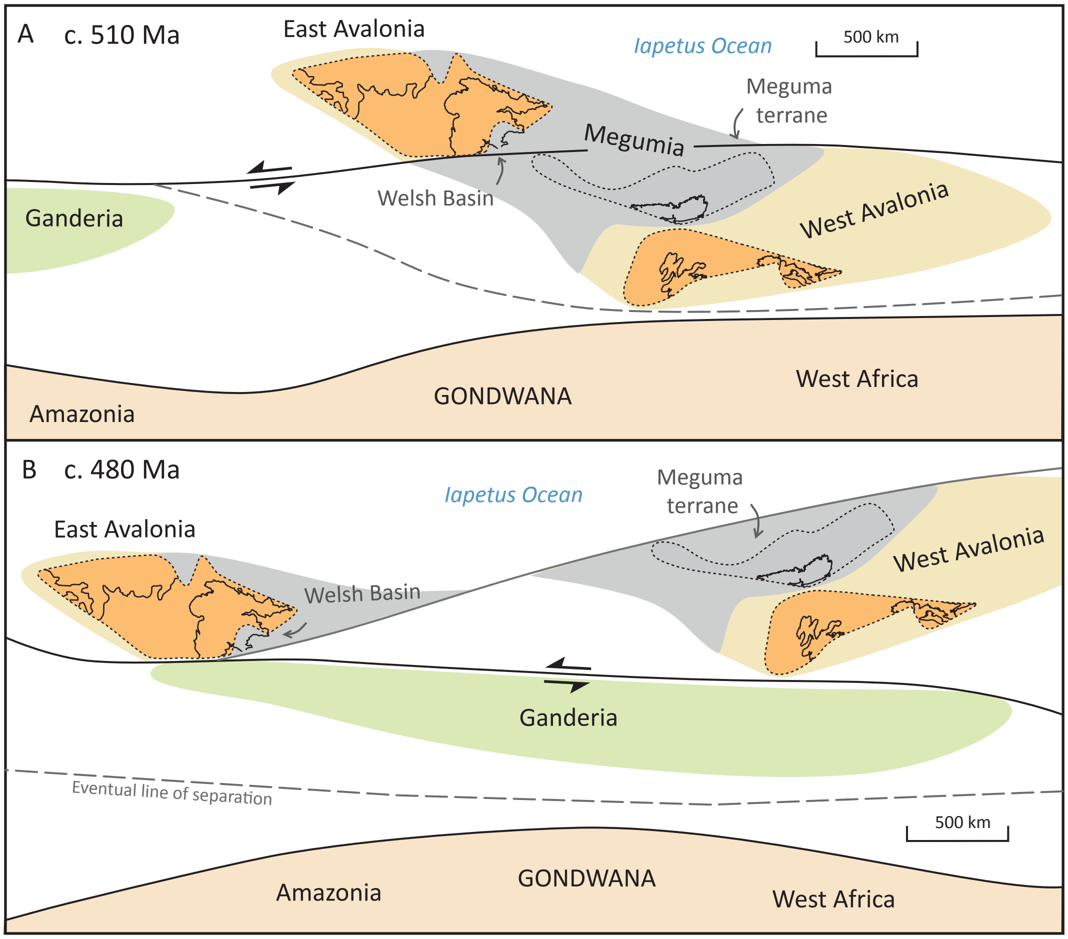

Figure 3.17: Possible paleogeographic reconstruction of the Gondwanan margin in the Cambrian and Early Ordovician in which the tectonic elements in Fig. 3.16 have been rotated 180º.

3.6 CONCLUSIONS

1) The depositional environments of the Bluestone formation and the Lumsden Dam formation of the Halifax Group represent slope related environments.

2) The detrital zircon results from the Lumsden Dam show similar results to the Upper Goldenville Group Government Point formation, with age populations consistent with a source region in the West African craton and possibly the Amazonian craton.

3) Although the age and depositional environment for the Lumsden Dam Formation and the Dol-cyn-afon Formation of the Harlech Dome are similar, their difference in detrital zircon age populations suggests that the histories of the basins diverge by the Tremadocian.

4) A possible explanation for the diversification in detrital zircon ages within the Meguma terrane succession, and the diverging histories of the Meguma terrane and North Wales, could be left-lateral migration of the Meguma terrane parallel to the margin of Gondwana along a strike-slip fault system that separated the once adjacent basins by the Tremadocian.

3.7 References

Ashton, K.E., Heaman, L.M., Lewry, J.F., Hartlaub, R.P. and Shi, R. 1999. Age and origin of the Jan Lake Complex: a glimpse at the buried Archean craton of the Trans-Hudson Orogen. Canadian Journal of Earth Sciences, 36: 185–208.

Barr, S.M., Doyle, E.M. and Trapasso, L.S. 1983. Geochemistry and tectonic implications of mafic sills in Lower Paleozoic formations of southwestern Nova Scotia. Maritime Sediments and Atlantic Geology, 19: 73–87.

Barr, S.M., Hamilton, M.A., Samson, S.D., Satkoski, A.M. and White, C.E. 2012. Provenance variations in northern Appalachian Avalonia based on detrital zircon age patterns in Ediacaran and Cambrian sedimentary rocks, New Brunswick and Nova Scotia, Canada. Canadian Journal of Earth Sciences, 49: 533–546.

Bouyx, E., Blaise, J., Brice, D., Degardin, J.M., Goujet, D., Gourvennec, R., Le Menn, J., Lardeux, H., Morzadec, P. and Paris, F. 1997. Biostratigraphie et paleobiogeographie du Siluro-Devonien de la zone de Meguma (Nouvelle-Écosse, Canada). Canadian Journal of Earth Sciences, 34: 1295–1309.

Clarke, D.B. and Halliday, A.N. 1980. Strontium isotope geology of the South Mountain batholith, Nova Scotia. Geochimica et Cosmochimica Acta, 44: 1045–1058.

Clarke, D.B., Halliday, A.N., and Hamilton, P.J. 1988. Neodymium and strontium isotopic constraints on the origin of the peraluminous granitoids of the South Mountain Batholith, Nova Scotia, Canada. Chemical Geology, 73: 15–24.

Cocks, L.R.M. and Torsvik, T.H. 2002. Earth geography from 500 to 400 million years ago: a faunal and palaeomagnetic review. Journal of the Geological Society, London, 159: 631–644.

Collins, A.S. and Buchan, C. 2004. Provenance and age constraints of the South Stack Group, Anglesey, UK: U-Pb SIMS detrital zircon data. Journal of the Geological Society, London, 161: 743–746.

Eberz, G.W., Clarke, D.B., Chatterjee, A.K., and Giles, P.S. 1991. Chemical and isotopic composition of the lower crust beneath the Meguma Lithotectonic Zone, Nova Scotia: Evidence from granulite facies xenoliths: Contributions to Mineralogy and Petrology, 109: 69–88.

Fyffe, L.R., Barr, S.M., et al. 2009. Detrital zircon ages from Neoproterozoic and Early Paleozoic conglomerate and sandstone units of New Brunswick and coastal Maine: Implications for the tectonic evolution of Ganderia. Atlantic Geology, 45: 110–144.

Gingras, M.K., Waldron, J.W.F., White, C.E. and Barr, S.M. 2011. The evolutionary significance of a Lower Cambrian trace-fossil assemblage from the Meguma terrane, Nova Scotia. Canadian Journal of Earth Sciences, 48: 71–85.

Gibbons, W. 1987. Menai Strait fault system: An early Caledonian terrane boundary in north Wales. Geology, 15: 744–747.

Gibbons, W. and Horák, J. 1990. Contrasting metamorphic terranes in northwest Wales.

Geological Society, London, Special Publications, 51: 315–327.

Gibling, M.R., Culshaw, N., Rygel, M.C. and Pascucci, V. 2008. The Maritimes Basin of Atlantic Canada: Basin Creation and Destruction in the Collisional Zone of Pangea. Sedimentary Basins of the World, 5: 211–244.

Greenough, J.D., Krogh, T.E., Kamo, S.L., Owen, J.V. and Ruffman, A. 1999. Precise U-Pb dating of Meguma basement xenoliths: new evidence for Avalonian underthrusting. Canadian Journal of Earth Sciences, 36: 15–22.

Harris, I.M. and Schenk P.E. 1976. The Meguma Group. Maritime Sediments, 11: 25–46.

Jackson, S.E., Pearson, N.J., Griffin, L. and Belousova, E.A. 2004. The application of laser ablation-inductively coupled plasma-mass spectrometry to in situ U-Pb zircon geochronology, 211: 47–69.

Jamieson, R.A., Hart, G.G., Chapman, G.G., and Tobey, N.W. 2012. The contact aureole of the South Mountain Batholith in Halifax, Nova Scotia: geology, mineral assemblages, and isograds. Canadian Journal of Earth Sciences, 49: 1280–1296.

Jamieson, R.A., Tobey, N., and ERTH 3020. 2005. Contact metamorphism of the Halifax Formation on the southeastern margin of the Halifax Pluton, Halifax, Nova Scotia. GAC-MAC-CSPG-CSSS Joint Annual Meeting, Halifax, Nova Scotia, Abstract Volume, 30: 95.

Jamieson, R.A., Waldron, J.W.F., and White, C.E. 2011. Bluestone formation of the Halifax Group: metamorphosed slope and mass-transport deposits, Halifax Peninsula, Nova Scotia. Atlantic Geology, 47: 24.

Keppie, J.D. 1977. Tectonics of Southern Nova Scotia. Nova Scotia Department of Mines Paper 77-1.

Keppie, J.D. and Dallmeyer, R.D. 1987. Dating transcurrent terrane accretion: an example from the Meguma and Avalon Composite terranes in the Northern Appalachians. Tectonics, 6: 831–847.

Keppie. J.D., Dostal, J., Murphy, J.B., and Cousens, B.L. 1997. Palaeozoic withinplate volcanic rocks in Nova Scotia reinterpreted: isotopic constraints on magmatic source and palaeocontinental reconstructions. Geological Magazine, 134: 425–447.

Keppie, J.D. and Krogh, T.E. 1999. U-Pb Geochronology of Devonian Granites in the Meguma Terrane of Nova Scotia, Canada: Evidence for Hotspot Melting of a Neoproterozoic Source. The Journal of Geology, 107: 555–568.

Keppie, J.D. and Krogh, T.E. 2000. 440 Ma igneous activity in the Meguma Terrane, Nova Scotia, Canada: part of the Appalachian overstep sequence. American Journal of Science, 300: 528–538.

Keppie, J.D. and Muecke, G.K. 1979. Metamorphic Map of Nova Scotia. Nova Scotia Department of Mines and Energy, Map 1979-01.

Klein, G.D. 1962. Triassic sedimentation, Maritime Provinces, Canada. Geological

Society of America Bulletin. 73: 1127–1146.

Krogh, T.E. and Keppie, J.D. 1990. Age of detrital zircon and titanite in the Meguma Group, southern Nova Scotia, Canada: Clues to the origin of the Meguma Terrane. Tectonophysics, 177: 307–323.

Landing, E. 2004. Precambrian-Cambrian boundary interval deposition and marginal platform of the Avalon microcontinent. Journal of Geodynamics, 37: 411–435.

Lane, T.E. 1976. Stratigraphy of the White Rock Formation. Maritime Sediments, 12: 119–140.

Lerouge, C., Cocheria, A., Toteu, S.F., Penaye, J., Milesi, J.P., Tchameni, R., Nsifa, E.N., Fanning, C.M., and Deloule, E. 2006. Shrimp U–Pb zircon age evidence for Paleoproterozoic sedimentation and 2.05Ga syntectonic plutonism in the Nyong Group, South-Western Cameroon: consequences for the Eburnean–Transamazonian belt of NE Brazil and Central Africa. Journal of African Earth Sciences, 44: 413–427.

Linnemann, U., Herbosch, A., Liegeois, J.P., Pin, C., Gartner, A., Hofmann, M. 2012. The Cambrian to Devonian odyssey of the Brabant Massif within Avalonia: A review with new zircon ages, geochemistry, Sm–Nd isotopes, stratigraphy and palaeogeography. Earth-Science Reviews, 112: 126–154.

Linnemann, U., McNaughton, N.J., Romer, R.L., Gehmlich, M., Drost, K. and Tonk, C. 2004. West African provenance for Saxo-Thuringia (Bohemian Massif): Did Armorica ever leave pre-Pangean Gondwana? U/Pb-SHRIMP zircon evidence and the Nd-isotopic record. International Journal of Earth Sciences, 93: 683–705.

Litherland, M., Klinck, B.A., O’Connor, E.A. and Pitfield, P.E.J. 1985. Andean-trending mobile belts in the Brazilian Shield. Nature, 314: 345–348.

Ludwig, K.R. 2003. User’s Manual for Isoplot 3.00. Berkeley Geochronology Center Special Publication, 4.

MacDonald, L.A., Barr, S.M., White, C.E. and Ketchum, J.W.F. 2002. Petrology, age, and tectonic setting of the White Rock Formation, Meguma terrane, Nova Scotia: evidence for Silurian continental rifting. Canadian Journal of Earth Sciences, 39: 259–277.

Martel, A.T. and McGregor, D.C. 1993. Stratigraphic significance of Upper Devonian and Lower Carboniferous miospores from the type area of the Horton Group, Nova Scotia. Canadian Journal of Earth Science. 30: 1091–1098.

Murphy, J.B., Fernandez-Suarez, J., Keppie, J.D., and Jeffries, T.E. 2004a. Contiguous rather than discrete Paleozoic histories for the Avalon and Meguma Terranes based on detrital zircon data. Geology, 32: 585–588.

Murphy, J.B., Fernandez-Suarez, J., Jeffries, T.E. and Strachan, R.A. 2004b. U-Pb (LA-ICP-M.S.) dating of detrital zircons from Cambrian clastic rocks in Avalonia: erosion of a Neoproterozoic arc along the northern Gondwanan margin. Journal of the Geological Society, London, 161: 243–254.

Nance, R.D., Murphy, J.B., Strahan, R.A., D'Lemos, R.S. and Taylor, G.K. 1991. Late Preoterozoic tectonostratigraphic evolution of the Avalonian and Cadomian terranes. Precambrian Research, 53: 41–78.

Nance, R.D. and Murphy, J.B. 1996. Basement isotopic signatures and Neoproterozoic paleogeography of Avalonian–Cadomian and related terranes in the Circum-North Atlantic. *In* Avalonian and Related Peri-Gondwanan Terranes of the Circum-North Atlantic. *Edited by* R.D. Nance and M.D. Thompson. Geological Society of America, Special Papers, 304: 333–346.

Nance,R.D., Murphy, J.B., Strachan, R.A., Keppie, D.J. Gutiérrez-Alonso, G., Fernández-Suárez, J., Quesada, C., Linnemann, U., D'lemos, R. and Pisarevsky, S.A. 2008. Neoproterozoic-early Palaeozoic tectonostratigraphy and palaeogeography of the peri-Gondwanan terranes: Amazonian v. West African connections. Geological Society, London, Special Publications, 297: 345–383.

Pollock, J.C., Hibbard, J.P. and Sylvester, P.J. 2009. Early Ordovician rifting of Avalonia and birth of the Rheic Ocean: U−Pb detrital zircon constraints from Newfoundland. Journal of the Geological Society, London, 166: 501–515.

Pratt, B.R. and Waldron, J.W.F. 1991. A Middle Cambrian trilobite faunule from the Meguma Group of Nova Scotia. Canadian Journal of Earth Sciences, 28: 1843–1853.

Robinson, P., Tucker, R.D., Bradley, D., Berry, H.N.V. and Osberg, P.H. 1998. Paleozoic orogens in New England, USA: Geologiska Föreningens Förhandlingar, 120: 119–148.

Rocci, G., Bronner, G. and Deschamps, M. 1991. Crystalline basement of the West African Craton. *In* The West African Orogens and Circum-Atlantic Correlatives. *Edited by* R.D. Dallmeyer and J.P. Lecorche. Berlin, Springer, pp. 31–61.

Rowley, D.B. and Pindell, J.L. 1989. End Paleozoic–early Mesozoic western Pangean reconstruction and its implications for the distribution of Precambrian and Paleozoic rocks around Meso-America: Precambrian Research, 42: 411–444.

Schenk, P.E. 1970. Regional variation of the flysch-like Meguma Group (Lower Palaeozoic) of Nova Scotia, compared to recent sedimentation off the Scotian shelf. Geological Association of Canada, Special Paper 7, 127–53.

Schenk, P.E. 1971. Southeastern Atlantic Canada, northwestern Africa, and continental drift. Canadian Journal of Earth Sciences, 8: 1218–1251.

Schenk, P.E. 1981. The Meguma zone of Nova Scotia: a remnant of western Europe, South America or Africa?. *In* Geology of North Atlantic borderlands. *Edited by* J.M Kerr, A.J. Ferguson and L.C. Machan. Canadian Society of Petroleum Geologists, Memoir 7, pp. 119–148.

Schenk, P.E. 1983. The Meguma terrane of Nova Scotia, Canada - An aid in trans-Atlantic correlation. *In* Regional trends in the geology of the Appalachian-Caledonian-Hercynian-Mauritanide orogen. *Edited by* P.E. Schenk. D. Reidel Publishing Co., pp. 121–130.

Schenk, P.E. 1995a. Meguma Zone. *In* Chapter 3 Geology of the Appalachian-Caledonian Orogen in Canada and Greenland. *Edited by* H. Williams. Geological Survey of Canada, Geology of Canada, 6: 261–277.

Schenk, P.E. 1995b. Annapolis Belt. *In* Chapter 4 Geology of the Appalachian-Caledonian Orogen in Canada and Greenland. *Edited by* H. Williams. Geological Survey of Canada, Geology of Canada, 6: 367–383.

Schenk, P.E. 1997. Sequence stratigraphy and provenance on Gondwana's margin: the Meguma Zone (Cambrian to Devonian) of Nova Scotia, Canada. Geological Society of America Bulletin, 109: 395–409.

Simonetti, A., Heaman, L.M., Hartlaub, R.P., Creaser, R.A., MacHattie, T.G. and Bohm, C. 2005. U-Pb zircon dating by laser ablation-MC-ICP-MS using a new multiple ion counting Faraday collector array. Journal of Analytical Atomic Spectrometry, 20: 677–686.

Simonetti, A., Heaman, L.M. and Chacko, T. 2008. Chapter 14: Use of discrete-dynode secondary electron multipliers with faradays – A 'reduced volume' approach for in situ U-Pb dating of accessory minerals within petrographic thin section by LA-ICP-MS. *In* Mineralogical Association of Canada Short Course 40, Vancouver, pp. 241–264.

Smitheringale, W.G. 1960. Geology of the Nictaux-Torbrook map-area, Annapolis and Kings counties, Nova Scotia. Geological Survey of Canada, Paper 60-13.

Smitheringale, W.G. 1973. Geology of parts of Digby, Bridgetown, and Gaspereau map-areas, Nova Scotia: Geological Survey of Canada Memoir 375.

Stevenson, I.M. 1959. Shubenacadie and Kennetcook map areas, Colchester, Hants, and Halifax counties, Nova Scotia. Geological Survey of Canada Memoir 302, 88 p.

Stow, D.A.V., Alam, M. and Piper, D.J.W. 1984. Sedimentology of the Halifax Formation, Nova Scotia: Lower Paleozoic fine-grained turbitites. *In* Fine grained sediments: deep water processes and facies. *Edited by* D.J.W. Piper and D.A.V. Stow. Geological Society of London, Special Publication 15, pp. 127–144.

Taylor, F.C. 1965. Silurian stratigraphy and Ordovician-Silurian relationships in southwestern Nova Scotia. Geological Survey of Canada, Department of Mines and Technical Surveys, Paper 64-13.

van Staal, C.R. 2007. Pre-Carboniferous tectonic evolution and metallogeny of the Canadian Appalachians. *In* Mineral Resources of Canada: A Synthesis of Major Deposit Types, Distinct Metallogeny, the Evolution of Geological Provinces, and Exploration Methods. *Edited by* W.D. Goodfellow. Geological Association of Canada, Mineral Deposits Division, Special Publication 5, pp. 793–818.

van Staal, C.R., Barr, S.B. and Murphy, J.B. 2012. Provenance and Tectonic Evolution of Ganderia: Constraints on the Evolution of the Iapetus and Rheic Oceans. Geology, 40: 987–990.

Waldron, J.W.F. 1987. Sedimentology of the Goldenville-Halifax transition in the

Tancook Island area, South Shore, Nova Scotia. Geological Survey of Canada, Open File Report 1525.

Waldron, J.W.F. 1992. The Goldenville–Halifax transition, Mahone Bay, Nova Scotia: relative sea-level rise in the Meguma source terrane. Canadian Journal of Earth Sciences, 29: 1091–1105.

Waldron, J.W.F. and Jensen, L.R. 1985. Sedimentology of the Goldenville Formation, Eastern Shore, Nova Scotia. Geological Survey of Canada, Paper, 85-15.

Waldron, J.W.F., Piper, D.J.W., and Pe-Piper, G. 1989. Deformation of the Cape Chignecto Pluton, Cobequid Highlands, Nova Scotia: thrusting at the Meguma-Avalon boundary. Atlantic Geology, 25: 51–62.

Waldron, J.W.F., Schofield, D.I., White, C.E. and Barr, S.M. 2011. Cambrian successions of the Meguma Terrane, Nova Scotia, and Harlech Dome, North Wales: dispersed fragments of a peri-Gondwanan basin?. Journal of the Geological Society, London, 168: 83–98.

Waldron, J.W.F., White, C.E., Barr, S.M., Simonetti, A. and Heaman, L.M. 2009. Provenance of the Meguma terrane, Nova Scotia: rifted margin of early Paleozoic Gondwana. Canadian Journal of Earth Sciences, 46: 1–9.

White, C.E. 2008. Defining the stratigraphy of the Meguma Supergroup in southern Nova Scotia: where do we go from here?. Atlantic Geology, 44, p. 48.

White, C.E. 2010a. Pre-Carboniferous bedrock geology of the Annapolis Valley area (NTS 21A/14, 15, and 16; 21H/01 and 02), southern Nova Scotia. *In* Mineral Resources Branch, Report of Activities 2009. *Edited by* D.R. MacDonald. Nova Scotia Department of Natural Resources, Report 2010-1, pp. 137–155.

White, C.E. 2010b. Stratigraphy of the Lower Paleozoic Goldenville and Halifax groups in the western part of southern Nova Scotia. Atlantic Geology, 46: 136–154.

White, C.E. and Barr, S.M. 2004. Age and Petrochemistry of Mafic Sills in Rocks of the Northwestern Margin of the Meguma Terrane, Bear River - Yarmouth Area of Southwestern Nova Scotia. *In* Mineral Resources Branch, Report of Activities 2003. *Edited by* D.R. MacDonald. Nova Scotia Department of Natural Resources, Report 2004-1, pp. 97–117.

White, C.E., Barr, S.M., Horne, R.J. and Hamilton, M.A. 2007. The Neoacadian orogeny in the Meguma terrane, Nova Scotia, Canada. *In* 42nd Annual Meeting Geological Society of America, Northeastern Section, March 12-14, Abstracts with Programs, 39: 69.

White, C.E., Barr, S.M. and Toole, R.M. 2006. New insights on the origin of the Meguma Group in southwestern Nova Scotia, Canada. Nova Scotia Department of Natural Resources, Mineral Resource Branch, Open File Illustration, ME 2006-2.

White, C.E., Bell, J.A., McLeish, D.F., Macdonald, M.A., Goodwin, T.A. and MacNeil, J.D. 2008. Geology of the Halifax Regional Municipality, Central Nova Scotia. *In* Mineral Resources Branch, Report of Activities 2007. Nova Scotia Department of

Natural Resources, Report 2008-1, pp. 125–139.

White, C.E., Horne, R.J., Muir, C. and Hunter, J.1999. Preliminary bedrock geology of the Digby map sheet (21A/12), southwestern Nova Scotia. In Mineral Resources Branch, Report of Activities 2008. Nova Scotia Department of Natural Resources, Report 2009-1, pp. 119–134.

White, C.E., Palacios, T., Jensen, S. and Barr, S.M. 2012. Cambrian-Ordovician acritarchs in the Meguma terrane, Nova Scotia, Canada: Resolution of early Paleozoic stratigraphy and implications for paleogeography. GSA Bulletin 124: 1773–1792.

Woodman, J.E. 1902. Geology of the Moose River district, Halifax County, Nova Scotia; together with the pre-Carboniferous history of the Meguma series. Unpublished Ph.D. thesis, Harvard University, Cambridge, Massachusetts.

CHAPTER 4: DISCUSSION AND CONCLUSIONS

This chapter summarizes previous interpretations for the tectonic setting and the position of Avalonia, Ganderia and the Meguma terrane along the Gondwanan margin during the late Neoproterozoic to the Tremadocian. It discusses two new tectonic models for the Gondwanan margin during the Cambrian to Tremadocian based on the detrital zircon results from Chapters 2 and 3, and closes with suggestions for future work that may provide further insight into the complex histories of these tectonic domains.

4.1 PREVIOUS PALEOGEOGRAPHIC INTERPRETATIONS

While it is widely accepted that Avalonia, Ganderia and the Meguma terrane all originated along the active continent margin of Gondwana (e.g., van Staal et al. 1996; Murphy et al. 2004; Thompson et al. 2007) their exact positions and relative arrangement are still uncertain. In most recent reconstructions Ganderia is placed along the Amazonian margin (e.g., van Staal et al. 1996; van Staal 2012) (Fig. 4.1). Major Mesoproterozoic detrital zircon populations of Ganderian basement and Cambrian sedimentary rocks match source regions within Amazonia (e.g., van Staal et al. 1996; van Staal et al. 2012). Avalonia is commonly placed near the boundary between Amazonia and West Africa (e.g., Nance et al. 2002; van Staal and Hatcher 2010) (Fig. 4.2). Detrital zircon and Sm/Nd data from West Avalonia have been interpreted by Satkoski et al. (2010) to indicate a change in source region from the Amazonian craton in the Neoproterozoic to the West African Craton by the early Cambrian. In many late Neoproterozoic and Cambrian peri-Gondwanan terrane reconstructions, the Meguma terrane is placed on the SE margin of West Avalonia and the Harlech Dome is placed in its current configuration within East Avalonia (e.g., Murphy et al. 2004; Linnemann et al. 2004). Given the lithostratigraphic and provenance similarities between the Harlech Dome succession and the Meguma Supergroup, Waldron et al. (2011) suggested three possible Cambrian paleogeographic reconstructions. In the first (Fig. 4.3a), the two basins were widely separated along the Gondwanan margin and underwent similar basin evolution histories. In the second (Fig. 4.3b), they were part of a single basin and were deposited in a rift system that developed between 'East' and 'West' Avalonia. In the third (Fig. 4.3c), they were deposited in a single basin in a rift that developed between Avalonia and Gondwana, which

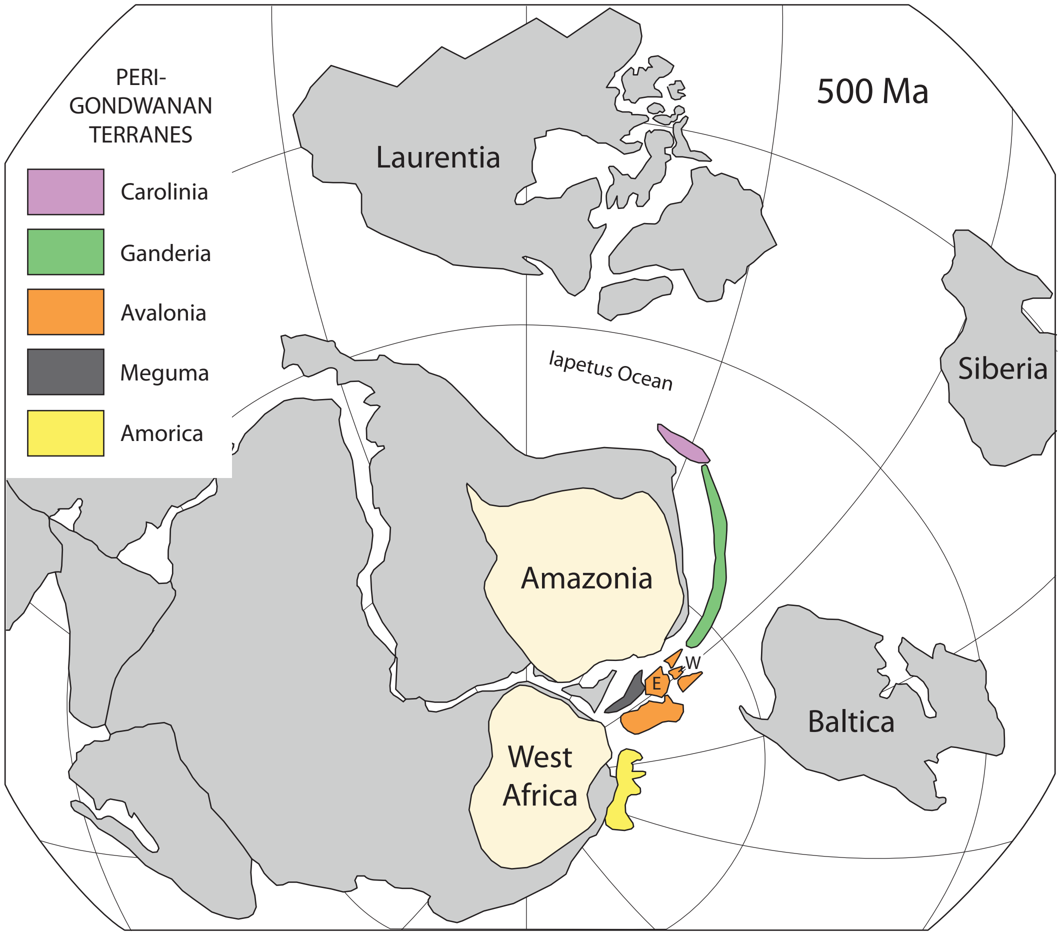

Figure 4.1: Paleogeographic reconstruction of the Gondwanan margin at c. 500 Ma (from van Staal et al. 2012). E=East Avalonia; W=West Avalonia.

involves the ~180º rotation of 'East' Avalonia relative to the Meguma terrane in their present day orientation.

4.2 DEPOSITIONAL ENVIRONMENT AND PROVENANCE

Detrital zircons studies have been an essential tool in unraveling the paleogeographic positions and evolution of terranes in ancient orogens. The detrital zircon record in North Wales shows a change from a restricted source region with age signatures characteristic of the West African craton in the mid-Cambrian Gamlan Formation, to those more characteristic of the Monian Composite Terrane by the Tremadocian Dol-cyn-afon Formation. The timing of this change also corresponds with the Monian deformation event, which we interpret to reflect the juxtaposition of North Wales with 'Ganderia'. None of the North Wales samples,

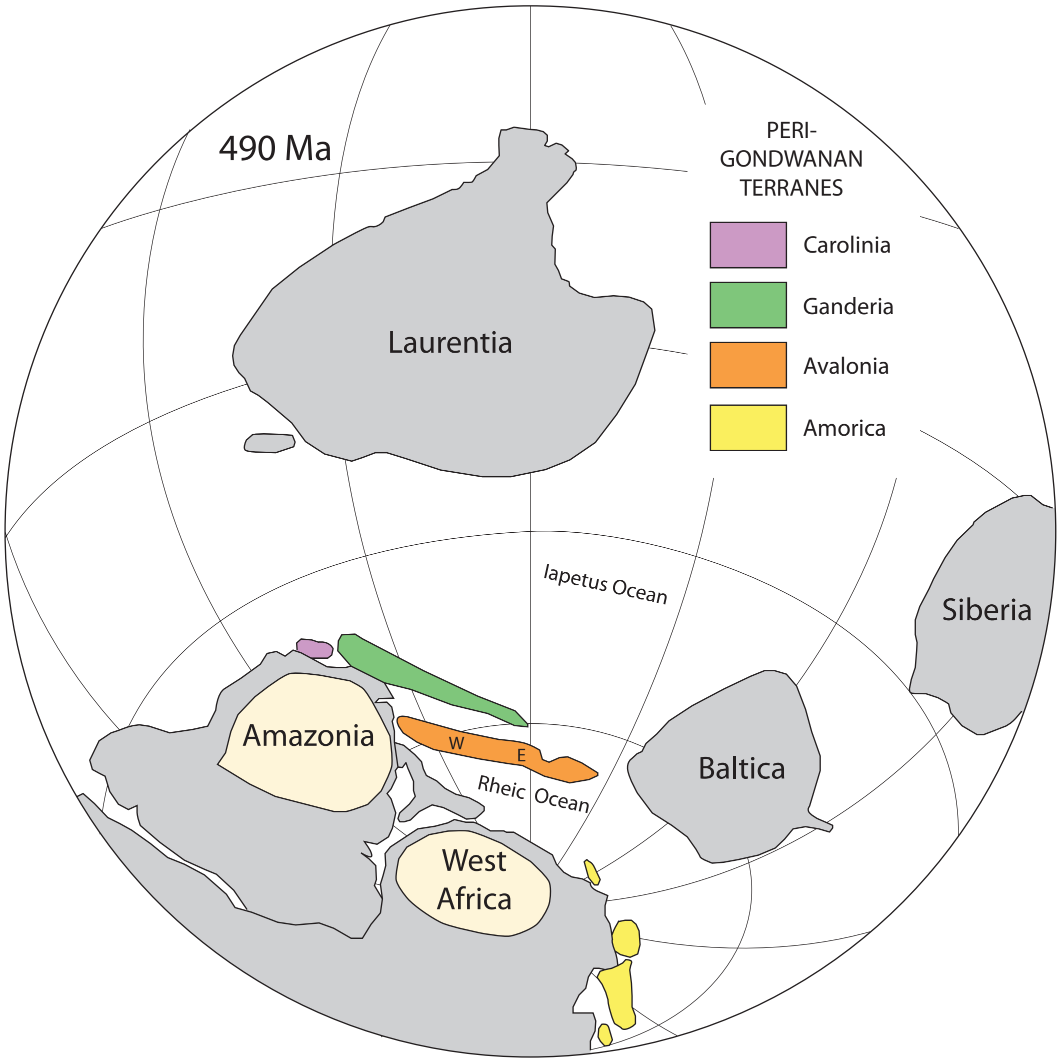

Figure 4.2: Paleogeographic reconstruction of the Gondwanan margin at 490 Ma (from van Staal and Hatcher 2010). E=East Avalonia; W=West Avalonia.

including the late Ordovician sedimentary rock of the Conway Castle Grit, exhibit a Laurentian source. This is in agreement with Soper and Woodcock (1990) and Cocks and Torsvick (2002) who interpreted that the collision of Avalonia with Laurentia occurred between 440 and 420 Ma. These data are further supported by unpublished detrital zircon data from the English Lake District in the Leinster-Lakesman terrane (Waldron et al. in prep. 2013), suggesting collision with Laurentia by the Wenlock.

The Arfon Basin, located along the Menai Strait Fault System between North Wales and the Monian Composite terrane, exhibits a distinctive detrital zircon

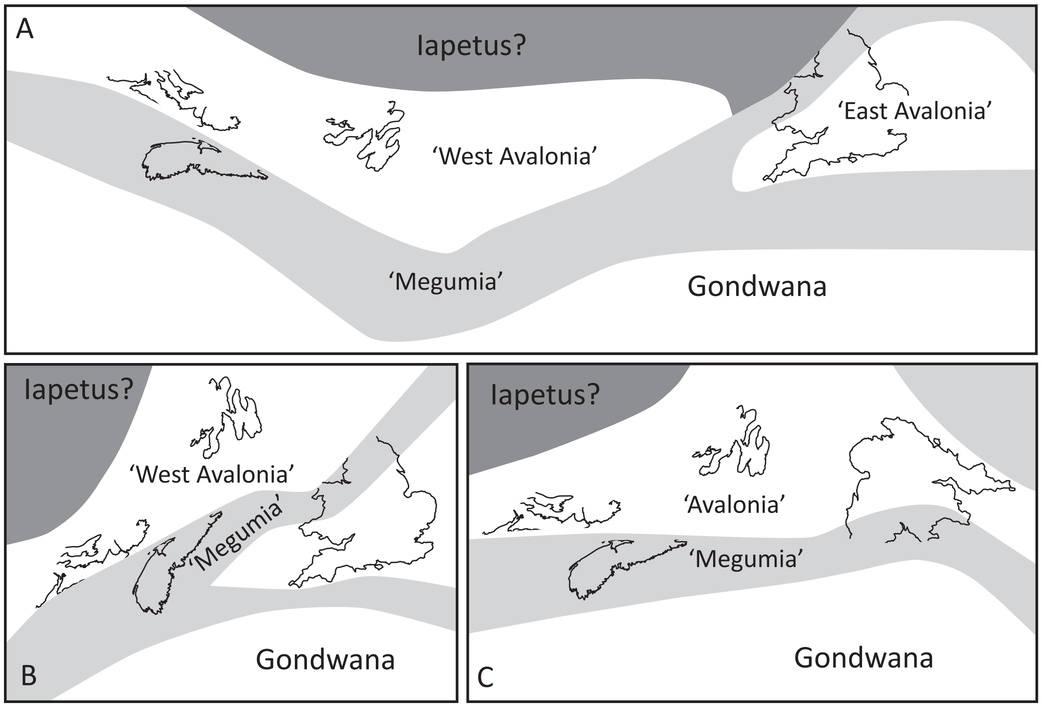

Figure 4.3: Three plate reconstructions proposed by Waldron et al. (2011) for the location of the Meguma terrane and North Wales in the early Cambrian.

signature. This suggests that it was neither part of East Avalonia nor the Monian Composite Terrane and was likely a transported slice caught up in the fault system.

The Meguma terrane exhibits similar Cambrian detrital zircon signatures to the Harlech Dome in North Wales, which also reflects a dominantly West African source region. The Tremadocian Lumsden Dam Formation of the Meguma Supergroup, deposited in a slope-related environment, also shows a diversification of detrital zircon ages as witnessed in the Welsh succession; however, the Mesoproterozoic and Paleoproterozoic grain populations in the Dol-cyn-afon Formation in North Wales are either absent or not as prominent in the Lumsden Dam Formation. If the two basins were once in close proximity, this difference would indicate separation by this time. This conclusion is consistent with their divergent Ordovician and Silurian histories.

4.3 TECTONIC MODELS

4.3.1 Late Neoproterozoic

During the Late Neoproterozoic (ca. 635 – 590 Ma) the active northern margin of Gondwana was characterized by oblique sinistral convergence and subduction (Nance et al. 2002; Murphy et al. 2004) and arc volcanism. Between 590 and 540 Ma subduction ceased and the Gondwanan margin underwent a transition here from an arc to a platform setting. The diachronous end of arc volcanism and the absence of a major collision event has been interpreted to reflect ridge-trench collision along the Gondwanan margin and a shift to a transform plate boundary (e.g., Murphy and Nance 1989; Keppie et al. 2000; Nance et al. 2002) and the development of extensional or transtensional basins (e.g., Smith and Hiscott 1984; Pauley 1990; Barr and White 1996; O'Brien et al. 1996). In East Avalonia and Cadomia sinistral motion along major faults is thought to be associated with this transition (e.g., Gibbons and Horák 1996; Nance et al. 1991; Strachan et al. 1996).

4.3.2 Cambrian to Tremadocian

Most models of the Iapetus Ocean during the Cambrian period do not include major strike-slip components (e.g., van Staal et al. 1998) and are dominated by subduction and rifting. However, Nance (2002) suggests that the transform fault along the Gondwana margin shifted inboard during the early Paleozoic, causing oblique rifting and the transfer of the peri-Gondwanan terranes, including Avalonia, Ganderia and the Meguma terrane, onto a formerly oceanic plate between 510 and 480 Ma. The closure of the Iapetus Ocean is thought to have begun in the mid-Cambrian (van Staal et al. 1998). The cause for the onset of closure is unknown. Van Staal et al. (2012) suggest it to be the result of far-field stresses induced by slab pull and slab rollback, while Waldron et al. (2012) proposed a Caribbean-style tectonics where a subduction zone migrated from an adjacent external ocean to explain the initiation of ocean closure.

Our results show that the Welsh Basin was juxtaposed with 'Ganderia' along the Menai Strait Fault System, which has a history of sinistral strike-slip movement suggesting that strike-slip tectonics persisted along the Gondwanan margin into the early Tremadocian. Strike-slip motion may also account for the diverging histories recorded in the Meguma terrane and the Harlech Dome succession in the Ordovician.

Contractional Deformation

Folding and uplift in North Wales occurred during the Monian deformation and resulted in a basin-wide sub-Floian unconformity which extends across the Menai Strait Fault System (Allen and Jackson 1985; Kokelaar 1988). The influx of 'Monian' detritus in the Tremadocian precedes this event, indicating that this event was likely caused the juxtaposition of the Welsh Basin with 'Ganderia'.

Penobscotian deformation in the northern Appalachian also records a soft collision event between 485 and 478 Ma (van Staal et al. 1998) that resulted from the obduction of the Penobscot backarc basin ophiolites onto the Gander margin (Colman-Sadd et al. 1992; Zagorevski et al. 2010).

Although the timing for the Monian and Penobscotian deformation events are contemporaneous, the nature of the deformation varies. If these events are related, then the different in kinematic setting could be caused by curvature of the plate boundary leading to strike-slip movement in North Wales and a convergent boundary at the Gander margin. Alternatively, both regions may have been in a sinistral transpressional setting.

4.3.3 Paleogeography

The paleogeographic reconstruction illustrated in Figure 2.10 places Avalonia and Ganderia in their traditional orientations relative to the Gondwanan margin. However, given the sinistral strike-slip tectonic regime this would place Ganderia adjacent to the West African Craton, when most believe it originated close to Amazonia (e.g., van Staal et al. 2012). To account for the juxtaposition of the Monian Composite Terrane and North Wales with Ganderia located adjacent to Amazonia and Avalonia closer to West Africa, the motion along the Menai Strait Fault System would have to have been dextral, which is inconsistent with the interpretations of structures exposed in the fault system (Gibbons 1987). Alternatively, if the Monian Composite Terrane and the Leinster-Lakesman terrane formed a separate continental slice from Ganderia of Atlantic Canada it could have resided closer to the West Africa in keeping with sinistral motion as interpreted by Gibbons (1987, 1996).

The reconstruction shown in Figure 2.11 places Avalonia and Ganderia in their traditional locations relative to each other, but their orientations have been rotated ~180º for consistency with the sinistral strike-slip tectonic model. This model requires significant clockwise rotation after the Monian – Penobscot event, but before collision with Laurentia, in order to get Avalonia, Ganderia and the Meguma terrane into their present-day orientations. This model is the preferred scenario because it agrees with the current understanding of the origin and positions of Avalonia, Ganderia and the Meguma terrane.

4.4 SUGGESTIONS FOR FUTURE WORK

To test whether the tectonic reconstruction outlined in Figure 2.11 is possible, additional paleomagnetic data must be collected in order to identify if the rotation necessary took place from the Early Ordovician to the mid-Silurian.

Further detrital zircon studies from the North Wales and the Meguma terrane could provide insight into the link between the Meguma terrane and Harlech Dome successions and to help complete the successions history. To further test the correlation between the two successions a sample from the Dolwen Formation at the base of the Harlech Dome succession could be compared to the lower Goldenville detrital zircon distributions in the Meguma terrane. Samples from the Furongian Maentwrog and Cunard formations would also be useful for comparison if enough zircons could be extracted from the fine-grained units. In the Meguma Supergroup, a diversification of zircon ages begins in the Cambrian Series 3; however, the Gamlan Formation of similar age does not show this trend. In addition, by analyzing the Maentwrog Formation it would better constrain the timing of first sign of influx of detritus from the Monian Composite Terrane. The Denbeigh Grits (Wenlock) are the first coarse-grained unit in the Silurian succession of North Wales. Sampling this unit would help complete the North Wales detrital zircon record, and also provide insight into timing of the first influx of Laurentian detritus into the basin.

To provide further insight into the origin of the Arfon Basin, the Fachwen Formation and the Marchlyn Formation, both of which have good age control, should be sampled. These samples could yield useful information about the late Neoproterozoic and late Cambrian source regions for the Arfon Basin and provide further insight into its relationship with the Harlech Dome succession or Monian Composite terrane by the Furongian.

Heavy mineral studies and paleocurrent analysis of the units that have been sampled for detrital zircon analyses would also prove useful for identifying different source regions.

4.5 REFERENCES

Allen, P.M. and Jackson, A.A. 1985. Geology of the country around Harlech. Memoir of the British Gevological Survey, Sheet 135 with part of 149. British Geological Survey, Keyworth, Nottingham.

Barr, S.M. and White, C.E. 1996. Contrasts in late Precambrian–early Paleozoic tectonothermal history between Avalon composite terrane sensu stricto and other possible peri-Gondwanan terranes in southern New Brunswick and Cape Breton Island, Canada. *In* Avalonian and Related Peri-Gondwanan Terranes of the Circum–North Atlantic: Boulder, Colorado. *Edited by* R. D. Nance and M.D. Thompson. Geological Society of America Special Paper 304.

Cocks, L.R.M. and Torsvik, T.H. 2002. Earth geography from 500 to 400 million years ago: a faunal and palaeomagnetic review. Journal of the Geological Society, London, 159: 31–644.

Colman-Sadd, S.P., Dunning, G.R. and Dec, T. 1992. Dunnage-Gander relationships and Ordovician orogeny in central Newfoundland: A sediment provenance and U/Pb age study: American Journal of Science, 292: 317–355.

Gibbons, W. and Horak, J.M. 1996. The Evolution of the Neoproterozoic Avalonian Subduction System: Evidence From the British Isles. Geological Society of America, Special Papers 304, pp. 269–280.

Keppie, J.B., Dostal, J., Dallmeyer, R.D. and Doig, R. 2000. Superposed Neoproterozoic and Silurian magmatic arcs in central Cape Breton Island, Canada: geochemical and geochronological constraints. Geological Magazine, 137: 137–153.

Kokelaar, B.P. 1988. Tectonic controls of Ordovician arc and marginal basin volcanism in Wales. Journal of the Geological Society, London, 145, 759–775.

Linnemann, U., McNaughton, N.J., Romer, R.L., Gehmlich, M., Drost, K. and Tonk, C. 2004. West African provenance for Saxo-Thuringia (Bohemian Massif): Did Armorica ever leave pre-Pangean Gondwana? U/Pb-SHRIMP zircon evidence and the Nd-isotopic record. International Journal of Earth Sciences, 93: 683–705.

Murphy, H. B. and Nance, R.D. 1989. Model for the Evolution of the Avalonia-Cadomian Belt. Geology 17: 735–738.

Murphy, J.B., Pisarevsky, S.A., Nance, R.D. and Keppie, J.D. 2004. Neoproterozoic-Early Paleozoic evolution of peri-Gondwanan terranes: implications for Laurentia-Gondwana connections. International Journal of Earth Sciences, 93: 659–682.

Nance, R.D., Murphy, J.B., Strahan, R.A., D'Lemos, R.S. and Taylor, G.K. 1991. Late Preoterozoic tectonostratigraphic evolution of the Avalonian and Cadomian terranes. Precambrian Research, 53: 41–78.

Nance, R.D., Murphy, J.B. and Keppie, J.D. 2002. A Cordilleran Model for the Evolution of Avalonia. Tectonophysics, 352: 11–31.

O'Brien, S.J., O'Brien, B.H., Dunning, G.R. and Tucker, R.D. 1996. Late Neoproterozoic Avalonian and Related Peri-Gondwanan Rocks of the Newfoundland Appalachians. Geological Society of America, 304: 9–28.

Pauley, J C. 1990. Sedimentology, Structural Evolution and Tectonic Setting of the Late Precambrian Longmyndian Supergroup of the Welsh Borderland, UK. Geological Society, London, Special Publications, 51: 341–351.

Satkoski, A.M, Barr, S.M. and Samson, S.D. 2010. Provenance of Late Neoproterozoic and Cambrian Sediments in Avalonia: Constraints From Detrital Zircon Ages and Sm-Nd Isotopic Compositions in Southern New Brunswick, Canada. The Journal of Geology, 118: 187–200.

Smith, S.A. and Hiscott, R.N. 1984. Latest Precambrian to Early Cambrian basin evolution, Fortune Bay, Newfoundland: fault-bounded basin to platform. Canadian Journal of Earth Sciences, 21: 1379–1392.

Soper, N J, and N H Woodcock. 1990. Silurian Collision and Sediment Dispersal Patterns in Southern Britain. Geological Magazine, London, 127: 527–542.

Strachan, R A, D'Lemos, R.S. and Dallmeyer, R.D. 1996. Neoproterozoic Evolution of an Active Plate Margin: North Armorican Massif, France. Geological Society of America, Special Papers 304, pp. 319–332.

Thompson, M.D., Grunow, A.M. and Ramezani, J. 2007. Late Neoproterozoic Paleogeography of the Southeastern New England Avalon Zone: Insights From U-Pb Geochronology and Paleomagnetism. Geological Society of America Bulletin 119: 681–696.

van Staal, C.R., Barr, S.B. and Murphy, J.B. 2012. Provenance and Tectonic Evolution of Ganderia: Constraints on the Evolution of the Iapetus and Rheic Oceans. Geology, 40: 987–990.

van Staal, C.R. and Hatcher, R.D., Jr. 2010. Global setting of Ordovician orogenesis. *In* The Ordovician Earth System. *Edited by* S.C. Finney and W.B.N. Berry. Geological Society of America, Special Paper 466, pp. 1–11.

van Staal, C.R., Sullivan, R.W. and Whalen, J.B. 1996. Provenance of tectonic history of the Gander Zone in the Caledonian/Appalachian Orogen: Implications for the origin and assembly of Avalon. Geological Society of America, Special Paper 304, pp. 347–367.

van Staal, C.R., Dewey, J.F., MacNiocaill, C. and McKerrow, W.S. 1998. The Cambrian–Silurian tectonic evolution of the northern Appalachians and British Caledonides: history of a complex, west and southwest Pacific-type segment of Iapetus. *In*: Lyell; the Past is the Key to the Present. *Edited by* D.J. Blundell and A.C. Scott. Geological Society, London, Special Publications, 143, pp. 199–242.

Waldron, J.W.F., Schofield, D.I., White, C.E. and Barr, S.M. 2011. Cambrian successions of the Meguma Terrane, Nova Scotia, and Harlech Dome, North Wales: dispersed fragments of a peri-Gondwanan basin?. Journal of the Geological Society, London, 168: 83–98.

Waldron, J.W.F., Murphy, J.B., Schofield, D.I. 2012. Why was the Iapetus Ocean so short lived? Northeastern Section 47th Annual Meeting, Geological Society of America Abstracts with Programs, 44, p. 39.

Zagorevski, A., van Staal, C.R., Rogers, N., McNicoll, V.J. and Pollock, J. 2010. Middle Cambrian to Ordovician arc-backarc development on the leading edge of Ganderia, Newfoundland Appalachians. Geological Society of America Memoirs, 206: 367–396.

APPENDIX A: THIN SECTION PHOTOGRAPHS OF SAMPLES

This appendix accompanies chapters 2 and 3 and shows examples of the thin section views from the petrographic analysis done of the five samples analyzed in this work.

ML001A - Gamlan Fm.

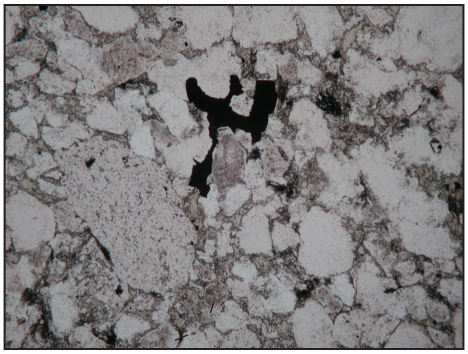

F.O.V. 2.25 mm PPL

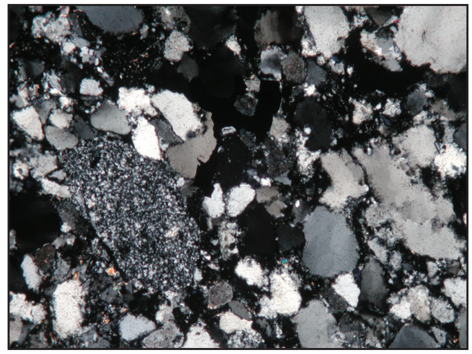

XN

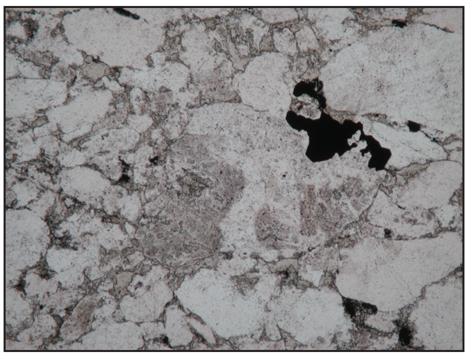

F.O.V. 2.25 mm PPL

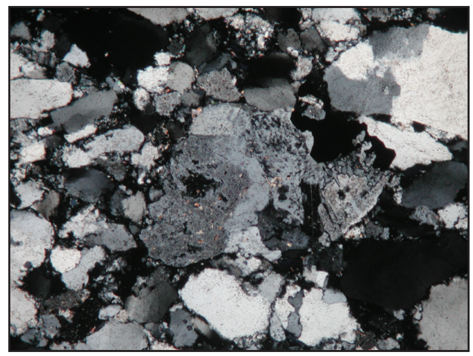

XN

ML010A - Dorothea Grit

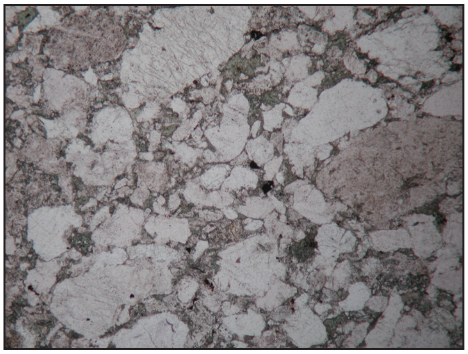

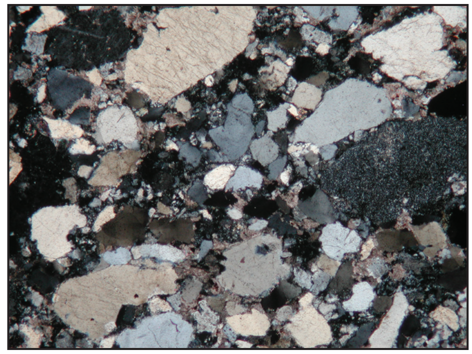

F.O.V. 4.5 mm PPL XN

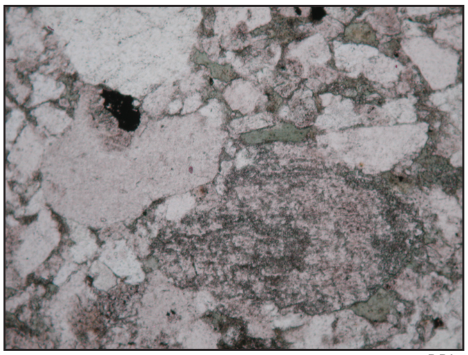

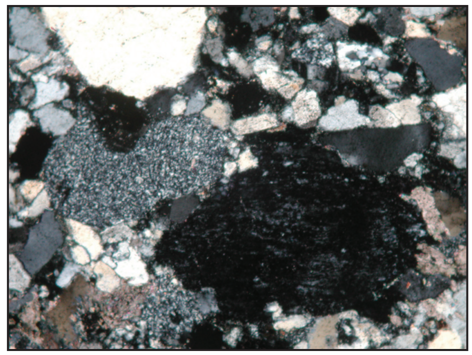

F.O.V. 2.25 mm PPL XN

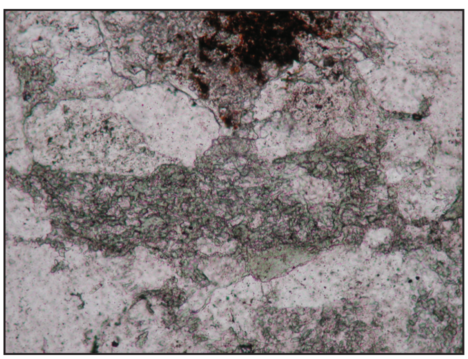

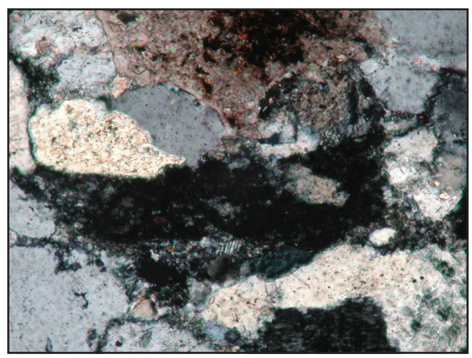

F.O.V. 1 mm PPL XN

NA031A - Conway Casatle Grit

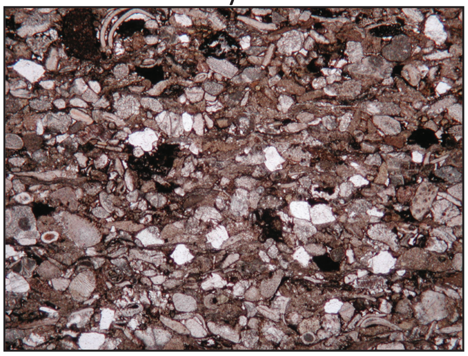

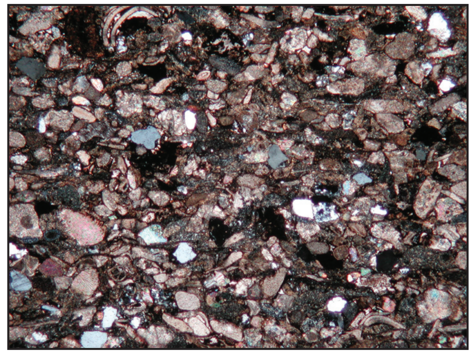

F.O.V. 4.5 mm PPL XN

F.O.V. 1 mm PPL XN

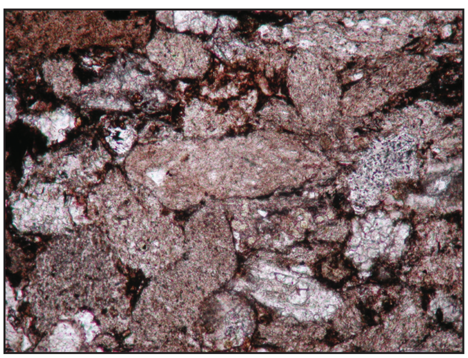

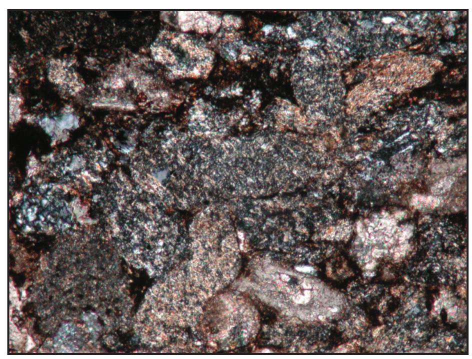

F.O.V. 1 mm PPL XN

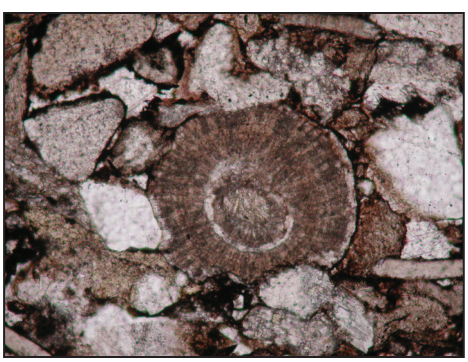

F.O.V. 1 mm PPL XN

NA041A - Dol-cyn-afon Fm.

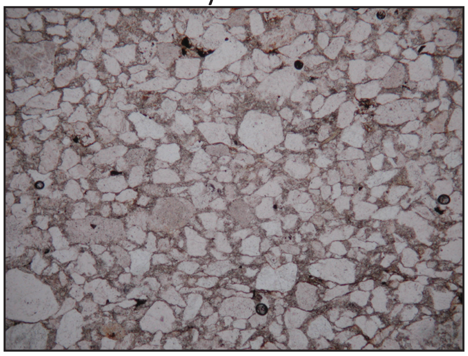

F.O.V. 4.5 mm PPL

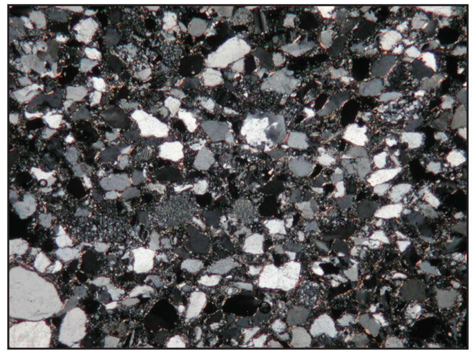

XN

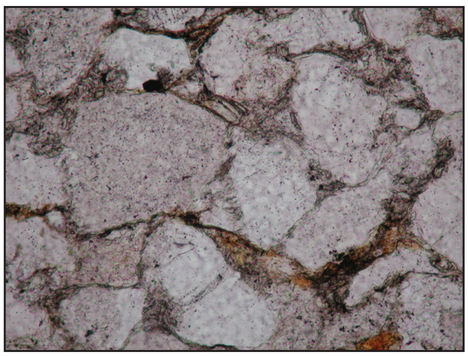

F.O.V. 1 mm PPL

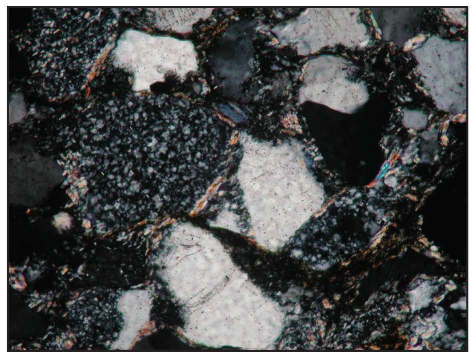

XN

F.O.V. 1 mm PPL

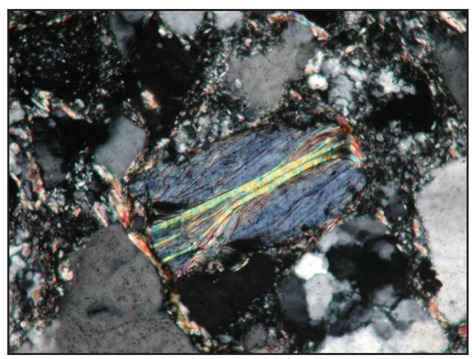

XN

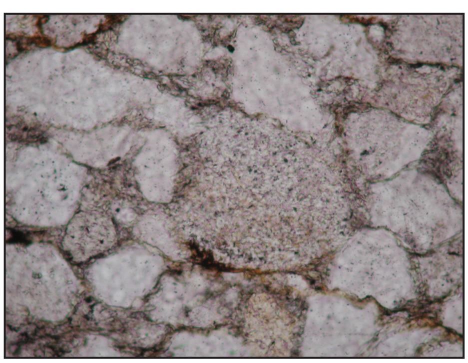

F.O.V. 1 mm PPL

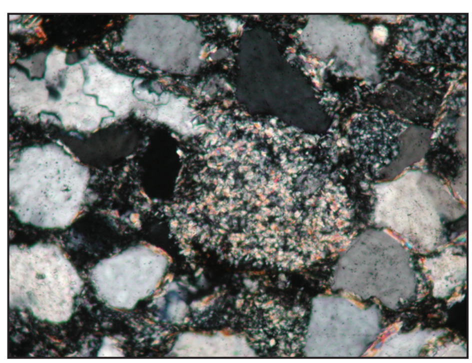

XN

NB027A - Lumsden Dam Fm.

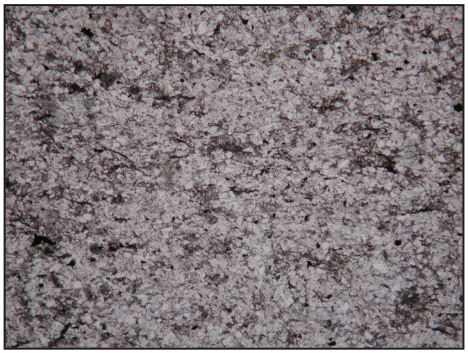

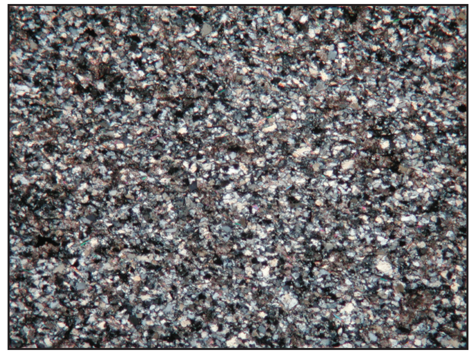

F.O.V. 4.5 mm PPL XN

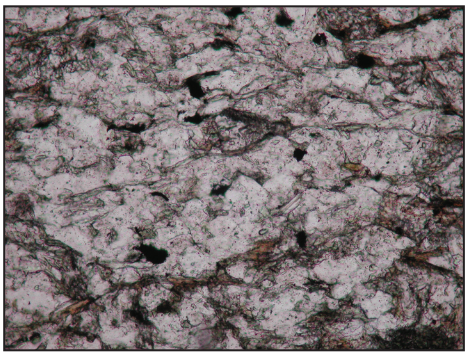

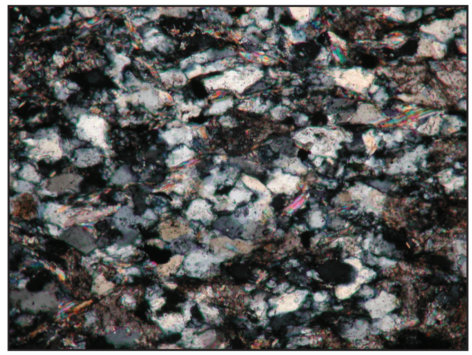

F.O.V. 1 mm PPL XN

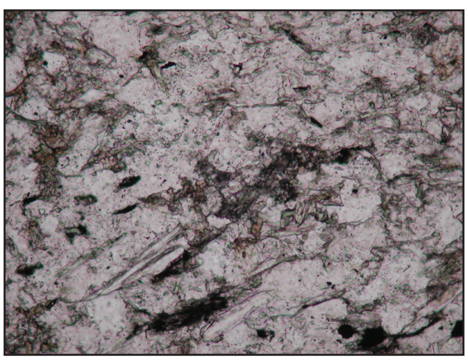

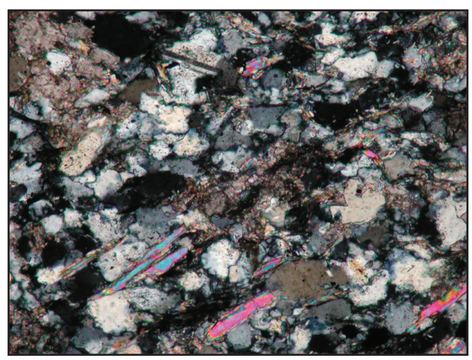

F.O.V. 1 mm PPL XN

APPENDIX B: DETRITAL ZIRCON RESULT TABLES

This appendix accompanies chapters 2 and 3 and shows the LA-ICP-MS analytical results of the five detrital zircon samples analyzed in this work. Records that are grayed out in the unknown samples were not used in interpretations because they did not meet the -10% to +10% discordance cut-off. Records that are grayed out in the standards were not used for normalizing the unknown data. Sample NA031A (Conway Castle Grit) was analyzed on two separate occassions. The results from both are listed separatly here.

Footnotes to data in tables:

1. cps = counts per second
2. $^{207}Pb/^{235}U$ calculated from $^{207}Pb/^{206}Pb$ and the natural $^{238}U/^{235}U$ ratio of 137.88.
3. Quadratic combination of standard deviation of standards and standard error of the single analysis.
4. ρ calculated using the equation below:

$$\rho = \frac{\left(\frac{^{207}Pb/^{235}U\ 2\sigma}{^{207}Pb/^{235}U}\right)^2 + \left(\frac{^{206}Pb/^{238}U\ 2\sigma}{^{206}Pb/^{238}U}\right)^2 - \left(\frac{^{207}Pb/^{206}Pb\ 2\sigma}{^{207}Pb/^{206}Pb}\right)^2}{2 \times \left(\frac{^{206}Pb/^{238}U\ 2\sigma}{^{206}Pb/^{238}U}\right) \times \left(\frac{^{207}Pb/^{206}Pb\ 2\sigma}{^{207}Pb/^{206}Pb}\right)}$$

5. Discordance calculated using the formula below:

$$\%\ discordance = \frac{(e^{0.000155125 \times 206Pb/207Pb\ age} - 1) - {^{206}Pb/^{238}U}\ ratio}{(e^{0.000155125 \times 206Pb/207Pb\ age} - 1)} \times 100$$

Sample ML001A Gamlan Formation

Results of all analyzed grains

*common lead corrected

			Isotopic Ratios							Apparent Age Summary						
Grain	^{206}Pb (cps) [1]	^{204}Pb (cps)	$^{207}Pb/^{206}Pb$	Absolute 2SE	$^{207}Pb/^{235}U$ [2]	Absolute 2SE [3]	$^{206}Pb/^{238}U$	Absolute 2SE	ρ [4]	$^{207}Pb/^{206}Pb$ Age (Ma)	error 2σ (Ma)	$^{207}Pb/^{235}U$ Age (Ma)	error 2σ (Ma)	$^{206}Pb/^{238}U$ Age (Ma)	error 2σ (Ma)	disc. [5] %
1	276811	4	0.08667	0.00106	2.76578	0.21546	0.23143	0.01781	0.988	1353	23	1346	56	1342	93	0.9
2	92386	3	0.05812	0.00095	0.67692	0.05892	0.08447	0.00722	0.982	534	36	525	35	523	43	2.3
3	49637	10	0.05690	0.00104	0.67137	0.05597	0.08558	0.00696	0.976	488	40	522	33	529	41	-8.9
4	17618	8	0.05443	0.00182	0.68870	0.06370	0.09177	0.00791	0.932	389	73	532	38	566	47	-47.6
5	115785	4	0.05811	0.00093	0.68576	0.05390	0.08559	0.00659	0.979	534	35	530	32	529	39	0.8
6	33451	3	0.05610	0.00145	0.67036	0.05691	0.08667	0.00701	0.952	456	56	521	34	536	41	-18.2
7	53825	4	0.05746	0.00113	0.66575	0.05159	0.08403	0.00630	0.968	509	42	518	31	520	37	-2.2
8	35044	8	0.05653	0.00125	0.66157	0.05530	0.08488	0.00684	0.964	473	48	516	33	525	41	-11.5
9	124423	5	0.05837	0.00089	0.69815	0.05311	0.08675	0.00647	0.980	544	33	538	31	536	38	1.4
10	66600	4	0.05810	0.00094	0.68067	0.05294	0.08497	0.00646	0.978	533	35	527	31	526	38	1.5
11	129820	62	0.05799	0.00094	0.72248	0.05370	0.09037	0.00656	0.976	529	35	552	31	558	39	-5.6
12	96723	80	0.06147	0.00208	0.97465	0.08076	0.11499	0.00869	0.913	656	71	691	41	702	50	-7.4
13	38910	32	0.05332	0.00162	0.65033	0.05788	0.08847	0.00740	0.940	342	67	509	35	546	44	-62.3
14	35112	39	0.05452	0.00286	0.63249	0.06300	0.08414	0.00713	0.851	392	113	498	38	521	42	-34.0
15	627709	78	0.06330	0.00103	0.98485	0.09345	0.11285	0.01055	0.985	718	34	696	47	689	61	4.2
16	29245	39	0.05076	0.00176	0.59224	0.04779	0.08463	0.00617	0.903	230	78	472	30	524	37	-133
17	77422	42	0.05667	0.00162	0.67146	0.05176	0.08594	0.00615	0.928	479	62	522	31	531	36	-11.5
18	582741	43	0.18039	0.00182	12.54879	1.59408	0.50452	0.06389	0.997	2657	17	2646	113	2633	268	1.1
19	89122	39	0.05717	0.00223	0.70225	0.07220	0.08909	0.00848	0.925	498	84	540	42	550	50	-10.9
20	60830	8	0.05495	0.00143	0.63474	0.06118	0.08378	0.00778	0.963	410	57	499	37	519	46	-27.5
21	134013	19	0.05739	0.00092	0.69932	0.05522	0.08838	0.00683	0.979	507	35	538	32	546	40	-8.1
22	84921	22	0.05656	0.00098	0.65405	0.05500	0.08387	0.00690	0.978	474	38	511	33	519	41	-9.8
23	141784	45	0.05747	0.00091	0.65778	0.05111	0.08300	0.00631	0.979	510	35	513	31	514	37	-0.9
24	54550	33	0.05402	0.00133	0.62123	0.04733	0.08341	0.00602	0.947	372	54	491	29	516	36	-40.5
25	98056	49	0.05876	0.00159	0.65148	0.05241	0.08042	0.00609	0.942	558	58	509	32	499	36	11.1
26	91414	68	0.05718	0.00166	0.58642	0.08054	0.07438	0.00998	0.977	499	63	469	50	462	60	7.5
27	90027	28	0.05630	0.00112	0.63927	0.04684	0.08236	0.00581	0.963	464	43	502	29	510	35	-10.3
28	68997	36	0.05585	0.00190	0.67640	0.06279	0.08783	0.00759	0.930	447	74	525	37	543	45	-22.4
29	107676	12	0.05750	0.00116	0.68878	0.05220	0.08687	0.00635	0.964	511	44	532	31	537	38	-5.3

Grain	^{206}Pb (cps) [1]	^{204}Pb (cps)	$^{207}Pb/^{206}Pb$	Absolute 2SE	$^{207}Pb/^{235}U$ [2]	Absolute 2SE [3]	$^{206}Pb/^{238}U$	Absolute 2SE	ρ [4]	$^{207}Pb/^{206}Pb$ Age (Ma)	error 2σ (Ma)	$^{207}Pb/^{235}U$ Age (Ma)	error 2σ (Ma)	$^{206}Pb/^{238}U$ Age (Ma)	error 2σ (Ma)	disc. [5] %
30	166195	15	0.05802	0.00087	0.70982	0.05013	0.08873	0.00612	0.977	531	33	545	29	548	36	-3.4
31	117721	42	0.05834	0.00095	0.69139	0.04871	0.08595	0.00589	0.973	543	35	534	29	532	35	2.1
32	296907	56	0.06292	0.00091	0.98753	0.06988	0.11383	0.00788	0.979	706	30	697	35	695	45	1.6
33	79833	32	0.05801	0.00106	0.72180	0.06001	0.09024	0.00732	0.976	530	40	552	35	557	43	-5.3
34	89939	39	0.05823	0.00129	0.72688	0.06242	0.09053	0.00751	0.966	539	48	555	36	559	44	-3.9
35	126893	42	0.05845	0.00091	0.69744	0.04984	0.08655	0.00603	0.976	547	34	537	29	535	36	2.2
36	64021	45	0.05753	0.00102	0.64597	0.05025	0.08144	0.00617	0.974	512	38	506	31	505	37	1.5
37	137987	38	0.05835	0.00089	0.69221	0.08379	0.08603	0.01033	0.992	543	33	534	49	532	61	2.1
38	108319	51	0.05869	0.00115	0.70296	0.05417	0.08687	0.00647	0.967	556	42	541	32	537	38	3.5
39	113253	28	0.05831	0.00091	0.65885	0.05350	0.08195	0.00653	0.981	541	34	514	32	508	39	6.4
40	64181	31	0.05813	0.00108	0.66962	0.05071	0.08355	0.00613	0.969	535	40	520	30	517	36	3.4
41	38839	24	0.05908	0.00227	0.71467	0.05737	0.08774	0.00619	0.879	570	81	548	33	542	37	5.1
42	39782	13	0.05686	0.00142	0.65746	0.04936	0.08386	0.00594	0.943	486	54	513	30	519	35	-7.1
43	99691	27	0.05891	0.00098	0.71022	0.05231	0.08744	0.00627	0.974	564	36	545	31	540	37	4.3
44	51023	39	0.05755	0.00153	0.67105	0.05007	0.08457	0.00590	0.935	513	57	521	30	523	35	-2.2
45	79332	66	0.06420	0.00170	0.99280	0.07182	0.11216	0.00755	0.930	748	55	700	36	685	44	8.9
46	69457	39	0.05929	0.00114	0.67952	0.04882	0.08312	0.00576	0.964	578	41	526	29	515	34	11.4
47	36198	55	0.05596	0.00125	0.63244	0.04603	0.08197	0.00568	0.952	451	49	498	28	508	34	-13.2
48	102095	50	0.05841	0.00096	0.67739	0.04755	0.08411	0.00574	0.972	545	36	525	28	521	34	4.7
49	73154	46	0.05835	0.00101	0.66727	0.04736	0.08294	0.00571	0.970	543	37	519	28	514	34	5.6
50	87676	105	0.05898	0.00114	0.66812	0.04845	0.08215	0.00574	0.964	567	41	520	29	509	34	10.6
51	42313	29	0.05740	0.00085	0.68514	0.04469	0.08658	0.00550	0.974	507	32	530	27	535	33	-5.9
52	55008	56	0.05846	0.00084	0.66691	0.04351	0.08273	0.00527	0.976	547	31	519	26	512	31	6.6
53	103643	63	0.06210	0.00058	0.75822	0.04633	0.08855	0.00535	0.988	678	20	573	26	547	32	20.1
54	79098	54	0.05818	0.00053	0.70375	0.04341	0.08773	0.00535	0.989	536	20	541	26	542	32	-1.1
55	85172	46	0.05788	0.00051	0.67610	0.04139	0.08472	0.00513	0.989	525	19	524	25	524	30	0.2
56	48136	52	0.06248	0.00128	0.96364	0.06114	0.11185	0.00672	0.946	691	43	685	31	684	39	1.1
57	86858	73	0.06105	0.00128	0.83333	0.05412	0.09900	0.00609	0.947	641	44	615	30	609	36	5.3
58	33807	70	0.06268	0.00187	0.69667	0.04889	0.08061	0.00512	0.905	698	62	537	29	500	30	29.5
59	58027	68	0.05801	0.00106	0.68044	0.04834	0.08508	0.00584	0.966	530	40	527	29	526	35	0.7
60	89715	30	0.05837	0.00045	0.67810	0.04457	0.08426	0.00550	0.993	544	17	526	27	521	33	4.3
61	300869	63	0.05859	0.00055	0.70085	0.05053	0.08675	0.00620	0.991	552	20	539	30	536	37	3.0
62	93983	61	0.05761	0.00055	0.64953	0.04091	0.08178	0.00509	0.989	515	21	508	25	507	30	1.6

Grain	^{206}Pb (cps) [1]	^{204}Pb (cps)	$^{207}Pb/^{206}Pb$	Absolute 2SE	$^{207}Pb/^{235}U$ [2]	Absolute 2SE [3]	$^{206}Pb/^{238}U$	Absolute 2SE	ρ [4]	$^{207}Pb/^{206}Pb$ Age (Ma)	error 2σ (Ma)	$^{207}Pb/^{235}U$ Age (Ma)	error 2σ (Ma)	$^{206}Pb/^{238}U$ Age (Ma)	error 2σ (Ma)	disc. [5] %
63	25636	32	0.05639	0.00105	0.64449	0.04511	0.08289	0.00559	0.964	468	41	505	27	513	33	-10.1
64	43275	59	0.05765	0.00077	0.67398	0.04609	0.08478	0.00569	0.981	517	29	523	28	525	34	-1.6
65	503780	73	0.06189	0.00036	0.96767	0.06754	0.11341	0.00789	0.997	670	12	687	34	692	46	-3.5
66	185914	88	0.06129	0.00086	0.81173	0.05037	0.09605	0.00581	0.974	650	30	603	28	591	34	9.4
67	410412	271	0.06328	0.00142	0.76023	0.05576	0.08713	0.00608	0.952	718	47	574	32	539	36	26.0
68	186104	66	0.05842	0.00047	0.70255	0.04475	0.08722	0.00551	0.992	546	18	540	26	539	33	1.2
69	66170	70	0.05798	0.00072	0.67724	0.04524	0.08472	0.00556	0.982	529	27	525	27	524	33	0.9
70	105561	76	0.05886	0.00051	0.71610	0.04899	0.08824	0.00599	0.992	562	19	548	29	545	35	3.1
71	312310	53	0.06312	0.00046	1.02897	0.06171	0.11824	0.00704	0.993	712	15	718	30	720	40	-1.2
72	64376	39	0.05669	0.00075	0.66152	0.04471	0.08463	0.00561	0.981	480	29	516	27	524	33	-9.6
73	137268	72	0.06016	0.00068	0.76940	0.05904	0.09276	0.00704	0.989	609	24	579	33	572	41	6.4
74	74432	50	0.05746	0.00055	0.68590	0.04168	0.08658	0.00520	0.988	509	21	530	25	535	31	-5.4
75	84844	57	0.05829	0.00087	0.68950	0.04441	0.08580	0.00538	0.973	541	32	532	26	531	32	1.9
76	90200	47	0.05916	0.00075	0.77030	0.05690	0.09443	0.00687	0.985	573	28	580	32	582	40	-1.6
77	66539	47	0.05880	0.00101	0.71656	0.05086	0.08839	0.00609	0.970	560	37	549	30	546	36	2.5
78	89153	71	0.05831	0.00070	0.67196	0.04784	0.08358	0.00587	0.986	541	26	522	29	517	35	4.6
79	74779	49	0.05780	0.00114	0.68347	0.04889	0.08576	0.00590	0.961	522	43	529	29	530	35	-1.6
80	92959	52	0.05817	0.00057	0.70309	0.04736	0.08766	0.00584	0.989	536	21	541	28	542	35	-1.1
81	161378	61	0.05813	0.00050	0.70842	0.04669	0.08839	0.00578	0.992	535	19	544	27	546	34	-2.2
82	60839	82	0.05942	0.00143	0.71285	0.04575	0.08701	0.00518	0.927	583	51	546	27	538	31	8.0
83	116948	84	0.05810	0.00061	0.71377	0.04659	0.08910	0.00574	0.987	534	23	547	27	550	34	-3.2
84	66664	68	0.05862	0.00134	0.68052	0.04279	0.08420	0.00493	0.932	553	49	527	26	521	29	6.0
85	86821	71	0.05802	0.00065	0.66799	0.04664	0.08350	0.00576	0.987	530	24	519	28	517	34	2.6
86	59481	41	0.05731	0.00065	0.66012	0.04055	0.08354	0.00504	0.983	503	25	515	25	517	30	-2.9
87	40640	60	0.05726	0.00087	0.65209	0.04476	0.08259	0.00553	0.975	502	33	510	27	512	33	-2.0
88	52208	97	0.05733	0.00089	0.68078	0.04607	0.08613	0.00567	0.973	504	34	527	27	533	34	-5.9
89	144698	86	0.05935	0.00080	0.71949	0.05720	0.08792	0.00689	0.986	580	29	550	33	543	41	6.6
90	79309	75	0.05868	0.00129	0.71154	0.04935	0.08795	0.00579	0.949	555	47	546	29	543	34	2.2
91	246177	121	0.05986	0.00058	0.77002	0.04869	0.09330	0.00583	0.988	598	21	580	28	575	34	4.1
92	38749	74	0.05663	0.00098	0.66407	0.04186	0.08505	0.00516	0.962	477	38	517	25	526	31	-10.7
93	104275	74	0.05842	0.00067	0.68697	0.04658	0.08528	0.00570	0.986	546	25	531	28	528	34	3.5
94	79546	103	0.05833	0.00071	0.75565	0.05507	0.09395	0.00675	0.986	542	26	571	31	579	40	-7.1
95	267933	145	0.05887	0.00053	0.71480	0.04531	0.08807	0.00553	0.990	562	20	548	26	544	33	3.4

Grain	^{206}Pb (cps) [1]	^{204}Pb (cps)	$^{207}Pb/^{206}Pb$	Absolute 2SE	$^{207}Pb/^{235}U$ [2]	Absolute 2SE [3]	$^{206}Pb/^{238}U$	Absolute 2SE	ρ [4]	$^{207}Pb/^{206}Pb$ Age (Ma)	error 2σ (Ma)	$^{207}Pb/^{235}U$ Age (Ma)	error 2σ (Ma)	$^{206}Pb/^{238}U$ Age (Ma)	error 2σ (Ma)	disc. [5] %
96	60058	67	0.05730	0.00053	0.69142	0.05153	0.08752	0.00647	0.992	503	20	534	30	541	38	-7.8
97	48763	59	0.05854	0.00123	0.66642	0.05192	0.08256	0.00619	0.963	550	45	519	31	511	37	7.3
98	257327	81	0.08170	0.00049	2.31295	0.16224	0.20532	0.01435	0.996	1238	12	1216	49	1204	76	3.1
99	131542	139	0.05866	0.00063	0.69092	0.04662	0.08543	0.00569	0.987	554	23	533	28	528	34	4.9
100	65908	78	0.05798	0.00111	0.69907	0.04464	0.08745	0.00533	0.954	529	42	538	26	540	31	-2.3
101	33573	74	0.05736	0.00154	0.68799	0.04750	0.08700	0.00553	0.921	505	58	532	28	538	33	-6.7
102	30258	74	0.05720	0.00118	0.66193	0.05025	0.08394	0.00613	0.962	499	45	516	30	520	36	-4.3
103	97589	65	0.05885	0.00066	0.68975	0.04602	0.08501	0.00559	0.986	561	24	533	27	526	33	6.6
104	110866	105	0.05898	0.00109	0.70513	0.04574	0.08671	0.00539	0.958	566	40	542	27	536	32	5.6
105	159359	48	0.05865	0.00075	0.66725	0.04445	0.08251	0.00539	0.981	554	28	519	27	511	32	8.1
106	209102	67	0.05839	0.00082	0.66504	0.04252	0.08260	0.00515	0.975	545	30	518	26	512	31	6.3
107	42251	34	0.05690	0.00095	0.64720	0.04539	0.08250	0.00562	0.971	488	36	507	28	511	33	-5.0
108	32299	43	0.05722	0.00119	0.67097	0.04711	0.08505	0.00570	0.955	500	45	521	28	526	34	-5.4
109	55866	29	0.05824	0.00085	0.67416	0.04689	0.08395	0.00571	0.978	539	32	523	28	520	34	3.7
110	45818	71	0.05963	0.00172	0.69623	0.05107	0.08468	0.00571	0.920	590	61	537	30	524	34	11.7
111	126729	79	0.05883	0.00077	0.71433	0.04765	0.08807	0.00576	0.981	561	28	547	28	544	34	3.1
112	28316	63	0.05627	0.00187	0.66804	0.04661	0.08610	0.00528	0.879	463	72	520	28	532	31	-15.6
113	48935	54	0.05837	0.00218	0.68646	0.05635	0.08530	0.00623	0.890	544	80	531	33	528	37	3.1
114	59507	110	0.06004	0.00150	0.70494	0.05697	0.08515	0.00654	0.951	605	53	542	33	527	39	13.5
115	51796	80	0.06064	0.00188	0.71781	0.05112	0.08586	0.00551	0.901	626	65	549	30	531	33	15.9
116	226134	47	0.12196	0.00071	6.07162	0.32781	0.36107	0.01938	0.994	1985	10	1986	46	1987	91	-0.1
117	710582	62	0.12177	0.00057	6.24543	0.30399	0.37197	0.01802	0.995	1982	8	2011	42	2039	84	-3.3
118	79916	77	0.05933	0.00141	0.66248	0.04701	0.08099	0.00541	0.942	579	51	516	28	502	32	13.8
119	125231	54	0.05809	0.00059	0.72270	0.05578	0.09023	0.00690	0.991	533	22	552	32	557	41	-4.6
120	58587	43	0.05726	0.00077	0.67468	0.04435	0.08546	0.00550	0.979	501	29	524	27	529	33	-5.7
121	121394	4	0.05804	0.00052	0.69300	0.04663	0.08660	0.00577	0.991	531	20	535	28	535	34	-0.8
122	125351	44	0.06018	0.00196	0.72812	0.06320	0.08775	0.00706	0.927	610	69	555	36	542	42	11.6
123	113942	32	0.05829	0.00069	0.72384	0.05371	0.09006	0.00660	0.987	541	26	553	31	556	39	-2.9
124	57356	18	0.05743	0.00127	0.67976	0.04580	0.08584	0.00546	0.945	508	48	527	27	531	32	-4.7
125	33963	19	0.05635	0.00117	0.63408	0.05684	0.08162	0.00712	0.973	466	45	499	35	506	42	-8.9
126*	108480	182	0.0621*	0.00548	0.74206*	0.08116	0.08666*	0.00560	0.590	678*	178	564*	46	536*	33	21.8
126	82044	37	0.06081	0.00069	0.74368	0.04743	0.08869	0.00557	0.984	633	24	565	27	548	33	14.0
127	153274	33	0.05903	0.00057	0.73379	0.05244	0.09016	0.00638	0.991	568	21	559	30	556	38	2.1

Grain	^{206}Pb (cps) [1]	^{204}Pb (cps)	$^{207}Pb/^{206}Pb$	Absolute 2SE	$^{207}Pb/^{235}U$ [2]	Absolute 2SE [3]	$^{206}Pb/^{238}U$	Absolute 2SE	ρ [4]	$^{207}Pb/^{206}Pb$ Age (Ma)	error 2σ (Ma)	$^{207}Pb/^{235}U$ Age (Ma)	error 2σ (Ma)	$^{206}Pb/^{238}U$ Age (Ma)	error 2σ (Ma)	disc. [5] %
128	210725	51	0.05907	0.00069	0.69500	0.04537	0.08533	0.00548	0.984	570	25	536	27	528	32	7.7
129	67423	47	0.05842	0.00104	0.70080	0.05324	0.08700	0.00642	0.972	546	39	539	31	538	38	1.5
130	105654	18	0.05803	0.00061	0.67444	0.04889	0.08429	0.00605	0.989	531	23	523	29	522	36	1.8
131	104433	23	0.05867	0.00093	0.67795	0.05424	0.08381	0.00657	0.980	555	34	526	32	519	39	6.7
132	120714	11	0.05841	0.00053	0.67598	0.04210	0.08394	0.00517	0.989	545	20	524	25	520	31	4.9
133	70430	7	0.05855	0.00080	0.71479	0.04749	0.08854	0.00576	0.978	550	30	548	28	547	34	0.7

Sample ML001A Gamlan Formation - Standards

*common lead corrected

Grain	^{206}Pb (cps)	^{204}Pb (cps)	^{206}Pbcom	^{207}Pbcom	^{207}Pb*	^{206}Pb*	Not Common Lead Corrected Isotopic Ratios: ^{207}Pb/^{206}Pb	Absolute 1SE	^{206}Pb/^{238}U	Absolute 1SE
LH94-15										
1	403476	185	2789	2804	400687	44391	0.115533	0.000253	0.370409	0.005896
2	559255	177	2673	2686	556581	61874	0.114113	0.000143	0.369075	0.009511
3	465513	202	3016	3062	462497	50269	0.113361	0.000144	0.389843	0.009665
4	412813	184	2813	2806	410000	44526	0.113564	0.000172	0.353976	0.008470
5	322944	199	3008	3018	319936	34120	0.113849	0.000149	0.365673	0.008407
6	1013479	56	853	851	1012625	115503	0.113711	0.000145	0.353901	0.007697
7	1290520	38	579	575	1289941	147357	0.113314	0.000120	0.345811	0.008611
12	1515283	30	454	453	1514829	173960	0.113854	0.000197	0.354928	0.008108
13	1184181	24	368	367	1183813	134871	0.112873	0.000103	0.352747	0.005053
14	2136910	40	609	606	2136300	245976	0.114280	0.000166	0.346314	0.005705
15	836190	54	821	818	835368	94886	0.113157	0.000154	0.352192	0.010932
17	576285	21	323	320	575962	65605	0.113125	0.000183	0.337932	0.004513
18	512062	13	199	196	511863	57960	0.112429	0.000118	0.333838	0.003962
19	630483	43	671	662	629812	71496	0.113067	0.000165	0.332858	0.004103
20	455619	27	421	416	455198	51593	0.113001	0.000140	0.332779	0.005817
21	719444	39	597	591	718847	82048	0.113222	0.000169	0.339145	0.007170
22	649423	40	620	611	648803	73680	0.113223	0.000116	0.328668	0.007216
23	691593	93	1430	1421	690163	77733	0.113424	0.000146	0.345917	0.009059
24	707553	81	1253	1236	706301	79865	0.113114	0.000165	0.330771	0.008513
25	490904	84	1303	1279	489600	55067	0.113317	0.000177	0.320980	0.008113
26	520843	63	977	961	519867	58735	0.113213	0.000176	0.326425	0.004725
27	567078	65	1003	989	566075	64054	0.113432	0.000170	0.331597	0.005537
28	597560	76	1178	1161	596381	67602	0.113021	0.000225	0.328205	0.007588
29	619733	205	3182	3125	616551	68004	0.113381	0.000153	0.322781	0.003957
30	594057	89	1386	1363	592672	66671	0.113162	0.000258	0.325741	0.005668
31	751416	125	1927	1901	749489	84767	0.113974	0.000173	0.331356	0.007000
32	661030	92	1421	1398	659609	74127	0.113066	0.000117	0.325845	0.004258
33	556209	36	563	550	555646	63247	0.113519	0.000184	0.312624	0.009196

	^{206}Pb	^{204}Pb						Absolute		Absolute
Grain	(cps)	(cps)	^{206}Pbcom	^{207}Pbcom	^{207}Pb*	^{206}Pb*	^{207}Pb/^{206}Pb	1SE	^{206}Pb/^{238}U	1SE
34	602236	26	399	391	601837	68552	0.113409	0.000129	0.319446	0.004617
35	603664	50	773	764	602891	68598	0.113648	0.000116	0.335587	0.005243
36	630795	26	402	396	630393	71928	0.113389	0.000121	0.324817	0.006527
37	754563	13	196	193	754367	86434	0.113505	0.000137	0.322972	0.005705
38	645321	16	242	238	645079	73677	0.113154	0.000206	0.329937	0.003667
39	745968	24	370	365	745598	85247	0.113578	0.000163	0.332421	0.004848
40	870738	32	487	482	870251	99337	0.113255	0.000114	0.336619	0.004908
GJ132										
1	187052	19	329	289	186723	11199	0.060479	0.000262	0.102042	0.001796
2	189236	19	332	292	188904	11401	0.060570	0.000219	0.105270	0.002128
13	173637	31	557	489	173079	10156	0.059877	0.000161	0.098441	0.002325
16	190088	31	557	489	189531	10963	0.059733	0.000156	0.097107	0.002309
18	211110	39	687	603	210423	12250	0.059476	0.000239	0.098540	0.001945
20	202831	37	658	577	202173	11861	0.060102	0.000143	0.097126	0.001743
22	237895	92	1631	1431	236264	13526	0.060716	0.000187	0.097949	0.001065
24	223656	74	1326	1160	222330	12660	0.060551	0.000221	0.092425	0.001855
26	211325	120	2139	1875	209186	11055	0.060518	0.000113	0.095949	0.002290
28	222782	93	1654	1450	221129	12323	0.060689	0.000177	0.096258	0.001311
30	221295	75	1338	1173	219957	12520	0.060876	0.000217	0.095959	0.001275
32	245200	90	1603	1407	243597	13731	0.060539	0.000149	0.098369	0.001575
34	263163	46	811	712	262353	15506	0.060618	0.000111	0.100495	0.002363
36	267713	55	968	851	266745	15645	0.060692	0.000098	0.101994	0.001808
38	289481	20	357	313	289125	17455	0.060455	0.000195	0.098803	0.001717
40	263599	9	157	138	263442	16036	0.060305	0.000191	0.098816	0.003113

Sample ML010A Dorothea Grit

Results of all analyzed grains

*common lead corrected

			Isotopic Ratios							Apparent Age Summary						
Grain	^{206}Pb (cps) [1]	^{204}Pb (cps)	$^{207}Pb/^{206}Pb$	Absolute 2SE	$^{207}Pb/^{235}U$ [2]	Absolute 2SE [3]	$^{206}Pb/^{238}U$	Absolute 2SE	ρ [4]	$^{207}Pb/^{206}Pb$ Age (Ma)	error 2σ (Ma)	$^{207}Pb/^{235}U$ Age (Ma)	error 2σ (Ma)	$^{206}Pb/^{238}U$ Age (Ma)	error 2σ (Ma)	disc. [5] %
1	373872	223	0.05934	0.00162	0.78438	0.06537	0.09587	0.00755	0.945	579	58	588	37	590	44	-1.9
2	40832	147	0.05976	0.00210	0.75697	0.06371	0.09188	0.00702	0.908	595	75	572	36	567	41	4.9
3	66274	135	0.06028	0.00174	0.76957	0.07698	0.09259	0.00887	0.957	614	61	580	43	571	52	7.3
4	63860	154	0.06048	0.00178	0.75570	0.05733	0.09062	0.00634	0.922	621	62	572	33	559	37	10.4
5	338415	152	0.06095	0.00167	0.89570	0.06667	0.10658	0.00738	0.930	638	58	649	35	653	43	-2.5
6	103761	154	0.05970	0.00166	0.74507	0.05722	0.09051	0.00648	0.932	593	59	565	33	559	38	6.0
7	113795	160	0.05939	0.00167	0.74537	0.05614	0.09102	0.00636	0.928	582	60	566	32	562	37	3.6
8	199382	176	0.05936	0.00162	0.74281	0.06211	0.09075	0.00717	0.945	580	58	564	36	560	42	3.7
9	94633	164	0.06032	0.00170	0.79212	0.06381	0.09524	0.00719	0.937	615	60	592	36	586	42	4.9
10	128476	158	0.05985	0.00178	0.75293	0.06616	0.09125	0.00755	0.941	598	63	570	38	563	44	6.1
11	41621	73	0.05779	0.00170	0.71234	0.05612	0.08940	0.00654	0.928	522	63	546	33	552	39	-6.1
12	98572	95	0.05932	0.00166	0.73853	0.05884	0.09030	0.00674	0.936	579	60	562	34	557	40	3.9
13	202336	65	0.05872	0.00161	0.72714	0.05589	0.08982	0.00645	0.934	557	59	555	32	554	38	0.4
14	92122	56	0.05854	0.00163	0.70775	0.05454	0.08768	0.00630	0.932	550	60	543	32	542	37	1.6
15	168134	68	0.05830	0.00163	0.69264	0.05820	0.08617	0.00683	0.943	541	60	534	34	533	40	1.6
16	122725	54	0.05823	0.00166	0.71761	0.05489	0.08938	0.00635	0.928	539	61	549	32	552	37	-2.6
17	30908	89	0.05598	0.00190	0.72353	0.06188	0.09373	0.00736	0.918	452	74	553	36	578	43	-29.1
18	80284	109	0.05951	0.00170	0.71497	0.05875	0.08714	0.00671	0.938	586	61	548	34	539	40	8.4
19	143869	131	0.05859	0.00161	0.71642	0.05785	0.08869	0.00673	0.940	552	59	549	34	548	40	0.7
20	42073	89	0.05832	0.00167	0.69952	0.05403	0.08699	0.00624	0.929	542	61	539	32	538	37	0.8
21	146097	125	0.05905	0.00169	0.71435	0.05507	0.08774	0.00628	0.929	569	61	547	32	542	37	4.9
22	73712	99	0.05595	0.00185	0.65360	0.05753	0.08472	0.00691	0.927	451	72	511	35	524	41	-17.0
23	100052	81	0.05718	0.00172	0.68069	0.07582	0.08634	0.00926	0.963	498	65	527	45	534	55	-7.4
24	32013	98	0.05194	0.00201	0.57982	0.05783	0.08096	0.00744	0.922	283	86	464	37	502	44	-80.4
25	68229	87	0.05713	0.00186	0.67187	0.05429	0.08530	0.00631	0.915	496	70	522	32	528	37	-6.6
26	64389	86	0.05729	0.00201	0.69240	0.05599	0.08765	0.00639	0.901	503	75	534	33	542	38	-8.0
27	152845	130	0.06325	0.00187	0.73144	0.06003	0.08387	0.00642	0.933	717	61	557	35	519	38	28.7
28	126831	52	0.05784	0.00160	0.70355	0.06813	0.08821	0.00819	0.958	524	60	541	40	545	48	-4.2
29	80848	129	0.05737	0.00171	0.71137	0.06224	0.08993	0.00740	0.940	506	64	546	36	555	44	-10.2

Grain	^{206}Pb (cps) [1]	^{204}Pb (cps)	$^{207}Pb/^{206}Pb$	Absolute 2SE	$^{207}Pb/^{235}U$ [2]	Absolute 2SE [3]	$^{206}Pb/^{238}U$	Absolute 2SE	ρ [4]	$^{207}Pb/^{206}Pb$ Age (Ma)	error 2σ (Ma)	$^{207}Pb/^{235}U$ Age (Ma)	error 2σ (Ma)	$^{206}Pb/^{238}U$ Age (Ma)	error 2σ (Ma)	disc. [5] %
30	129953	140	0.05827	0.00166	0.69144	0.05447	0.08607	0.00632	0.932	540	61	534	32	532	37	1.5
31	90730	221	0.05957	0.00198	0.74850	0.06927	0.09113	0.00787	0.933	588	71	567	39	562	46	4.6
32	66920	202	0.05992	0.00263	0.67005	0.07057	0.08110	0.00777	0.909	601	92	521	42	503	46	17.0
33	39569	220	0.05527	0.00190	0.66120	0.05293	0.08676	0.00627	0.903	423	75	515	32	536	37	-27.9
34	54412	218	0.05732	0.00173	0.67316	0.05074	0.08518	0.00588	0.916	504	65	523	30	527	35	-4.8
35	77435	180	0.05791	0.00169	0.66360	0.05525	0.08312	0.00648	0.937	526	63	517	33	515	38	2.3
36	94358	207	0.05809	0.00189	0.73473	0.05844	0.09173	0.00666	0.913	533	70	559	34	566	39	-6.4
37	61404	143	0.05621	0.00175	0.65645	0.05339	0.08469	0.00637	0.924	461	67	512	32	524	38	-14.3
38	51802	135	0.05425	0.00169	0.62300	0.05267	0.08329	0.00655	0.930	381	69	492	32	516	39	-36.6
39	259830	183	0.05845	0.00162	0.68843	0.06196	0.08543	0.00732	0.951	547	59	532	37	528	43	3.5
40	86088	305	0.06667	0.00259	0.73666	0.06652	0.08014	0.00654	0.903	827	79	560	38	497	39	41.5
41	45331	216	0.05607	0.00176	0.68795	0.05554	0.08899	0.00662	0.922	455	68	532	33	550	39	-21.7
42	140019	194	0.05793	0.00160	0.68991	0.05398	0.08637	0.00632	0.936	527	59	533	32	534	37	-1.4
43	141566	258	0.05779	0.00160	0.68182	0.06753	0.08556	0.00814	0.960	522	60	528	40	529	48	-1.5
44	126897	296	0.05740	0.00172	0.68308	0.05804	0.08631	0.00686	0.936	507	64	529	34	534	41	-5.5
45	93159	265	0.05579	0.00177	0.66802	0.05835	0.08684	0.00707	0.932	444	69	520	35	537	42	-21.7
46	183975	306	0.05835	0.00162	0.74408	0.05776	0.09249	0.00671	0.934	543	59	565	33	570	39	-5.3
47	60502	261	0.05676	0.00180	0.67713	0.06156	0.08653	0.00737	0.937	482	69	525	37	535	44	-11.4
48	107210	258	0.05910	0.00181	0.70924	0.05881	0.08703	0.00671	0.930	571	65	544	34	538	40	6.0
49	86387	259	0.05863	0.00200	0.73806	0.05856	0.09130	0.00654	0.903	553	73	561	34	563	39	-1.9
50	77038	219	0.05651	0.00172	0.69341	0.05310	0.08900	0.00626	0.918	472	66	535	31	550	37	-17.1
51	109848	326	0.05756	0.00159	0.72413	0.05886	0.09124	0.00697	0.940	513	60	553	34	563	41	-10.1
52	158108	305	0.05896	0.00165	0.76116	0.05712	0.09364	0.00652	0.928	565	60	575	32	577	38	-2.1
53	80464	271	0.05583	0.00164	0.67939	0.06037	0.08826	0.00740	0.944	446	64	526	36	545	44	-23.3
54	181800	289	0.05808	0.00162	0.74136	0.06662	0.09258	0.00791	0.951	533	60	563	38	571	47	-7.5
55	122450	303	0.05709	0.00161	0.68848	0.06529	0.08747	0.00792	0.955	495	61	532	39	541	47	-9.6
56	1258491	44	0.07874	0.00171	2.20363	0.27167	0.20297	0.02463	0.984	1166	42	1182	83	1191	131	-2.4
57	625408	683	0.06526	0.00187	0.79662	0.06535	0.08853	0.00681	0.937	783	59	595	36	547	40	31.4
58	797923	422	0.05914	0.00161	0.76843	0.06638	0.09424	0.00773	0.949	572	58	579	37	581	45	-1.5
59	59509	294	0.05562	0.00213	0.68937	0.05790	0.08990	0.00672	0.890	437	83	532	34	555	40	-28.2
60	36794	328	0.05358	0.00181	0.61698	0.05189	0.08352	0.00644	0.916	353	74	488	32	517	38	-48.3
61	119302	400	0.05835	0.00185	0.69129	0.06242	0.08592	0.00726	0.936	543	68	534	37	531	43	2.2
62	115777	373	0.05767	0.00191	0.69263	0.06220	0.08710	0.00727	0.929	517	71	534	37	538	43	-4.2

Grain	^{206}Pb (cps) [1]	^{204}Pb (cps)	$^{207}Pb/^{206}Pb$	Absolute 2SE	$^{207}Pb/^{235}U$ [2]	Absolute 2SE [3]	$^{206}Pb/^{238}U$	Absolute 2SE	ρ [4]	$^{207}Pb/^{206}Pb$ Age (Ma)	error 2σ (Ma)	$^{207}Pb/^{235}U$ Age (Ma)	error 2σ (Ma)	$^{206}Pb/^{238}U$ Age (Ma)	error 2σ (Ma)	disc. [5] %
63	118518	385	0.05773	0.00159	0.76587	0.06699	0.09622	0.00799	0.949	519	59	577	38	592	47	-14.7
64	104486	308	0.05780	0.00172	0.68516	0.05896	0.08598	0.00694	0.938	522	64	530	35	532	41	-1.9
65	200492	294	0.05761	0.00159	0.66156	0.05759	0.08329	0.00687	0.948	515	60	516	35	516	41	-0.2
66	758536	426	0.05910	0.00161	0.77794	0.06568	0.09547	0.00763	0.947	571	58	584	37	588	45	-3.1
67	113706	442	0.06139	0.00198	0.80084	0.06248	0.09461	0.00672	0.910	653	68	597	35	583	39	11.3
68	75287	384	0.05710	0.00180	0.71499	0.06134	0.09082	0.00725	0.930	495	68	548	36	560	43	-13.7
69	172349	436	0.05755	0.00159	0.71378	0.05650	0.08995	0.00667	0.937	513	60	547	33	555	39	-8.6
70	67568	390	0.05618	0.00176	0.66790	0.05337	0.08623	0.00634	0.920	459	68	519	32	533	38	-16.8
71	205540	390	0.05788	0.00168	0.73693	0.06326	0.09234	0.00746	0.941	525	63	561	36	569	44	-8.7
72	75114	348	0.05734	0.00172	0.66952	0.05856	0.08468	0.00696	0.940	505	65	520	35	524	41	-4.0
73	96447	178	0.06192	0.00163	0.75602	0.04991	0.08856	0.00536	0.917	671	55	572	28	547	32	19.3
74	934064	342	0.05956	0.00157	0.73964	0.05016	0.09007	0.00563	0.921	588	56	562	29	556	33	5.6
75	118803	178	0.06082	0.00171	0.69792	0.05073	0.08323	0.00558	0.922	633	59	538	30	515	33	19.3
76	615258	555	0.06678	0.00224	0.79283	0.06522	0.08611	0.00647	0.913	831	68	593	36	532	38	37.4
77	1560258	356	0.05855	0.00159	0.74740	0.05257	0.09258	0.00601	0.923	551	58	567	30	571	35	-3.8
78	99159	176	0.06078	0.00169	0.75861	0.05405	0.09052	0.00594	0.921	632	59	573	31	559	35	12.1
79	341302	316	0.05862	0.00159	0.72039	0.05279	0.08913	0.00607	0.929	553	58	551	31	550	36	0.5
80	152477	319	0.06245	0.00199	0.78354	0.06025	0.09100	0.00637	0.910	690	67	587	34	561	38	19.4
81	114505	166	0.06068	0.00166	0.73773	0.04874	0.08817	0.00530	0.910	628	58	561	28	545	31	13.8
82	135391	152	0.05974	0.00161	0.70433	0.04756	0.08550	0.00529	0.917	594	57	541	28	529	31	11.5
83	132316	169	0.06243	0.00166	0.88150	0.06092	0.10240	0.00653	0.923	689	56	642	32	628	38	9.2
84	347060	167	0.05758	0.00153	0.69180	0.04697	0.08714	0.00545	0.920	514	57	534	28	539	32	-5.0
85	288649	375	0.06541	0.00178	0.79756	0.07074	0.08843	0.00746	0.952	788	56	595	39	546	44	32.0
86	376449	200	0.05853	0.00155	0.76418	0.05663	0.09469	0.00655	0.934	550	57	576	32	583	38	-6.4
87	135239	180	0.06059	0.00201	0.77888	0.05886	0.09323	0.00633	0.899	625	70	585	33	575	37	8.4
88	314232	118	0.05751	0.00152	0.70330	0.04889	0.08870	0.00570	0.925	511	57	541	29	548	34	-7.5
89	343418	170	0.05716	0.00151	0.70780	0.04682	0.08980	0.00545	0.917	498	57	543	27	554	32	-11.9
90	130435	199	0.05960	0.00161	0.71586	0.05005	0.08711	0.00562	0.922	589	58	548	29	538	33	9.0
91	97275	191	0.06069	0.00180	0.71728	0.05299	0.08572	0.00580	0.916	628	63	549	31	530	34	16.2
92	401661	254	0.05824	0.00156	0.73717	0.05188	0.09180	0.00598	0.925	539	57	561	30	566	35	-5.3
93	297150	287	0.06262	0.00169	0.69374	0.05679	0.08034	0.00621	0.944	695	57	535	33	498	37	29.5
94	143169	193	0.06487	0.00175	0.80667	0.05673	0.09019	0.00586	0.924	770	56	601	31	557	35	28.9
95	159123	91	0.05824	0.00156	0.70522	0.04794	0.08783	0.00549	0.919	539	57	542	28	543	32	-0.8

Grain	^{206}Pb (cps) [1]	^{204}Pb (cps)	$^{207}Pb/^{206}Pb$	Absolute 2SE	$^{207}Pb/^{235}U$ [2]	Absolute 2SE [3]	$^{206}Pb/^{238}U$	Absolute 2SE	ρ [4]	$^{207}Pb/^{206}Pb$ Age (Ma)	error 2σ (Ma)	$^{207}Pb/^{235}U$ Age (Ma)	error 2σ (Ma)	$^{206}Pb/^{238}U$ Age (Ma)	error 2σ (Ma)	disc. [5] %
96	235044	340	0.06888	0.00220	0.77126	0.05680	0.08120	0.00539	0.901	895	65	580	32	503	32	45.5
97	82277	105	0.06048	0.00168	0.70641	0.05032	0.08472	0.00556	0.921	621	59	543	30	524	33	16.2
98	621097	104	0.05695	0.00151	0.70463	0.05242	0.08973	0.00624	0.934	490	57	542	31	554	37	-13.7
99	287572	80	0.05777	0.00156	0.68595	0.04439	0.08612	0.00507	0.909	521	58	530	26	533	30	-2.3
100	228564	194	0.05979	0.00163	0.76222	0.05489	0.09246	0.00616	0.926	596	58	575	31	570	36	4.6
101	155979	60	0.05828	0.00156	0.67921	0.04658	0.08452	0.00534	0.921	540	58	526	28	523	32	3.3
102	165707	97	0.05928	0.00159	0.75418	0.04948	0.09227	0.00553	0.913	577	57	571	28	569	33	1.5
103	237096	89	0.05804	0.00156	0.70344	0.04847	0.08790	0.00557	0.920	531	58	541	28	543	33	-2.3
104	96955	61	0.05872	0.00162	0.68451	0.05395	0.08455	0.00624	0.937	557	59	529	32	523	37	6.2
105	147010	74	0.05839	0.00158	0.70839	0.04795	0.08798	0.00546	0.917	545	58	544	28	544	32	0.2
106	109931	39	0.05856	0.00159	0.70844	0.04781	0.08774	0.00542	0.916	551	58	544	28	542	32	1.6
107	86397	74	0.05902	0.00160	0.74779	0.04983	0.09189	0.00559	0.914	568	58	567	29	567	33	0.2
108	220503	128	0.05759	0.00153	0.69723	0.04719	0.08780	0.00547	0.920	514	57	537	28	543	32	-5.7
109	199207	124	0.05857	0.00160	0.70699	0.04644	0.08755	0.00523	0.910	551	58	543	27	541	31	1.9
111	1055899	39	0.05655	0.00149	0.68246	0.04563	0.08753	0.00538	0.919	474	57	528	27	541	32	-14.8
112	187135	43	0.05745	0.00155	0.67677	0.04528	0.08544	0.00523	0.915	509	58	525	27	528	31	-4.0
113	207142	107	0.06290	0.00185	0.65115	0.04860	0.07508	0.00515	0.919	705	61	509	29	467	31	35.0
114	320097	141	0.06044	0.00166	0.76142	0.05335	0.09137	0.00589	0.920	619	58	575	30	564	35	9.4
115	656301	896	0.05851	0.00172	0.70849	0.04643	0.08782	0.00514	0.893	549	63	544	27	543	30	1.2
116	168844	30	0.05734	0.00153	0.67361	0.04311	0.08520	0.00495	0.909	505	58	523	26	527	29	-4.6
117	120793	24	0.05802	0.00157	0.69228	0.04890	0.08654	0.00564	0.923	531	58	534	29	535	33	-0.9
118	165540	41	0.05794	0.00154	0.69895	0.05101	0.08749	0.00595	0.931	528	57	538	30	541	35	-2.6
119	2368357	98	0.18014	0.00248	11.75920	1.05122	0.47343	0.04182	0.988	2654	23	2585	80	2499	180	7.1
120	231065	74	0.05742	0.00153	0.70374	0.04640	0.08889	0.00536	0.915	508	58	541	27	549	32	-8.5

Sample ML010A Dorothea Grit - Standards

*common lead corrected

Grain	^{206}Pb (cps)	^{204}Pb (cps)	^{206}Pbcom	^{207}Pbcom	^{207}Pb*	^{206}Pb*	$^{207}Pb/^{206}Pb$	Absolute 1SE	$^{206}Pb/^{238}U$	Absolute 1SE
							Not Common Lead Corrected Isotopic Ratios			
LH94-15										
4	216258	158	2473	2419	213785	23371	0.117453	0.000258	0.315035	0.004752
5	149126	100	1583	1534	147544	15922	0.116516	0.000219	0.296134	0.017413
6	289026	111	1735	1702	287292	32280	0.116986	0.000184	0.320899	0.004387
7	414339	140	2170	2142	412170	46501	0.115908	0.000156	0.333188	0.009993
8	347460	105	1626	1599	345835	39300	0.116666	0.000287	0.325193	0.008615
9	159269	94	1463	1441	157806	17117	0.115437	0.000174	0.328214	0.009607
10	97787	58	913	887	96874	10578	0.116242	0.000324	0.300364	0.008813
11	118077	23	355	347	117722	13416	0.115132	0.000420	0.317507	0.011075
12	275423	105	1635	1604	273788	30779	0.116017	0.000275	0.320415	0.009564
13	219418	117	1821	1787	217597	23811	0.115350	0.000321	0.320420	0.005308
14	268025	192	3007	2934	265018	28146	0.114808	0.000219	0.309024	0.004629
15	224432	205	3217	3138	221215	22997	0.114788	0.000291	0.308366	0.006243
16	455591	180	2806	2748	452785	50389	0.115126	0.000246	0.316422	0.007722
17	142011	174	2736	2664	139275	13628	0.113613	0.000178	0.304665	0.011082
18	501247	271	4226	4145	497021	54343	0.114760	0.000277	0.320025	0.006533
19	254990	247	3848	3778	251142	25582	0.113478	0.000272	0.321594	0.007991
20	246203	363	5615	5541	240588	23006	0.114141	0.000220	0.332494	0.010859
21	338184	380	5867	5800	332317	33550	0.115254	0.000189	0.335999	0.008449
22	544791	125	1929	1912	542862	62761	0.117857	0.000257	0.341194	0.007474
23	360417	211	3253	3217	357163	39557	0.117519	0.000221	0.336458	0.005516
24	476908	155	2427	2376	474481	54065	0.116553	0.000270	0.315820	0.008417
25	500848	95	1499	1460	499349	57522	0.116652	0.000268	0.306248	0.007423
26	613678	171	2697	2623	610980	70091	0.116866	0.000331	0.303077	0.005599
27	567875	106	1670	1628	566205	65041	0.116232	0.000149	0.307120	0.008786
28	554507	119	1848	1815	552659	63510	0.116216	0.000303	0.322108	0.007200
29	548293	129	2037	1983	546256	62347	0.116172	0.000245	0.304164	0.009146
30	634621	21	335	327	634286	74021	0.115883	0.000235	0.312714	0.009057
31	732523	35	544	533	731980	85196	0.115814	0.000216	0.320461	0.007376

Grain	^{206}Pb (cps)	^{204}Pb (cps)	$^{206}Pb_{com}$	$^{207}Pb_{com}$	$^{207}Pb^*$	$^{206}Pb^*$	$^{207}Pb/^{206}Pb$	Absolute 1SE	$^{206}Pb/^{238}U$	Absolute 1SE
32	669425	4	68	66	669357	78137	0.115578	0.000177	0.298137	0.005531
33	425810	21	332	323	425478	49440	0.115238	0.000189	0.303366	0.006916
GJ132										
1	75035	147	2624	2292	72410	2613	0.064988	0.000388	0.089161	0.001401
2	71352	243	4314	3777	67038	1126	0.066352	0.000361	0.093816	0.001155
3	66226	188	3347	2923	62879	1455	0.065091	0.000435	0.088645	0.001451
4	174403	174	3102	2710	171301	8429	0.063731	0.000352	0.089487	0.001355
5	161013	157	2802	2450	158211	7748	0.062838	0.000188	0.090880	0.003022
8	183745	118	2099	1834	181646	9739	0.061827	0.000255	0.089717	0.001680
9	172142	154	2728	2392	169414	8633	0.062295	0.000283	0.096658	0.002274
10	232959	73	1300	1137	231659	13405	0.061217	0.000200	0.092371	0.001632
11	191442	69	1227	1071	190215	10730	0.061060	0.000190	0.088260	0.002072
12	258429	178	3168	2771	255261	13281	0.061451	0.000212	0.091595	0.001341
13	252096	167	2975	2605	249121	13162	0.061775	0.000183	0.093650	0.001218
14	244153	234	4162	3649	239991	11519	0.061107	0.000188	0.096257	0.002972
15	244373	239	4262	3720	240111	11438	0.061445	0.000126	0.087657	0.001738
16	286657	245	4370	3818	282287	13856	0.060968	0.000151	0.089217	0.000966
17	304052	337	5990	5254	298061	13695	0.061462	0.000157	0.097277	0.002315
18	260276	337	5998	5254	254279	10837	0.060826	0.000165	0.094625	0.001469
19	263006	314	5594	4895	257412	11219	0.060383	0.000184	0.092566	0.000764
20	284109	412	7328	6418	276781	11126	0.060873	0.000156	0.094317	0.002055
21	276029	469	8329	7298	267700	10076	0.061471	0.000351	0.095234	0.002135
22	302318	251	4447	3902	297871	16086	0.064852	0.000404	0.097949	0.002197
23	367336	283	5029	4407	362307	19085	0.063290	0.000148	0.095400	0.002423
24	227995	169	3001	2626	224995	12036	0.063561	0.000188	0.092764	0.001654
25	207297	188	3351	2932	203946	10423	0.063930	0.000173	0.092821	0.002781
26	227565	191	3391	2973	224174	11581	0.063512	0.000285	0.096505	0.002022
27	232842	177	3149	2759	229692	12159	0.063422	0.000186	0.094837	0.002258
28	219427	147	2613	2286	216813	12263	0.064654	0.000832	0.091768	0.001471
29	206540	139	2478	2169	204061	10951	0.062807	0.000172	0.092438	0.002777
30	259245	72	1281	1119	257964	15213	0.062339	0.000156	0.089774	0.001341
31	238228	56	995	870	237233	14129	0.062422	0.000144	0.091509	0.001527

Grain	^{206}Pb (cps)	^{204}Pb (cps)	^{206}Pbcom	^{207}Pbcom	^{207}Pb*	^{206}Pb*	$^{207}Pb/^{206}Pb$	Absolute 1SE	$^{206}Pb/^{238}U$	Absolute 1SE
32	218113	41	722	631	217390	13260	0.062930	0.000190	0.089854	0.002128
33	229200	17	306	267	228894	14227	0.062406	0.000148	0.090834	0.001248

Sample NA031A Conway Castle Grit, 1st Run

Results of all analyzed grains

*common lead corrected

Grain	^{206}Pb (cps) [1]	^{204}Pb (cps)	Isotopic Ratios: $^{207}Pb/^{206}Pb$	Absolute 2SE	$^{207}Pb/^{235}U$ [2]	Absolute 2SE [3]	$^{206}Pb/^{238}U$	Absolute 2SE	ρ [4]	Apparent Age Summary: $^{207}Pb/^{206}Pb$ Age (Ma)	error 2σ (Ma)	$^{207}Pb/^{235}U$ Age (Ma)	error 2σ (Ma)	$^{206}Pb/^{238}U$ Age (Ma)	error 2σ (Ma)	disc. [5] %
1	926314.6	73.59	0.22228	0.00116	16.52625	0.95800	0.53922	0.03113	0.996	2997	8	2908	54	2780	129	8.9
2	99559.91	66.21	0.06081	0.00106	0.55264	0.04211	0.06591	0.00489	0.974	633	37	447	27	411	30	36.1
4	36001.14	49.26	0.06560	0.00132	0.84359	0.06753	0.09326	0.00722	0.968	794	42	621	37	575	42	28.8
5	312702.9	64.36	0.06337	0.00082	0.89516	0.07556	0.10245	0.00855	0.988	721	27	649	40	629	50	13.4
6	101660.4	122.7	0.06263	0.00236	0.57413	0.04745	0.06649	0.00489	0.890	696	78	461	30	415	30	41.6
7	26084.52	46.09	0.06819	0.00356	0.59543	0.06647	0.06333	0.00625	0.884	874	105	474	41	396	38	56.4
8	84857.54	126.5	0.06082	0.00236	0.54060	0.04380	0.06447	0.00459	0.878	633	81	439	28	403	28	37.5
9	114160.5	73.03	0.06049	0.00234	0.53533	0.04321	0.06418	0.00455	0.878	621	81	435	28	401	27	36.5
10	159083.7	62.3	0.05728	0.00089	0.51736	0.03799	0.06551	0.00470	0.977	502	34	423	25	409	28	19.1
11	33056.28	75.25	0.07603	0.00188	1.71146	0.11985	0.16327	0.01070	0.936	1096	49	1013	44	975	59	11.9
12	15696.4	109.9	0.06927	0.00941	0.64590	0.10132	0.06763	0.00530	0.499	907	257	506	61	422	32	55.2
13	124908	90.78	0.05626	0.00078	0.48740	0.03544	0.06284	0.00448	0.982	462	30	403	24	393	27	15.5
14	262152.7	86.03	0.05603	0.00076	0.50120	0.03709	0.06487	0.00472	0.983	454	30	413	25	405	29	11.0
15*	974005.7	1096	0.20217	0.00198	12.21408	0.95500	0.43817	0.03399	0.992	2844	16	2621	71	2342	151	21.0
16	675570.7	107.2	0.18659	0.00171	12.33365	0.82911	0.47941	0.03193	0.991	2712	15	2630	61	2525	138	8.4
17	130429.4	318.6	0.07821	0.00462	0.74227	0.06613	0.06884	0.00459	0.749	1152	113	564	38	429	28	64.8
18	38751.22	186.5	0.06042	0.00451	0.53830	0.05802	0.06462	0.00502	0.721	618	154	437	38	404	30	35.8
19	302091.8	187.8	0.09970	0.00203	3.44041	0.21563	0.25026	0.01484	0.946	1619	37	1514	48	1440	76	12.3
20	99040.36	261.4	0.06914	0.00780	0.63203	0.09803	0.06630	0.00706	0.687	903	217	497	59	414	43	55.9
21	17344.72	57.07	0.06508	0.00316	0.74243	0.08460	0.08274	0.00853	0.905	777	99	564	48	512	51	35.4
22	136067.2	92.82	0.05996	0.00110	0.52869	0.03806	0.06395	0.00445	0.967	602	39	431	25	400	27	34.7
23	41098.3	63.81	0.06112	0.00140	0.55778	0.04747	0.06618	0.00543	0.963	644	48	450	30	413	33	37.0
24	147895.9	54.85	0.13470	0.00097	6.14436	0.32491	0.33082	0.01733	0.991	2160	12	1997	45	1842	83	16.9
25	118467.1	86.3	0.06092	0.00094	0.67761	0.04837	0.08068	0.00562	0.977	636	33	525	29	500	33	22.2
26	257021.1	149.5	0.06290	0.00095	0.54287	0.04215	0.06260	0.00477	0.981	705	32	440	27	391	29	45.8
27	43770.64	51.67	0.06483	0.00112	0.80023	0.05910	0.08953	0.00643	0.972	769	36	597	33	553	38	29.3
28	40485.64	70.95	0.06630	0.00347	0.60593	0.05237	0.06628	0.00456	0.796	816	106	481	33	414	27	50.9
29	41329.03	47.48	0.06125	0.00144	0.51999	0.04673	0.06157	0.00534	0.965	648	50	425	31	385	32	41.8
30	237683.5	47.15	0.06166	0.00088	0.76305	0.05888	0.08976	0.00681	0.983	662	30	576	33	554	40	17.0

Grain	^{206}Pb (cps) [1]	^{204}Pb (cps)	$^{207}Pb/^{206}Pb$	Absolute 2SE	$^{207}Pb/^{235}U$ [2]	Absolute 2SE [3]	$^{206}Pb/^{238}U$	Absolute 2SE	ρ [4]	$^{207}Pb/^{206}Pb$ Age (Ma)	error 2σ (Ma)	$^{207}Pb/^{235}U$ Age (Ma)	error 2σ (Ma)	$^{206}Pb/^{238}U$ Age (Ma)	error 2σ (Ma)	disc. [5] %
31	21571.79	67.86	0.07436	0.00919	0.64804	0.09260	0.06321	0.00453	0.502	1051	231	507	56	395	27	64.3
32	67076.08	101.3	0.06319	0.00179	0.58034	0.05462	0.06661	0.00598	0.954	715	59	465	35	416	36	43.2
33	1410500	68.28	0.19329	0.00097	12.58508	0.82678	0.47222	0.03093	0.997	2770	8	2649	60	2493	134	12.0
34	120098.8	46.04	0.06083	0.00114	0.64718	0.05508	0.07716	0.00641	0.976	633	40	507	33	479	38	25.2
35*	**908169.2**	**261.2**	**0.19072**	**0.00144**	**12.93113**	**0.81806**	**0.49174**	**0.03089**	**0.993**	**2748**	**12**	**2675**	**58**	**2578**	**132**	**7.5**
36	134184.1	66.05	0.05805	0.00097	0.52747	0.03947	0.06590	0.00481	0.975	532	36	430	26	411	29	23.3
37	166543.5	137.7	0.05840	0.00120	0.54399	0.04496	0.06756	0.00541	0.968	545	44	441	29	421	33	23.4
38	241400.3	372.6	0.07661	0.00220	0.66021	0.05441	0.06250	0.00483	0.938	1111	56	515	33	391	29	66.8
39	180656.6	278.1	0.07679	0.00150	0.99343	0.07973	0.09383	0.00730	0.970	1116	38	700	40	578	43	50.3
40	32948.44	65.14	0.06108	0.00137	0.55973	0.04463	0.06646	0.00509	0.960	642	47	451	29	415	31	36.6
41	21346.66	157.1	0.07825	0.00649	0.73719	0.09231	0.06833	0.00641	0.749	1153	156	561	53	426	39	65.1
42*	3908678	36168	0.17447	0.00765	10.09146	1.02067	0.41951	0.03824	0.901	2601	71	2443	89	2258	171	15.6
43	135361.9	193.7	0.06053	0.00262	0.57452	0.04835	0.06883	0.00497	0.858	623	91	461	31	429	30	32.1
44	204230.8	141.9	0.05767	0.00077	0.58562	0.04526	0.07364	0.00561	0.985	517	29	468	29	458	34	11.9
45	201139.4	114	0.09710	0.00066	3.33519	0.19774	0.24912	0.01467	0.993	1569	13	1489	45	1434	75	9.6
46	71392.14	495.4	0.10907	0.01336	1.49964	0.21003	0.09972	0.00677	0.485	1784	208	930	82	613	40	68.7
47	60690.77	180.1	0.07176	0.00273	1.02330	0.09156	0.10342	0.00838	0.905	979	75	716	45	634	49	37.0
48	124564.7	111.8	0.06030	0.00074	0.59504	0.04420	0.07157	0.00524	0.986	614	26	474	28	446	31	28.4
49	161849.4	138.4	0.05788	0.00047	0.52996	0.03982	0.06641	0.00496	0.994	525	18	432	26	414	30	21.8
50	16337.27	133.9	0.07648	0.00370	0.78846	0.06672	0.07477	0.00519	0.820	1108	94	590	37	465	31	60.1
51	114797.2	242.5	0.06699	0.00115	0.72115	0.06929	0.07807	0.00738	0.984	838	35	551	40	485	44	43.7
52	153480.3	153.8	0.06043	0.00079	0.62754	0.05402	0.07532	0.00641	0.988	619	28	495	33	468	38	25.3
53	136369.7	224.2	0.06562	0.00194	0.63577	0.05310	0.07027	0.00549	0.936	794	61	500	32	438	33	46.4
54	148285.3	663.8	0.08845	0.01221	0.89658	0.13896	0.07352	0.00519	0.455	1392	244	650	72	457	31	69.5
55	530927.5	533	0.06680	0.00307	0.83778	0.07052	0.09097	0.00642	0.838	831	93	618	38	561	38	33.9
56	272483.4	170.7	0.05761	0.00089	0.56850	0.04475	0.07157	0.00552	0.980	515	34	457	29	446	33	14.0
57	33450.83	260	0.10231	0.01252	1.30632	0.17891	0.09261	0.00569	0.448	1666	211	849	76	571	33	68.6
58	210579.6	183.4	0.13387	0.00158	6.46796	0.36821	0.35043	0.01952	0.978	2149	20	2042	49	1937	92	11.4
59	147238.9	286.3	0.07566	0.00156	1.12064	0.07525	0.10742	0.00687	0.952	1086	41	763	35	658	40	41.5
60	202304	243.9	0.06539	0.00229	0.75929	0.06359	0.08422	0.00641	0.908	787	72	574	36	521	38	35.1
61	84630.91	111.2	0.06244	0.00100	0.70604	0.05587	0.08202	0.00636	0.979	689	34	542	33	508	38	27.3
62	98819.83	140.2	0.06007	0.00105	0.55720	0.04138	0.06727	0.00486	0.972	606	37	450	27	420	29	31.8
63	180457.7	307.3	0.05954	0.00105	0.56110	0.04301	0.06835	0.00510	0.973	587	38	452	28	426	31	28.3

Grain	^{206}Pb (cps) [1]	^{204}Pb (cps)	$^{207}Pb/^{206}Pb$	Absolute 2SE	$^{207}Pb/^{235}U$ [2]	Absolute 2SE [3]	$^{206}Pb/^{238}U$	Absolute 2SE	ρ [4]	$^{207}Pb/^{206}Pb$ Age (Ma)	error 2σ (Ma)	$^{207}Pb/^{235}U$ Age (Ma)	error 2σ (Ma)	$^{206}Pb/^{238}U$ Age (Ma)	error 2σ (Ma)	disc. [5] %
64*	253952.4	5412	0.08055	0.14085	0.61746	1.08697	0.05560	0.01131	0.116	1210	1780	488	522	349	69	73.1
65	85682.59	532.5	0.12828	0.00979	3.05134	0.29323	0.17251	0.01007	0.607	2075	129	1421	71	1026	55	54.6
66	140257.7	709.5	0.09232	0.01382	0.89642	0.14950	0.07042	0.00517	0.440	1474	260	650	77	439	31	72.6
67	432740.9	102.7	0.08011	0.00054	2.10618	0.15000	0.19067	0.01352	0.996	1200	13	1151	48	1125	73	6.8
68	72586.01	108.4	0.06109	0.00139	0.57050	0.04365	0.06773	0.00495	0.955	642	48	458	28	422	30	35.4
69	94813.8	146.9	0.06339	0.00184	0.62929	0.05647	0.07200	0.00611	0.946	721	60	496	35	448	37	39.2
70	56927.67	89.71	0.06480	0.00182	0.74703	0.05766	0.08361	0.00601	0.932	768	58	566	33	518	36	33.9
71	121115.5	64.06	0.13173	0.00087	6.34076	0.42189	0.34912	0.02311	0.995	2121	12	2024	57	1930	110	10.4
72	75806.74	122.9	0.06268	0.00143	0.60137	0.04855	0.06959	0.00539	0.959	697	48	478	30	434	32	39.1
73	1416398	110.8	0.12745	0.00068	5.96317	0.42724	0.33934	0.02424	0.997	2063	9	1970	60	1883	116	10.0
74	245832.2	126.6	0.06161	0.00096	0.81884	0.07595	0.09639	0.00881	0.986	661	33	607	42	593	52	10.7
75	77670	85.5	0.06147	0.00116	0.59866	0.04361	0.07063	0.00497	0.966	656	40	476	27	440	30	34.0
76	24801.19	112.1	0.08379	0.00464	0.84432	0.08126	0.07308	0.00575	0.818	1288	104	622	44	455	34	67.0
77	570520.5	83.13	0.20416	0.00109	14.58466	0.79256	0.51811	0.02802	0.995	2860	9	2789	50	2691	118	7.2
78	1158460	228.3	0.17830	0.00196	8.40607	0.54348	0.34194	0.02179	0.985	2637	18	2276	57	1896	104	32.3
79	12543.1	62.63	0.08212	0.00701	0.88701	0.09650	0.07833	0.00529	0.621	1248	158	645	51	486	32	63.3
80	55586.02	70.76	0.06416	0.00172	0.61379	0.04865	0.06938	0.00517	0.941	747	56	486	30	432	31	43.5
81	53438.11	40.05	0.06123	0.00104	0.55344	0.04550	0.06556	0.00527	0.978	647	36	447	29	409	32	37.9
82	421425.7	69.58	0.19732	0.00213	12.98124	0.71012	0.47714	0.02559	0.980	2804	18	2678	50	2515	111	12.4
83	43277.83	69.59	0.06458	0.00232	0.62546	0.04875	0.07025	0.00486	0.888	761	74	493	30	438	29	43.9
84	24052.96	33.43	0.10222	0.00215	3.63649	0.23472	0.25802	0.01575	0.946	1665	38	1558	50	1480	80	12.4
85	94699.22	88.28	0.05962	0.00084	0.58899	0.05523	0.07165	0.00664	0.989	590	30	470	35	446	40	25.2
86	119556.2	79.53	0.06199	0.00093	0.69332	0.05680	0.08112	0.00653	0.983	674	32	535	33	503	39	26.4
87	169578.4	194.9	0.09739	0.00139	3.35774	0.23568	0.25005	0.01718	0.979	1575	27	1495	53	1439	88	9.6
88	165673.8	295.7	0.06829	0.00194	0.91225	0.07612	0.09689	0.00760	0.940	877	58	658	40	596	45	33.5
89	133796	189.1	0.06422	0.00151	0.63214	0.04598	0.07139	0.00491	0.946	749	49	497	28	445	29	42.0
90	119021.1	152.1	0.06266	0.00205	0.60126	0.04727	0.06959	0.00498	0.910	697	68	478	30	434	30	39.0
91	1874153	88.06	0.18237	0.00094	12.37705	0.65293	0.49223	0.02584	0.995	2675	9	2633	48	2580	111	4.3
92	32601.8	62.14	0.06872	0.00268	0.63878	0.05818	0.06742	0.00555	0.904	890	78	502	35	421	33	54.5
93	167530	92.85	0.06168	0.00116	0.62453	0.04711	0.07344	0.00536	0.968	663	40	493	29	457	32	32.2
94	63390.27	50.98	0.06531	0.00109	0.94113	0.07414	0.10451	0.00804	0.977	784	35	673	38	641	47	19.2
95	34639.98	93.32	0.08015	0.00503	0.75691	0.06982	0.06849	0.00463	0.733	1201	119	572	40	427	28	66.5
96	223373.7	70.73	0.13678	0.00109	6.78480	0.33752	0.35977	0.01766	0.987	2187	14	2084	43	1981	83	10.9

Grain	^{206}Pb (cps) [1]	^{204}Pb (cps)	$^{207}Pb/^{206}Pb$	Absolute 2SE	$^{207}Pb/^{235}U$ [2]	Absolute 2SE [3]	$^{206}Pb/^{238}U$	Absolute 2SE	ρ [4]	$^{207}Pb/^{206}Pb$ Age (Ma)	error 2σ (Ma)	$^{207}Pb/^{235}U$ Age (Ma)	error 2σ (Ma)	$^{206}Pb/^{238}U$ Age (Ma)	error 2σ (Ma)	disc. [5] %
97	85794.72	210.8	0.17145	0.00402	10.38529	0.60964	0.43931	0.02364	0.917	2572	39	2470	53	2348	105	10.4
98	103157.6	102.8	0.06130	0.00114	0.56943	0.04229	0.06737	0.00484	0.968	650	39	458	27	420	29	36.5
99	38207.91	228.2	0.13206	0.01351	1.33652	0.15537	0.07340	0.00405	0.475	2126	169	862	65	457	24	81.2
100	81349.57	49.1	0.06147	0.00103	0.53939	0.04250	0.06364	0.00490	0.977	656	36	438	28	398	30	40.6
101*	319913.4	605.8	0.05306	0.00309	0.50348	0.04568	0.06882	0.00479	0.767	331	127	414	30	429	29	-30.4
102	60703.07	127.4	0.06930	0.00184	0.95711	0.07251	0.10016	0.00711	0.936	908	54	682	37	615	42	33.8
103	28234.17	112.9	0.07300	0.00414	0.68710	0.05707	0.06826	0.00415	0.731	1014	111	531	34	426	25	59.9
104	78835.66	211	0.07837	0.00263	0.72477	0.05670	0.06707	0.00474	0.903	1156	65	553	33	418	29	65.9
105	102055.3	197.1	0.07098	0.00351	0.71129	0.05793	0.07268	0.00470	0.795	957	98	546	34	452	28	54.6
106	93240.09	107	0.06298	0.00122	0.71586	0.05250	0.08243	0.00583	0.965	708	41	548	31	511	35	29.0
107	196371.4	92.61	0.08204	0.00082	2.18284	0.12752	0.19298	0.01111	0.985	1246	19	1176	40	1137	60	9.5
108	209225.2	94.36	0.06177	0.00105	0.80556	0.05534	0.09458	0.00630	0.969	666	36	600	31	583	37	13.1
109	244117	154.4	0.05947	0.00120	0.57582	0.04131	0.07022	0.00483	0.960	584	43	462	26	438	29	26.0
110*	177854.6	612.6	0.05023	0.00565	0.48162	0.06305	0.06955	0.00465	0.511	205	242	399	42	433	28	-115
111	131372.5	111.5	0.05883	0.00117	0.55289	0.03840	0.06816	0.00454	0.958	561	43	447	25	425	27	25.0
112	126498.2	109.5	0.05993	0.00111	0.58312	0.04292	0.07057	0.00503	0.968	601	40	466	27	440	30	27.8
113	93867.93	107.4	0.05838	0.00109	0.60178	0.04857	0.07476	0.00587	0.973	544	40	478	30	465	35	15.1
114	417574.1	105.3	0.10039	0.00381	3.62980	0.23679	0.26223	0.01391	0.813	1631	69	1556	51	1501	71	8.9
115	156698.8	70.27	0.06109	0.00108	0.72513	0.05163	0.08609	0.00594	0.969	642	38	554	30	532	35	17.8
116	158152	138	0.09550	0.00096	3.25591	0.19656	0.24726	0.01472	0.986	1538	19	1471	46	1424	76	8.2
117*	630626	1172	0.09394	0.00133	3.33390	0.22154	0.25741	0.01671	0.977	1507	27	1489	51	1477	85	2.2
118	52112	75	0.06999	0.00351	0.82857	0.06885	0.08585	0.00569	0.798	928	100	613	38	531	34	44.6
119	26155	242	0.07482	0.00272	0.99520	0.07163	0.09647	0.00599	0.863	1064	72	701	36	594	35	46.2
120	238703	67	0.13099	0.00089	6.30573	0.32966	0.34914	0.01810	0.992	2111	12	2019	45	1930	86	9.9
121	238703	139	0.13099	0.00089	6.30573	0.32966	0.34914	0.01810	0.992	2111	12	2019	45	1930	86	9.9
122	25593	108	0.07144	0.00491	0.68985	0.06546	0.07003	0.00459	0.690	970	134	533	39	436	28	56.9
123	58772	97	0.06167	0.00150	0.59936	0.04911	0.07049	0.00552	0.955	663	51	477	31	439	33	34.9
124*	359829	836	0.05639	0.00145	0.65136	0.05274	0.08377	0.00643	0.948	468	56	509	32	519	38	-11.3
125	49478	261	0.06306	0.00126	0.62177	0.04795	0.07151	0.00533	0.966	710	42	491	30	445	32	38.6
126	69591	114	0.06886	0.00194	0.92976	0.06460	0.09793	0.00622	0.914	895	57	668	33	602	36	34.2
127	1194948	235	0.19303	0.00107	11.32033	0.85995	0.42534	0.03222	0.997	2768	9	2550	69	2285	144	20.7
128	67028	132	0.06095	0.00099	0.58793	0.04088	0.06997	0.00473	0.973	637	34	470	26	436	28	32.7
129	70408	102	0.07615	0.00411	1.05018	0.08940	0.10002	0.00659	0.774	1099	104	729	43	615	39	46.2

Grain	^{206}Pb (cps) [1]	^{204}Pb (cps)	$^{207}Pb/^{206}Pb$	Absolute 2SE	$^{207}Pb/^{235}U$ [2]	Absolute 2SE [3]	$^{206}Pb/^{238}U$	Absolute 2SE	ρ [4]	$^{207}Pb/^{206}Pb$ Age (Ma)	error 2σ (Ma)	$^{207}Pb/^{235}U$ Age (Ma)	error 2σ (Ma)	$^{206}Pb/^{238}U$ Age (Ma)	error 2σ (Ma)	disc. [5] %
130	132889	112	0.05862	0.00098	0.54956	0.04092	0.06800	0.00493	0.974	553	36	445	26	424	30	24.1
131	81994	79	0.06094	0.00126	0.63721	0.05099	0.07583	0.00586	0.966	637	44	501	31	471	35	27.0
132	111761	199	0.07102	0.00488	0.69826	0.06655	0.07131	0.00471	0.692	958	135	538	39	444	28	55.5
133	62023	65	0.06164	0.00127	0.61866	0.04424	0.07279	0.00499	0.958	662	43	489	27	453	30	32.7
134	49186	71	0.06611	0.00274	0.66256	0.05473	0.07268	0.00519	0.865	810	84	516	33	452	31	45.7
135	14049	58	0.07361	0.00247	0.79689	0.06745	0.07851	0.00610	0.918	1031	66	595	37	487	36	54.7
136	62498	151	0.07574	0.00497	0.69069	0.06625	0.06614	0.00463	0.729	1088	126	533	39	413	28	64.0
137	50903	60	0.06378	0.00150	0.63375	0.05321	0.07206	0.00581	0.960	734	49	498	33	449	35	40.3
138	167815	140	0.06179	0.00124	0.63233	0.04889	0.07422	0.00554	0.966	667	42	498	30	462	33	31.9
139	92079	159	0.06323	0.00146	0.64589	0.04467	0.07408	0.00483	0.943	716	48	506	27	461	29	36.9
140	108860	94	0.10377	0.00117	3.66609	0.28948	0.25624	0.02003	0.990	1693	21	1564	61	1471	102	14.7
141	30524	44	0.06834	0.00208	0.77368	0.05677	0.08210	0.00548	0.910	879	62	582	32	509	33	43.8
142	236735	49	0.09582	0.00075	3.34292	0.22019	0.25304	0.01655	0.993	1544	15	1491	50	1454	85	6.5
143	284923	258	0.06641	0.00117	0.70860	0.05805	0.07738	0.00619	0.977	819	36	544	34	480	37	42.9
144	139003	70	0.06250	0.00135	0.80156	0.08733	0.09302	0.00993	0.980	691	45	598	48	573	58	17.8
145	73909	57	0.06120	0.00144	0.59027	0.04757	0.06995	0.00539	0.957	646	50	471	30	436	32	33.7
146	147714	151	0.06348	0.00260	0.62529	0.05150	0.07143	0.00511	0.868	725	84	493	32	445	31	39.9
147	23396	72	0.07700	0.00400	0.76004	0.06530	0.07159	0.00490	0.797	1121	100	574	37	446	29	62.3
148	288799	118	0.09771	0.00122	3.20351	0.24676	0.23778	0.01807	0.987	1581	23	1458	58	1375	93	14.4
149	109000	122	0.06242	0.00126	0.62310	0.04544	0.07240	0.00507	0.961	688	42	492	28	451	30	35.8
150	136494	77	0.06298	0.00116	0.71290	0.05143	0.08210	0.00572	0.967	707	39	546	30	509	34	29.2
151	28024	50	0.10221	0.00187	3.61449	0.22308	0.25648	0.01512	0.955	1665	33	1553	48	1472	77	12.9
152	22273	43	0.06878	0.00203	0.66651	0.04920	0.07029	0.00475	0.916	892	60	519	30	438	29	52.6
153	134398	79	0.07363	0.00137	1.63915	0.11881	0.16147	0.01131	0.967	1031	37	985	45	965	62	6.9
154	67097	70	0.06084	0.00149	0.61855	0.05106	0.07373	0.00581	0.955	634	52	489	32	459	35	28.6
155	50231	63	0.06794	0.00124	1.02421	0.08457	0.10934	0.00880	0.975	867	38	716	42	669	51	24.0
156	30384	71	0.07425	0.00243	0.85271	0.06285	0.08330	0.00550	0.896	1048	65	626	34	516	33	52.8
157	131190	89	0.06204	0.00123	0.68960	0.05377	0.08062	0.00608	0.967	675	42	533	32	500	36	27.0
158	190934	1077	0.09653	0.00120	2.78004	0.22709	0.20889	0.01686	0.988	1558	23	1350	59	1223	89	23.6
159	131576	90	0.05929	0.00117	0.59175	0.04340	0.07239	0.00511	0.963	578	42	472	27	451	31	22.8

Grain	^{206}Pb (cps) [1]	^{204}Pb (cps)	^{207}Pb/^{206}Pb	Absolute 2SE	^{207}Pb/^{235}U [2]	Absolute 2SE [3]	^{206}Pb/^{238}U	Absolute 2SE	ρ [4]	^{207}Pb/^{206}Pb Age (Ma)	error 2σ (Ma)	^{207}Pb/^{235}U Age (Ma)	error 2σ (Ma)	^{206}Pb/^{238}U Age (Ma)	error 2σ (Ma)	disc. [5] %
160	48167	177	0.08843	0.00807	0.91176	0.10696	0.07478	0.00552	0.629	1392	166	658	55	465	33	69.0
161	75137	60	0.05931	0.00115	0.56357	0.05040	0.06892	0.00602	0.976	578	42	454	32	430	36	26.6
162	62922	253	0.08265	0.00507	0.84568	0.08540	0.07421	0.00596	0.795	1261	115	622	46	461	36	65.7
163	116037	65	0.06315	0.00094	0.88481	0.07040	0.10162	0.00794	0.982	713	31	644	37	624	46	13.1
164	147829	88	0.05876	0.00113	0.54538	0.04338	0.06731	0.00520	0.970	558	41	442	28	420	31	25.6
165	77731	74	0.06074	0.00136	0.58248	0.04278	0.06955	0.00486	0.952	630	48	466	27	433	29	32.3
166	292805	121	0.13642	0.00109	7.12436	0.41938	0.37877	0.02209	0.991	2182	14	2127	51	2071	102	6.0
167	94192	215	0.07714	0.00641	0.78222	0.08592	0.07355	0.00528	0.654	1125	157	587	48	457	32	61.4
168	17157	70	0.07422	0.00296	1.09610	0.08918	0.10710	0.00760	0.872	1048	78	751	42	656	44	39.3
169	96728	56	0.05925	0.00095	0.58310	0.04132	0.07138	0.00493	0.974	576	34	466	26	444	30	23.7
170	38720	70	0.06601	0.00136	0.87845	0.05886	0.09651	0.00616	0.952	807	42	640	31	594	36	27.6
171	24753	63	0.06990	0.00213	0.79974	0.05768	0.08298	0.00542	0.906	925	61	597	32	514	32	46.2
172	140872	159	0.06938	0.00206	1.03108	0.07109	0.10779	0.00671	0.903	910	60	719	35	660	39	28.9
173	132306	134	0.06406	0.00115	0.61643	0.04403	0.06979	0.00483	0.968	744	37	488	27	435	29	42.9
174	103743	112	0.06320	0.00190	0.65035	0.05139	0.07463	0.00545	0.924	715	63	509	31	464	33	36.4
175	61142	165	0.07184	0.00591	0.71988	0.07474	0.07268	0.00460	0.610	981	159	551	43	452	28	55.8
176	71782	74	0.06565	0.00140	0.95092	0.07490	0.10506	0.00797	0.963	795	44	679	38	644	46	20.0
177	291555	95	0.13416	0.00075	6.85856	0.38358	0.37077	0.02063	0.995	2153	10	2093	48	2033	96	6.5
178	73191	93	0.06241	0.00127	0.77710	0.05912	0.09031	0.00662	0.963	688	43	584	33	557	39	19.8
179*	415068	1137	0.06066	0.00378	0.69980	0.06251	0.08366	0.00535	0.716	627	129	539	37	518	32	18.1
180	134394	255	0.06979	0.00356	0.70781	0.05988	0.07356	0.00496	0.797	922	102	543	35	458	30	52.2
181	46607	111	0.06892	0.00287	0.65976	0.05576	0.06942	0.00511	0.871	896	84	514	34	433	31	53.5
182	93443	313	0.08341	0.00892	1.11141	0.13778	0.09664	0.00607	0.506	1279	195	759	64	595	36	56.0
183	63271	308	0.11042	0.01126	1.07076	0.12712	0.07033	0.00427	0.512	1806	175	739	60	438	26	78.3
184	231250	94	0.05730	0.00083	0.56414	0.03885	0.07140	0.00481	0.978	503	32	454	25	445	29	12.0
185	85168	133	0.06381	0.00219	0.62697	0.05344	0.07126	0.00556	0.915	735	71	494	33	444	33	41.0
186	316870	118	0.05723	0.00089	0.54421	0.04430	0.06896	0.00551	0.982	500	34	441	29	430	33	14.6
187	344954	100	0.05667	0.00088	0.55627	0.03997	0.07120	0.00499	0.976	479	34	449	26	443	30	7.6
188*	547077	374	0.10299	0.00163	4.00179	0.28444	0.28182	0.01953	0.975	1679	29	1635	56	1601	97	5.3
189*	383712	999	0.05099	0.00320	0.47083	0.04327	0.06697	0.00450	0.730	240	139	392	29	418	27	-76.3
190	94178	72	0.05887	0.00106	0.58855	0.04332	0.07250	0.00518	0.970	562	39	470	27	451	31	20.5
191	37775	77	0.05745	0.00140	0.55439	0.04124	0.06999	0.00492	0.945	509	53	448	27	436	30	14.8
192	21241	73	0.06442	0.00320	0.85587	0.07157	0.09636	0.00648	0.804	755	102	628	38	593	38	22.5

Grain	^{206}Pb (cps) [1]	^{204}Pb (cps)	$^{207}Pb/^{206}Pb$	Absolute 2SE	$^{207}Pb/^{235}U$ [2]	Absolute 2SE [3]	$^{206}Pb/^{238}U$	Absolute 2SE	ρ [4]	$^{207}Pb/^{206}Pb$ Age (Ma)	error 2σ (Ma)	$^{207}Pb/^{235}U$ Age (Ma)	error 2σ (Ma)	$^{206}Pb/^{238}U$ Age (Ma)	error 2σ (Ma)	disc. [5] %
193	193955	74	0.09473	0.00084	3.26698	0.18842	0.25013	0.01425	0.988	1523	17	1473	44	1439	73	6.1
194	118821	237	0.06905	0.00336	0.73251	0.06585	0.07694	0.00582	0.841	900	97	558	38	478	35	48.7
195	166961	63	0.06105	0.00089	0.85012	0.06225	0.10100	0.00725	0.980	641	31	625	34	620	42	3.4
196	265185	123	0.05869	0.00097	0.58796	0.04320	0.07266	0.00520	0.975	556	36	470	27	452	31	19.3
197	196698	143	0.06899	0.00174	1.18975	0.09323	0.12507	0.00928	0.947	899	51	796	42	760	53	16.4
198	225690	104	0.09508	0.00082	3.27301	0.20550	0.24968	0.01553	0.990	1530	16	1475	48	1437	80	6.8
199	28491	60	0.06229	0.00149	0.75044	0.05855	0.08737	0.00649	0.952	684	50	568	33	540	38	22.0
200	1077318	141	0.12169	0.00052	5.00709	0.25715	0.29842	0.01527	0.996	1981	8	1821	43	1683	75	17.1

Sample NA031A Conway Castle Grit, 1st Run - Standards

*common lead corrected

Grain	^{206}Pb (cps)	^{204}Pb (cps)	$^{206}Pbcom$	$^{207}Pbcom$	$^{207}Pb*$	$^{206}Pb*$	Not Common Lead Corrected Isotopic Ratios: $^{207}Pb/^{206}Pb$	Absolute 1SE	$^{206}Pb/^{238}U$	Absolute 1SE
LH94-15										
1	649175	41	617	623	648558	74045	0.113613	0.000276	0.378535	0.006999
2	289832	64	970	976	288862	32445	0.114572	0.000257	0.371475	0.007214
3	320935	87	1304	1323	319631	36204	0.116641	0.000464	0.388311	0.006535
4	445707	78	1157	1174	444549	50065	0.114113	0.000228	0.388127	0.011739
5	327823	86	1275	1296	326548	35989	0.112023	0.000184	0.391944	0.008028
6	534696	74	1115	1125	533580	59405	0.111818	0.000176	0.377658	0.007777
7	1133872	113	1702	1712	1132170	126674	0.111956	0.000128	0.371082	0.007145
8	1336996	115	1721	1740	1335275	149394	0.111798	0.000124	0.382500	0.008157
9	533692	91	1367	1379	532325	59722	0.113050	0.000174	0.377795	0.006177
10	550220	87	1311	1317	548909	60938	0.111893	0.000117	0.368522	0.007117
11	351302	73	1098	1108	350204	38621	0.111886	0.000211	0.378349	0.008464
12	752903	43	652	654	752251	84520	0.111892	0.000188	0.365663	0.006516
13	741427	54	804	812	740623	82888	0.111670	0.000161	0.379470	0.007066
14	386506	67	1012	1021	385495	43095	0.112065	0.000172	0.377395	0.008018
15	434822	48	716	722	434106	48443	0.111641	0.000153	0.377966	0.008827
18	798792	99	1490	1498	797301	88425	0.111501	0.000104	0.369669	0.007691
19	476307	114	1709	1723	474598	52322	0.111998	0.000169	0.376320	0.005721
20	900667	116	1739	1753	898928	99901	0.111711	0.000138	0.375301	0.008501
21	836933	109	1648	1654	835285	92621	0.111503	0.000113	0.367153	0.006164
22	882520	168	2513	2542	880008	97014	0.111565	0.000157	0.383488	0.006392
23	529322	152	2300	2310	527022	57907	0.112303	0.000170	0.367880	0.006169
24	992358	114	1724	1736	990634	110560	0.111933	0.000123	0.373517	0.004634
25	1107470	102	1529	1540	1105941	123740	0.112049	0.000118	0.373303	0.009886
26	987609	86	1307	1310	986302	110067	0.111616	0.000115	0.364260	0.009301
27	797203	72	1088	1092	796115	88498	0.111207	0.000120	0.366717	0.007808
28	849895	51	780	777	849115	95125	0.111479	0.000106	0.351301	0.007070
29	906299	38	572	573	905727	101626	0.111761	0.000091	0.360316	0.006813
30	459851	57	858	862	458993	51746	0.113370	0.000174	0.369209	0.007151

Grain	^{206}Pb (cps)	^{204}Pb (cps)	$^{206}Pb_{com}$	$^{207}Pb_{com}$	$^{207}Pb^*$	$^{206}Pb^*$	$^{207}Pb/^{206}Pb$	Absolute 1SE	$^{206}Pb/^{238}U$	Absolute 1SE
31	511579	58	877	885	510702	57273	0.112516	0.000152	0.377393	0.007053
32	783410	55	826	831	782584	88570	0.112906	0.000126	0.372721	0.005508
33	796600	54	811	818	795789	89818	0.112477	0.000128	0.376229	0.003923
34	874358	90	1358	1367	873000	98060	0.112628	0.000097	0.372574	0.007739
35	1554870	99	1501	1508	1553369	175965	0.112913	0.000124	0.369261	0.007770
36	590992	108	1630	1638	589362	65848	0.113024	0.000102	0.369446	0.007276
37	610442	114	1723	1727	608719	67691	0.112606	0.000122	0.364186	0.005043
38	782622	96	1458	1454	781164	87885	0.113033	0.000121	0.354273	0.006792
39	1136719	102	1534	1542	1135185	128331	0.113170	0.000153	0.370070	0.008767
40	384672	93	1400	1407	383272	42630	0.113297	0.000121	0.370393	0.007106
41	764838	86	1311	1313	763526	85856	0.112673	0.000133	0.361825	0.007731
42	684682	46	691	693	683991	77351	0.112953	0.000095	0.365958	0.006609
43	714047	55	829	833	713218	80390	0.112490	0.000111	0.369348	0.007871
44	745147	71	1066	1073	744081	84478	0.113120	0.000162	0.373611	0.005663
45	523184	60	887	905	522297	59021	0.113248	0.000112	0.399846	0.009499
46	579395	48	723	725	578672	65650	0.113241	0.000156	0.365426	0.009454
47	786006	55	828	838	785177	88909	0.112982	0.000115	0.381837	0.007913
48	645409	64	959	971	644450	72931	0.113279	0.000168	0.385704	0.004332
49	662033	65	974	983	661059	74386	0.112733	0.000111	0.379073	0.007356
50	726004	58	883	887	725121	81923	0.112792	0.000130	0.367499	0.006102
51	614727	63	955	960	613772	68965	0.112676	0.000077	0.369570	0.005837
52	753510	76	1151	1154	752359	84576	0.112692	0.000078	0.364671	0.008628
53	751263	67	1005	1010	750258	84462	0.112726	0.000090	0.369130	0.004221
54	462230	57	878	874	461352	51849	0.112706	0.000102	0.348872	0.008253
55	601577	76	1148	1153	600429	67262	0.112635	0.000115	0.367878	0.005935
56	1044000	74	1124	1130	1042876	117356	0.112105	0.000102	0.369287	0.007538
57	802568	76	1142	1154	801426	89554	0.111707	0.000123	0.380511	0.007181
58	768130	64	965	966	767165	85869	0.111994	0.000120	0.361006	0.006520
59	1101663	90	1361	1371	1100302	123665	0.111945	0.000151	0.374706	0.009900
GJ132										
1	192225	46	817	723	191408	11312	0.062158	0.000127	0.115486	0.002233
2	178902	42	736	652	178166	10527	0.061920	0.000155	0.115942	0.002647

Grain	^{206}Pb (cps)	^{204}Pb (cps)	$^{206}Pb_{com}$	$^{207}Pb_{com}$	$^{207}Pb^*$	$^{206}Pb^*$	$^{207}Pb/^{206}Pb$	Absolute 1SE	$^{206}Pb/^{238}U$	Absolute 1SE
3	182281	55	973	861	181308	10523	0.062009	0.000202	0.114387	0.002393
4	166484	62	1093	964	165391	9422	0.061732	0.000169	0.108259	0.001541
5	244042	62	1086	958	242955	13827	0.059961	0.000102	0.108430	0.002834
6	221380	65	1153	1018	220227	12376	0.059758	0.000174	0.110376	0.002901
7	247411	73	1285	1136	246126	13997	0.060653	0.000144	0.112374	0.002612
8	248572	69	1206	1067	247366	14103	0.060383	0.000099	0.115208	0.002710
12	305391	43	762	672	304630	18061	0.060740	0.000129	0.110406	0.002609
13	261647	43	749	662	260898	15354	0.060567	0.000148	0.112609	0.001635
14	288750	41	713	631	288037	17023	0.060566	0.000115	0.114884	0.001969
15	298204	46	804	714	297400	17537	0.060337	0.000118	0.120454	0.002461
18	361819	128	2259	1994	359560	20763	0.062275	0.000141	0.109762	0.002219
19	334894	125	2205	1947	332689	19186	0.062381	0.000144	0.110713	0.002615
20	334082	119	2093	1847	331989	18508	0.060403	0.000111	0.108618	0.001602
21	317492	131	2321	2043	315171	17350	0.060611	0.000145	0.103836	0.001837
22	323001	142	2501	2203	320500	17645	0.060888	0.000152	0.106014	0.001466
23	334151	126	2231	1964	331920	18509	0.060632	0.000103	0.105114	0.001973
24	350818	87	1531	1349	349287	20158	0.060644	0.000121	0.105952	0.001776
25	356308	101	1774	1565	354535	20400	0.060863	0.000173	0.109629	0.001521
26	305437	95	1670	1476	303768	17280	0.060733	0.000119	0.112468	0.001883
27	313121	77	1363	1204	311758	18125	0.061139	0.000103	0.111923	0.001360
28	285906	61	1078	955	284827	16619	0.060694	0.000130	0.116129	0.002021
29	275151	59	1046	926	274104	16049	0.061166	0.000130	0.114505	0.002407
30	307653	55	971	857	306683	18052	0.060953	0.000118	0.111049	0.001330
31	324625	49	863	761	323763	19163	0.060818	0.000104	0.109036	0.001655
32	332152	50	874	773	331277	19585	0.060684	0.000097	0.112814	0.001799
33	333705	62	1089	962	332616	19575	0.060780	0.000091	0.112286	0.001462
34	326436	93	1646	1448	324790	18926	0.061691	0.000147	0.103566	0.001319
35	337500	90	1599	1406	335901	19468	0.061202	0.000112	0.103187	0.001489
36	294691	118	2088	1841	292603	16498	0.061360	0.000093	0.107791	0.001676
37	314917	115	2026	1787	312890	17687	0.061083	0.000126	0.107888	0.001955
38	330262	96	1690	1489	328571	19163	0.061883	0.000138	0.105951	0.001566
39	320036	104	1832	1614	318204	18424	0.061738	0.000148	0.106195	0.001714
40	305083	106	1855	1642	303228	17627	0.062617	0.000163	0.115979	0.001971

Grain	^{206}Pb (cps)	^{204}Pb (cps)	$^{206}Pb_{com}$	$^{207}Pb_{com}$	$^{207}Pb^*$	$^{206}Pb^*$	$^{207}Pb/^{206}Pb$	Absolute 1SE	$^{206}Pb/^{238}U$	Absolute 1SE
41	293740	90	1593	1407	292146	16733	0.061178	0.000100	0.110431	0.001562
42	289950	60	1052	929	288897	16977	0.061137	0.000129	0.111144	0.002450
43	282288	48	843	745	281445	16612	0.060969	0.000112	0.112908	0.001613
44	291229	36	638	563	290590	17357	0.060891	0.000085	0.108794	0.001216
45	299943	42	735	648	299208	17856	0.061083	0.000107	0.108598	0.001963
46	228321	44	782	689	227540	13422	0.061410	0.000166	0.108829	0.001521
47	247422	43	755	665	246667	14712	0.061483	0.000118	0.104809	0.001364
48	260407	68	1202	1060	259204	15039	0.061267	0.000107	0.107410	0.002137
49	274059	81	1440	1268	272619	15738	0.061514	0.000154	0.105479	0.001859
50	265324	70	1239	1092	264085	15351	0.061281	0.000152	0.107417	0.002106
51	285339	76	1348	1189	283991	16436	0.061113	0.000119	0.108232	0.002411
52	305952	81	1434	1264	304518	17736	0.061443	0.000159	0.107624	0.001335
53	266908	81	1426	1258	265481	15263	0.061283	0.000130	0.108985	0.002120
54	272588	75	1339	1174	271249	15776	0.061286	0.000125	0.097022	0.001672
55	261608	57	1010	888	260598	15342	0.061186	0.000165	0.101469	0.001860
56	312867	61	1086	956	311781	18386	0.061238	0.000090	0.103840	0.001028
57	287597	59	1035	912	286562	16645	0.060513	0.000097	0.106459	0.001857
58	254789	48	841	740	253948	14727	0.060105	0.000082	0.103513	0.002328
59	259369	58	1019	898	258350	14967	0.060473	0.000142	0.107079	0.002278

Sample NA031A Conway Castle Grit, 2nd Run

Results of all analyzed grains

*common lead corrected

			Isotopic Ratios							Apparent Age Summary						
Grain	^{206}Pb (cps) [1]	^{204}Pb (cps)	$^{207}Pb/^{206}Pb$	Absolute 2SE	$^{207}Pb/^{235}U$ [2]	Absolute 2SE [3]	$^{206}Pb/^{238}U$	Absolute 2SE	ρ [4]	$^{207}Pb/^{206}Pb$ Age (Ma)	error 2σ (Ma)	$^{207}Pb/^{235}U$ Age (Ma)	error 2σ (Ma)	$^{206}Pb/^{238}U$ Age (Ma)	error 2σ (Ma)	disc. [5] %
2A	94190	212	0.05879	0.00072	0.59626	0.02392	0.07356	0.00281	0.952	559	26	475	15	458	17	18.9
2B	113417	209	0.05755	0.00060	0.55705	0.01748	0.07020	0.00208	0.943	513	23	450	11	437	13	15.2
4	32615	51	0.06204	0.00099	0.87254	0.03203	0.10201	0.00337	0.900	675	34	637	17	626	20	7.7
5	205332	58	0.06329	0.00085	1.01881	0.03900	0.11675	0.00418	0.936	718	28	713	19	712	24	0.9
6A	97147	202	0.05731	0.00037	0.57899	0.01894	0.07327	0.00235	0.980	503	14	464	12	456	14	9.8
6B	72938	226	0.06171	0.00070	0.62260	0.02108	0.07317	0.00233	0.941	664	24	491	13	455	14	32.6
7A	15611	231	0.07652	0.00368	0.84589	0.04914	0.08018	0.00261	0.561	1109	93	622	27	497	16	57.3
7B	20216	212	0.06682	0.00109	0.66561	0.02384	0.07224	0.00230	0.890	832	34	518	14	450	14	47.6
8	40015	318	0.09670	0.00706	1.01317	0.08079	0.07599	0.00244	0.403	1561	131	710	40	472	15	72.3
9A	68897	280	0.06132	0.00084	0.61081	0.02182	0.07224	0.00238	0.924	651	29	484	14	450	14	32.0
9B	91066	404	0.07455	0.00402	0.79820	0.05215	0.07766	0.00287	0.565	1056	105	596	29	482	17	56.4
10	35016	258	0.06062	0.00115	0.61836	0.02305	0.07398	0.00237	0.861	626	40	489	14	460	14	27.4
12	11065	298	0.32282	0.03701	5.41000	0.71649	0.12154	0.00806	0.501	3583	166	1886	108	739	46	83.7
13	109719	295	0.06095	0.00107	0.63690	0.02231	0.07579	0.00230	0.866	637	37	500	14	471	14	27.1
17	89236	122	0.06130	0.00146	0.64557	0.02484	0.07638	0.00230	0.784	650	50	506	15	474	14	28.0
18A	24902	205	0.11011	0.00327	1.12587	0.04637	0.07416	0.00212	0.693	1801	53	766	22	461	13	77.0
18B	65347	126	0.05776	0.00102	0.57206	0.02161	0.07183	0.00240	0.883	521	38	459	14	447	14	14.6
20	138588	161	0.06014	0.00120	0.60469	0.03020	0.07292	0.00334	0.916	609	43	480	19	454	20	26.4
21	35128	60	0.05731	0.00133	0.56471	0.02178	0.07146	0.00221	0.800	504	50	455	14	445	13	12.1
26	92972	124	0.05971	0.00090	0.60673	0.02157	0.07370	0.00237	0.906	593	32	481	14	458	14	23.5
27	38748	57	0.06102	0.00114	0.82504	0.03086	0.09806	0.00317	0.865	640	40	611	17	603	19	6.1
28	34211	341	0.18508	0.03314	1.57666	0.29160	0.06179	0.00285	0.250	2699	269	961	109	386	17	88.1
29	26116	99	0.05611	0.00109	0.55781	0.01892	0.07210	0.00201	0.820	457	42	450	12	449	12	1.8
30*	421904	541	0.05643	0.00237	0.73525	0.03774	0.09450	0.00279	0.575	469	90	560	22	582	16	-25.2
31	20476	142	0.06414	0.00157	0.63370	0.02395	0.07165	0.00206	0.762	746	51	498	15	446	12	41.6
32	44874	138	0.05822	0.00097	0.57981	0.02086	0.07223	0.00230	0.887	538	36	464	13	450	14	17.0
34	352829	84	0.05883	0.00078	0.70469	0.02432	0.08688	0.00277	0.922	561	29	542	14	537	16	4.4
37	75590	146	0.05762	0.00097	0.55717	0.02087	0.07013	0.00235	0.893	515	37	450	14	437	14	15.7
39	158856	84	0.06229	0.00111	0.83163	0.03068	0.09683	0.00312	0.875	684	38	615	17	596	18	13.5

Grain	^{206}Pb (cps) [1]	^{204}Pb (cps)	$^{207}Pb/^{206}Pb$	Absolute 2SE	$^{207}Pb/^{235}U$ [2]	Absolute 2SE [3]	$^{206}Pb/^{238}U$	Absolute 2SE	ρ [4]	$^{207}Pb/^{206}Pb$ Age (Ma)	error 2σ (Ma)	$^{207}Pb/^{235}U$ Age (Ma)	error 2σ (Ma)	$^{206}Pb/^{238}U$ Age (Ma)	error 2σ (Ma)	disc. [5] %
40A	18057	149	0.05755	0.00156	0.62694	0.02769	0.07901	0.00276	0.790	513	58	494	17	490	16	4.5
40B	19985	150	0.05716	0.00104	0.62694	0.02216	0.07954	0.00241	0.858	498	39	494	14	493	14	0.9
43	92870	174	0.05975	0.00121	0.60235	0.02157	0.07312	0.00216	0.826	595	43	479	14	455	13	24.3
44	117365	78	0.05659	0.00081	0.55516	0.01805	0.07115	0.00208	0.899	476	31	448	12	443	12	7.1
46	72017	59	0.06115	0.00090	0.82084	0.02668	0.09736	0.00282	0.892	644	31	609	15	599	17	7.4
48	93208	89	0.05776	0.00102	0.61336	0.02169	0.07702	0.00236	0.868	521	38	486	14	478	14	8.4
49	73003	164	0.05845	0.00093	0.58657	0.02014	0.07278	0.00222	0.887	547	34	469	13	453	13	17.8
62	43470	157	0.05958	0.00133	0.58766	0.02211	0.07153	0.00217	0.805	588	48	469	14	445	13	25.2
63	54227	201	0.06574	0.00187	0.66615	0.02743	0.07349	0.00218	0.721	798	59	518	17	457	13	44.2
64	163644	645	0.05724	0.00087	0.56481	0.02000	0.07157	0.00229	0.903	501	33	455	13	446	14	11.4
68	91266	308	0.05653	0.00088	0.55194	0.01868	0.07081	0.00213	0.888	473	34	446	12	441	13	7.0
69	54052	227	0.05577	0.00084	0.55033	0.01937	0.07157	0.00228	0.903	443	33	445	13	446	14	-0.6
72	141052	189	0.05667	0.00078	0.55602	0.02118	0.07116	0.00253	0.932	479	30	449	14	443	15	7.7
75	63105	197	0.06004	0.00130	0.58831	0.02238	0.07107	0.00222	0.822	605	46	470	14	443	13	27.8
81A	46765	194	0.05678	0.00085	0.55595	0.01876	0.07101	0.00215	0.895	483	33	449	12	442	13	8.7
81B	54180	217	0.05894	0.00094	0.58873	0.02006	0.07244	0.00218	0.884	565	34	470	13	451	13	20.9
83	37791	218	0.06098	0.00170	0.59649	0.02504	0.07094	0.00222	0.746	639	59	475	16	442	13	31.9
85A	27353	207	0.05796	0.00127	0.56489	0.02122	0.07069	0.00216	0.811	528	47	455	14	440	13	17.2
85B	71396	86	0.05823	0.00091	0.56309	0.02189	0.07014	0.00250	0.916	538	34	454	14	437	15	19.5
85C	44665	103	0.05889	0.00109	0.57095	0.02089	0.07032	0.00222	0.862	563	40	459	13	438	13	22.9
92	15185	155	0.12529	0.01101	1.38652	0.12788	0.08026	0.00225	0.304	2033	148	883	53	498	13	78.4
95	19571	147	0.10016	0.00545	1.11936	0.06773	0.08106	0.00215	0.439	1627	98	763	32	502	13	71.8
100	94461	96	0.05923	0.00094	0.59284	0.02156	0.07260	0.00238	0.901	575	34	473	14	452	14	22.3
103	14474	79	0.06183	0.00230	0.68367	0.03239	0.08020	0.00235	0.617	668	78	529	19	497	14	26.6
104A	42517	188	0.06498	0.00316	0.63929	0.03834	0.07136	0.00251	0.586	774	99	502	23	444	15	44.0
104B	39421	166	0.06219	0.00218	0.60845	0.02892	0.07096	0.00227	0.674	681	73	483	18	442	14	36.3
111	87684	56	0.05639	0.00084	0.55610	0.02030	0.07152	0.00238	0.913	468	33	449	13	445	14	5.0
112A	43243	30	0.05570	0.00091	0.53832	0.02012	0.07010	0.00236	0.900	440	36	437	13	437	14	0.8
112B	40550	41	0.05691	0.00092	0.56665	0.02165	0.07221	0.00250	0.907	488	35	456	14	449	15	8.2
112C	70407	72	0.06373	0.00172	0.63609	0.02814	0.07238	0.00253	0.791	733	56	500	17	451	15	39.9
112D	78464	75	0.05982	0.00120	0.58278	0.02143	0.07066	0.00217	0.837	597	43	466	14	440	13	27.2
112E	68563	39	0.05571	0.00080	0.54638	0.02043	0.07113	0.00246	0.924	441	32	443	13	443	15	-0.5
122	28830	39	0.05880	0.00165	0.56111	0.02429	0.06922	0.00228	0.763	560	60	452	16	431	14	23.7

Grain	^{206}Pb (cps) [1]	^{204}Pb (cps)	$^{207}Pb/^{206}Pb$	Absolute 2SE	$^{207}Pb/^{235}U$ [2]	Absolute 2SE [3]	$^{206}Pb/^{238}U$	Absolute 2SE	ρ [4]	$^{207}Pb/^{206}Pb$ Age (Ma)	error 2σ (Ma)	$^{207}Pb/^{235}U$ Age (Ma)	error 2σ (Ma)	$^{206}Pb/^{238}U$ Age (Ma)	error 2σ (Ma)	disc. [5] %
125	37376	38	0.05563	0.00109	0.53298	0.02153	0.06948	0.00246	0.875	438	43	434	14	433	15	1.1
128	23439	37	0.05457	0.00134	0.52540	0.02155	0.06983	0.00229	0.800	395	54	429	14	435	14	-10.6
130	42379	34	0.05962	0.00167	0.57945	0.02392	0.07049	0.00214	0.736	590	59	464	15	439	13	26.4
132	78098	50	0.05684	0.00088	0.56389	0.02103	0.07195	0.00244	0.909	485	34	454	14	448	15	8.0
134	41225	50	0.05582	0.00109	0.54482	0.02272	0.07079	0.00261	0.884	445	43	442	15	441	16	1.0
136	79234	98	0.06107	0.00104	0.64134	0.02671	0.07617	0.00289	0.912	642	36	503	16	473	17	27.2
137	17182	178	0.15100	0.01976	1.83165	0.24539	0.08798	0.00253	0.215	2357	208	1057	84	544	15	80.1
145	66861	109	0.06385	0.00161	0.65213	0.02653	0.07408	0.00237	0.786	737	52	510	16	461	14	38.8
146	110285	53	0.05735	0.00088	0.58468	0.02336	0.07394	0.00273	0.923	505	34	467	15	460	16	9.3
147	39922	72	0.06119	0.00151	0.63420	0.02580	0.07517	0.00243	0.794	646	52	499	16	467	15	28.7
152A	27911	57	0.05700	0.00121	0.63265	0.02524	0.08050	0.00272	0.847	491	46	498	16	499	16	-1.6
152B	17401	48	0.05425	0.00132	0.59149	0.02469	0.07907	0.00268	0.813	382	54	472	16	491	16	-29.7
161	54254	83	0.06289	0.00130	0.63042	0.02398	0.07271	0.00232	0.840	704	43	496	15	452	14	37.0
164	105234	80	0.05912	0.00122	0.58903	0.02120	0.07226	0.00213	0.820	571	44	470	13	450	13	22.0
169	92086	47	0.05732	0.00088	0.58234	0.02239	0.07369	0.00260	0.917	504	33	466	14	458	16	9.3
173	109919	200	0.06153	0.00260	0.63817	0.03456	0.07523	0.00254	0.624	658	88	501	21	468	15	30.0
181	30927	63	0.07185	0.00316	0.74937	0.04035	0.07565	0.00236	0.579	982	87	568	23	470	14	54.0
186	264865	121	0.06006	0.00083	0.58490	0.02193	0.07063	0.00246	0.930	606	30	468	14	440	15	28.3
191	23093	70	0.07255	0.00329	0.73596	0.04060	0.07358	0.00231	0.569	1001	89	560	23	458	14	56.2

Sample NA031A Conwa Castle Grit 2nd Run - Standards

*common lead corrected

Grain	^{206}Pb (cps)	^{204}Pb (cps)	$^{206}Pbcom$	$^{207}Pbcom$	$^{207}Pb*$	$^{206}Pb*$	Not Common Lead Corrected Isotopic Ratios: $^{207}Pb/^{206}Pb$	Absolute 1SE	$^{206}Pb/^{238}U$	Absolute 1SE
LH94-15										
1	741687	90	1437	1385	740250	85266	0.115722	0.000146	0.284664	0.003015
2	498709	92	1463	1417	497246	56152	0.114378	0.000105	0.293390	0.002818
3	532665	106	1673	1621	530992	59739	0.114143	0.000115	0.295519	0.001495
4	558449	77	1216	1181	557233	62953	0.113807	0.000102	0.300303	0.001806
5	789258	106	1677	1620	787581	89095	0.113916	0.000122	0.289443	0.004918
6	510156	87	1385	1339	508770	57315	0.114025	0.000105	0.290218	0.003070
7	522563	123	1950	1882	520613	58634	0.114834	0.000129	0.287766	0.003449
8	700873	157	2497	2409	698376	78003	0.113736	0.000105	0.286402	0.004150
9	598726	141	2243	2165	596483	66288	0.113362	0.000120	0.287530	0.003452
10	709786	168	2659	2571	707127	78855	0.113711	0.000085	0.290741	0.001592
11	751684	151	2386	2312	749298	84149	0.114078	0.000099	0.295436	0.003408
12	541153	274	4326	4197	536827	58378	0.114603	0.000104	0.297695	0.003298
13	649947	269	4276	4133	645671	70752	0.114189	0.000100	0.290366	0.004571
14	413257	66	1046	1009	412210	47260	0.115665	0.000156	0.285373	0.003367
15	603686	205	3242	3137	600444	66631	0.114392	0.000153	0.292433	0.004005
16	505720	73	1160	1122	504560	57168	0.114264	0.000090	0.291024	0.003013
17	510314	58	919	889	509396	57887	0.114028	0.000096	0.292579	0.004639
18	338287	65	1036	1002	337251	37926	0.113930	0.000132	0.291840	0.002089
19	287461	63	1008	971	286453	32750	0.116154	0.000196	0.283357	0.003174
20	251463	68	1080	1040	250383	28379	0.116074	0.000136	0.281780	0.002162
21	317618	110	1747	1691	315870	35287	0.115083	0.000144	0.292807	0.002939
22	284236	79	1249	1208	282987	31698	0.114672	0.000163	0.291335	0.003470
24	403949	80	1273	1231	402677	45536	0.114965	0.000127	0.291745	0.004494
GJ132										
1	199805	82	1469	1280	198336	11149	0.061685	0.000101	0.083674	0.000575
2	193764	100	1783	1553	191981	10560	0.061707	0.000146	0.083351	0.001031
3	207367	87	1562	1362	205805	11560	0.061774	0.000115	0.085089	0.000763

Grain	^{206}Pb (cps)	^{204}Pb (cps)	$^{206}Pb_{com}$	$^{207}Pb_{com}$	$^{207}Pb^*$	$^{206}Pb^*$	$^{207}Pb/^{206}Pb$	Absolute 1SE	$^{206}Pb/^{238}U$	Absolute 1SE
4	206092	96	1714	1495	204378	11333	0.061720	0.000129	0.086110	0.000473
5	198752	129	2300	2005	196452	10339	0.061577	0.000150	0.085256	0.001291
6	236157	117	2092	1825	234065	12875	0.061518	0.000117	0.086667	0.000822
7	220689	147	2625	2289	218064	11473	0.061774	0.000118	0.085539	0.000901
8	212069	269	4793	4189	207277	9284	0.062893	0.000149	0.090488	0.002486
9	178655	104	1846	1625	176809	9504	0.061594	0.000157	0.104344	0.009272
11	229771	219	3904	3405	225867	10762	0.061098	0.000113	0.085655	0.000671
12	200619	96	1719	1497	198900	11048	0.061974	0.000116	0.083587	0.000731
13	206702	70	1250	1089	205452	11723	0.061446	0.000141	0.083626	0.000687
14	199847	84	1492	1301	198355	11253	0.062134	0.000095	0.086111	0.001535
20	211242	88	1568	1367	209673	11765	0.061335	0.000113	0.084470	0.000709
21	209398	94	1679	1463	207719	11610	0.061746	0.000143	0.084204	0.000689
22	202422	76	1364	1188	201058	11357	0.061299	0.000133	0.084352	0.001271
23	196342	92	1649	1436	194693	10664	0.061056	0.000123	0.082637	0.000778

Sample NA041A Dol-cyn-afon Formation

Results of all analyzed grains

*common lead corrected

			Isotopic Ratios							Apparent Age Summary						
Grain	^{206}Pb (cps) [1]	^{204}Pb (cps)	$^{207}Pb/^{206}Pb$	Absolute 2SE	$^{207}Pb/^{235}U$ [2]	Absolute 2SE [3]	$^{206}Pb/^{238}U$	Absolute 2SE	ρ [4]	$^{207}Pb/^{206}Pb$ Age (Ma)	error 2σ (Ma)	$^{207}Pb/^{235}U$ Age (Ma)	error 2σ (Ma)	$^{206}Pb/^{238}U$ Age (Ma)	error 2σ (Ma)	disc. [5] %
1	64479	105	0.06451	0.00139	0.99791	0.06297	0.11219	0.00665	0.940	758	45	703	32	685	38	10.2
2	58727	210	0.08588	0.00301	1.06429	0.11150	0.08988	0.00888	0.943	1336	66	736	53	555	52	61.0
3	49075	100	0.05870	0.00133	0.69134	0.03502	0.08541	0.00387	0.894	556	49	534	21	528	23	5.2
4	39740	114	0.06166	0.00190	0.74466	0.04981	0.08759	0.00520	0.887	662	65	565	29	541	31	19.1
5	32493	99	0.06086	0.00141	0.79489	0.04572	0.09473	0.00499	0.916	634	49	594	26	583	29	8.4
6	280504	107	0.17763	0.00089	11.46919	0.60599	0.46830	0.02463	0.996	2631	8	2562	48	2476	107	7.1
7	178288	103	0.08074	0.00119	2.23078	0.15187	0.20038	0.01332	0.976	1215	29	1191	47	1177	71	3.4
8	106929	135	0.06277	0.00144	0.77128	0.04333	0.08911	0.00457	0.913	700	48	580	25	550	27	22.4
9	613892	125	0.12794	0.00060	6.45999	0.50482	0.36621	0.02857	0.998	2070	8	2040	66	2012	133	3.3
10	57734	111	0.06172	0.00136	0.77518	0.04610	0.09109	0.00503	0.928	665	47	583	26	562	30	16.1
11	187471	271	0.07065	0.00395	0.95591	0.07686	0.09813	0.00567	0.718	947	110	681	39	603	33	38.0
12	40426	124	0.05707	0.00259	0.57928	0.04572	0.07362	0.00475	0.818	494	97	464	29	458	28	7.6
13	92165	122	0.07424	0.00240	1.65591	0.11614	0.16176	0.01007	0.888	1048	64	992	43	967	56	8.4
14	574684	122	0.13481	0.00068	7.22434	0.36820	0.38865	0.01971	0.995	2162	9	2140	44	2117	91	2.4
15	37784	129	0.06060	0.00260	0.79453	0.05592	0.09508	0.00530	0.792	625	90	594	31	586	31	6.6
16	1957078	130	0.18485	0.00093	12.01023	0.80841	0.47123	0.03163	0.997	2697	8	2605	61	2489	137	9
17	782166	104	0.28617	0.00124	24.92386	1.79572	0.63167	0.04543	0.998	3397	7	3305	68	3156	177	8.9
18	31056	120	0.06102	0.00305	0.69143	0.05608	0.08219	0.00525	0.788	640	104	534	33	509	31	21.2
19	55276	137	0.06070	0.00279	0.72564	0.05448	0.08670	0.00515	0.791	629	96	554	32	536	30	15.3
20	175911	126	0.06072	0.00254	0.77636	0.05981	0.09274	0.00600	0.840	629	88	583	34	572	35	9.5
21	114586	130	0.06643	0.00303	0.89448	0.06215	0.09765	0.00511	0.754	820	93	649	33	601	30	28.0
22	20658	73	0.06325	0.00283	0.80906	0.07412	0.09277	0.00742	0.872	717	92	602	41	572	44	21.1
23	107046	92	0.06417	0.00262	0.86255	0.06342	0.09749	0.00596	0.832	747	84	632	34	600	35	20.7
24	46152	78	0.06386	0.00280	0.88743	0.06866	0.10079	0.00643	0.824	737	90	645	36	619	38	16.8
25	36533	82	0.05790	0.00250	0.57753	0.04164	0.07234	0.00418	0.800	526	92	463	26	450	25	14.9
26*	1187373	312	0.19830	0.00234	13.00905	0.82721	0.47580	0.02973	0.983	2812	19	2680	58	2509	129	13.0
27	160415	81	0.10762	0.00145	4.35911	0.30265	0.29377	0.02001	0.981	1760	24	1705	56	1660	99	6.4
28	68580	105	0.06051	0.00283	0.71696	0.05263	0.08593	0.00487	0.771	622	98	549	31	531	29	15.1
29	314162	84	0.12483	0.00129	5.88256	0.42374	0.34179	0.02437	0.990	2026	18	1959	61	1895	116	7.5

Grain	^{206}Pb (cps) [1]	^{204}Pb (cps)	$^{207}Pb/^{206}Pb$	Absolute 2SE	$^{207}Pb/^{235}U$ [2]	Absolute 2SE [3]	$^{206}Pb/^{238}U$	Absolute 2SE	ρ [4]	$^{207}Pb/^{206}Pb$ Age (Ma)	error 2σ (Ma)	$^{207}Pb/^{235}U$ Age (Ma)	error 2σ (Ma)	$^{206}Pb/^{238}U$ Age (Ma)	error 2σ (Ma)	disc. [5] %
30	27165	82	0.06171	0.00271	0.82329	0.05684	0.09676	0.00515	0.771	664	91	610	31	595	30	10.8
31	1171222	129	0.11641	0.00116	5.13362	0.36391	0.31985	0.02245	0.990	1902	18	1842	59	1789	109	6.8
32	531048	91	0.10840	0.00132	4.58111	0.35404	0.30651	0.02339	0.988	1773	22	1746	62	1724	114	3.2
33	56848	93	0.06129	0.00262	0.80795	0.05653	0.09561	0.00529	0.791	649	89	601	31	589	31	9.8
34	324334	98	0.09594	0.00192	3.27462	0.22387	0.24756	0.01618	0.956	1547	37	1475	52	1426	83	8.7
35	41366	134	0.07562	0.00577	0.92503	0.09857	0.08871	0.00660	0.698	1085	146	665	51	548	39	51.6
36	270347	114	0.06438	0.00253	1.08197	0.08635	0.12189	0.00847	0.871	754	81	745	41	741	48	1.8
37	138971	93	0.05813	0.00241	0.65628	0.05292	0.08187	0.00566	0.857	535	88	512	32	507	34	5.4
38	272132	121	0.06076	0.00252	0.74866	0.06074	0.08936	0.00623	0.859	631	87	567	35	552	37	13.1
39	95857	118	0.06289	0.00273	0.87789	0.06510	0.10124	0.00609	0.811	705	90	640	35	622	36	12.3
40	51381	114	0.06155	0.00267	0.84514	0.06782	0.09958	0.00673	0.842	659	90	622	37	612	39	7.4
41*	257694	603	0.05744	0.00445	0.76682	0.06942	0.09683	0.00455	0.519	508	162	578	39	596*	27	-18.0
42	169076	96	0.05925	0.00246	0.76427	0.05900	0.09356	0.00609	0.843	576	88	576	33	577	36	-0.1
43	56160	76	0.06350	0.00256	0.93560	0.06409	0.10686	0.00592	0.808	725	83	671	33	654	34	10.2
44	94191	66	0.06151	0.00258	0.83773	0.05941	0.09878	0.00565	0.806	657	87	618	32	607	33	7.9
45	51113	77	0.06158	0.00270	0.80847	0.06555	0.09522	0.00650	0.842	660	91	602	36	586	38	11.6
46	32216	53	0.05856	0.00261	0.63861	0.05190	0.07910	0.00537	0.836	551	94	501	32	491	32	11.3
47	81783	56	0.05956	0.00253	0.72922	0.05771	0.08879	0.00593	0.844	588	89	556	33	548	35	7.0
48	279406	55	0.12426	0.00125	5.79433	0.42179	0.33819	0.02438	0.990	2018	18	1946	61	1878	116	8.0
49	65857	55	0.06009	0.00276	0.80553	0.06316	0.09723	0.00618	0.811	607	96	600	35	598	36	1.5
50	52755	73	0.06213	0.00264	0.73296	0.06660	0.08556	0.00687	0.884	679	88	558	38	529	41	22.9
51	286204	73	0.06455	0.00255	1.07192	0.07222	0.12044	0.00657	0.810	760	81	740	35	733	38	3.7
52	54145	43	0.06119	0.00259	0.79147	0.06521	0.09381	0.00663	0.858	646	88	592	36	578	39	11.0
53	114294	47	0.09349	0.00205	3.11229	0.23639	0.24144	0.01756	0.957	1498	41	1436	57	1394	91	7.7
54	75661	45	0.06167	0.00260	0.80653	0.06134	0.09485	0.00600	0.832	663	88	601	34	584	35	12.4
55	219479	54	0.06437	0.00252	1.04254	0.07483	0.11747	0.00706	0.838	754	81	725	37	716	41	5.3
56	108573	44	0.05876	0.00248	0.70838	0.05142	0.08744	0.00517	0.814	558	89	544	30	540	31	3.3
57	568549	43	0.08784	0.00218	2.81939	0.20475	0.23278	0.01589	0.940	1379	47	1361	53	1349	83	2.4
58	291831	42	0.06017	0.00250	0.81659	0.07391	0.09843	0.00791	0.888	610	87	606	40	605	46	0.8
59	24393	49	0.05791	0.00352	0.76487	0.07271	0.09579	0.00700	0.769	526	128	577	41	590	41	-12.6
60	102723	46	0.06060	0.00256	0.79539	0.06104	0.09520	0.00609	0.834	625	89	594	34	586	36	6.5
61	182098	202	0.06241	0.00284	0.78233	0.06361	0.09091	0.00612	0.828	688	94	587	36	561	36	19.3
62	173838	37	0.06035	0.00251	0.77007	0.07550	0.09254	0.00822	0.905	616	87	580	42	571	48	7.8

Grain	^{206}Pb (cps) [1]	^{204}Pb (cps)	$^{207}Pb/^{206}Pb$	Absolute 2SE	$^{207}Pb/^{235}U$ [2]	Absolute 2SE [3]	$^{206}Pb/^{238}U$	Absolute 2SE	ρ [4]	$^{207}Pb/^{206}Pb$ Age (Ma)	error 2σ (Ma)	$^{207}Pb/^{235}U$ Age (Ma)	error 2σ (Ma)	$^{206}Pb/^{238}U$ Age (Ma)	error 2σ (Ma)	disc. [5] %
63	145081	108	0.06288	0.00267	0.87856	0.06311	0.10134	0.00588	0.807	704	88	640	34	622	34	12.2
64	68567	39	0.06183	0.00254	0.89073	0.06332	0.10448	0.00606	0.816	668	86	647	33	641	35	4.3
65	129947	88	0.06745	0.00287	1.09305	0.08336	0.11754	0.00744	0.830	852	86	750	40	716	43	16.8
66	252769	47	0.09053	0.00214	2.31832	0.17487	0.18573	0.01331	0.950	1437	44	1218	52	1098	72	25.6
67*	1308848	406	0.12836	0.00152	6.17626	0.40982	0.34898	0.02279	0.984	2076	21	2001	56	1930	108	8.1
68	508081	70	0.12510	0.00130	4.71328	0.41325	0.27326	0.02379	0.993	2030	18	1770	71	1557	119	26.2
69	51556	25	0.05908	0.00252	0.76721	0.06943	0.09418	0.00751	0.882	570	90	578	39	580	44	-1.8
70	59260	64	0.05621	0.00092	0.59757	0.03931	0.07710	0.00491	0.968	461	36	476	25	479	29	-4.1
72	61719	33	0.05911	0.00252	0.73828	0.05825	0.09058	0.00601	0.842	571	90	561	33	559	35	2.2
73	82459	46	0.06022	0.00252	0.76730	0.05438	0.09240	0.00529	0.808	612	88	578	31	570	31	7.2
74	25423	36	0.05574	0.00279	0.55897	0.04297	0.07273	0.00425	0.760	442	108	451	28	453	25	-2.5
75	51695	33	0.06066	0.00260	0.80373	0.05610	0.09609	0.00529	0.789	627	90	599	31	591	31	6.0
76	300857	39	0.08138	0.00235	2.18998	0.16103	0.19517	0.01320	0.920	1231	56	1178	50	1149	71	7.2
77*	678767	3513	0.11053	0.00589	1.84576	0.15446	0.12111	0.00782	0.771	1808	94	1062	54	737	45	62.6
78	491605	50	0.09821	0.00181	3.83514	0.27165	0.28321	0.01937	0.965	1590	34	1600	56	1608	97	-1.2
79	19019	46	0.05300	0.00262	0.60157	0.04326	0.08232	0.00431	0.727	329	108	478	27	510	26	-57.3
80	980221	75	0.21877	0.00245	14.62714	1.08445	0.48491	0.03554	0.989	2972	18	2791	68	2549	152	17.2
81	1011221	40	0.08524	0.00222	2.64469	0.21963	0.22502	0.01775	0.950	1321	50	1313	59	1308	93	1.1
82	518068	58	0.12324	0.00109	5.92690	0.52509	0.34880	0.03075	0.995	2004	16	1965	74	1929	145	4.3
83*	843162	358	0.12501	0.00159	5.80540	0.50303	0.33681	0.02887	0.989	2029	22	1947	72	1871	138	8.9
84	130711	42	0.05767	0.00241	0.67190	0.04836	0.08450	0.00495	0.815	517	89	522	29	523	29	-1.1
85	330612	48	0.05992	0.00248	0.75067	0.05035	0.09087	0.00480	0.787	601	87	569	29	561	28	6.9
86	191334	30	0.11202	0.00108	4.69063	0.38965	0.30370	0.02506	0.993	1832	17	1766	67	1710	123	7.6
87	350715	42	0.08121	0.00232	2.18371	0.16672	0.19502	0.01380	0.927	1227	55	1176	52	1149	74	6.9
88	292564	49	0.08688	0.00218	2.58676	0.18201	0.21594	0.01420	0.934	1358	48	1297	50	1260	75	7.9
89	382845	71	0.05863	0.00243	0.71148	0.05650	0.08802	0.00596	0.853	553	88	546	33	544	35	1.8
90	159502	60	0.06228	0.00253	0.93465	0.06936	0.10884	0.00676	0.836	684	85	670	36	666	39	2.7
91	33754	56	0.05871	0.00279	0.75843	0.06402	0.09369	0.00654	0.827	556	100	573	36	577	38	-3.9
92	70159	57	0.05867	0.00249	0.63412	0.05072	0.07839	0.00532	0.848	555	90	499	31	486	32	12.8
93	13994	57	0.05647	0.00487	0.80953	0.08574	0.10397	0.00638	0.580	471	180	602	47	638	37	-37.2
94	359548	97	0.06086	0.00258	0.74408	0.06021	0.08867	0.00611	0.852	634	89	565	34	548	36	14.2
95	86570	58	0.06265	0.00259	0.94374	0.07217	0.10926	0.00703	0.841	696	86	675	37	668	41	4.2
96	33026	64	0.05611	0.00267	0.61927	0.04882	0.08005	0.00503	0.797	457	102	489	30	496	30	-9.1

Grain	^{206}Pb (cps) [1]	^{204}Pb (cps)	$^{207}Pb/^{206}Pb$	Absolute 2SE	$^{207}Pb/^{235}U$ [2]	Absolute 2SE [3]	$^{206}Pb/^{238}U$	Absolute 2SE	ρ [4]	$^{207}Pb/^{206}Pb$ Age (Ma)	error 2σ (Ma)	$^{207}Pb/^{235}U$ Age (Ma)	error 2σ (Ma)	$^{206}Pb/^{238}U$ Age (Ma)	error 2σ (Ma)	disc. [5] %
97	267041	66	0.07884	0.00240	1.99517	0.15031	0.18354	0.01264	0.914	1168	59	1114	50	1086	68	7.6
98	46709	70	0.05524	0.00277	0.55890	0.04702	0.07338	0.00496	0.803	422	108	451	30	457	30	-8.5
99	119543	64	0.06010	0.00254	0.77900	0.05466	0.09401	0.00526	0.798	607	89	585	31	579	31	4.8
100	29344	61	0.05353	0.00262	0.53973	0.04392	0.07312	0.00475	0.798	351	107	438	29	455	28	-30.5
101	1067781	154	0.21940	0.00198	16.54695	1.45536	0.54700	0.04786	0.995	2976	14	2909	81	2813	196	6.8
102	1431344	73	0.18557	0.00125	11.98148	1.01359	0.46829	0.03949	0.997	2703	11	2603	76	2476	171	10.1
103*	243179	3111	0.07609*	0.01352	0.93142*	0.18454	0.08878*	0.00777	0.442	1098*	320	668*	93	548*	46	52.2
104	88992	57	0.05938	0.00252	0.75185	0.06144	0.09183	0.00642	0.855	581	90	569	35	566	38	2.7
105	235246	72	0.13853	0.00129	7.28475	0.65655	0.38140	0.03419	0.995	2209	16	2147	77	2083	158	6.7
106*	1582339	631	0.09853	0.00159	3.48208	0.25172	0.25632	0.01806	0.975	1596	30	1523	55	1471	92	8.8
107	61144	57	0.05990	0.00253	0.83815	0.05611	0.10148	0.00526	0.775	600	89	618	31	623	31	-4.0
108	58224	92	0.06338	0.00292	0.84937	0.06266	0.09719	0.00559	0.780	721	95	624	34	598	33	17.9
109	1768611	150	0.19952	0.00152	14.43259	0.88145	0.52464	0.03179	0.992	2822	12	2779	56	2719	133	4.5
110	182058	41	0.05971	0.00250	0.71313	0.05040	0.08662	0.00494	0.806	593	88	547	29	536	29	10.1
111	83949	25	0.05772	0.00244	0.68796	0.05275	0.08645	0.00553	0.834	519	90	532	31	535	33	-3.1
112	107981	27	0.05878	0.00249	0.70238	0.04643	0.08666	0.00440	0.768	559	90	540	27	536	26	4.4
113	77419	35	0.06064	0.00262	0.77245	0.05634	0.09238	0.00543	0.805	627	91	581	32	570	32	9.5
114	414676	75	0.06344	0.00258	1.02920	0.09106	0.11767	0.00925	0.888	723	84	719	45	717	53	0.8
115	84229	87	0.06018	0.00264	0.77663	0.05222	0.09359	0.00477	0.759	610	92	584	29	577	28	5.7
116	269264	80	0.05881	0.00244	0.70761	0.04753	0.08726	0.00461	0.787	560	88	543	28	539	27	3.9
117	171431	74	0.05876	0.00246	0.68045	0.04576	0.08398	0.00442	0.783	558	89	527	27	520	26	7.2
118	645295	68	0.11386	0.00103	4.79794	0.41080	0.30562	0.02602	0.994	1862	16	1785	70	1719	127	8.7
119	141834	63	0.05923	0.00248	0.78765	0.05424	0.09645	0.00527	0.794	576	88	590	30	594	31	-3.3
120	133596	67	0.05937	0.00249	0.78385	0.05769	0.09576	0.00579	0.821	581	89	588	32	590	34	-1.6
121	169059	96	0.09735	0.00091	3.74774	0.27282	0.27921	0.02016	0.992	1574	17	1582	57	1587	101	-1.0
122	630212	89	0.09468	0.00090	3.59581	0.26971	0.27546	0.02049	0.992	1522	18	1549	58	1568	103	-3.5
123	164132	84	0.06199	0.00081	0.94512	0.06401	0.11057	0.00735	0.981	674	28	676	33	676	43	-0.3
124	265491	22	0.06244	0.00085	0.94356	0.06377	0.10959	0.00726	0.980	689	29	675	33	670	42	2.9
125	76048	29	0.05950	0.00103	0.69691	0.04860	0.08495	0.00574	0.969	585	37	537	29	526	34	10.7
126	23405	27	0.05901	0.00170	0.56995	0.04447	0.07005	0.00508	0.930	568	61	458	28	436	31	23.9
127*	900121	2391	0.12276	0.00289	4.58602	0.38613	0.27094	0.02190	0.960	1997	41	1747	68	1546	110	25.4
128	46826	21	0.06161	0.00101	0.77593	0.05301	0.09134	0.00606	0.971	661	35	583	30	563	36	15.4
129	187631	17	0.09979	0.00090	4.08354	0.33404	0.29680	0.02413	0.994	1620	17	1651	65	1675	119	-3.9

Grain	^{206}Pb (cps) [1]	^{204}Pb (cps)	$^{207}Pb/^{206}Pb$	Absolute 2SE	$^{207}Pb/^{235}U$ [2]	Absolute 2SE [3]	$^{206}Pb/^{238}U$	Absolute 2SE	ρ [4]	$^{207}Pb/^{206}Pb$ Age (Ma)	error 2σ (Ma)	$^{207}Pb/^{235}U$ Age (Ma)	error 2σ (Ma)	$^{206}Pb/^{238}U$ Age (Ma)	error 2σ (Ma)	disc. [5] %
130	128452	19	0.05871	0.00083	0.68796	0.04822	0.08498	0.00584	0.980	557	30	532	29	526	35	5.8
131	836593	67	0.11360	0.00081	5.22379	0.37482	0.33350	0.02381	0.995	1858	13	1857	59	1855	114	0.2
132	171960	92	0.06093	0.00084	0.85174	0.06315	0.10138	0.00739	0.983	637	29	626	34	623	43	2.4
133	120746	96	0.05785	0.00081	0.63338	0.04999	0.07940	0.00617	0.984	524	30	498	31	493	37	6.3
134	238767	88	0.05870	0.00080	0.70367	0.04884	0.08694	0.00592	0.980	556	30	541	29	537	35	3.5
135	892827	92	0.17993	0.00146	12.48846	0.92933	0.50339	0.03724	0.994	2652	13	2642	68	2628	158	1.1
136	131950	82	0.06044	0.00085	0.80554	0.05561	0.09666	0.00653	0.979	619	30	600	31	595	38	4.2
137	186074	103	0.06066	0.00083	0.83501	0.07245	0.09984	0.00855	0.987	627	29	616	39	613	50	2.3
138	117234	98	0.06098	0.00093	0.83638	0.06441	0.09947	0.00751	0.980	639	32	617	35	611	44	4.5
139	362510	123	0.08597	0.00092	2.97552	0.24750	0.25103	0.02071	0.992	1337	21	1401	61	1444	106	-8.9
140	129231	79	0.07717	0.00092	1.87878	0.15397	0.17658	0.01432	0.989	1126	24	1074	53	1048	78	7.4
141	65664	95	0.06113	0.00119	0.79581	0.06175	0.09441	0.00709	0.968	644	41	594	34	582	42	10.1
142	107367	94	0.05845	0.00091	0.65642	0.05035	0.08146	0.00612	0.979	547	34	512	30	505	36	7.9
143	131604	97	0.08304	0.00149	2.26974	0.18734	0.19824	0.01597	0.976	1270	35	1203	57	1166	85	9.0
144	33256	86	0.06021	0.00110	0.78333	0.05935	0.09435	0.00694	0.971	611	39	587	33	581	41	5.1
145	66252	90	0.07851	0.00102	2.02031	0.13862	0.18663	0.01257	0.982	1160	26	1122	46	1103	68	5.3
146	400950	155	0.06128	0.00084	0.74994	0.05595	0.08876	0.00651	0.983	649	29	568	32	548	38	16.2
147	191291	101	0.05847	0.00079	0.69487	0.04718	0.08619	0.00573	0.980	548	29	536	28	533	34	2.8
148C	107606	105	0.06075	0.00091	0.84398	0.05939	0.10077	0.00693	0.977	630	32	621	32	619	40	1.9
128D	216522	101	0.05988	0.00080	0.80157	0.05572	0.09708	0.00662	0.981	599	29	598	31	597	39	0.4
149	932166	107	0.08757	0.00088	3.00682	0.21052	0.24903	0.01725	0.990	1373	19	1409	52	1433	88	-4.9
150	379248	101	0.09261	0.00088	3.18971	0.23589	0.24980	0.01832	0.992	1480	18	1455	56	1437	94	3.2

Sample NA041A Dol-cyn-afon Fromation - Standards

*common lead corrected

							Not Common Lead Corrected Isotopic Ratios			
Grain	^{206}Pb (cps)	^{204}Pb (cps)	^{206}Pbcom	^{207}Pbcom	^{207}Pb*	^{206}Pb*	^{207}Pb/^{206}Pb	Absolute 1SE	^{206}Pb/^{238}U	Absolute 1SE
LH94-15										
1	152304	77	1232	1186	151073	16528	0.115248	0.000205	0.281892	0.005273
2	263916	75	1179	1144	262737	29278	0.114465	0.000201	0.298600	0.006433
3	185768	60	953	922	184815	20490	0.114222	0.000205	0.291631	0.004699
4	254710	66	1049	1012	253661	28185	0.113439	0.000138	0.286851	0.005250
5	254947	123	1971	1895	252977	27238	0.113106	0.000231	0.279998	0.006201
6	242530	113	1813	1735	240717	26041	0.113364	0.000177	0.271265	0.006066
7	316985	128	2038	1962	314947	34375	0.112911	0.000268	0.282136	0.006187
8	260811	133	2132	2047	258678	27922	0.113363	0.000241	0.276248	0.004407
9	507490	73	1143	1117	506347	57518	0.114404	0.000275	0.311139	0.004970
10	370911	66	1051	1018	369860	41362	0.113251	0.000175	0.294318	0.005592
11	390439	90	1426	1377	389013	43511	0.113854	0.000257	0.289043	0.003717
12	388867	83	1327	1274	387540	43331	0.113088	0.000285	0.277188	0.003954
13	614993	98	1552	1498	613441	69125	0.113177	0.000279	0.288249	0.004797
14	542650	92	1466	1417	541184	60290	0.112594	0.000154	0.290522	0.004155
15	517943	64	1009	976	516934	57961	0.112602	0.000193	0.292640	0.006105
16	434668	53	839	812	433830	48575	0.112498	0.000200	0.293536	0.002611
17	515121	37	592	574	514528	58073	0.112394	0.000203	0.295915	0.003581
18	567100	42	666	643	566434	63780	0.112187	0.000219	0.290212	0.003736
19	451135	40	638	614	450496	50431	0.112127	0.000190	0.281958	0.003137
20	407593	34	540	517	407054	45613	0.112078	0.000187	0.270992	0.003303
21	351704	32	507	488	351196	39358	0.112152	0.000166	0.281328	0.002481
22	401309	48	767	735	400542	44819	0.112347	0.000229	0.272069	0.003003
23	502730	38	610	584	502120	56140	0.111754	0.000174	0.271547	0.003312
24	633193	55	876	842	632317	70972	0.111933	0.000187	0.279716	0.003473
25	549955	59	952	911	549003	61825	0.112697	0.000180	0.272006	0.002788
26	594418	56	898	867	593520	66556	0.112324	0.000207	0.287842	0.003238
27	232790	31	496	481	232294	25763	0.111540	0.000215	0.293711	0.006311
28	430320	38	599	582	429721	48246	0.112287	0.000239	0.303953	0.008030

Sample NA041A Dol-cyn-afon Fromation - Standards

*common lead corrected

Grain	^{206}Pb (cps)	^{204}Pb (cps)	$^{206}Pb_{com}$	$^{207}Pb_{com}$	$^{207}Pb^*$	$^{206}Pb^*$	Not Common Lead Corrected Isotopic Ratios: $^{207}Pb/^{206}Pb$	Absolute 1SE	$^{206}Pb/^{238}U$	Absolute 1SE
LH94-15										
1	152304	77	1232	1186	151073	16528	0.115248	0.000205	0.281892	0.005273
2	263916	75	1179	1144	262737	29278	0.114465	0.000201	0.298600	0.006433
3	185768	60	953	922	184815	20490	0.114222	0.000205	0.291631	0.004699
4	254710	66	1049	1012	253661	28185	0.113439	0.000138	0.286851	0.005250
5	254947	123	1971	1895	252977	27238	0.113106	0.000231	0.279998	0.006201
6	242530	113	1813	1735	240717	26041	0.113364	0.000177	0.271265	0.006066
7	316985	128	2038	1962	314947	34375	0.112911	0.000268	0.282136	0.006187
8	260811	133	2132	2047	258678	27922	0.113363	0.000241	0.276248	0.004407
9	507490	73	1143	1117	506347	57518	0.114404	0.000275	0.311139	0.004970
10	370911	66	1051	1018	369860	41362	0.113251	0.000175	0.294318	0.005592
11	390439	90	1426	1377	389013	43511	0.113854	0.000257	0.289043	0.003717
12	388867	83	1327	1274	387540	43331	0.113088	0.000285	0.277188	0.003954
13	614993	98	1552	1498	613441	69125	0.113177	0.000279	0.288249	0.004797
14	542650	92	1466	1417	541184	60290	0.112594	0.000154	0.290522	0.004155
15	517943	64	1009	976	516934	57961	0.112602	0.000193	0.292640	0.006105
16	434668	53	839	812	433830	48575	0.112498	0.000200	0.293536	0.002611
17	515121	37	592	574	514528	58073	0.112394	0.000203	0.295915	0.003581
18	567100	42	666	643	566434	63780	0.112187	0.000219	0.290212	0.003736
19	451135	40	638	614	450496	50431	0.112127	0.000190	0.281958	0.003137
20	407593	34	540	517	407054	45613	0.112078	0.000187	0.270992	0.003303
21	351704	32	507	488	351196	39358	0.112152	0.000166	0.281328	0.002481
22	401309	48	767	735	400542	44819	0.112347	0.000229	0.272069	0.003003
23	502730	38	610	584	502120	56140	0.111754	0.000174	0.271547	0.003312
24	633193	55	876	842	632317	70972	0.111933	0.000187	0.279716	0.003473
25	549955	59	952	911	549003	61825	0.112697	0.000180	0.272006	0.002788
26	594418	56	898	867	593520	66556	0.112324	0.000207	0.287842	0.003238
27	232790	31	496	481	232294	25763	0.111540	0.000215	0.293711	0.006311
28	430320	38	599	582	429721	48246	0.112287	0.000239	0.303953	0.008030

Grain	^{206}Pb (cps)	^{204}Pb (cps)	$^{206}Pb_{com}$	$^{207}Pb_{com}$	$^{207}Pb^*$	$^{206}Pb^*$	$^{207}Pb/^{206}Pb$	Absolute 1SE	$^{206}Pb/^{238}U$	Absolute 1SE
29	618203	17	274	264	617929	70734	0.113283	0.000268	0.280216	0.004994
30	348055	13	211	204	347844	39324	0.112369	0.000168	0.295435	0.002902
31	346878	68	1097	1052	345780	38818	0.113721	0.000248	0.273571	0.002966
32	202984	74	1182	1139	201802	22123	0.113386	0.000149	0.285234	0.002641
33	304683	50	799	763	303884	34238	0.113985	0.000163	0.266380	0.005672
34	152644	66	1064	1014	151580	16448	0.113170	0.000234	0.262097	0.003738
35	177351	91	1469	1397	175882	18893	0.113266	0.000210	0.257198	0.005959
36	209172	96	1553	1481	207619	22341	0.112780	0.000168	0.263933	0.006401
37	249208	97	1558	1489	247650	26936	0.112918	0.000208	0.268329	0.006958
38	166921	93	1506	1437	165415	17617	0.113085	0.000241	0.265054	0.003480
39	154047	59	942	903	153105	16777	0.113521	0.000216	0.274017	0.003651
40	169683	74	1181	1134	168502	18290	0.113196	0.000202	0.278119	0.006637
41	159718	61	977	936	158741	17370	0.112665	0.000262	0.272703	0.005218
42	308177	72	1150	1110	307028	34191	0.113269	0.000192	0.288258	0.005371
GJ132										
1	58754	60	1082	941	57672	2682	0.061071	0.000285	0.081382	0.000962
2	48745	56	994	866	47751	2223	0.061803	0.000357	0.082676	0.001201
3	53168	79	1416	1230	51753	2055	0.061138	0.000248	0.078651	0.000981
4	68636	67	1206	1048	67431	3253	0.061596	0.000354	0.079417	0.000742
5	53891	99	1765	1535	52126	1769	0.060410	0.000429	0.080577	0.000922
6	47983	110	1969	1713	46014	1263	0.060397	0.000392	0.081175	0.001184
7	55297	135	2426	2111	52871	1323	0.060302	0.000529	0.081697	0.001369
8	73680	123	2208	1922	71472	2631	0.060030	0.000283	0.081827	0.000912
9	105902	58	1033	900	104869	5771	0.062129	0.000145	0.082857	0.000848
10	97861	58	1033	900	96828	5267	0.062512	0.000280	0.083924	0.001042
11	85085	83	1481	1288	83604	3979	0.061267	0.000270	0.080455	0.000519
12	109550	88	1574	1368	107977	5355	0.060856	0.000201	0.079403	0.000516
13	117395	93	1665	1448	115730	5710	0.060217	0.000220	0.080039	0.000788
14	104823	82	1461	1273	103362	5207	0.060565	0.000301	0.084180	0.000674
15	69372	50	889	774	68483	3429	0.059833	0.000259	0.083868	0.000517
16	89462	38	675	587	88787	4856	0.060087	0.000200	0.079584	0.000785
17	111800	38	688	599	111112	6188	0.059641	0.000234	0.082278	0.000844

Grain	^{206}Pb (cps)	^{204}Pb (cps)	^{206}Pbcom	^{207}Pbcom	^{207}Pb*	^{206}Pb*	^{207}Pb/^{206}Pb	Absolute 1SE	^{206}Pb/^{238}U	Absolute 1SE
18	119352	37	668	580	118684	6711	0.060424	0.000147	0.079315	0.000739
19	46538	22	393	342	46145	2453	0.058817	0.000308	0.083182	0.000737
20	53963	34	612	532	53351	2809	0.060523	0.000331	0.080773	0.000509
21	62935	38	688	599	62247	3192	0.059499	0.000332	0.082528	0.000687
22	58143	34	604	526	57539	3026	0.060517	0.000219	0.083404	0.000603
23	78916	59	1050	914	77867	3843	0.059217	0.000219	0.082030	0.000894
24	53005	35	625	544	52380	2657	0.059475	0.000403	0.080496	0.000720
25	55338	46	819	712	54520	2555	0.058268	0.000293	0.081462	0.000575
26	91577	51	918	799	90659	4693	0.059535	0.000222	0.080769	0.000599
27	68785	20	364	317	68422	3791	0.058707	0.000249	0.083761	0.000577
28	81246	19	349	304	80897	4564	0.059161	0.000183	0.081460	0.000491
29	39629	10	182	159	39447	2154	0.057036	0.000443	0.084395	0.001202
30	116468	18	320	278	116148	6766	0.058986	0.000238	0.077824	0.001006
31	146853	76	1365	1185	145487	7942	0.061141	0.000151	0.076077	0.001395
32	38976	62	1106	963	37871	1462	0.061166	0.000472	0.083099	0.000839
33	132090	77	1381	1202	130708	6882	0.060583	0.000174	0.080531	0.001861
34	111245	71	1279	1112	109965	5817	0.060736	0.000215	0.078888	0.001856
35	113252	73	1311	1140	111941	5822	0.060632	0.000180	0.080200	0.001519
36	134194	90	1604	1397	132590	6850	0.060636	0.000208	0.082337	0.001813
37	100755	79	1417	1232	99338	4890	0.060033	0.000199	0.079208	0.001207
38	103916	77	1375	1197	102542	5111	0.060256	0.000202	0.082981	0.001919
39	73314	46	830	721	72485	3793	0.060629	0.000250	0.078615	0.000915
40	97843	48	863	752	96980	5281	0.060932	0.000306	0.083681	0.001334
41	73373	45	809	705	72564	3763	0.059920	0.000256	0.084387	0.001174
42	63360	50	888	774	62472	3127	0.060299	0.000298	0.085681	0.001542

Sample NB027A Lumsden Dam Formation

Results of all analyzed grains

*common lead corrected

			Isotopic Ratios							Apparent Age Summary						
	^{206}Pb	^{204}Pb		Absolute		Absolute		Absolute		$^{207}Pb/^{206}Pb$	error 2σ	$^{207}Pb/^{235}U$	error 2σ	$^{206}Pb/^{238}U$	error 2σ	disc. [5]
Grain	(cps) [1]	(cps)	$^{207}Pb/^{206}Pb$	2SE	$^{207}Pb/^{235}U$ [2]	2SE [3]	$^{206}Pb/^{238}U$	2SE	ρ [4]	Age (Ma)	(Ma)	Age (Ma)	(Ma)	Age (Ma)	(Ma)	%
1	312011	500	0.06825	0.00337	0.90278	0.10018	0.09594	0.00953	0.895	876	99	653	52	591	56	34.1
2	761848	840	0.07220	0.00310	1.09981	0.11439	0.11049	0.01047	0.911	991	85	753	54	676	60	33.5
3	82722	294	0.06418	0.00300	0.83410	0.10463	0.09426	0.01097	0.928	748	96	616	56	581	64	23.3
4	1771085	507	0.13927	0.00135	5.43662	0.33957	0.28311	0.01747	0.988	2218	17	1891	52	1607	87	31.1
5	508295	530	0.06522	0.00121	0.89413	0.09772	0.09943	0.01071	0.985	782	39	649	51	611	62	22.9
6	49127	100	0.06502	0.00195	1.01246	0.10805	0.11293	0.01157	0.960	775	62	710	53	690	67	11.6
7	841177	324	0.06511	0.00217	0.96817	0.10252	0.10785	0.01084	0.949	778	69	688	52	660	63	15.9
8	106014	98	0.06121	0.00136	0.84882	0.09294	0.10057	0.01078	0.979	647	47	624	50	618	63	4.7
9	397851	205	0.06297	0.00166	0.89527	0.09736	0.10312	0.01088	0.970	707	55	649	51	633	63	11.1
10	259853	140	0.07353	0.00167	1.48307	0.16189	0.14629	0.01562	0.978	1029	45	923	64	880	87	15.4
11	852294	153	0.12998	0.00094	7.24248	0.55777	0.40412	0.03099	0.996	2098	13	2142	66	2188	141	-5.1
12	21088	125	0.07325	0.00459	1.59668	0.23757	0.15809	0.02133	0.907	1021	122	969	89	946	118	7.9
13	474233	195	0.11007	0.00094	3.58468	0.29864	0.23621	0.01957	0.995	1800	15	1546	64	1367	101	26.7
14	94060	168	0.06360	0.00190	0.98146	0.10545	0.11192	0.01155	0.961	728	62	694	53	684	67	6.5
15	244625	151	0.07616	0.00120	1.89014	0.17691	0.17999	0.01660	0.986	1099	31	1078	60	1067	90	3.2
16	357464	111	0.06095	0.00110	0.89335	0.09454	0.10631	0.01109	0.985	637	38	648	49	651	64	-2.3
17	124463	148	0.06192	0.00118	0.83182	0.09448	0.09743	0.01091	0.986	671	40	615	51	599	64	11.2
18	688774	137	0.13024	0.00117	5.70945	0.49893	0.31794	0.02764	0.995	2101	16	1933	73	1780	134	17.5
19	1401723	263	0.12488	0.00095	5.82293	0.36399	0.33818	0.02098	0.993	2027	13	1950	53	1878	100	8.5
20	651631	215	0.12420	0.00152	4.18036	0.34975	0.24411	0.02021	0.989	2017	21	1670	66	1408	104	33.6
21	64510	159	0.06443	0.00217	0.95700	0.10034	0.10773	0.01070	0.947	756	70	682	51	660	62	13.4
22	364456	166	0.06048	0.00106	0.83693	0.09431	0.10036	0.01117	0.988	621	38	617	51	617	65	0.7
24	207168	240	0.06284	0.00153	0.87500	0.09593	0.10099	0.01080	0.975	703	51	638	51	620	63	12.3
25	608298	368	0.15762	0.00133	8.70570	0.83379	0.40059	0.03822	0.996	2430	14	2308	84	2172	174	12.5
26	230836	1756	0.15652	0.01143	2.15533	0.23419	0.09987	0.00803	0.740	2418	119	1167	73	614	47	78.1
27	136656	303	0.06518	0.00175	0.87379	0.09579	0.09722	0.01033	0.969	780	56	638	51	598	60	24.4
28	718193	252	0.12088	0.00106	5.56229	0.40935	0.33373	0.02438	0.993	1969	16	1910	61	1856	117	6.6
29	412214	282	0.06085	0.00112	0.86599	0.11061	0.10322	0.01305	0.990	634	39	633	58	633	76	0.1
30	254299	348	0.07242	0.00294	1.20655	0.13120	0.12084	0.01219	0.928	998	80	804	59	735	70	27.8

Grain	^{206}Pb (cps) [1]	^{204}Pb (cps)	$^{207}Pb/^{206}Pb$	Absolute 2SE	$^{207}Pb/^{235}U$ [2]	Absolute 2SE [3]	$^{206}Pb/^{238}U$	Absolute 2SE	ρ [4]	$^{207}Pb/^{206}Pb$ Age (Ma)	error 2σ (Ma)	$^{207}Pb/^{235}U$ Age (Ma)	error 2σ (Ma)	$^{206}Pb/^{238}U$ Age (Ma)	error 2σ (Ma)	disc. [5] %
31	941517	776	0.06142	0.00150	0.87407	0.09181	0.10321	0.01054	0.973	654	52	638	49	633	61	3.3
32	458382	153	0.06850	0.00131	1.32463	0.12631	0.14025	0.01310	0.980	884	39	857	54	846	74	4.5
33	265131	138	0.13046	0.00166	7.09237	0.42042	0.39429	0.02283	0.977	2104	22	2123	51	2143	105	-2.2
34	378954	167	0.06263	0.00163	0.82971	0.08640	0.09609	0.00969	0.968	696	55	613	47	591	57	15.7
35	218831	105	0.06391	0.00214	0.94659	0.13145	0.10743	0.01448	0.970	739	69	676	66	658	84	11.5
36	788664	159	0.06063	0.00113	0.79066	0.08205	0.09459	0.00966	0.984	626	40	592	45	583	57	7.2
37	111273	194	0.08095	0.00391	1.18694	0.11751	0.10635	0.00919	0.873	1220	92	795	53	651	53	49.0
38	252555	653	0.10847	0.00394	4.48597	0.56768	0.29994	0.03636	0.958	1774	65	1728	100	1691	178	5.3
39	455433	1517	0.05807	0.00398	0.92551	0.10305	0.11560	0.01014	0.788	532	143	665	53	705	58	-34.3
40	396952	626	0.17844	0.00458	11.13943	0.72145	0.45277	0.02692	0.918	2638	42	2535	59	2408	118	10.5
41	758693	283	0.06521	0.00136	1.11543	0.10245	0.12406	0.01110	0.974	781	43	761	48	754	63	3.7
42	811513	817	0.06065	0.00172	0.82701	0.09172	0.09889	0.01060	0.967	627	60	612	50	608	62	3.2
43	498484	284	0.11625	0.00200	3.86856	0.27402	0.24135	0.01658	0.970	1899	31	1607	56	1394	86	29.6
44	648152	958	0.06070	0.00228	0.80854	0.08285	0.09661	0.00921	0.930	629	79	602	45	594	54	5.7
45	378919	55	0.12633	0.00097	6.34555	0.43390	0.36429	0.02475	0.994	2048	14	2025	58	2002	116	2.6
46	67083	133	0.09227	0.00547	1.47875	0.17777	0.11623	0.01215	0.870	1473	109	922	70	709	70	54.7
47	964118	546	0.07111	0.00148	1.61535	0.15591	0.16476	0.01553	0.976	961	42	976	59	983	85	-2.5
48	135128	218	0.08134	0.00268	1.18348	0.12108	0.10553	0.01022	0.947	1230	63	793	55	647	59	49.8
49	131372	678	0.05309	0.00918	0.67741	0.12758	0.09254	0.00692	0.397	333	351	525	74	571	41	-74.8
50	470173	162	0.15264	0.00120	7.22130	0.38192	0.34312	0.01795	0.989	2376	13	2139	46	1902	86	23.0
51	644226	1019	0.06111	0.00227	0.84594	0.08769	0.10039	0.00972	0.934	643	78	622	47	617	57	4.3
52	57793	241	0.09747	0.01640	1.43263	0.27220	0.10660	0.00941	0.465	1576	286	903	108	653	55	61.5
53	861315	82	0.12880	0.00099	6.99603	0.57813	0.39395	0.03241	0.996	2082	13	2111	71	2141	148	-3.4
54	1313991	89	0.15532	0.00113	9.34260	0.58097	0.43624	0.02694	0.993	2405	12	2372	55	2334	120	3.5
55	619325	202	0.06139	0.00164	0.74997	0.08018	0.08860	0.00917	0.968	653	56	568	45	547	54	16.9
56	1450830	1261	0.08969	0.00133	1.81950	0.15778	0.14713	0.01257	0.985	1419	28	1053	55	885	70	40.2
57	1320690	762	0.12166	0.00134	6.28287	0.40259	0.37456	0.02364	0.985	1981	20	2016	55	2051	110	-4.1
58	550078	1865	0.07308	0.00414	1.15106	0.11150	0.11423	0.00898	0.811	1016	111	778	51	697	52	33.1
59	420796	716	0.06175	0.00279	0.94413	0.09401	0.11090	0.00984	0.891	665	94	675	48	678	57	-2.0
60	488718	219	0.06915	0.00117	1.08148	0.10712	0.11343	0.01107	0.985	903	35	744	51	693	64	24.6
61	743026	181	0.06257	0.00097	0.97587	0.05491	0.11311	0.00612	0.961	694	33	691	28	691	35	0.4
62	465102	1031	0.06029	0.00318	0.87201	0.06258	0.10490	0.00511	0.678	614	110	637	33	643	30	-5.0
64	625519	2313	0.10831	0.00411	5.44391	0.57016	0.36454	0.03559	0.932	1771	68	1892	86	2004	166	-15.3

Grain	^{206}Pb (cps) [1]	^{204}Pb (cps)	$^{207}Pb/^{206}Pb$	Absolute 2SE	$^{207}Pb/^{235}U$ [2]	Absolute 2SE [3]	$^{206}Pb/^{238}U$	Absolute 2SE	ρ [4]	$^{207}Pb/^{206}Pb$ Age (Ma)	error 2σ (Ma)	$^{207}Pb/^{235}U$ Age (Ma)	error 2σ (Ma)	$^{206}Pb/^{238}U$ Age (Ma)	error 2σ (Ma)	disc. [5] %
71	952446	7304	0.06219	0.00853	0.83596	0.14279	0.09750	0.00993	0.596	681	269	617	76	600	58	12.4
72	319457	108	0.06838	0.00622	0.99397	0.21210	0.10542	0.02035	0.905	880	178	701	103	646	118	27.9
73	718034	69	0.19731	0.00202	14.75157	2.07715	0.54223	0.07615	0.997	2804	17	2799	126	2793	311	0.5
74	404279	1671	0.08704	0.00538	1.55715	0.14923	0.12975	0.00951	0.764	1361	115	953	58	786	54	44.8
76	214472	68	0.06206	0.00107	0.74631	0.03706	0.08722	0.00406	0.937	676	37	566	21	539	24	21.1
77	206076	26	0.06355	0.00159	0.93429	0.09526	0.10663	0.01054	0.969	727	52	670	49	653	61	10.6
78	293873	434	0.06984	0.00292	1.51820	0.10712	0.15766	0.00897	0.806	924	83	938	42	944	50	-2.3
79	171483	312	0.08580	0.00620	1.25939	0.11295	0.10646	0.00565	0.592	1334	134	828	50	652	33	53.7
80	716699	84	0.17545	0.00148	11.42439	0.86497	0.47227	0.03553	0.994	2610	14	2558	68	2494	154	5.4
81	558953	49	0.12590	0.00102	6.54608	0.42278	0.37711	0.02416	0.992	2041	14	2052	55	2063	112	-1.2
84	183348	475	0.10642	0.00488	3.18286	0.49147	0.21693	0.03198	0.955	1739	82	1453	113	1266	167	29.9
85	115534	131	0.07353	0.00260	1.12779	0.09792	0.11125	0.00882	0.914	1028	70	767	46	680	51	35.7
86	210034	186	0.07405	0.00205	0.98082	0.05737	0.09606	0.00495	0.880	1043	55	694	29	591	29	45.3
89	195258	818	0.05883	0.00629	0.73504	0.09323	0.09062	0.00617	0.537	561	218	560	53	559	36	0.3
90	631245	3	0.11664	0.00102	5.16370	0.37146	0.32109	0.02293	0.993	1905	16	1847	59	1795	111	6.6
92	273887	942	0.06564	0.00465	0.82906	0.07164	0.09161	0.00453	0.572	795	142	613	39	565	27	30.2
97	338417	53	0.06311	0.00132	0.80695	0.04585	0.09274	0.00490	0.929	712	44	601	25	572	29	20.6
99	672720	465	0.19064	0.00213	8.81103	0.62889	0.33521	0.02363	0.988	2748	18	2319	63	1864	113	36.9
102	271077	158	0.07119	0.00159	1.06805	0.05702	0.10880	0.00528	0.908	963	45	738	28	666	31	32.5
104	252304	180	0.06534	0.00182	0.88697	0.06047	0.09846	0.00613	0.913	785	57	645	32	605	36	24.0
105	168217	130	0.06765	0.00177	0.90923	0.06969	0.09748	0.00702	0.940	858	53	657	36	600	41	31.5
106	1109753	345	0.09732	0.00222	2.28812	0.19782	0.17053	0.01422	0.965	1573	42	1209	59	1015	78	38.3
108	624701	211	0.06598	0.00131	1.13722	0.07175	0.12501	0.00748	0.949	806	41	771	34	759	43	6.1
109	133944	31	0.06209	0.00120	0.95159	0.03719	0.11116	0.00378	0.869	677	41	679	19	679	22	-0.4
110	624029	192	0.12153	0.00188	3.93390	0.36512	0.23476	0.02148	0.986	1979	27	1621	72	1359	111	34.7
111	1014140	4361	0.06184	0.00460	0.86723	0.10636	0.10171	0.00992	0.795	669	152	634	56	624	58	6.9
114	474793	208	0.11062	0.00198	4.07868	0.34065	0.26742	0.02182	0.977	1810	32	1650	66	1528	110	17.5
115	804396	241	0.06011	0.00117	0.84583	0.04567	0.10205	0.00514	0.932	608	42	622	25	626	30	-3.2
116	462354	6984	0.06919	0.01752	0.93895	0.24658	0.09842	0.00685	0.265	905	450	672	122	605	40	34.7
118	154442	543	0.06488	0.00563	0.81126	0.14102	0.09068	0.01366	0.867	771	173	603	76	560	80	28.6
120	251761	556	0.06202	0.00699	0.67072	0.09995	0.07844	0.00765	0.654	675	224	521	59	487	46	28.9
121	41019	198	0.10673	0.01162	1.63292	0.20056	0.11096	0.00631	0.463	1744	187	983	75	678	37	64.3
122	217380	172	0.06919	0.00252	0.94907	0.05556	0.09948	0.00456	0.783	904	73	678	29	611	27	34.0

Grain	^{206}Pb (cps) [1]	^{204}Pb (cps)	$^{207}Pb/^{206}Pb$	Absolute 2SE	$^{207}Pb/^{235}U$ [2]	Absolute 2SE [3]	$^{206}Pb/^{238}U$	Absolute 2SE	ρ [4]	$^{207}Pb/^{206}Pb$ Age (Ma)	error 2σ (Ma)	$^{207}Pb/^{235}U$ Age (Ma)	error 2σ (Ma)	$^{206}Pb/^{238}U$ Age (Ma)	error 2σ (Ma)	disc. [5] %
123	73937	51	0.06545	0.00227	0.91175	0.05474	0.10103	0.00495	0.816	789	71	658	29	620	29	22.4
124	139967	34	0.06129	0.00136	0.82461	0.06103	0.09757	0.00689	0.954	650	47	611	33	600	40	8.0
127	829305	1438	0.08224	0.00214	1.85457	0.13481	0.16355	0.01110	0.934	1251	50	1065	47	976	61	23.7
130	159698	100	0.13277	0.00256	6.27939	0.48885	0.34301	0.02587	0.969	2135	33	2016	66	1901	123	12.6
131	253791	78	0.06443	0.00135	0.90780	0.04608	0.10219	0.00472	0.910	756	44	656	24	627	28	17.8
133	366355	30	0.06025	0.00090	0.76713	0.04062	0.09235	0.00469	0.959	612	32	578	23	569	28	7.3
134	103084	31	0.09026	0.00143	2.95284	0.15992	0.23726	0.01228	0.956	1431	30	1396	40	1372	64	4.6
135	81051	111	0.07203	0.00311	0.98981	0.07953	0.09966	0.00675	0.843	987	86	699	40	612	39	39.8
136	398732	106	0.09459	0.00241	2.01129	0.18330	0.15421	0.01349	0.960	1520	47	1119	60	925	75	42.0
137	1010069	460	0.18413	0.00397	8.40025	0.56157	0.33087	0.02094	0.947	2690	35	2275	59	1843	101	36.1
138	17675	52	0.08674	0.00812	1.42260	0.16255	0.11894	0.00780	0.574	1355	170	898	66	724	45	49.1
140	297381	12	0.06168	0.00095	0.84113	0.05172	0.09891	0.00589	0.968	663	33	620	28	608	34	8.7
142	54340	9	0.06353	0.00187	0.91007	0.05283	0.10390	0.00519	0.861	726	61	657	28	637	30	12.8
143	23874	35	0.07832	0.00972	1.15545	0.16672	0.10700	0.00787	0.510	1155	228	780	76	655	46	45.5
144	388112	1170	0.06559	0.00368	0.76027	0.07733	0.08407	0.00713	0.834	793	114	574	44	520	42	35.8
146	81009	35	0.06641	0.00305	0.92766	0.06313	0.10131	0.00508	0.737	819	93	666	33	622	30	25.2
148	120637	93	0.08349	0.00805	1.12778	0.14055	0.09797	0.00773	0.633	1281	177	767	65	602	45	55.4
149	212340	135	0.06849	0.00337	0.99514	0.09811	0.10538	0.00901	0.867	883	98	701	49	646	52	28.2
150	775281	695	0.06307	0.00163	0.97630	0.06858	0.11226	0.00733	0.930	711	54	692	35	686	42	3.7

Sample NB027A Lumsden Dam Fromation - Standards

*common lead corrected

Grain	^{206}Pb (cps)	^{204}Pb (cps)	^{206}Pbcom	^{207}Pbcom	^{207}Pb*	^{206}Pb*	$^{207}Pb/^{206}Pb$	Absolute 1SE	$^{206}Pb/^{238}U$	Absolute 1SE
							Not Common Lead Corrected Isotopic Ratios			
LH94-15										
1	639913	148	2239	2243	637674	71831	0.114428	0.000178	0.363308	0.007552
2	619481	157	2377	2388	617104	68777	0.113481	0.000152	0.368800	0.012490
3	527319	111	1673	1687	525647	58464	0.112949	0.000114	0.376697	0.009489
4	1128627	142	2157	2153	1126470	127248	0.113369	0.000125	0.355618	0.005251
5	1430559	165	2524	2517	1428035	161075	0.113136	0.000135	0.353422	0.007994
6	1211828	129	1963	1958	1209865	136812	0.113373	0.000170	0.354570	0.006318
7	940468	40	609	613	939859	106979	0.113219	0.000141	0.372288	0.012712
8	620445	86	1311	1308	619134	69466	0.112706	0.000121	0.354319	0.010684
9	605366	87	1327	1319	604039	67674	0.112542	0.000144	0.347232	0.005106
10	702913	86	1300	1301	701613	78438	0.112348	0.000145	0.360222	0.010120
11	713491	257	3897	3903	709595	77444	0.112373	0.000132	0.362536	0.007774
12	1010957	145	2208	2202	1008750	112962	0.112656	0.000134	0.353659	0.005956
13	736653	73	1120	1115	735533	82966	0.112835	0.000129	0.350185	0.007447
14	708684	59	894	891	707790	79930	0.112817	0.000109	0.353440	0.004315
15	769174	56	848	849	768326	86527	0.112305	0.000124	0.361155	0.009591
16	577145	25	380	377	576765	65313	0.112599	0.000123	0.342647	0.007217
17	577245	17	259	257	576986	65438	0.112427	0.000121	0.342775	0.005512
18	855330	39	603	592	854727	97801	0.113822	0.000171	0.321954	0.004384
19	505110	10	149	146	504961	57427	0.113105	0.000135	0.320852	0.004948
20	556476	66	1029	1015	555447	62454	0.113017	0.000128	0.330760	0.008354
21	460456	37	567	559	459889	51963	0.113005	0.000106	0.330112	0.008704
22	548538	55	848	834	547690	62230	0.113664	0.000217	0.323758	0.009099
23	1373642	17	266	263	1373376	157362	0.113420	0.000150	0.330183	0.006534
24	655505	103	1592	1566	653913	73457	0.112752	0.000179	0.325205	0.003991
25	612945	53	824	815	612121	68679	0.112429	0.000122	0.336790	0.004539
26	806407	77	1189	1172	805217	91138	0.113170	0.000191	0.330018	0.005110
27	1492852	78	1211	1195	1491641	171321	0.113804	0.000286	0.332647	0.010453
28	689235	30	473	466	688762	78533	0.113259	0.000275	0.328129	0.009065

Grain	^{206}Pb (cps)	^{204}Pb (cps)	$^{206}Pb_{com}$	$^{207}Pb_{com}$	$^{207}Pb^*$	$^{206}Pb^*$	$^{207}Pb/^{206}Pb$	Absolute 1SE	$^{206}Pb/^{238}U$	Absolute 1SE
30	631119	8	116	114	631003	71613	0.112540	0.000090	0.337346	0.008402
31	461354	34	515	511	460839	52031	0.112766	0.000157	0.341463	0.008487
32	382946	30	458	451	382488	43254	0.112882	0.000212	0.327218	0.004337
33	629772	200	3081	3046	626691	70733	0.114442	0.000438	0.335939	0.008950
34	481125	45	704	694	480421	54262	0.112764	0.000208	0.330708	0.004240
36	322267	28	431	423	321836	36398	0.113099	0.000193	0.321084	0.007143
37	432702	166	2585	2534	430117	47142	0.113064	0.000177	0.318769	0.007563
38	359960	21	328	320	359632	40731	0.112866	0.000184	0.310964	0.007123
39	564859	28	436	429	564423	64246	0.113279	0.000133	0.325427	0.005553
40	429428	27	414	406	429014	48720	0.112706	0.000210	0.319619	0.004710
41	511271	6	99	99	511172	58148	0.112725	0.000153	0.342129	0.006130
42	259352	30	473	464	258879	29417	0.112912	0.000389	0.322092	0.006975
44	369869	15	233	231	369636	42320	0.113381	0.000341	0.335442	0.007404
45	428788	5	75	74	428712	48887	0.113010	0.000190	0.330254	0.009808
GJ132										
1	193061	204	3587	3167	189474	8656	0.060451	0.000210	0.110501	0.001982
2	211971	198	3498	3084	208473	9921	0.060532	0.000205	0.107494	0.002597
8	215160	62	1093	963	214066	12307	0.060755	0.000148	0.105146	0.003079
10	238103	86	1519	1336	236584	13394	0.060703	0.000174	0.103859	0.002716
12	225270	238	4207	3703	221063	10393	0.061246	0.000331	0.104118	0.001814
14	287075	125	2212	1950	284863	16621	0.063716	0.000339	0.107846	0.002431
17	266833	28	503	441	266330	16356	0.061872	0.000331	0.096898	0.002430
18	255287	7	116	102	255171	15614	0.060949	0.000155	0.095106	0.001586
21	300529	113	2004	1762	298525	17323	0.061576	0.000276	0.102109	0.002446
23	262403	21	375	329	262028	15686	0.060307	0.000137	0.095307	0.001384
25	253636	114	2031	1781	251605	13771	0.060119	0.000253	0.096335	0.000968
27	280734	4	69	60	280665	17070	0.060184	0.000132	0.094605	0.001818
29	274147	36	644	565	273502	16145	0.060038	0.000120	0.096522	0.001699
32	260189	25	441	386	259748	15638	0.060587	0.000161	0.093140	0.002707
34	262941	38	673	590	262269	15476	0.060068	0.000137	0.097616	0.001049
37	274229	61	1085	951	273144	16120	0.061138	0.000365	0.096896	0.002018
39	292112	38	683	599	291429	17392	0.060762	0.000262	0.096766	0.001733

Grain	^{206}Pb (cps)	^{204}Pb (cps)	^{206}Pbcom	^{207}Pbcom	$^{207}Pb^*$	$^{206}Pb^*$	$^{207}Pb/^{206}Pb$	Absolute 1SE	$^{206}Pb/^{238}U$	Absolute 1SE
41	305381	9	154	134	305228	18744	0.061000	0.000143	0.094569	0.000965
42	114111	115	2038	1785	112073	5460	0.060652	0.000575	0.094523	0.002151
43	141790	1	20	17	141771	8860	0.060997	0.000431	0.094700	0.001431